JAERI-M
82-178

JAPANESE CONTRIBUTIONS TO IAEA INTOR WORKSHOP, PHASE IIA

CHAPTER XI : MECHANICAL CONFIGURATION

November 1982

Satoshi NISHIO, Noburo FUJISAWA, Yuzo FUKAI*
Yoshio SAWADA*, Mitsugi YAMAGUCHI
Takao UCHIDA*, Nobuharu MIKI,* Takataro HAMAJIMA*
Masamitsu NAGANUMA*, Tadashi MUNAKATA*
Nobuo TACHIKAWA, Mikihiko GOTO
Katsuyuki EBISAWA*, Tsutomu HONDA* and Kusuo ASHIBE*

日本原子力研究所
Japan Atomic Energy Research Institute

JAERI-M レポートは，日本原子力研究所が不定期に公刊している研究報告書です。
入手の問合わせは，日本原子力研究所技術情報部情報資料課（〒319—11 茨城県那珂郡東海村）あて，お申しこしください。なお，このほかに財団法人原子力弘済会資料センター（〒319-11 茨城県那珂郡東海村日本原子力研究所内）で複写による実費頒布をおこなっております。

JAERI-M reports are issued irregularly.
Inquiries about availability of the reports should be addressed to Information Section, Division of Technical Information, Japan Atomic Energy Research Institute, Tokai-mura, Naka-gun, Ibaraki-ken 319-11, Japan.

© Japan Atomic Energy Research Institute, 1982

編集兼発行　日本原子力研究所
印　　刷　山田軽印刷所

JAERI-M 82-178

Japanese Contribution to IAEA INTOR Workshop, Phase II A

Chapter XI : Mechanical Configuration

Satoshi NISHIO , Noboru FUJISAWA , Yuzo FUKAI*, Yoshio SAWADA*
Mitsugi YAMAGUCHI*, Takao UCHIDA*, Nobuharu MIKI*, Takataro HAMAJIMA*
Masamitsu NAGANUMA*, Tadashi MUNAKATA*, Nobuo TACHIKAWA*
Mikihiko GOTO*, Katsuyuki EBISAWA*, Tsutomu HONDA* and
Kusuo ASHIBE*

Fusion Research and Development Center
Tokai Research Establishment, JAERI

(Received November 1, 1982)

This report corresponds to Chapter XI of Japanese contribution report to IAEA INTOR Workshop, Phase II A. This report describes a new concept with a significant reduction in the device size and cost while maintaing the plasma size and performance from Phase I. This concept can be realized mainly by mitigating the allowable field ripple from 0.75% to 1.2%.

Keywords : INTOR, Shield, Pump Limiter, Blanket, Toroidal Field Coil, Poloidal Field Coil, Remote Maintenance.

---

* Toshiba Electric Co., Ltd.

JAERI－M 82－178

INTORフェーズⅡAワークショップ検討報告書
第Ⅺ章：炉構造概念

日本原子力研究所東海研究所核融合研究開発推進センター

西尾　敏・藤沢　登・深井　佑造*
沢田　芳夫*・山口　貢*・内田　高穂*
三木　信晴*・浜島高太郎*・長沼　正光*
崇像　正*・立川　信夫*・五島　幹彦*
海老沢克之*・本田　力*・芦部　楠夫*

（1982年11月1日受理）

国際トカマク炉（INTOR）フェーズⅡAにおける主要課題は分解修理性を確保しつつ可能な限りコンパクトで低コストの炉概念を確立することである。本報告書ではシールド，ブランケット，リミタ等のトーラス構造物をトロイダル磁場コイル間から直線引抜方式で交換する方式を採用し，かつ小型化された炉概念を示す。炉構造物引抜空間，真空境界，炉構造物の分割法，コイルの支持法等が詳細に考察され，今後の検討課題を明確にした。

＊　東京芝浦電気㈱

CONTENTS

1. Introduction 1

1.1 Objectives 1

1.2 Design requirements 1

1.3 Brief summary of results 2

2. TF System 4

2.1 Evaluation of coil size 4

2.1.1 Ripple requirement 4

2.1.2 Winding configuration 4

2.1.3 Structural design implication 7

2.2 Design description 11

2.3 Coil maintenance and replacement approach ... 21

2.4 Supporting analysis 31

3. PF System (related to mechanical configuration) .. 46

3.1 Configuration drivers 46

3.1.1 Maintenance and access philosophy 46

3.1.2 Pumped limiter configuration 52

3.1.3 Poloidal divertor configuration 68

3.1.4 Design optimization (universal PF concept).. 69

3.2 Design description 74

3.3 Supporting analysis 80

4. Vacuum boundary 88

4.1 Design options 88

4.2 Evaluation and selection 93

4.3 Design description 105

4.4 Supporting analysis 112

5. Torus System 116

5.1 Segmentation options 116

5.2 Evaluation and selection 116

5.3 Design description 124

5.4 Supporting analysis 139

6. Impurity control 142

6.1 Pumped limiter configuration 142

6.2 Poloidal divertor configuration 151

6.3 Universal concept 154

6.4 Maintenance and segmentation 160

7. Heating systems 175

7.1 NBI configurations 175

7.2 RF configurations 175

8. Conclusions and Recommendations 186

Acknowledgment 187

目　　次

1. 序　論 …… 1
1.1 目　的 …… 1
1.2 設計条件 …… 1
1.3 概　要 …… 2
2. トロイダル磁場コイルシステム …… 4
2.1 コイル寸法の評価 …… 4
2.2 設　計 …… 11
2.3 分解及び修理 …… 21
2.4 支持構造 …… 31
3. ポロイダル磁場コイルシステム …… 46
3.1 コイル配置 …… 46
3.2 設　計 …… 74
3.3 支持構造 …… 80
4. 真空境界 …… 88
4.1 幾つかの方式例 …… 88
4.2 検討評価 …… 93
4.3 設　計 …… 105
4.4 支持構造 …… 112
5. トーラス分割方式 …… 116
5.1 幾つかの例 …… 116
5.2 検討評価 …… 116
5.3 設　計 …… 124
5.4 支持構造 …… 139
6. 不純物制御機構 …… 142
6.1 ポンプリミタ方式 …… 142
6.2 ポロイダルダイバータ方式 …… 151
6.3 ポンプリミタ・ポロイダルダイバータ共通方式 …… 154
6.4 分割修理 …… 160
7. プラズマ加熱方式 …… 175
7.1 NBI方式 …… 175
7.2 RF方式 …… 175
8. 結　論 …… 186
謝　辞 …… 187

1. Introduction

1.1 Objectives

As one of the main characteristics of INTOR Phase I, the 12 TF coils were sized with sufficient bore dimensions so that a complete torus sector, consisting of 1/12 of the total, can be withdrawn by a simple straight motion between TF coils. Consequently the remote maintenance system was greatly simplified. However, a large-size reactor structure configuration is required to perform this approach, and may lead to high cost of reactor.

In order to establish the INTOR system concept with high reliability and reasonable cost, further more detailed approach is required from both standpoints of reactor structure configuration and remote maintenance technology. The objective of the engineering studies on INTOR J-IIa is to evaluate different mechanical configuration concepts and the corresponding maintenance and assembly/disassembly approaches that might be used to reduce the size and cost.

1.2 Design requirements

The principal engineering parameters such as major plasma parameters of INTOR J-IIa are the same as those used in Phase 1. Primary design considerations carried out on INTOR J-IIa include; (1) minimization of the TF

coil and reactor size, (2) adoption of pumped limiter for impurity control, (3) adoption of RF heating instead of NBI heating.

The different specifications are follows.

(1) The bore of the toroidal field coil is reduced from 7.7 m wide × 10.7 m high for Phase I reference design to 6.6 m wide × 9.3 m high. Number of toroidal field coil amounts to 12.

(2) Ripple condition at R = 6.5 m is ±1.2%.

(3) Plasma start up is carried out with 35 V, 0.3 sec.

(4) The pumped limiter is used in order to control the impurities.

1.3 Brief summary of results

The four options of repair and maintenance method are considered taking into account the reduction of the TF coil bore.

Replacement of the blanket/first wall and the pumped limiter is performed by single straight motion. The torus structures of both limiter and blanket are divided into 24 sectors (2 sectors/TF coil).
Each of two sectors between two TF coils is retracted in radial direction with different angle.

Concerning the vacuum boundary, 4 options are considered and the separate vacuum boundary for the torus and superconducting magnet vacuum system is selected.

The vacuum boundary of the plasma chamber is located on the inner side of the shielding structure. This vacuum boundary is connected with the blanket access door through which the blanket and the limiter sectors are retracted. A common vacuum cryostat contains all of the superconducting coils.

Five cases of limiter or divertor operation as impurity control are considered. Our reference system is limiter case of the PF coil maximum radius 11 m. The adoption of the limiter permits the reduction of the PF coil ampere turn 98 MAT (Phase I) to 83 MAT, accordingly, the capacity of power supply is reduced from 15 GW (Phase I) to 4 GW.
The out-of-plane force (MZ) resulting on TF coil (±239 MN-m/coil) is also considerably reduced by 35%.

The size of the reactor is reduced and the cost becomes lower than phase one's.
As PF coil distribution, the Universal-INTOR type is taken into consideration.

The Universal type has the divertor type PF coil distribution permitting the limiter operaiton.
The conceptual study on the Universal-INTOR type reactor concept is carried out under the following specifications.

i) combined type vacuum boundary

ii) torus closure without access port

iii) torus segmentation by 1 ∿ 2 sectors/TF coil

2. TF System

2.1 Evaluation of coil size

2.1.1 Ripple requirement

The number and bore of TF coil is determined, taking into account accessebility and maintainability for the remote handling of blanket, pump limiter, etc. and also considering the achievement of an acceptable field (ripple ±1.2% at R = 6.5 m) at plasma region.

In the limit of the TF coil bore width 6.6 m, the blanket sector segmented as 2 sectors/TF coil can be retracted with straight single motion.

The attained field ripple is ±0.92% at R = 6.5 m.

2.1.2 Winding configuration

The key design issue of TF magnet is the establishment of cryogenic stability and mechanical rigidity.

Besides those, there are many conflicting constraints; AC loss, coil protection against normal zone propagation, electrical insulation, joint requirement, fabricability, economics and such.

There are many discussion with regard to the choice of cooling concept of large bore TF magnet; pool boiling, forced cooling, etc. However, none of them satisfies all above requirements. Each cooling method has individual features and one cooling method is, in many case, devoid of advantages the other one displays.
The adopted cooling method in this phase is the concept of pool boiling in preference to other cooling concepts. The reason for this choice is that pool boiling is simple and more reliable, and is considered a more mature technology as shown in the achievement of a number of large magnets, and further the mechanism of cryostability is more understood.

On the other hand, forced-cooling method are short of achievement with large magnets. But, forced cooled magnets have some interesting advantages and potentialities especially concerning the heat transfer characteristics, mechanical integrity of the magnet, high voltage endurance, etc., overcoming the difficulties of supplying the supercritical helium or cooling down the large magnet. It is worth noting that cable-in-conduit conductors may exhibit an outstanding cryogenic

stability as typically shown by zero flow stability. NbTi based conductors may have useful performances for constructing large TF magnets to be operated at 12^T and reduced temperatures and if so, this type conductor might be put to use in place of brittle Nb_3Sn conductors.

Anyway, many uncertainties to be solved still remain on other cooling concepts notwithstanding the active research and development, but it is not true that pool boiling concept is decisively advantageous way. It could be envisioned that other cooling concepts will be introduced to large TF magnets as their technologies are advanced. It does not seem at the present stage that the determination of the cooling concept is the most critical issue for the definition of TF magnet for INTOR.

Pancake winding of pool boiling conductors are favored primarily due to the fact that ventilation of vapor bubbles is better and the transmission of expanding forces through the winding to the coil case is reliable. It is another merit that the pancake winding approach simplifies the coil winding process significantly.

2.1.3 Structural design implication

Fig. XI-2-1 shows the TF coil structure and Fig. XI-2-2 shows the cross section of the coil/helium vessel.

The main features of TF coil are shown below.

(a) The helium vessel material is 316 stainless steel.

(b) The helium vessel structure consists of inner ring wall, outer ring wall and two side plates. These parts are assembled by welding.

(c) In the centerpost region, the outer wall is thickened in order to be supported against the centering force by means of the wedging action of helium vessels.

(d) The electromagnetic hoop force is supported by the TF coil conductor and the helium vessels.

(e) In the outer region, the outer supporting frame is welded to the outer wall in order to support the out-of-plane force.

(f) In order to permit the removal of torus sectors, there is an open window region between adjacent TF coils.
A bending moment is produced on the outboard portion of the TF coil because of the out-of-plane force.
As shown in Fig. XI-2-1, the support structure is attached on the outer ring wall of the outboard portion of the TF coils.
This support structure has a forme of trapezoid.

(g) At the lower portion of the TF coils, the pedestal supports for the dead weight of the shield structure and the vacuum duct penetrate the space between adjacent TF coils. Therefore, the support structure of inter TF coil is partially installed in order to permit the penetration of the vacuum duct and shield support pedestal as shown in Fig. XI-2-1.

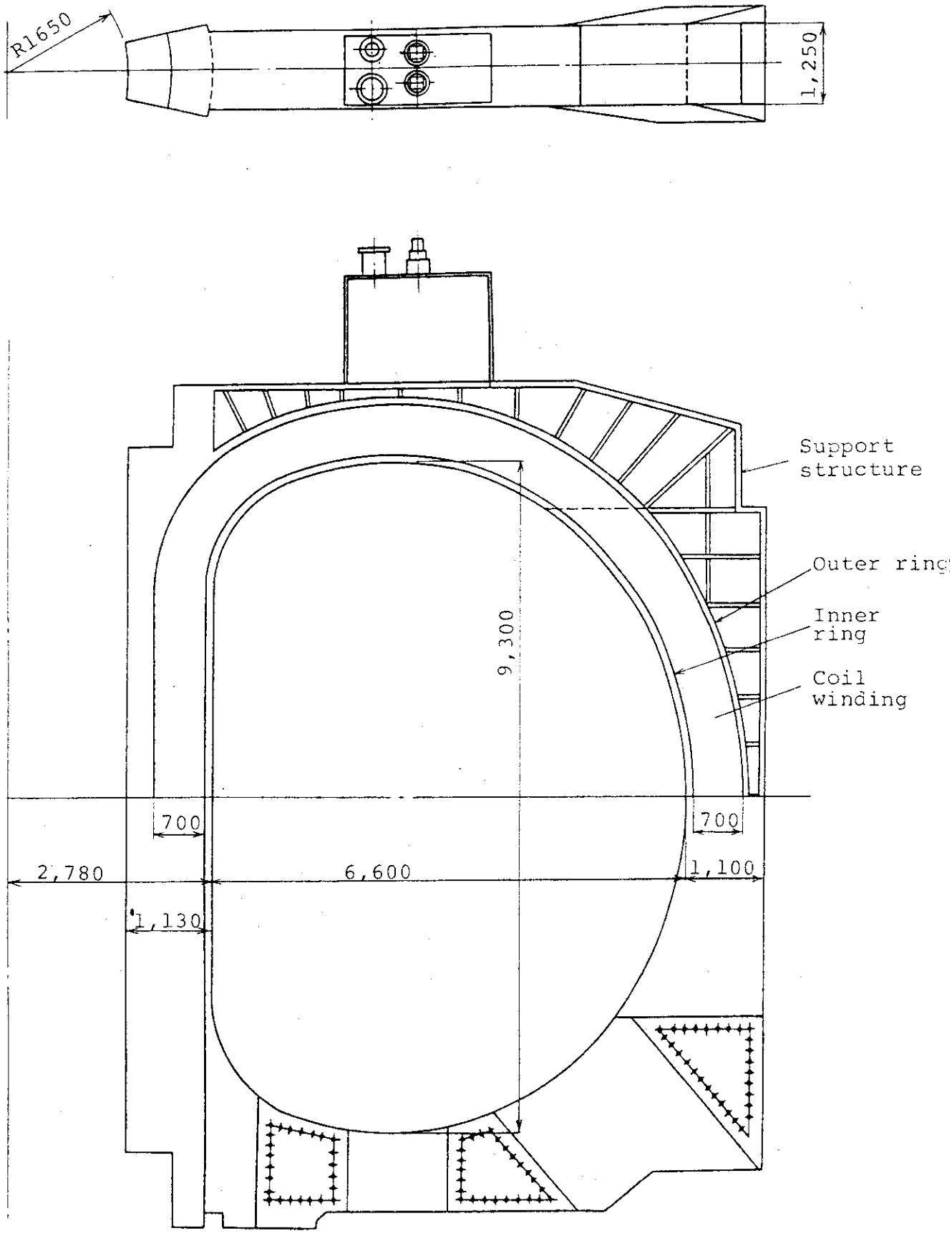

Fig. XI-2-1 TF coil structure

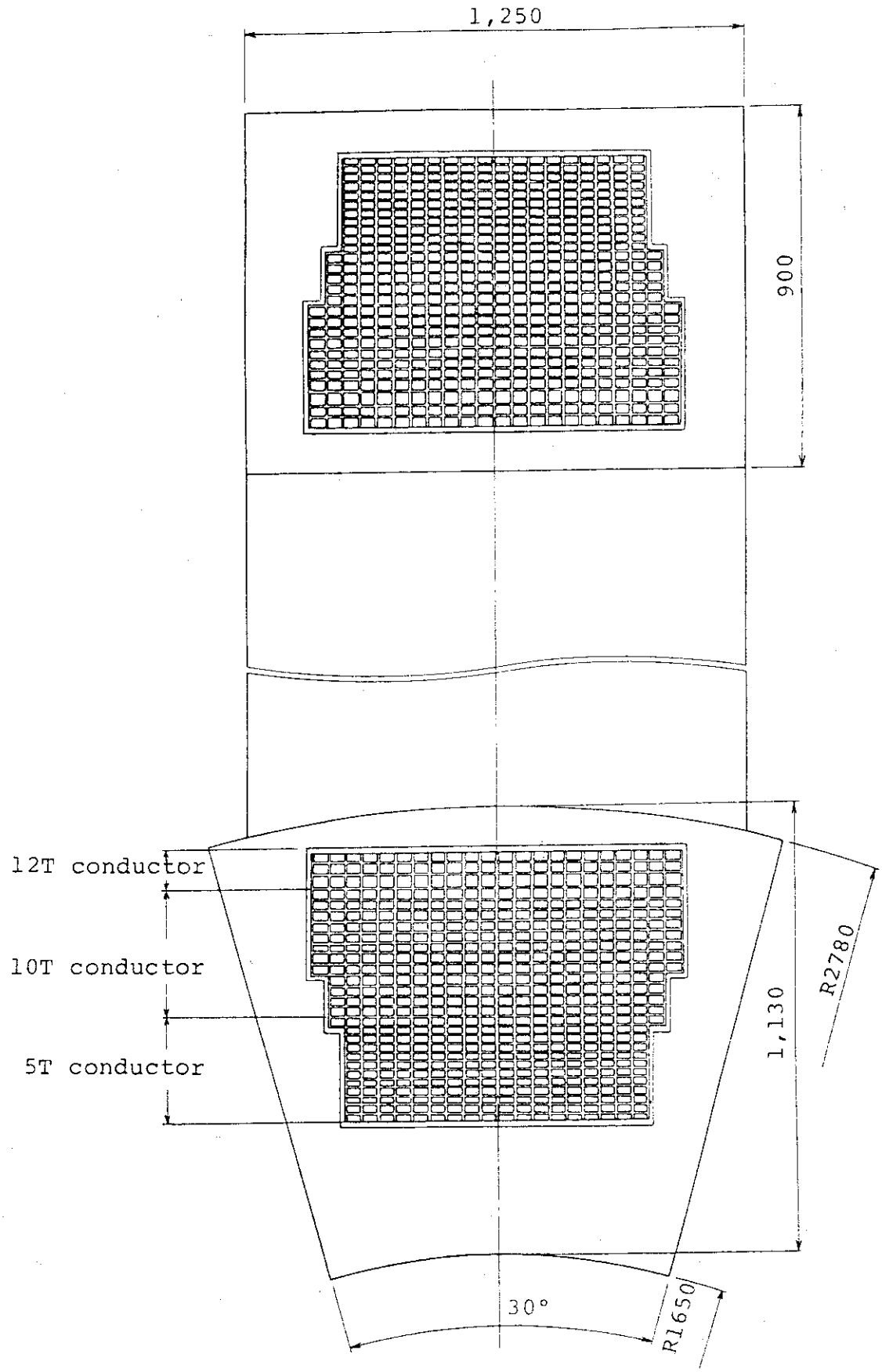

Fig. XI-2-2 Coil/helium vessel cross sections

2.2 Design description

The number and bore of TF coil are determined, taking into account accessibility and maintainability for the remote handling of blanket, pump limiter, etc. and also considering the achievement of an acceptable field at plasma region.

The TF coil main parameter is shown in Table XI-2-1 ∿ Table XI-2-3.

The main characteristics of TF coil is summarized below.

(a) The major requirement for the INTOR TF magnet is to provide total ampere-turns of 143 MAT required to generate the 5.5^{T} field at plasma major radius of 5.2m.

(b) The TF coil bore is 6.6 × 9.3m. The number of TF coils is 12 which satisfy the field ripple limit of 1.2% at the plasma edge.
The attained field ripple is ±0.92% at R=6.5m.
The TF coil structure size is shown in Fig. XI-2-3.

(c) The overall current density in the winding of TF magnet is 19.4A/mm^2 and the maximum field is 11.4^{T} at the magnet bore. The pool boiling method is adopted and fulfils the cryogenic stabilization. The magnet is graded at three fields: the nominal field of 12^{T}, 10^{T} and 5^{T} as

shown in Fig. XI-2-4.

The conductors of 12^T and 10^T are consist of the conductor of copper stabilized Nb_3Sn.

The conductor of 5^T is consist of copper stabilized NbTi conductor.

(d) For cooling of magnet, the pool boiling concept is used.

(e) One coil has 22 pancakes, each separated with 3mm thick cooling spacers for the establishment of cooling channels and pancake-to-pancake electrical insulations. One pancake is wound flatwise with 27 turns at most and between which insulated 5mm thick inter-turn reinforcements are inserted with the objective of holding each turn tightly and preparing cooled space on the flat surface of conductors.

(f) Fig. XI-2-5 indicates toroidal field distribution at a centerline of a toroidal coil and between toroidal coils on a mid-plane.

In-plane force distribution for TF coils is shown in Fig. XI-2-6. The total expanding force per coil is 1144^{MN} and centering force and vertical force F_Z are 379^{MN} and $\pm 253^{MN}$ respectively.

Besides those electromagnetic forces which are caused by TF magnet itself, TF coil must be sustained against torque which is caused by the

interaction between toroidal field current and poloidal coil field. Fig. XI-2-7 gives the out-of-plane force distribution for case 1. The torque around the horizontal axis is 213^{MN-m}, while the one around the vertical axis is $\pm 239^{MN-m}$.

(g) The copper stabilizer houses cabled and compacted Nb_3Sn strands. Both mechanical and chemical treatment on four surfaces of the copper stabilizer are made in order not only to enhance the heat transfer but to increase the cooling surface area.

(h) The recovery process at the operating current can be simulated, if the disturbance energy is determined. It is assumed that the disturbances are caused by AC loss, the nuclear heating and the frictional heating.

It is concluded that the each of three conductors can be operated stably against expected disturbances.

(i) The AC loss is caused by the changing poloidal field mainly at the superconductor, the helium vessel and the coil support in the TF coils.

For the case 1, the average AC loss is 56kW (See Table XI-2-4).

Table XI-2-1 Major characteristics of the TF magnet system

1.	Total ampere-turns	143 MAT
2.	No. of coils	12
3.	Ampere-turns per coil	11.9 MAT
4.	Plasma major radius	5.3 m
5.	Field at plasma axis	5.5 T
6.	Helium condition	Pool boiling
7.	Grading concept	3 grades (12, 10, 5^T)
8.	Winding configuration	Flat wound in pancakes
9.	Superconductor	Copper stabilized Nb_3Sn and NbTi
10.	No. of turns per coil	540
11.	No. of pies per coil	22
12.	Operation current	22.07 kA
13.	Critical current	33 kA
14.	Avg. winding current density	19.4 A/mm^2
15.	Maximum field	11.4 T
16.	Cooling spacer thickness	3.0 mm
17.	Cooling surface	Rough surface (mechanical and chemical treatment)
18.	Inductance	∿120 H
19.	Magnetic field energy	∿30 GJ

Table XI-2-2 Characteristics of one TF magnet

1. Ampere turns	11.9 MAT (12^T portion 1.456 MAT; 10^T 5.649; 5^T 4.811)
2. Operation current	22.07 kA
3. Maximum field	(12^T portion 11.4 T; 10^T 10.2 T; 5^T 4.9 T)
4. No. of turns	540 (12^T portion 66; 10^T 256; 5^T 218)
5. No. of pies	22
6. No. of layers	27 12^T portion 3; 10^T 12; 5^T 12
7. Magnet bore	6.6m × 9.3m
8. Magnet cross section	maximum 700mm thick × 949mm wide
9. Turn insulation	5mm thick including steel
10. Cooling spacer	3mm thick
11. Electromagnetic force	
Expanding force	1144 MN
Centering force	379 MN
Vertical force	±253 MN
Torque	213 MN.m against X axis ±239 MN.m against Z axis

Table XI-2-3 Characteristics of the superconductor

		12^T conductor	10^T conductor	5^T conductor
1.	Superconducting wire	Copper stabilized Nb_3Sn	Copper stabilizee Nb_3Sn	Copper stabilized NbTi
2.	Maximum field	11.4^T	10.2^T	4.9^T
3.	Conductor current	22.07 kA	22.07 kA	22.07 kA
4.	Ic at 4.2 k	33 kA	33 kA	33 kA
5.	Conductor size	30×39 mm^2	21×39 mm^2	16×39 mm^2
6.	Element size	35×42 mm^2	26×42 mm^2	21×42 mm^2
7.	Cable size	8×18.4 mm^2	8×10.2 mm^2	3.6×9.3 mm^2
8.	Conductor current density	18.8 A/mm^2	26.9 A/mm^2	35.4 A/mm^2
9.	Element current density	15.0 A/mm^2	20.2 A/mm^2	25.0 A/mm^2
10.	Conductor copper ratio	15.5	18.2	42.5
11.	Interturn reinforcement	5 mm	5 mm	5 mm
12.	$\rho 0$	6.2×10^{-6} Ωcm	5.6×10^{-8} Ωcm	3.4×10^{-8} Ωcm
13.	$\Delta\rho$ (1.1×10^{18} n/cm^2)	9×10^{-8} Ωcm	5.3×10^{-8} Ωcm	0.6×10^{-8} Ωcm
14.	ρt	15.2×10^{-8} Ωcm	10.9×10^{-8} Ωcm	3.9×10^{-8} Ωcm
15.	Heat flux	0.39 w/cm^2	0.47 w/cm^2	0.24 w/cm^2
16.	No. of strands	9	5	11
17.	Cooling surface	Rough surface (mechanical and chemical treatment)		
18.	Minimum winding radius	2.21 m	2.32 m	2.63 m
19.	Maximum winding strain	0.18%	0.17%	0.06%

Table XI-2-4 AC losses in TF coils

	Case 1 (Pump limiter R=11m)	Case 2 (Pump limiter R=13m)	Case 4a (Divertor)
Superconductors	15.4 kW	14.5 kW	42.8 kW
Helium vessels	14.4 kW	14.1 kW	35.8 kW
Coil supports	26.2 kW	20.0 kW	70.5 kW
Sum	56.0 kW	48.6 kW	149.1 kW

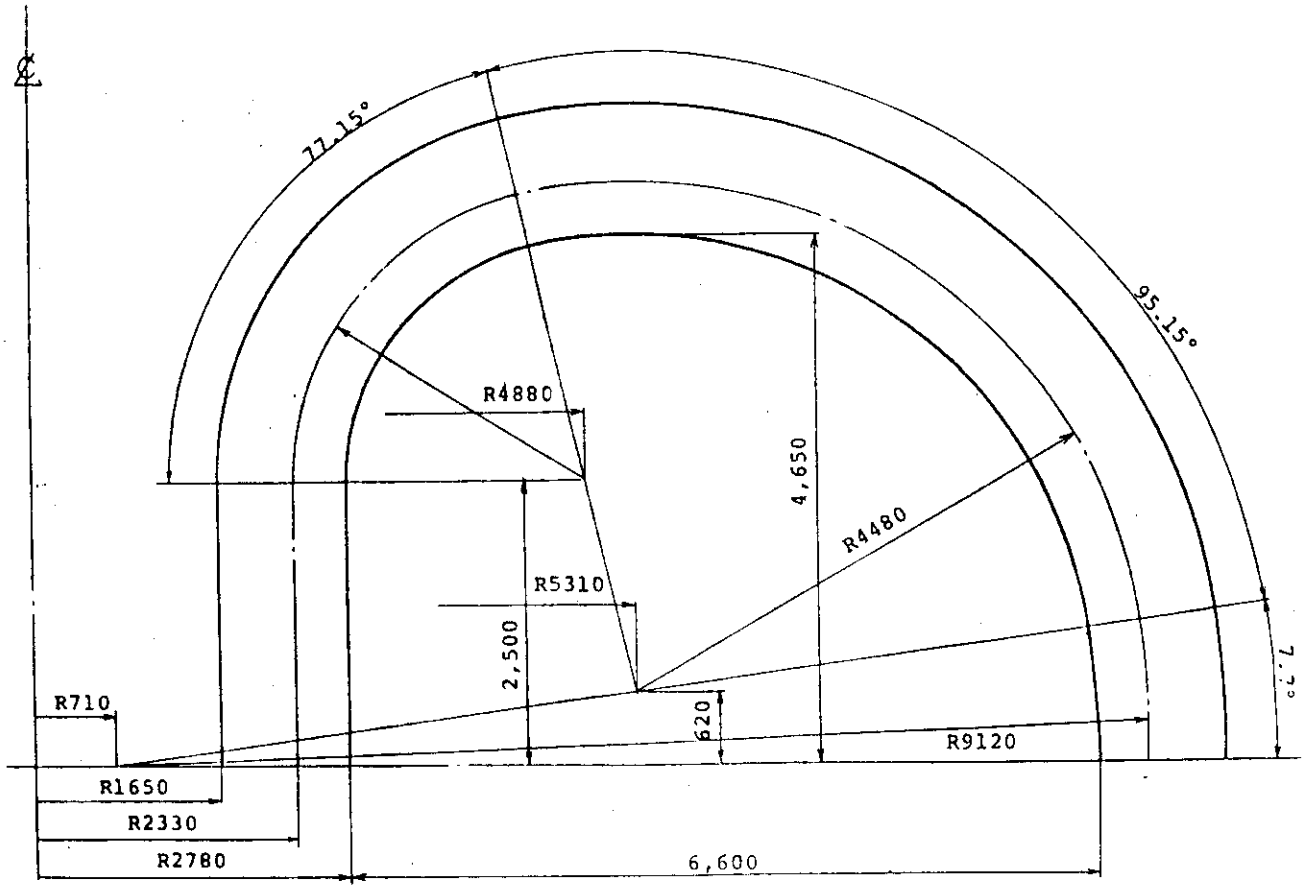

Fig. XI-2-3 TF coil dimension

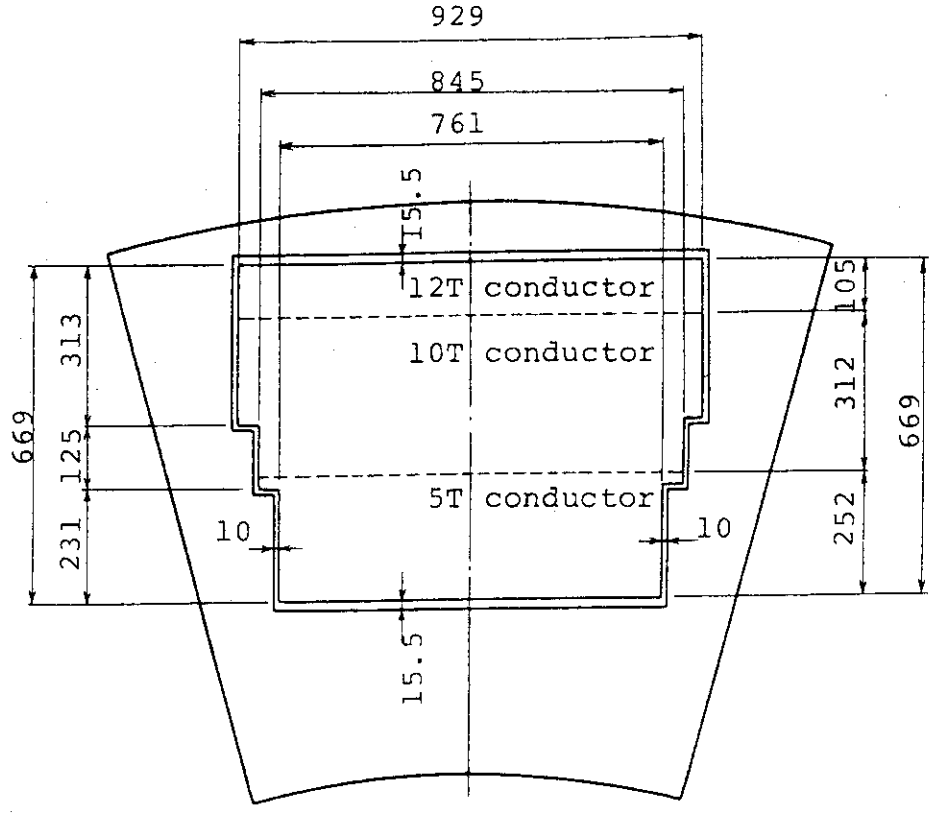

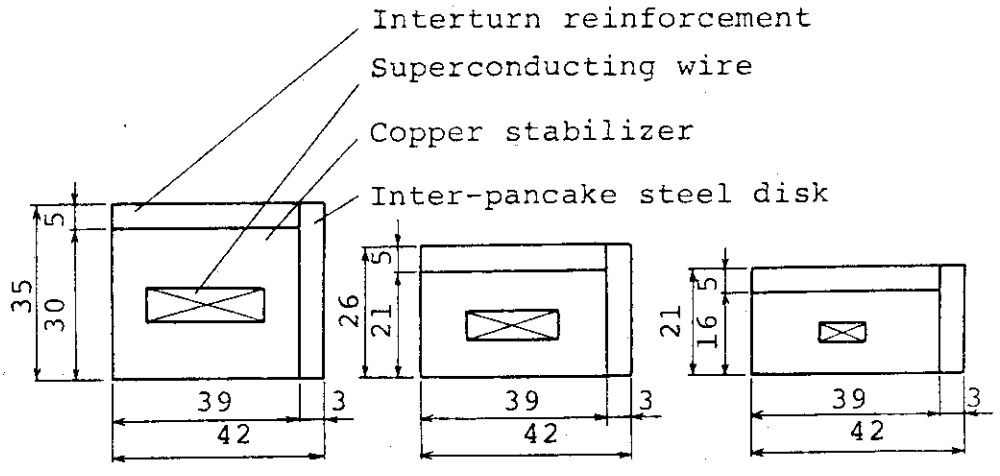

(1) 12T conductof (2) 10T conductor (3) 5T conductor

Fig. Ⅱ-2-4 TF coil winding concept and its conductors

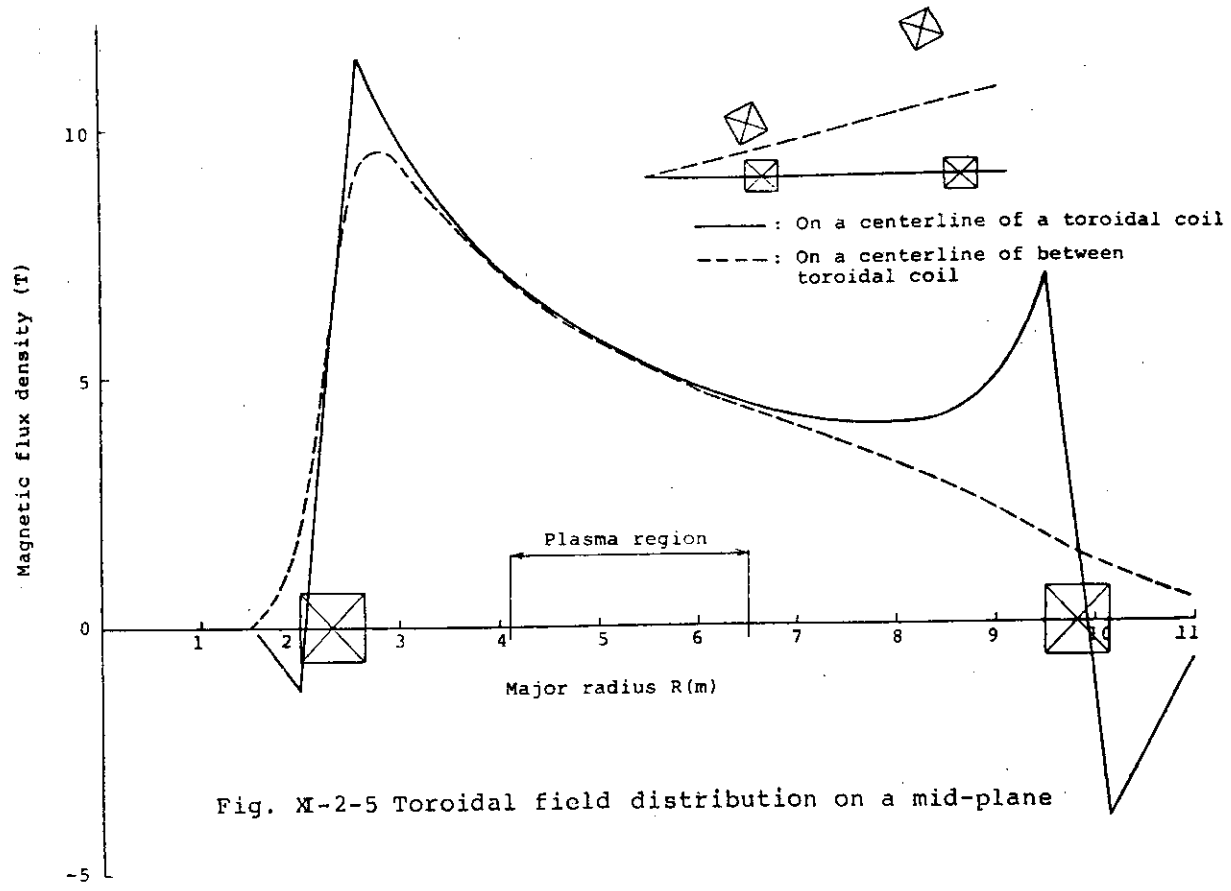

Fig. XI-2-5 Toroidal field distribution on a mid-plane

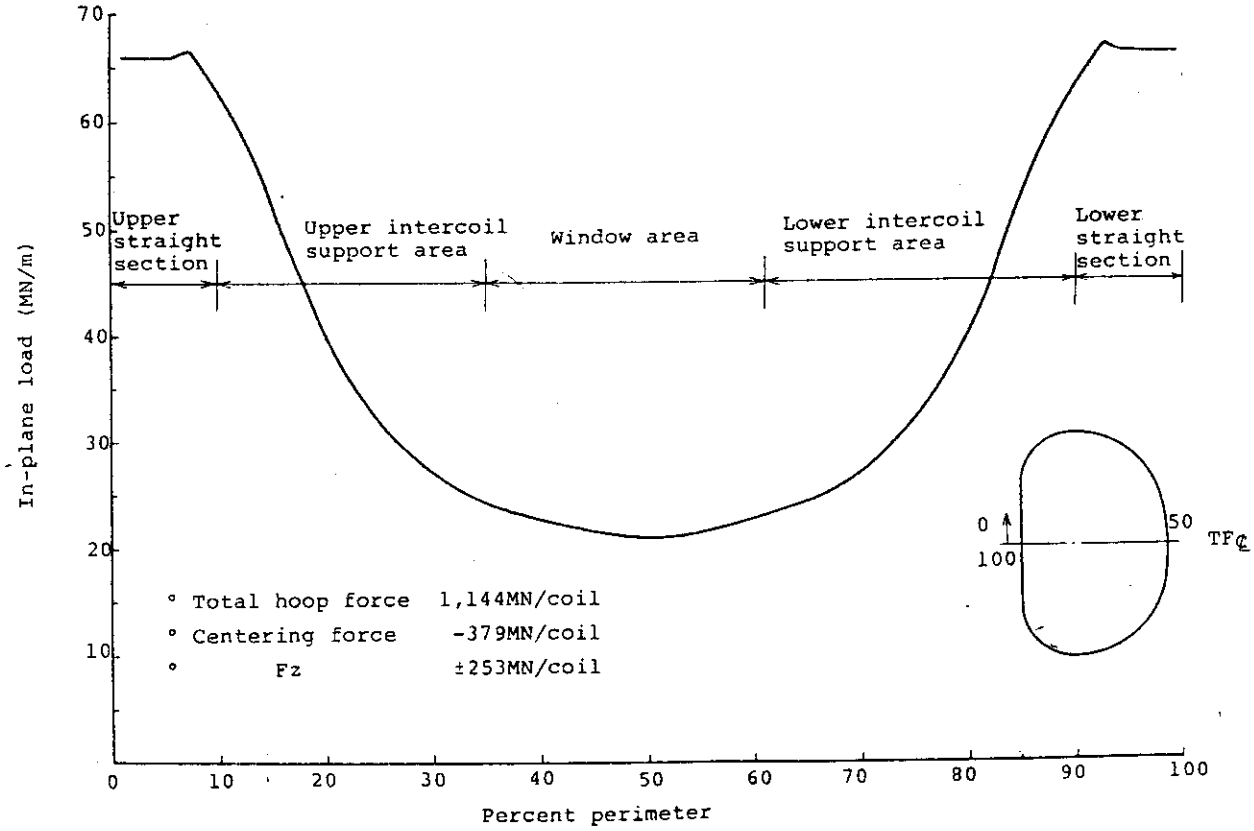

Fig. XI-2-6 In-plane force distribution for TF coils
(Component of force normal to coil centerline)

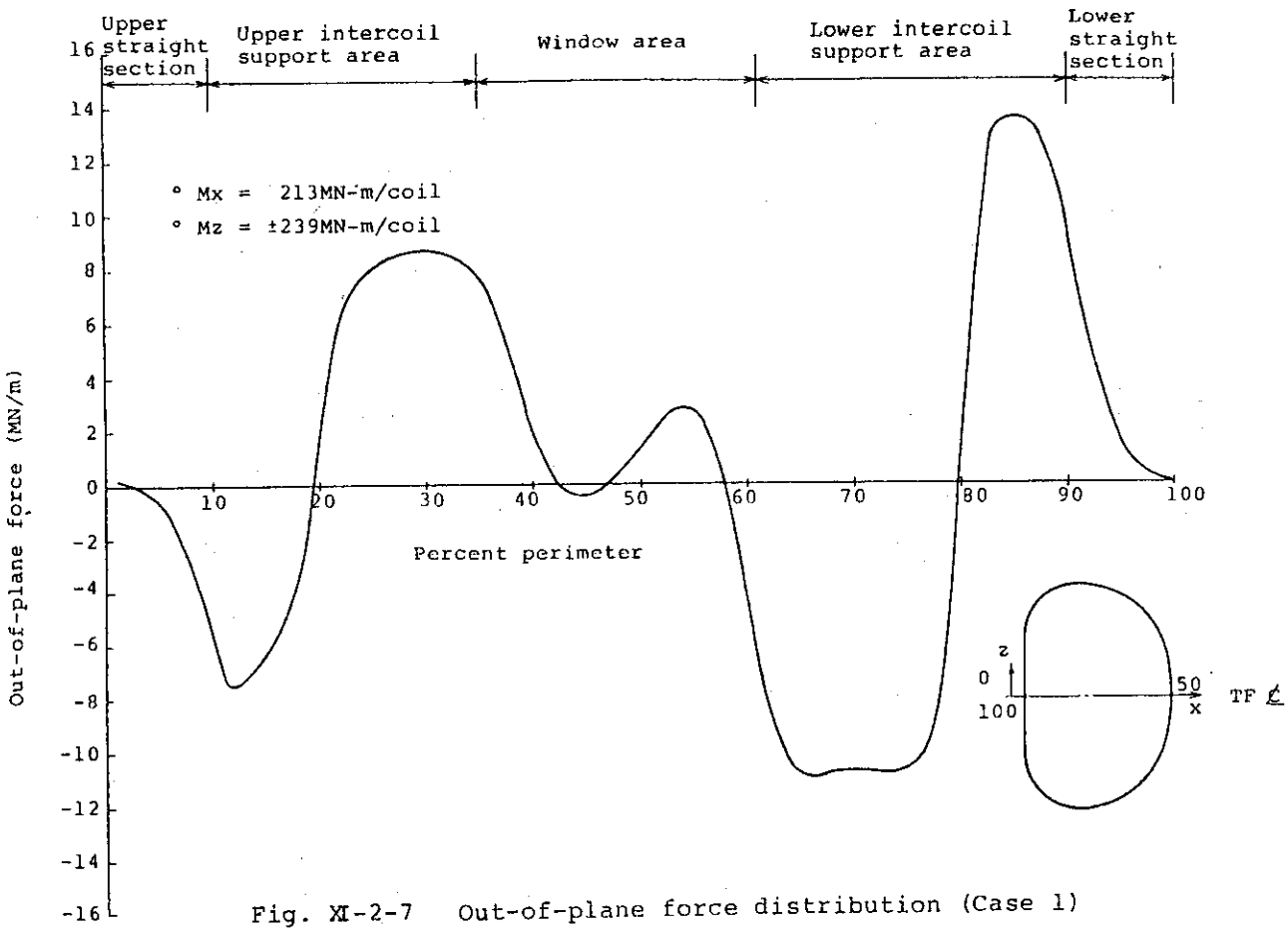

Fig. XI-2-7 Out-of-plane force distribution (Case 1)

2.3 Coil maintenance and replacement approach

1. Assembly/disassembly

The maintenance procedure of one troubled TF coil is slightly different from the replacement procedure of whole TF coils in torus.

The disassembly/assembly procedures are considered for the bay where ICRF coaxial cable duct is not installed.

(i) Disassembly of TF coil.

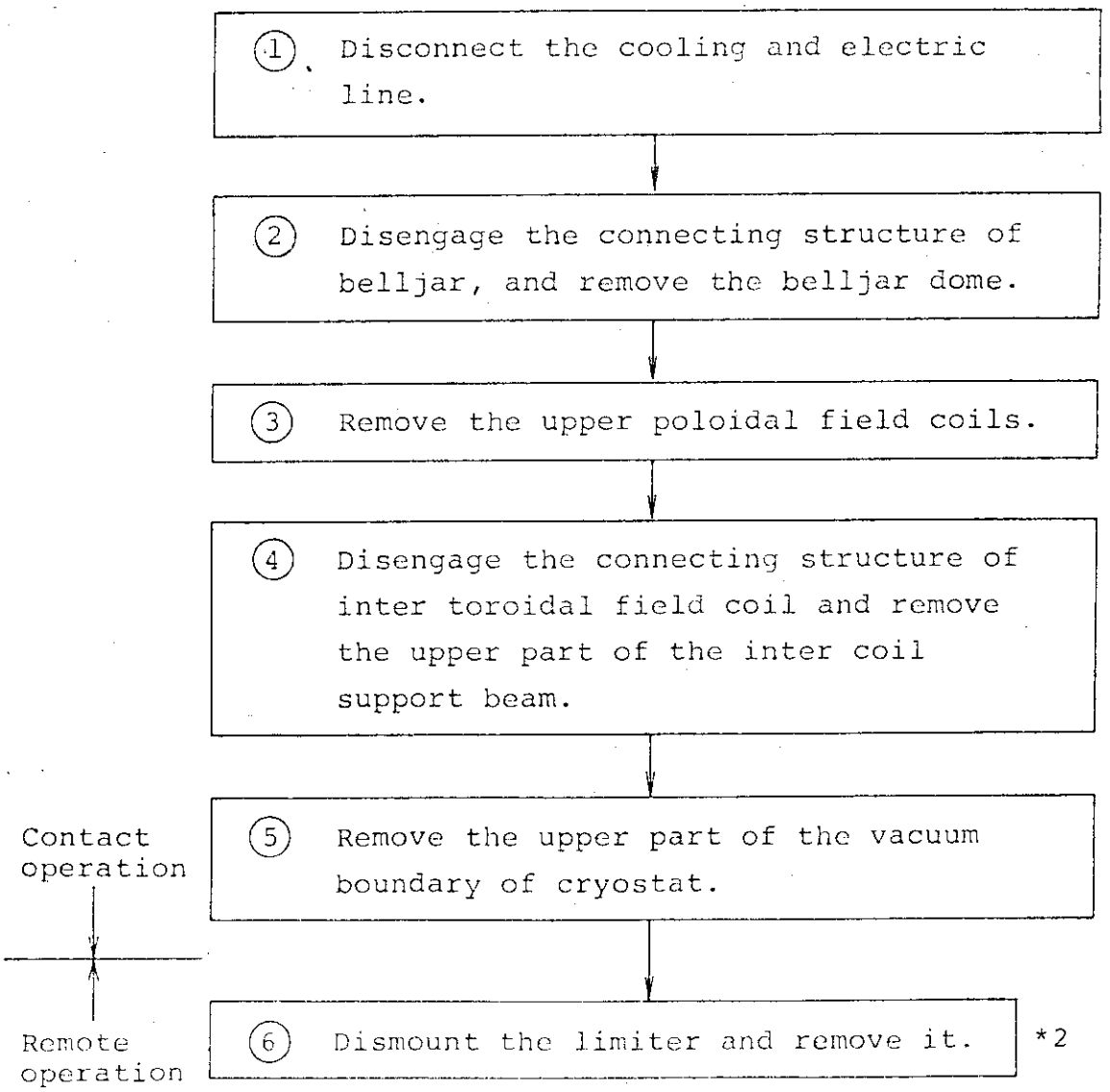

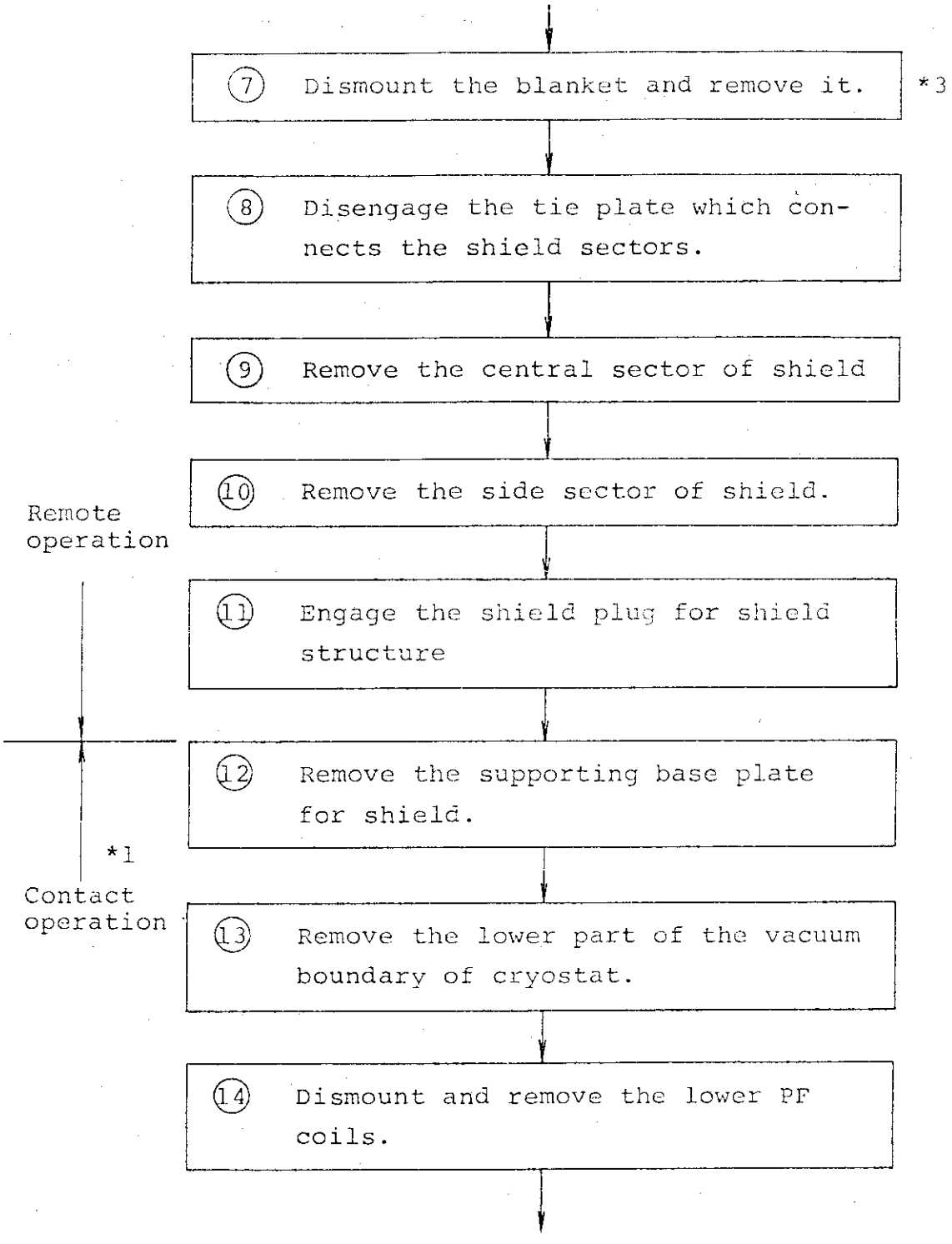
⑦ Dismount the blanket and remove it.
*3
⑧ Disengage the tie plate which connects the shield sectors.
⑨ Remove the central sector of shield
⑩ Remove the side sector of shield.
Remote operation
⑪ Engage the shield plug for shield structure
⑫ Remove the supporting base plate for shield.
*1
Contact operation
⑬ Remove the lower part of the vacuum boundary of cryostat.
⑭ Dismount and remove the lower PF coils.

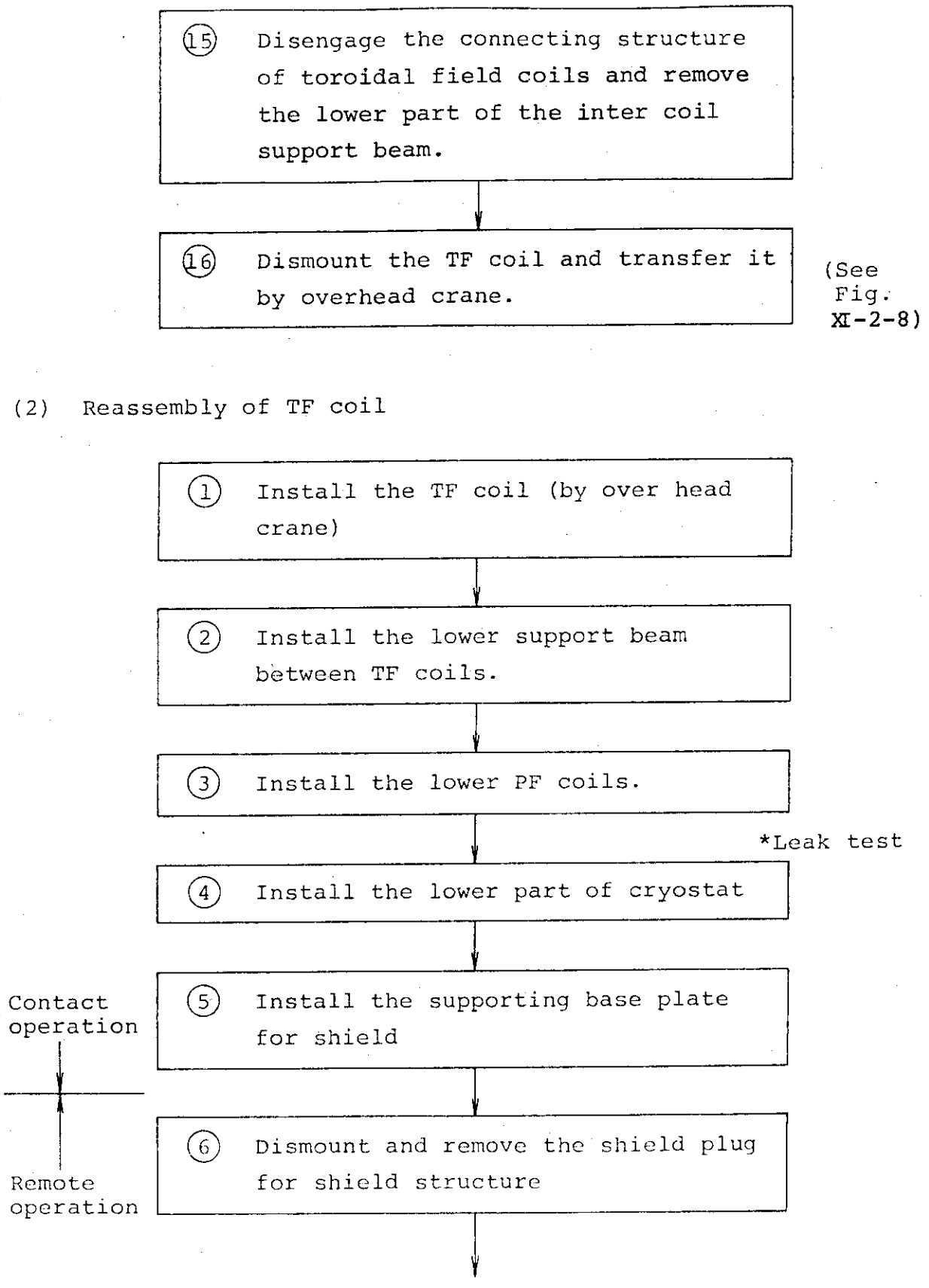
⑮ Disengage the connecting structure of toroidal field coils and remove the lower part of the inter coil support beam.
⑯ Dismount the TF coil and transfer it by overhead crane.
(See Fig. XI-2-8)
(2) Reassembly of TF coil
① Install the TF coil (by over head crane)
② Install the lower support beam between TF coils.
③ Install the lower PF coils.
*Leak test
④ Install the lower part of cryostat
Contact operation
⑤ Install the supporting base plate for shield
⑥ Dismount and remove the shield plug for shield structure
Remote operation

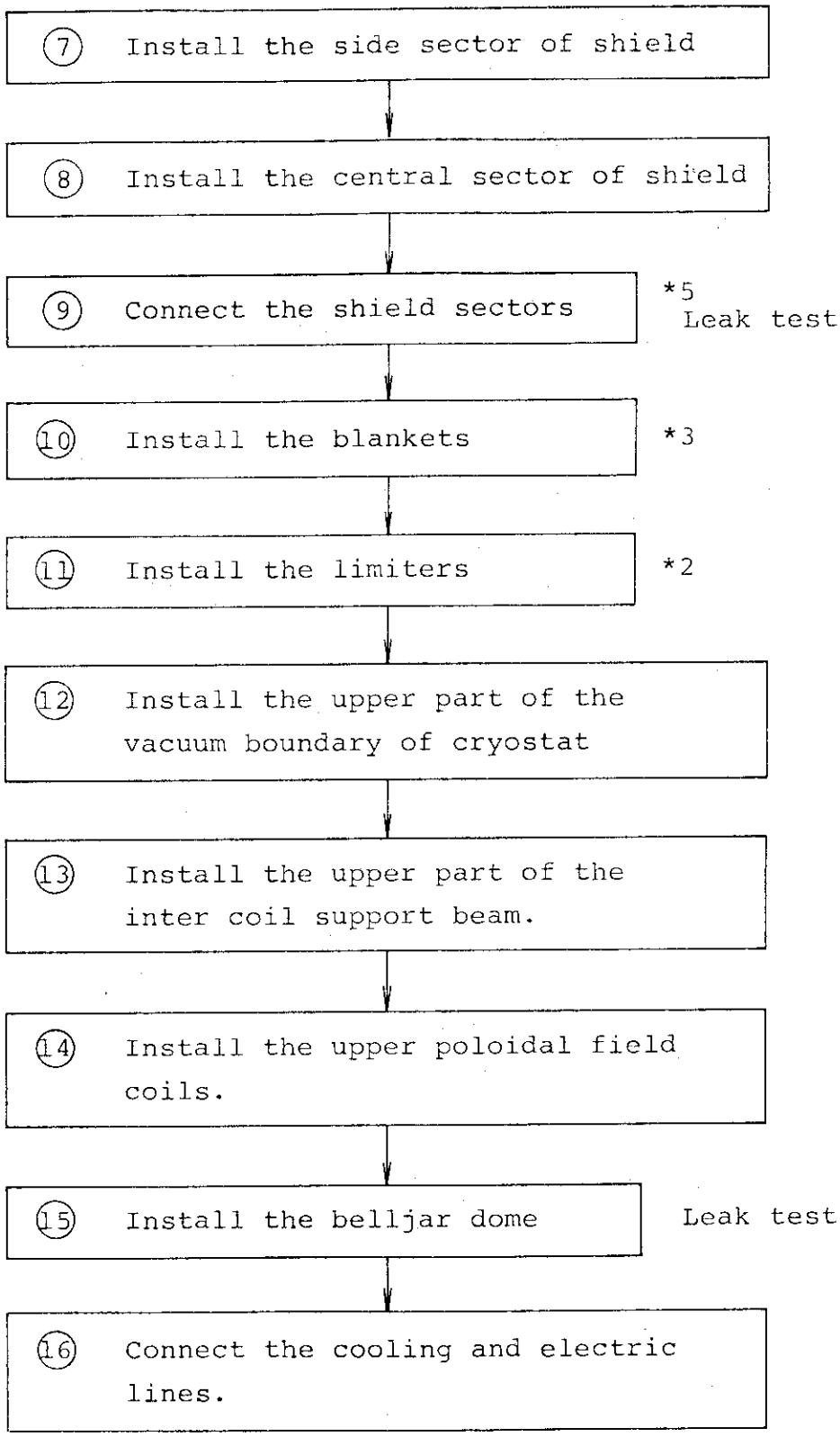
⑦ Install the side sector of shield
⑧ Install the central sector of shield
⑨ Connect the shield sectors
*5
Leak test
⑩ Install the blankets
*3
⑪ Install the limiters
*2
⑫ Install the upper part of the vacuum boundary of cryostat
⑬ Install the upper part of the inter coil support beam.
⑭ Install the upper poloidal field coils.
⑮ Install the belljar dome
Leak test
⑯ Connect the cooling and electric lines.
Leaktest(cooling pipes)

*1 : Operations ⑫ ∿ ⑯ are supposed to be performed by contact operation with a shielding measure against the induced activity.

*2 : Refer XI-6-1 for the assembly/disassembly of limiters

*3 : Refer XI-5-3 for the assembly/disassembly of blankets.

*4 : Leak test will be performed after setting provisionally the upper cryostat and the belljar dome.

*5 : Leak test will be performed with the blanket access door using the viton O-ring.

2. Estimation of the time required for assembly/disassembly of TF coil

In maintenance of TF coil, almost operations require remote handling. As the examination on remote maintenance is not sufficiently accomplished in this stage, it might be so early to estimate the time of assembly/disassembly of TF coil. However, a very rough estimation may be possible with the assumptions mentioned below.

(i) Only one damaged TF coil is replaced by a spare TF coil after disassembling.

(ii) The following parts should be at least dismounted in order to replace one TF coil.

- o Cooling pipes for 2 baies.
- o Pumped limiters for 2 baies.
- o Dome of belljar
- o PF coils, #9 ∿ #12, #22 ∿ #24.
- o Support beams between TF coils; both lower and upper beams for 2 baies
- o Cryostat for 2 baies
- o Disconnection of vacuum ducts for 2 baies
- o Shields and base plates (including support legs) for 2 baies.

(iii) Disassembly is considered only for the bay where ICRF coaxial cable duct is lacking.

(iv) Installation of the shield plug is considered after removal of the shield sectors.

(v) The time required for assembly/disassembly is estimated under the assumption that the maintenance operation is carried out 12 hours per day.

The time required for each operation is shown in Table XI-2-5 and XI-2-6. The disassembly of one TF coil requires 65 days and the reassembly 63 days. The sum total amounts 228 days (7.6 month).

Table XI-2-5 Time required for maintenance of the TF coil (Disassembly)

Disassembly of TF coil	Time and sequence (days) 20 40 60
① After shut down, bake and evacuate	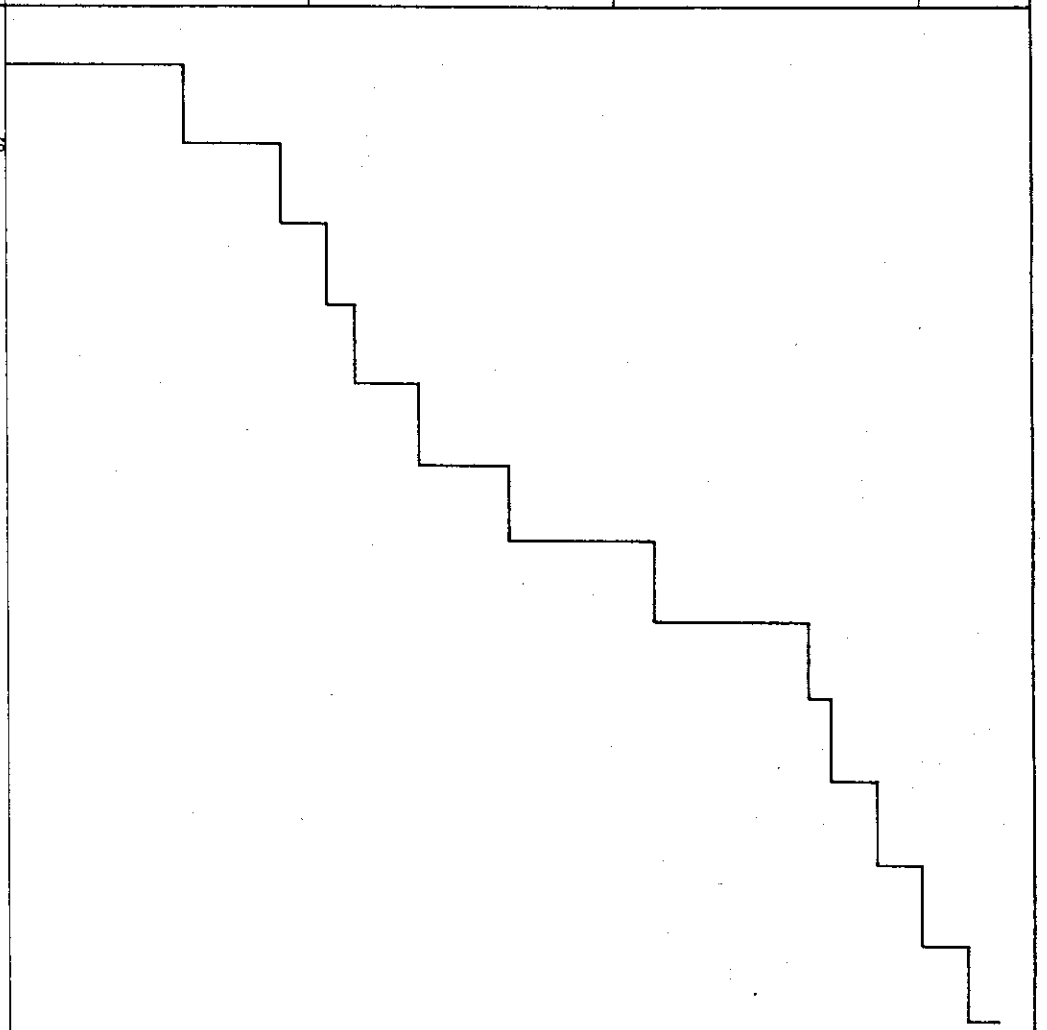
② Disconnect the cooling and electric lines	
③ Remove the belljar dome	
④ Remove the upper PF coils	
⑤ Remove the upper support beams between TF coils and dismount the cryostat	
⑥ Remove the pump limiters	
⑦ Remove the blanket sectors	
⑧ Remove the shield sectors and install the shield plug	
⑨ Dismount the base plate of the shield	
⑩ Remove the lower part of cryostat	
⑪ Remove the lower PF coils	
⑫ Remove the lower support beams between TF coils	
⑬ Remove the TF coils	
Total time for one TF coil	65 days

Table XI-2-6 Time required for maintenance of the TF coil (Assembly)

Assembly of one TF coil	Time and sequence (days) 50 100 150
① Install the TF coil	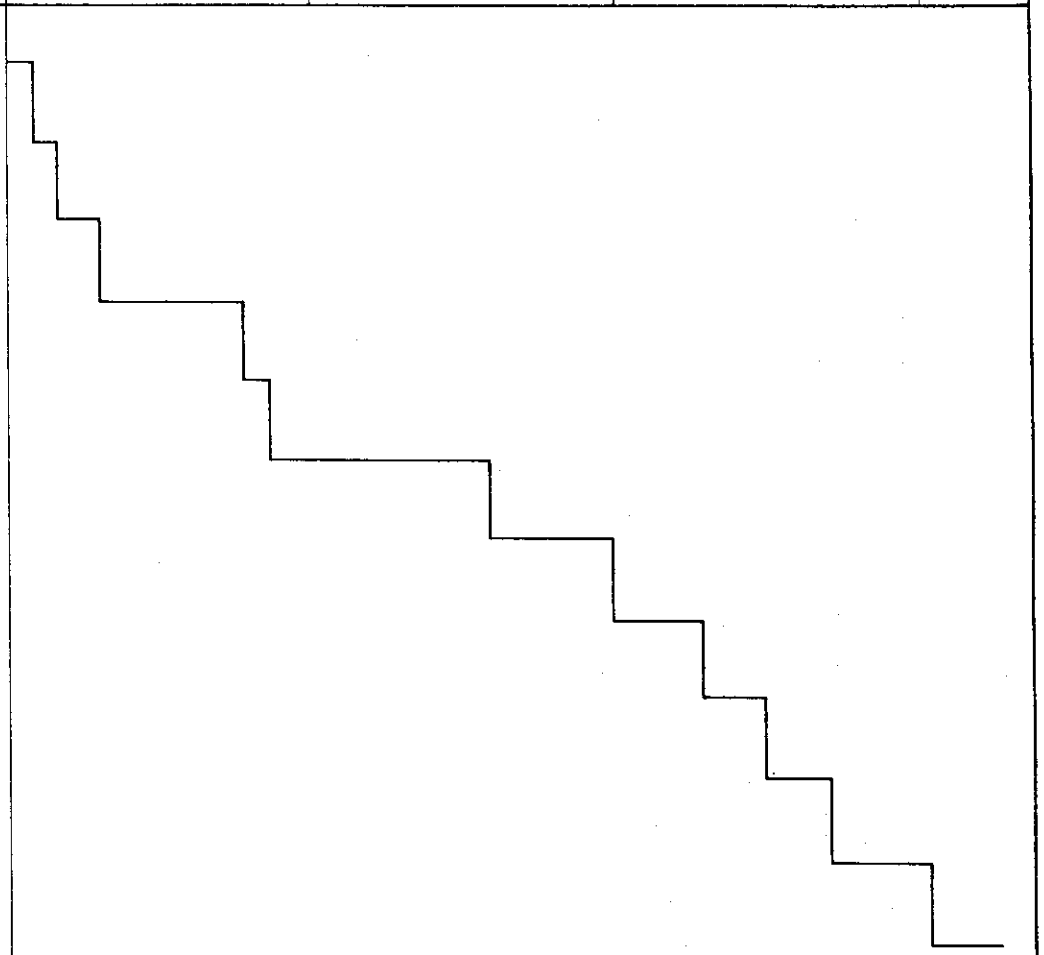
② Install the lower support beams between TF coils	
③ Install the lower PF coils	
④ Install the lower part of the cryostat	
⑤ Install the base plate supporting the shield	
⑥ Remove the shield plug and install the shield sectors	
⑦ Install the blankets	
⑧ Install the pump limiters	
⑨ Install the upper part of the cryostat	
⑩ Install the upper PF coils	
⑪ Install the belljar dome	
⑫ Connect the cooling and electric lines	
Total time for one TF coil	163 days

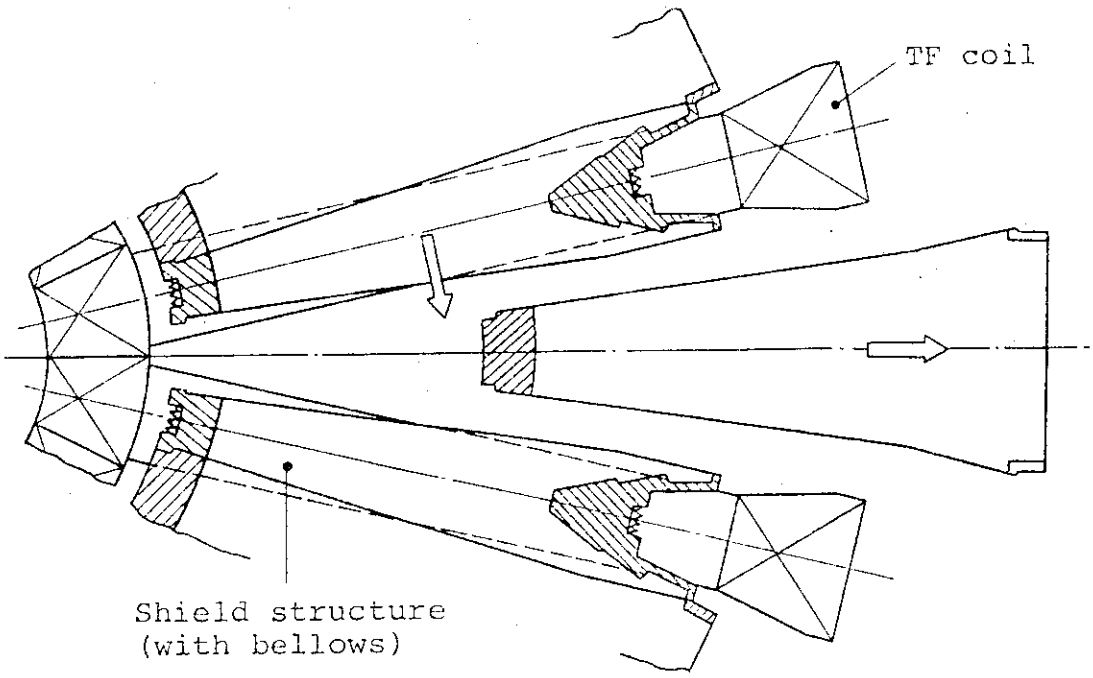

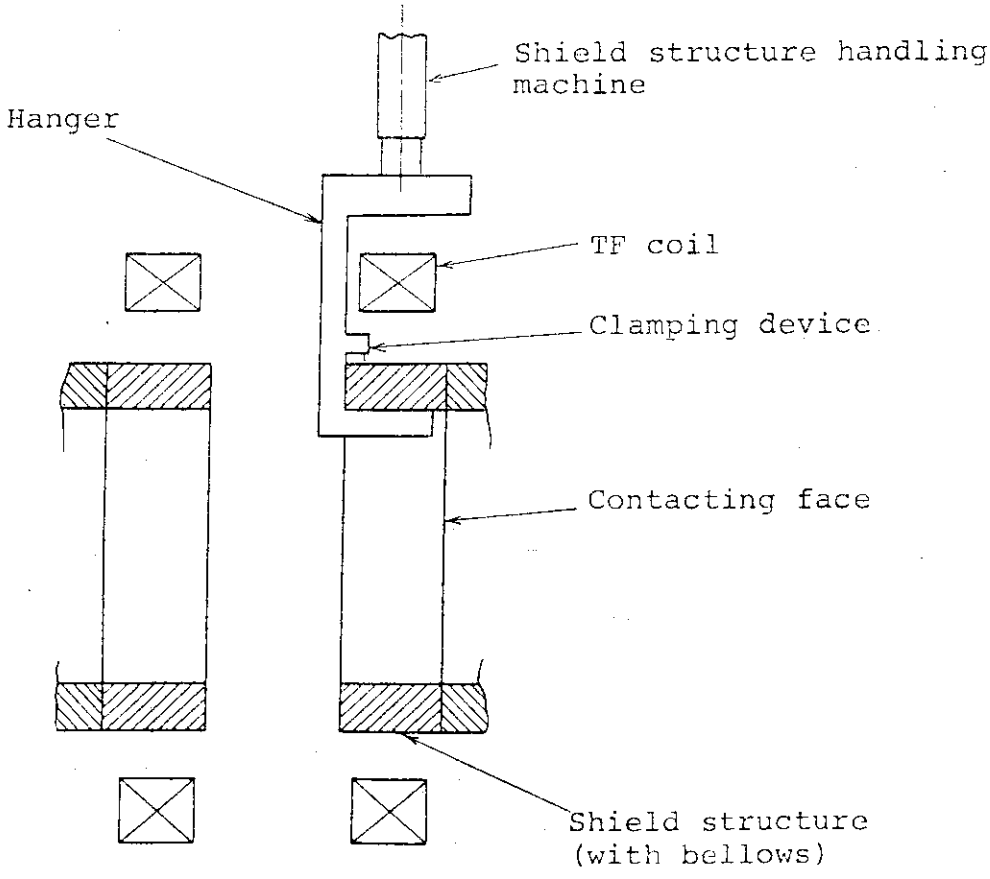

Fig. XI-2-8 Schematic view of replacement of the shield structure

2.4 Supporting analysis

1. TF coil loading condition

Three cases of PF coil distribution are considered in order to evaluate the TF coil strength for the out-of-plane load:

a) Case 1: Pump limiter operation with small ring coil (Max. radius of ring coil = 11 m)

b) Case 2: Pump limiter operation with large ring coil (Max. radius of ring coil = 13 m)

c) Case 4a: Divertor operation

Figure XI-2-9 ∿ Fig. XI-2-11 show the PF coil location for each cases.

The in-plane electromagnetic force as a function of TF coil perimeter is given in Fig. XI-2-12.

a) Total hoop force per coil : 1,144 MN

b) Centering force per coil : -379 MN

c) Vertical direction force per coil : ±253 MN

The out-of-plane magnetic forces as a function of TF coil perimeter are shown in Fig. XI-2-13 ∿ Fig. XI-2-15 for each cases.

a) Case 1:
- Moment around horizontal axis per coil (Mx) : 213 MN-m
- Moment around vertical axis per coil (M_Z) : ±239 MN-m

b) Case 2:
- M_X : 188 MN-m
- M_Z : ±263 MN-m

c) Case 4a: ° M_X : 164 MN-m

° M_Z : ±234 MN-m

2. Structural analysis for electromagnetic force

(i) Overall stress analysis

The finite element model for the structural analysis is shown in Fig. XI-2-16. TF coils, upper and lower intercoil support structure between TF coils, and support legs are modeled with beam element.
The wedged portion of TF coils, which mainly receive the compression, are modeled with beam elements.
This three dimensional beam element model treats both in-plane electromagnetic force and out-of-plane electromagnetic force of TF coils.
The deformations of TF coils for three loading conditions are shown in Fig. XI-2-17 ∿ Fig. XI-2-19.
The maximum displacements in vertical direction are the same value of 7 mm for three cases and the maximum displacements in toroidal direction are as follows:

a) Case 1 : 27 mm

b) Case 2 : 26 mm

c) Case 4a : 29 mm

(ii) Local stress analysis

It should be noted that the local bending stress on the side plate of the helium vessel due to the out-of-plane force cannot be calculated with the above-mentioned model.

The local bending stress (σ_{3b}) is given by

$$\sigma_{3b} = \frac{M}{Z}$$

where,

$$M = \frac{P\ell^2}{8}$$

P = Out-of-plane force shown in Fig. XI-2-13 ∿ Fig. XI-2-15

ℓ = Supporting length subjected to the force (0.7 m)

Z = Section modules of side plate

The side plate thickness is assumed to be 150 mm in the nose region, where the two adjacent side plate will support the out-of-plane force. In the other region where the torus support leg and exhaust duct may restrict the thickness of side plate, the side plate thickness is assumed to be 200 mm.

(iii) Resultant stress

The calculated stresses of TF coil are shown in Table XI-2-7 ∿ Table XI-2-9 for three cases.

Mechanical strength and design stress intensity value of used materials are shown in Table XI-2-10. Table XI-2-11 shows the evaluation of maximum stress intensities in TF coil for three cases. The maximum stress intensities for pump limiter operation (Case 1 & Case 2) are below the allowable value, but the maximum stress intensity for divertor operation (Case 4a) is over the allowable value.

Cyclic bending stresses due to out-of-plane force occur in the helium vessel of the TF coil. As shown

in Table XI-2-7 ∿ Table XI-2-9, the maximum values of cyclic stress ranges for case 1, case 2 and Case 4a are 261 MPa, 235 MPa and 464 MPa respectively, so that maximum cyclic stress amplitudes for case 1, case 2 and case 4a are 131 MPa, 118 MPa and 232 MPa.

Taking into account the mean stress, the equivalent cyclic stress amplitude is given by

$$S_{eq} = \frac{S_{alt}}{1 - \frac{S_{mean}}{Su}}$$

where,

S_{alt} : Cyclic stress amplitude

S_{mean} : Modified mean stress

Su : Ultimate strength

The equivalent maximum cyclic stress amplitude for case 1, case 2 and case 4a are 152 MPa, 147 MPa and 321 MPa, respectively.

Fig. XI-2-20 shows the design fatigue curve of SS 316, which is determined taking into account both the stress safety factor of 2 and the cycle safety factor of 20. Maximum cyclic stress amplitudes for pump limiter operation (case 1 & case 2) are less than the design fatigue stress of 310 MPa for the design cyclic number of 10^6.

Table XI-2-7 TF coil stress due to electromagnetic force (Case 1)

Unit : MPa

Location		Stress due to in-plane force			Stress due to out-of-plane force		P_m	P_L+P_b
		σ_{1m} *1)	σ_{1b}	σ_{3m}	σ_{1b}	σ_{3b}		
A	He vessel	108.39	±52.23	-286.26	±35.57	±1.86	394.65	484.32
	Conductor	74.19	±35.67	-86.53	±24.40	—	160.72	220.79
B	He vessel	87.91	±100.16	-88.49 *2)	±49.98	±158.76	176.40	485.30
	Conductor	60.17	±68.60	-50.96	±32.4	—	111.13	213.93
C	He vessel	80.16	±88.20	-28.91	±60.47	±141.12	109.07	398.86
	Conductor	54.88	±60.37	-28.91	±41.36	—	83.79	185.51
D	He vessel	73.79	±35.97	-25.09	±114.95	±142.10	98.88	391.90
	Conductor	50.47	±24.60	-25.87	±76.69	—	76.34	179.63
E	He vessel	48.71	±14.70	-25.87	±141.02	±120.05	74.58	350.35
	Conductor	33.32	±10.00	-25.87	±96.53	—	59.19	165.72
F	He vessel	86.93	±10.58	-19.80	±34.20	±23.42	106.72	174.93
	Conductor	59.49	±7.25	-19.80	±23.42	—	79.28	109.96

Note: *1) σ_1, σ_2, σ_3 show the stress direction. δ_m and δ_b show the membrane stress and the bending stress.

*2) The values in parentheses indicate σ_{2m}.

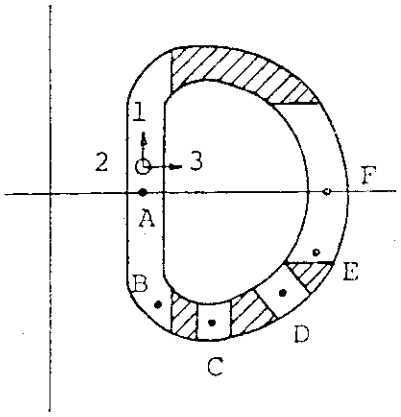

Table XI-2-8 TF coil stress due to electromagnetic force (Case 2)

Unit : MPa

Location		Stress due to in-plane force			Stress due to out-of-plane force			
		σ_{1m} *1)	σ_{1b}	σ_{3m}	σ_{1b}	σ_{3b}	P_m	P_L+P_b
A	He vessel	108.39	±52.23	-286.26 *2)	±32.05	±1.67	394.65	480.59
	Conductor	74.19	±35.67	-86.53	±21.95	___	160.72	218.34
B	He vessel	87.91	±100.16	-88.49 *2)	±48.22	±156.60	176.40	481.38
	Conductor	60.17	±68.60	-50.96	±33.03	___	111.13	212.76
C	He vessel	80.16	±88.20	-28.91	±104.37	±131.03	109.07	432.67
	Conductor	54.88	±60.37	-28.91	±71.44	___	83.79	215.60
D	He vessel	73.79	±35.97	-25.09	±103.29	±121.52	98.88	359.66
	Conductor	50.47	±24.60	-25.87	±70.66	___	76.34	171.60
E	He vessel	48.71	±14.70	-25.87	±132.59	±95.84	74.58	317.72
	Conductor	33.32	±10.00	-25.87	±90.75	___	59.19	159.94
F	He vessel	86.93	±10.58	-19.80	±39.79	±9.31	106.72	166.40
	Conductor	59.49	±7.25	-19.80	±27.24	___	79.28	113.78

Note: *1) σ_1, σ_2, σ_3 show the stress direction. δ_m and δ_b show the membrane stress and the bending stress.

*2) The values in parentheses indicate σ_{2m}.

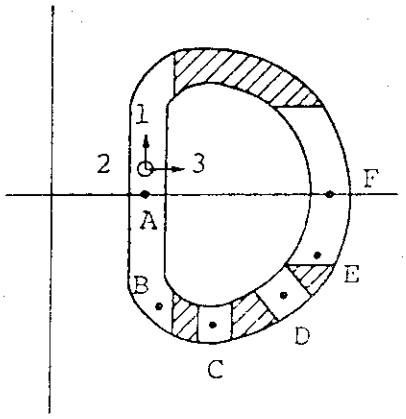

Table XI-2-9 TF coil stress due to electromagnetic force (Case 4a)

Unit : MPa

Location		Stress due to in-plane force			Stress due to out-of-plane force			
		σ_{1m} *1)	σ_{1b}	σ_{3m}	σ_{1b}	σ_{3b}	P_m	P_L+P_b
A	He vessel	108.39	±52.23	-286.26 *2)	±30.77	±18.62	394.65	496.27
	Conductor	74.19	±35.67	-86.53	±21.07	—	160.72	217.46
B	He vessel	87.91	±100.16	-88.49 *2)	±127.30	±315.56	176.40	719.42
	Conductor	60.17	±68.60	-50.96	±87.12	—	111.13	266.85
C	He vessel	80.16	±88.20	-28.91	±184.14	±280.18	109.07	661.60
	Conductor	54.88	±60.37	-28.91	±126.32	—	83.79	270.48
D	He vessel	73.79	±35.97	-25.09	±169.74	±260.68	98.88	565.26
	Conductor	50.47	±24.60	-25.87	±116.13	—	76.34	217.07
E	He vessel	48.71	±14.70	-25.87	±133.57	±109.47	74.58	332.32
	Conductor	33.32	±10.00	-25.87	±91.43	—	59.19	160.62
F	He vessel	86.93	±10.58	-19.80	±77.81	±47.73	106.72	242.84
	Conductor	59.49	±7.25	-19.80	±53.21	—	79.28	139.75

Note: *1) σ_1, σ_2, σ_3 show the stress direction. δ_m and δ_b show the membrane stress and the bending stress.

*2) The values in parentheses indicate σ_{2m}.

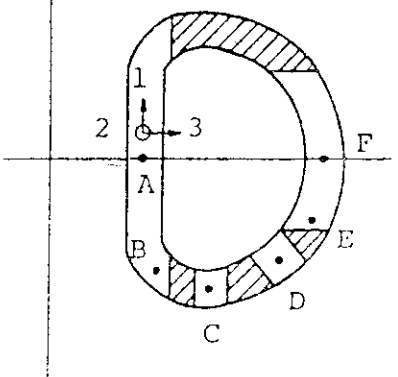

Table XI-2-10 Mechanical strength and allowable stress of materials

Part		Materials	Ultimate strength σu (MPa)	Yield strength σy (MPa)	sm (MPa)
Helium vessel		SUS316L	1,580	670	440
Winding	Stainless steel reinforcement				
	Copper stabilizer	OFHC$\frac{1}{2}$ H	440	330	220

Table XI-2-11 Evaluation of maximum stress intensities in TF coil

Unit : MPa

		Pm (<Sm)	P_L+P_b (<1.5Sm)
He vessel	Allowable stress	440	670
	Case 1	395	485
	Case 2	395	481
	Case 4a	395	791
Conductor	Allowable stress	220	330
	Case 1	161	221
	Case 2	161	218
	Case 4a	161	270

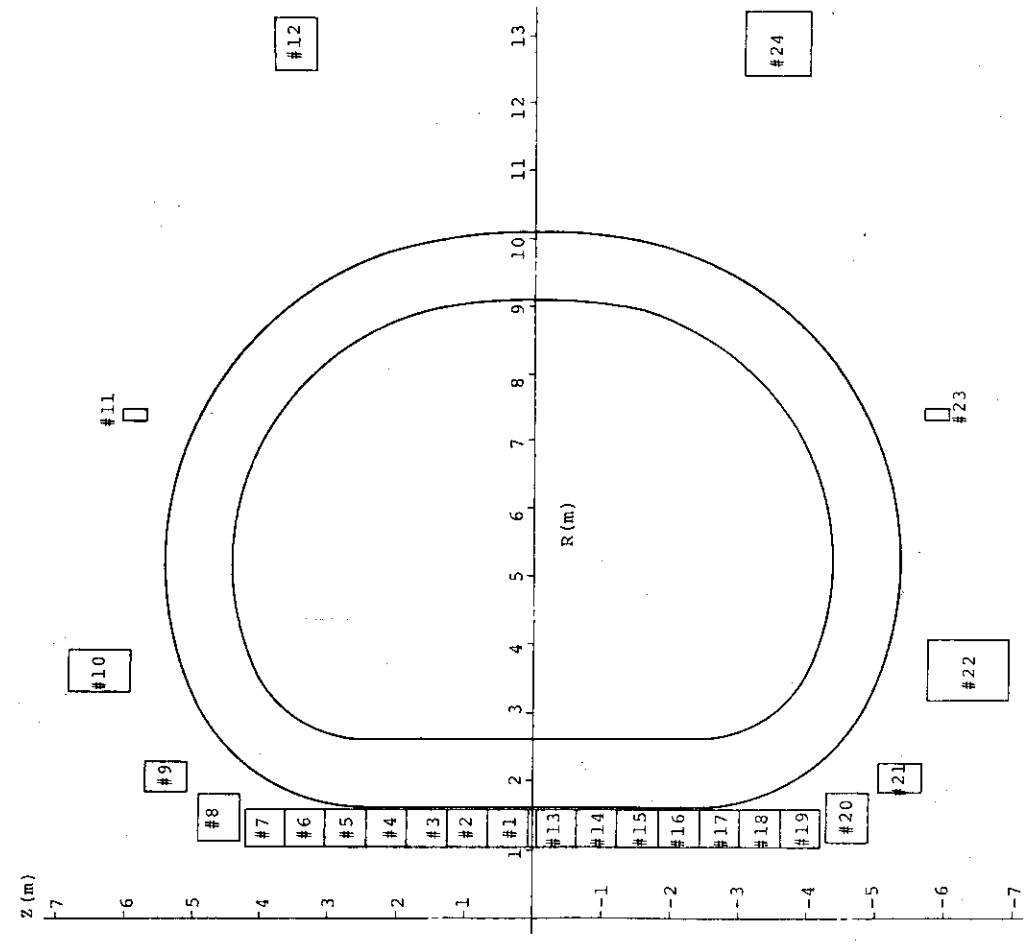

Fig. XI-2-10 Poloidal coil location for pump limiter operation (Case 2)

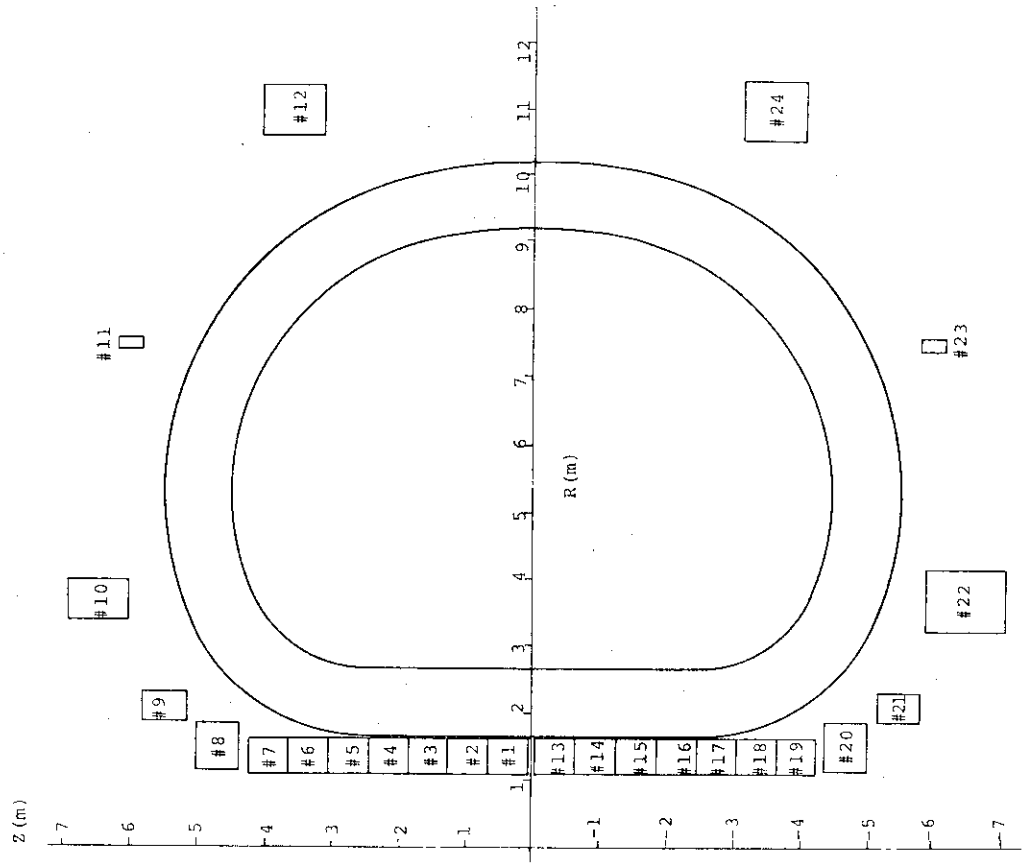

Fig. XI-2-9 Poloidal coil location for pump limiter operation (Case 1)

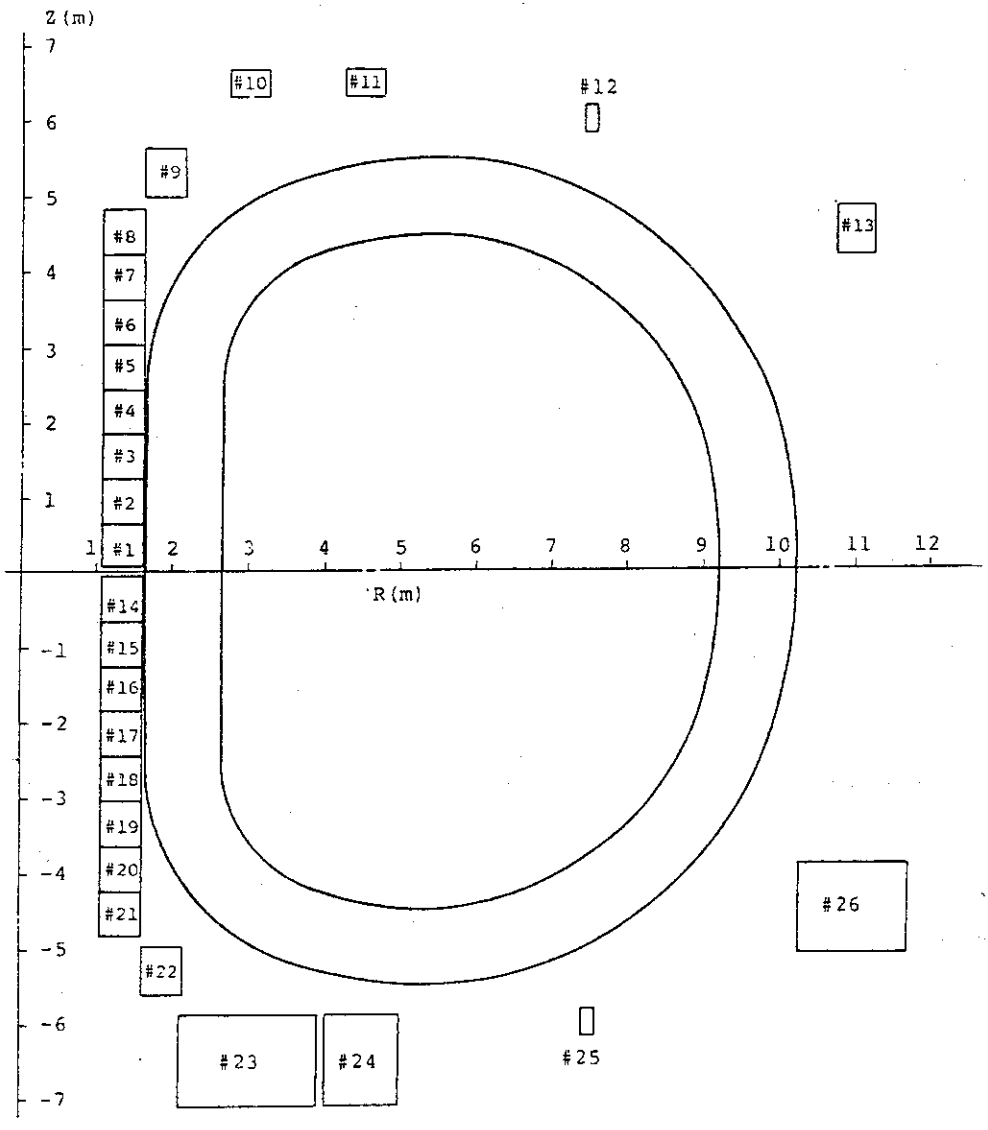

Fig. XI-2-11 Poloidal coil location for divertor operation (Case 4)

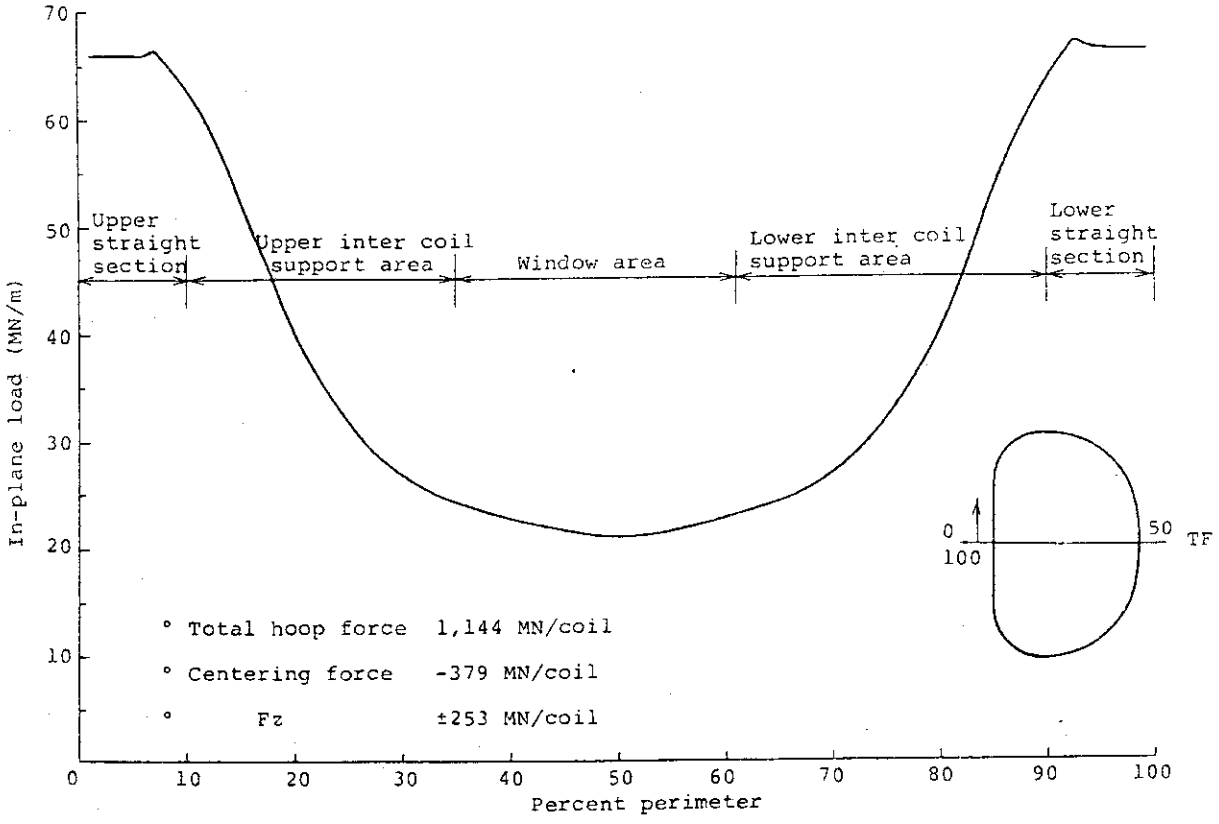

Fig. XI-2-12 In-plane force distribution for TF coils (Component of force normal to coil centerline)

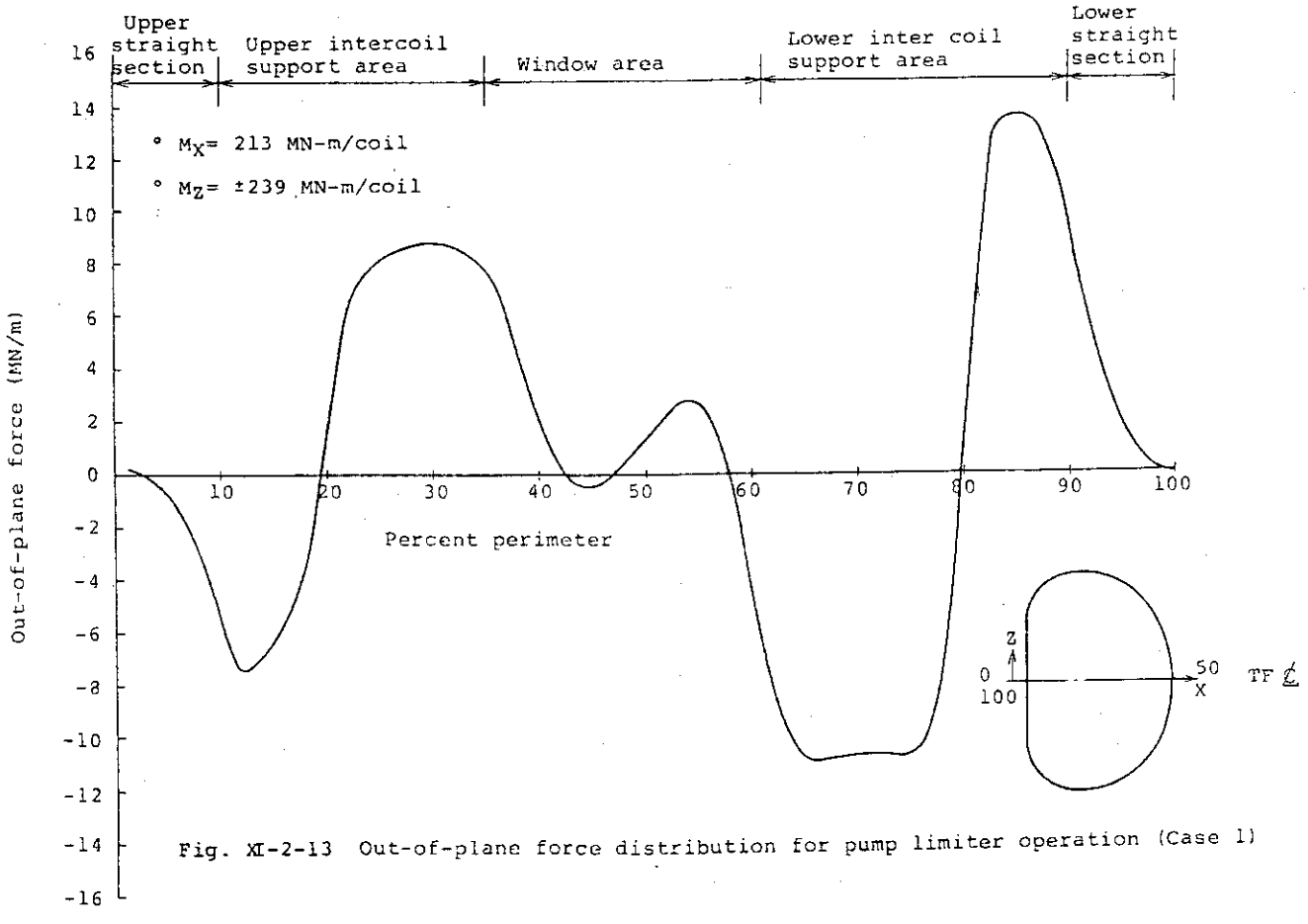

Fig. XI-2-13 Out-of-plane force distribution for pump limiter operation (Case 1)

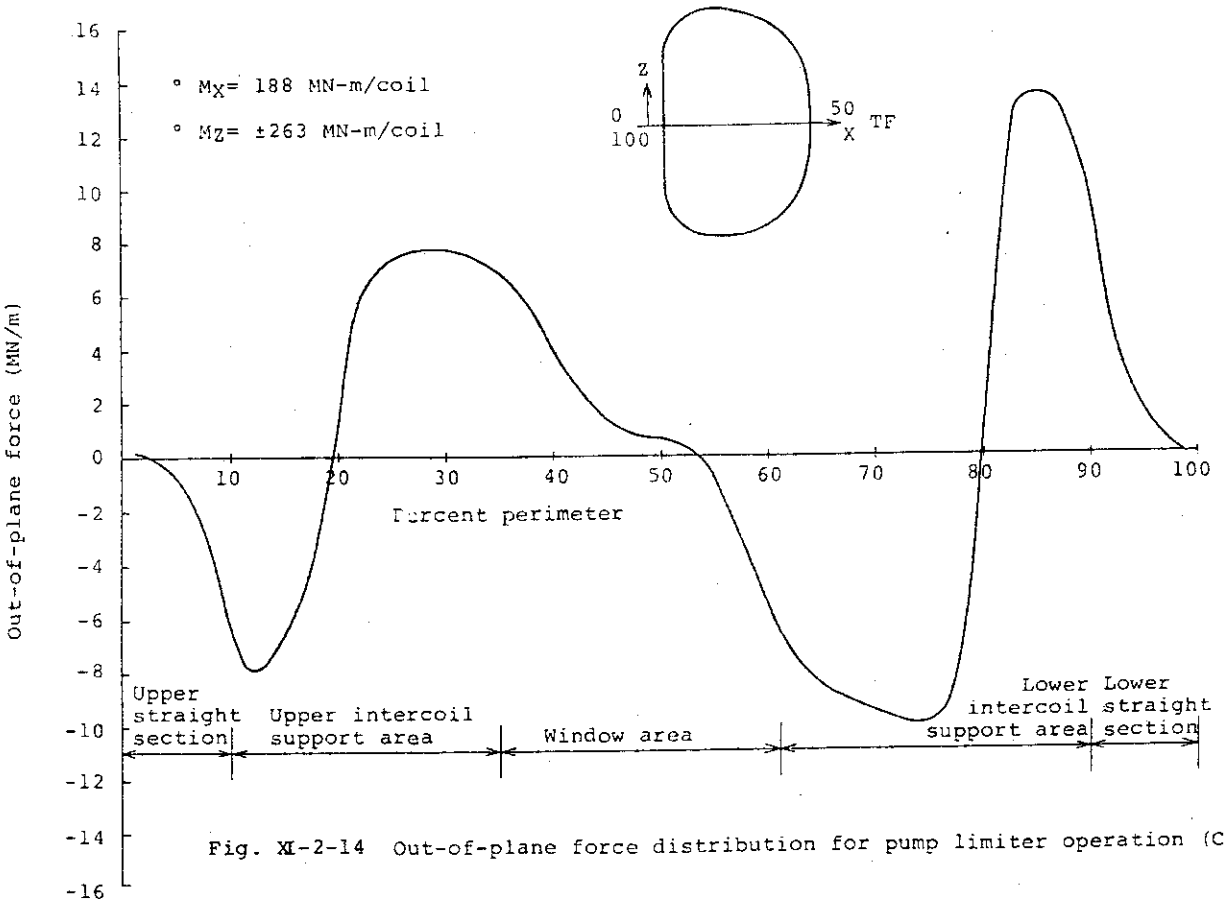

Fig. XI-2-14 Out-of-plane force distribution for pump limiter operation (Case 2)

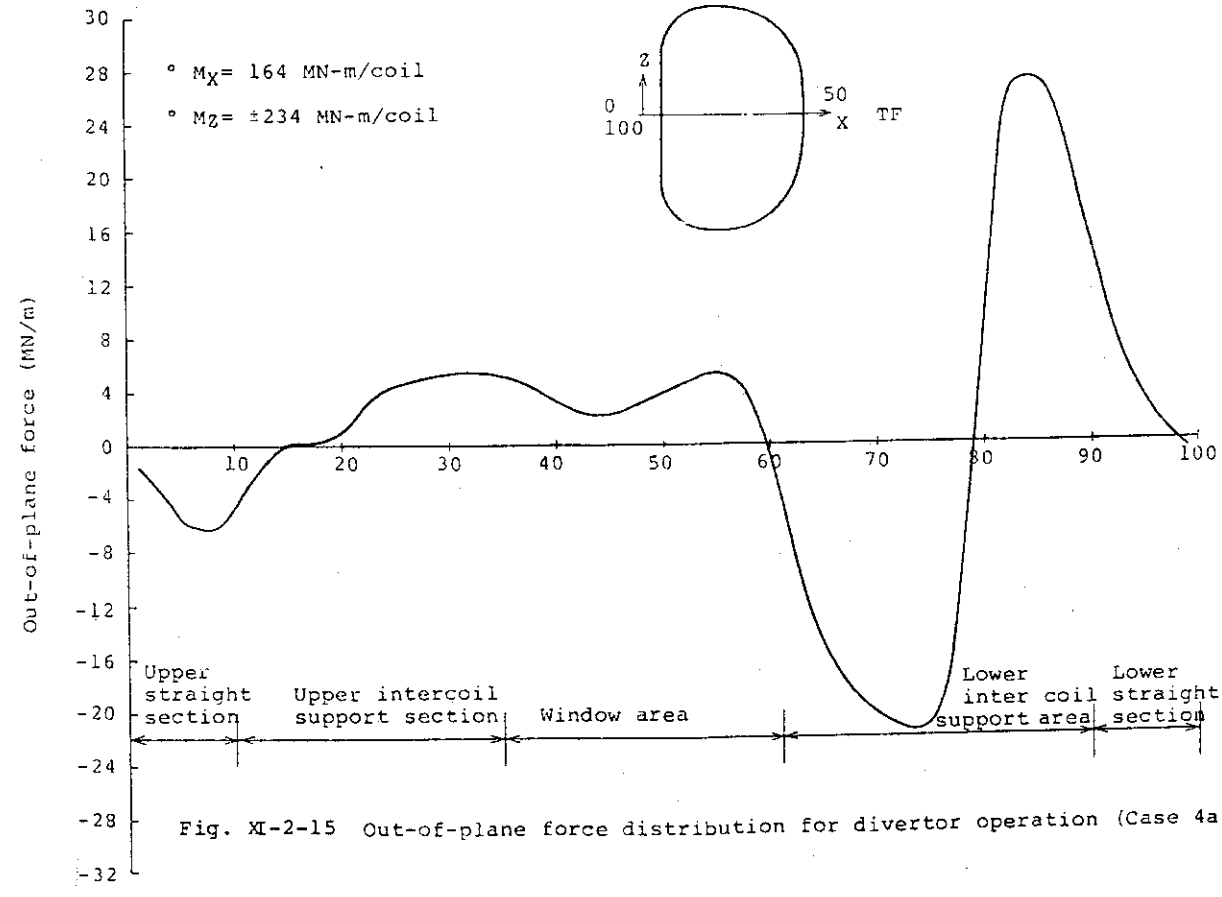

Fig. XI-2-15 Out-of-plane force distribution for divertor operation (Case 4a)

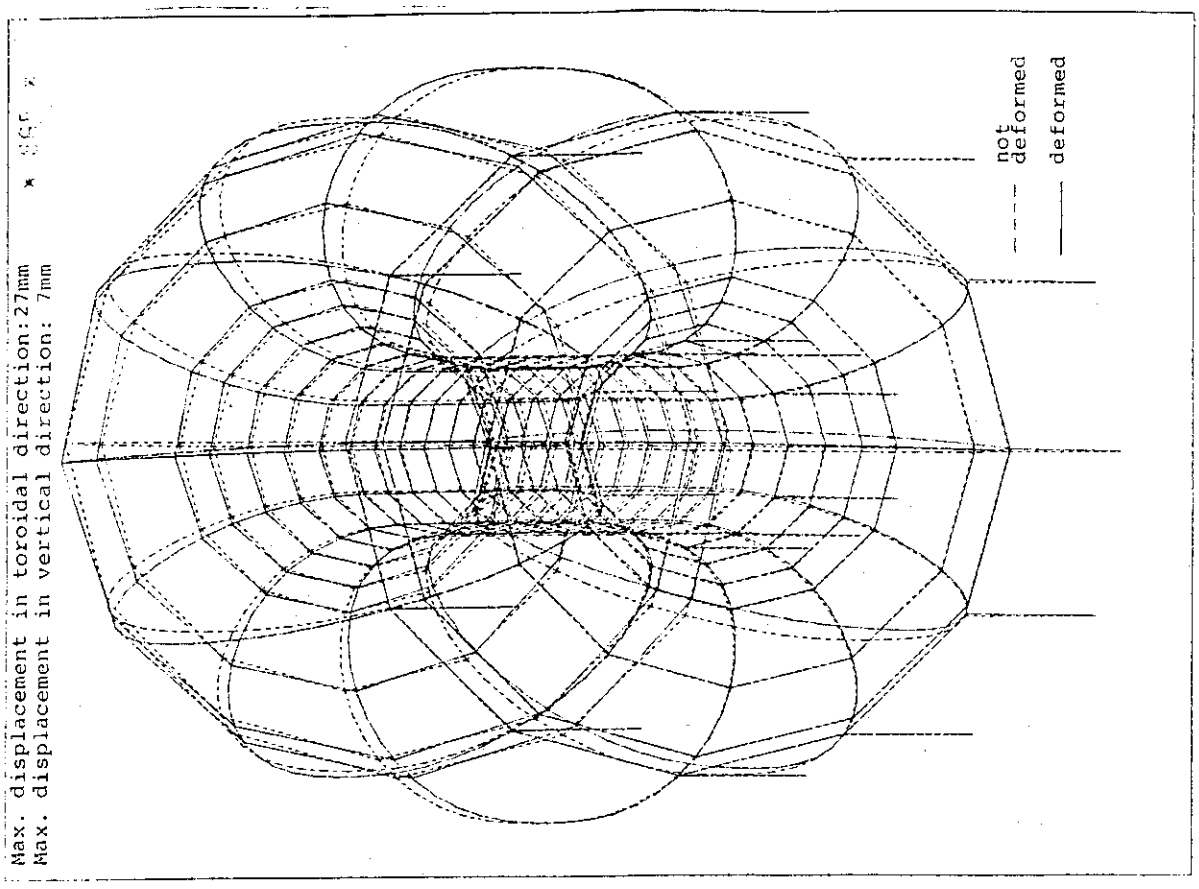

Fig. M-2-17 Deformation of TF coil due to in-plane force and out-of-plane force (Case 1)

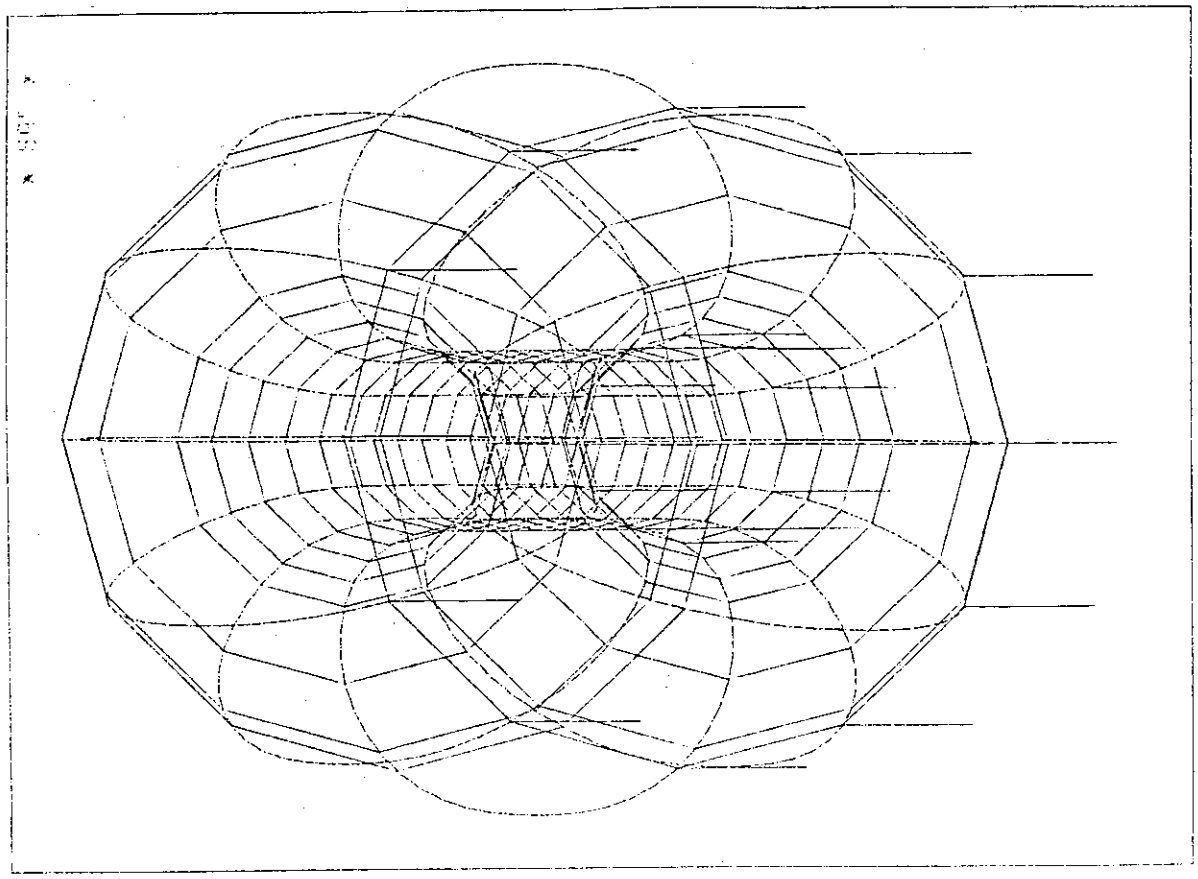

Fig. M-2-16 Three-dimensional stress analysis model of TF coil

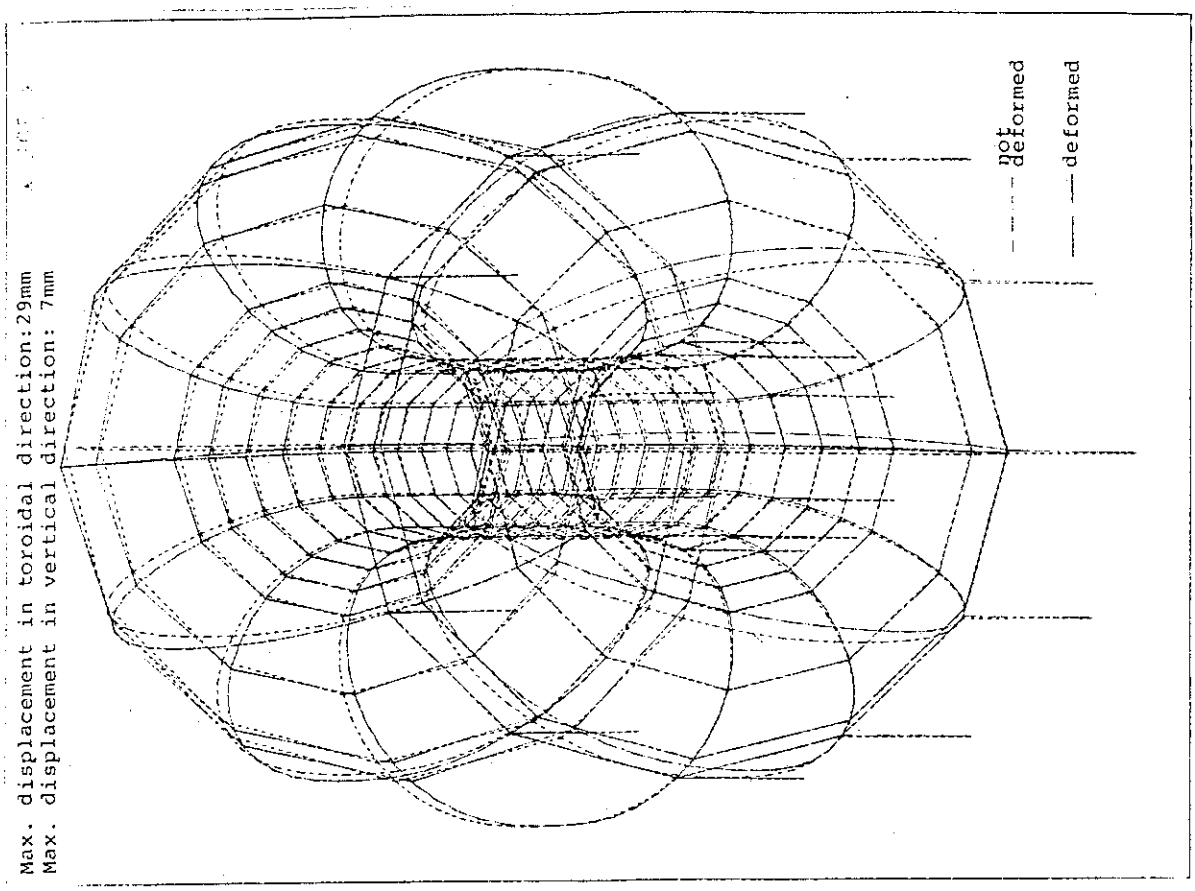

Fig. M-2-18 Deformation of TF coil due to in-plane force and out-of-plane force (Case 2)

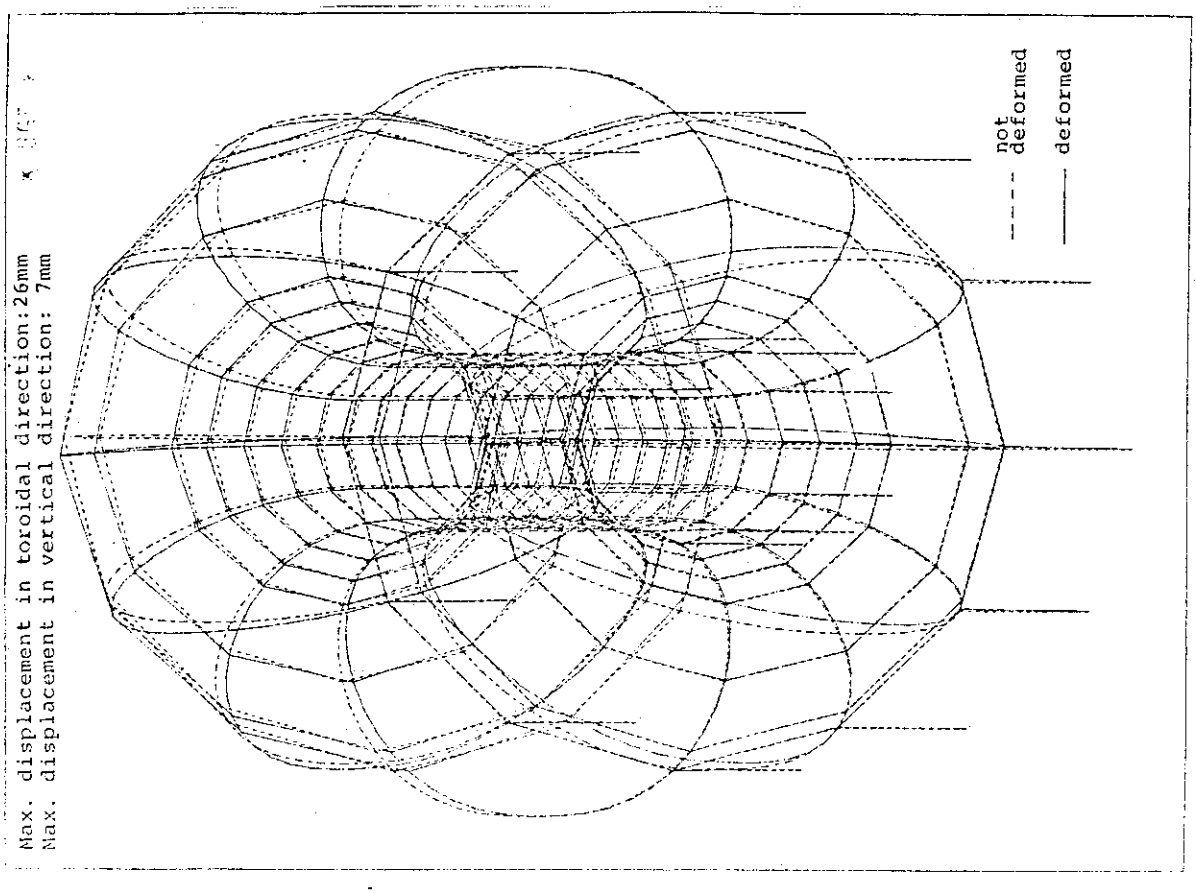

Fig. M-2-19 Deformation of TF coil due to in-plane force and out-of-plane force (Case 4a)

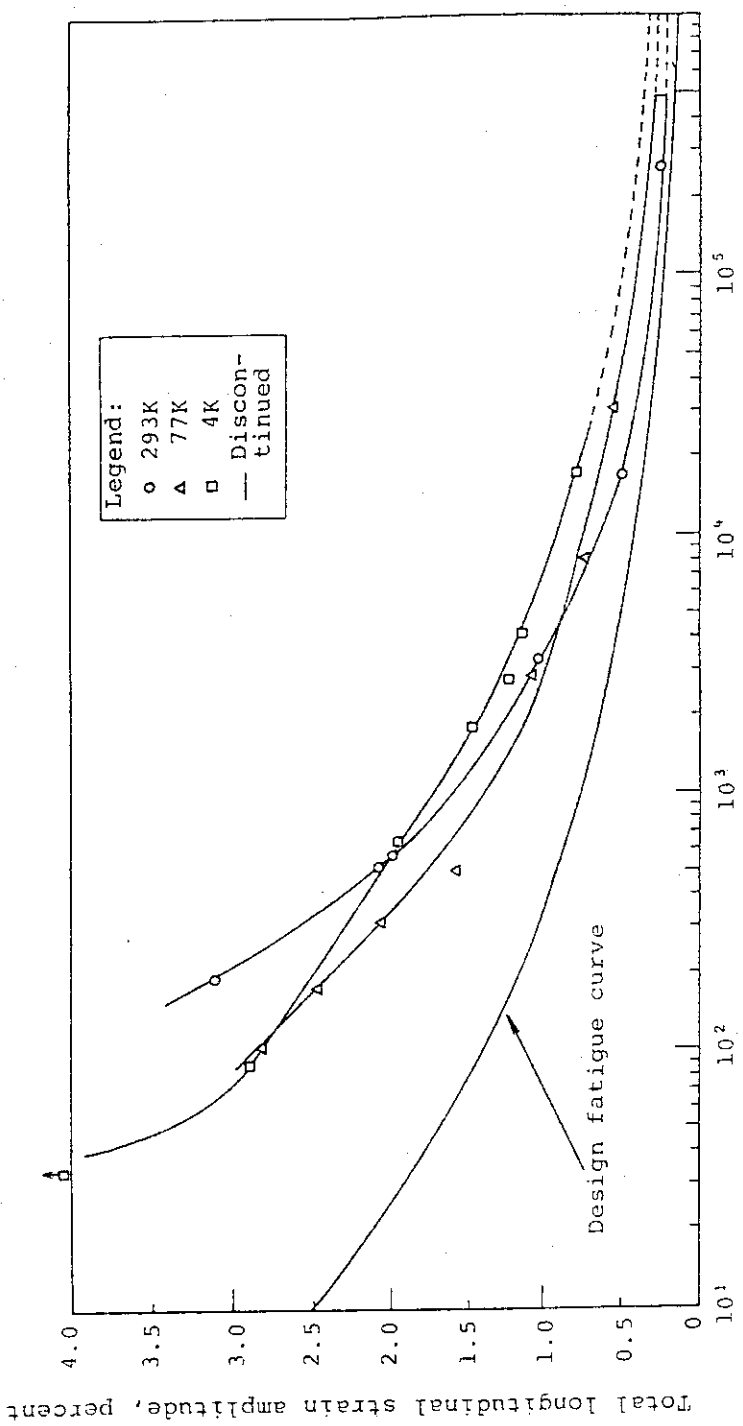

Fig. M-2-20 Fatigue life curves for SS 316

3. PF System

3.1 Configuration drivers

3.1.1 Maintenance and access philosophy

(1) Requirements for reactor structure maintenance

The reactor structure components of Tokamak fusion reactors are expected to be exposed to various kinds of severe stresses during operations such as thermal and neutron loads and electromagnetic forces. In particular, the reactor core components such as first walls, blanket and divertor plates wall be very severely stressed and are expected to have relatively short life. Therefore, reactor structure which enables easy maintenance of those components is required.

The following items must be considered in relation to maintenance requirements.

(a) Maintenance frequency and its scale

Maintenance frequency and its scale for each component are classified as shown in Table XI-3-1. Because of the complex nature of the Tokamak geometry, replacement of certain structures within the device will severely impact device availability. Those structures are designed for the life of the device, and classified as semi-permanent installations. However, capability to accommodate their unexpected repair or replacement will be a

design criterion even though such an occurrence represents a prolonged downtime. They include, but may not be limited to, the TF coils and the PF coils.

(b) Reliability of remote maintenance system

Since most remote maintenance works will be performed in highly radio-active environment, it is rather difficult to send another maintenance equipment to the rescue of the failed one. Therefore, highly reliable remote maintenance equipment and reliable maintenance procedures are required to minimize the possibility of those accidents.

(c) Maintenance time minimization

It is very important to reduce the maintenance time, in order to achieve the high availability required for the INTOR system. Since the life of divertor plates is rather short and its maintenance frequency is fairly high, it is particularly important to reduce the maintenance time for them.

(d) Heavy components handling

The weight of the divertor components which must be removed from the reactor core region, is an order of several tons. It is required to develop remotely controlled manipulators

and retraction vehicles which can handle removing process of those heavy components.

(2) Basic considerations on maintenability

(a) Modes of operation

The device components to be handled in the reactor cell range in size from very large (i.e., TF coils and torus sectors) to very small (i.e., valves and pipes), and many of the operations to disassemble and replace them will require varying degrees of handling ranging from contact to fully remote. In general, the areas within the shield envelope of the device require remote handling operations and the outside surface of the shield is the "hands-on" boundary.

Two modes of operation around the device can be defined: contact and fully remote.

1) Contact operations allow the maintenance worker to use direct touch (hands-on) and sight without intermediate protective shielding. All components which are located outside the shield structure are maintained using hands-on procedures. Some examples of these are: inspection, setup of diagnostics, electrical connections, coolant connections, and engineering instrumentation. The outer shield thickness is sized to limit surface dose rates to 2.5 rmem/hr, 24 hours after machine shut-down. This is the design level for contact maintenance and is only exceeded when the inner surfaces of the machine are opened to the reactor cell. Contact operations are very significant for simplification and high reliability of the maintenance system which will lead to reduction of machine downtime.

2) Fully remote operations do not allow direct touch or sight. These operations are required for all components which are within the shield boundary of the torus, as well as the beam-lines, and the divertor ducting, and will be required in the reactor cell when the plasma chamber is disassembled. The worker is separated

from the device by a biological shield and maintenance tasks are accomplished by the use of remote handling equipment and viewing systems.

(b) Basic considerations on structure configuration

Because of the complex Tokamak geometry and limited space inside the shield boundary, the maintenance system will be greatly affected by structure design. In general, if machine design is focused on getting smaller machine and smaller structure segments to replace, the maintenance system will become more sophistcated and complicated.

With "Phase-I" design, structure components are removed in horizontal direction with single straight motion, and all vacuum seal lines and mechanical joints to be released are provided on the front side of the reactor shield boundary.

In "Phase-I", with combination of this structure configuration and allowable radio-activity level for human beings, the assembling and disassembling process is rather simplified, though this system has such a drawback that some structure components, particularly toroidal and poloidal field magnets, were

designed to be big sized to allow horizontal access for replacement of internal reactor components. This is a tradeoff between simplified maintenance process and size of structure components.

In "Phase-IIa", the efforts are conducted on the reduction of the reactor size in order reduce the reactor cost without complication of the assembling and disassembling press in maintenance operation.

Table XI-3-1 Frequency of repair

Type of repair	Frequency of repair (per year)	Components
Small scale	2 - 10	Pumped limiter
Medium scale	1	First wall, blanket (removable torus sector), farady shield of ICRF antenna
Large scale	0.1	Magnet, shield structure (semi-permanent torus sector)

3.1.2 Pumped limiter/poloidal divertor configuration

(1) PF coil location and ampere turn

The examinations on several cases of PF coil location and ampere turn is carried out. The discussion is mainly focused on the following four principle points. The case of the pumped limiter (bottom type, maximum PF coil radius R = 11m) is finally selected as our reference design.

(a) Relevancy with the reactor structure system.

(b) Reduction of power capacity of electrical supply.

(c) Out-of-plane force acting on TF coil structure.

(d) Reduction of AC loss in superconducting conductor and coil case structure induced by pulsed magnetic field.

The above items are considered for four cases shown Table XI-3-2.

The PF coil location for each case are shown in Fig. XI-3-1 ∿ Fig. XI-3-4. The PF coil ampere turns for each case are shown in Table XI-3-3 ∿ Table XI-3-6.

In order to determine the PF coil distribution, the region necessary for limiter and blanket maintenance is presupposed. This space available for maintenance is estimated under the assumption that the blanket sector is retracted horizontally in radial direction.

(a) Incorporation with the reactor structure

The main objects of Phase IIa are to reduce the reactor size, to make more reliable and to reduce the construction cost.

Concerning the PF coil, the case 1 and case 4a have a largest PF coil of radius R=11m, the case 2 and case 3 have a largest PF coil of radius R=13m.

If the belljar type cryostat is supposed to be used, the outer radius of belljar for case 1 and case 4a is R=24.5m, the case 2 and case 3, R=28.7m. As the space required for the maintenance of blanket and other structure is supposed to be same, the size of the reactor room increases propotinally to the PF coil maximum radius.

Concerning the support structure of the PF coil of maximum radius, in the case 1 and case 4a, the PF coil of maximum radius can be supported easily from the TF coil.

In the case 2 and case 3, as the PF coil of maximum radius is located at the 2m from the TF coil, in order to support the PF coil from the TF coil, long support arms which have sufficient rigidity for bending are necessary and these support arms brings about an increase of dead weight and heating due to AC loss.

Another option such as PF coil supported independently from the floor is proposed.
However, this concept is not desirable from the view point of heat penetration.

(b) Reduction of electric power capacity

Among the systems constituting the tokamak reactor, the electric power system occupies a great part of the construction cost.
Therefore, the cost reduction of the electrical power system is of great importance from the view point of the reactor system design.
The optimization of operation and control of PF coil should be also examined.
The stored energy and MG peak power of three cases are listed in Table XI-3-7(a).

Table XI-3-7(a)

		Case 1 Phase-II A Pump limiter	Case 2 Phase-II A Pump limiter	Case 4a Phase-II A Divertor
PF coil	Stored energy	4.3GJ	5.75GJ	8.09GJ
Power supply (*)	MG peak power	0.86GW	1.1GW	2.3GW

* Remarks

During the plasma start-up phase (0 ∿ 0.3s), the voltages of PF coil are assumed to be generated by resistances. So thyristor controlled DC power supply capacity is not included in start-up phase.

(c) Out-of-plane force acting on TF coil

Increasing the size of TF coil, the ampere turn of the PF coil and the distance of PF coil from the plasma, the out-of-plane magnetic forces acting on the TF coil becomes greater in general. The out-of-plane magnetic force as a function of TF coil perimeter is shown in Table XI-3-8. The stress produced by the out-of-plane-force is shown in Table XI-3-9.

(d) Reduction of AC loss in S.C. conductor and surrounding structure

The AC loss caused by changing poloidal field appears mainly in the superconductor, the helium vessel and the coil support in the TF coil. The averaged AC losses are summarized in Table XI-3-10 for each case.
The loss in the case 1 and 2 is small. On the other hand, the loss for case 4a is about three times greater than that for the other two cases.

Table XI-3-2

	Case 1	Case 2	Case 3	Case 4a
Impurity control	Pump limiter	Pump limiter	Pump limiter	Single divertor
Location and configuration	bottom 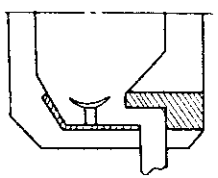	bottom 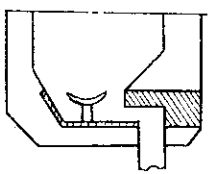	outboard 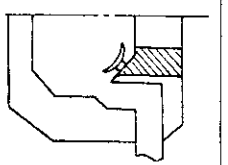	bottom 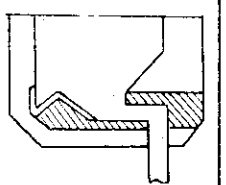
PF coil max. radius (m)	11	13	13	11
Plasma offset (m)	0.4	0.4	0	0.4

Table XI-3-3 Coordinate and ampere-turns of PF coils (Case 1)

Coil No.	Block No.	Coil location		Turns No.	Time (sec)						
		R(m)	Z(m)		0.	0.3	5.0	11.0	211.0	226.0	246.0
1	1	1.35	0.35	72	3.683	2.879	-2.476	-2.777	-3.698	0.	3.683
2	2	1.35	0.95	72	3.108	2.495	-2.317	-2.777	-3.554	0.	3.108
3	3	1.35	1.55	72	3.396	2.688	-2.397	-2.777	-3.626	0.	3.396
4	4	1.35	2.15	72	3.217	2.568	-2.347	-2.777	-3.581	0.	3.217
5	5	1.35	2.75	72	3.369	2.670	-2.389	-2.777	-3.619	0.	3.369
6	6	1.35	3.35	72	3.180	2.543	-2.337	-2.777	-3.572	0.	3.180
7	7	1.35	3.95	72	3.964	2.647	-1.092	0.	-0.991	0.	3.964
8	8	1.50	4.70	88	4.341	2.899	-1.196	0.	-1.085	0.	4.341
9	8	2.10	5.50	56	2.857	1.908	-0.787	0.	-0.714	0.	2.857
10	9	3.70	6.50	132	1.771	2.942	6.191	6.565	6.122	0.	1.771
11	8	7.50	6.00	8	0.416	0.278	-0.115	0.	-0.104	0.	0.416
12	10	11.00	4.60	138	0.181	-0.387	-4.311	-6.937	-6.982	0.	0.181
13	11	1.35	-0.35	72	3.677	2.875	-2.474	-2.777	-3.696	0.	3.677
14	12	1.35	-0.95	72	3.117	2.502	-2.320	-2.777	-3.556	0.	3.117
15	13	1.35	-1.55	72	3.377	2.675	-2.391	-2.777	-3.621	0.	3.377
16	14	1.35	-2.15	72	3.248	2.589	-2.356	-2.777	-3.588	0.	3.248
17	15	1.35	-2.75	72	3.312	2.632	-2.373	-2.777	-3.605	0.	3.312
18	16	1.35	-3.35	72	3.280	2.610	-2.365	-2.777	-3.597	0.	3.280
19	7	1.35	-3.95	72	3.779	2.523	-1.041	0.	-0.945	0.	3.779
20	8	1.50	-4.70	92	4.568	3.050	-1.258	0.	-1.142	0.	4.568
21	8	2.10	-5.50	56	2.787	1.861	-0.768	0.	-0.697	0.	2.787
22	17	3.70	-6.50	272	1.624	3.212	11.177	13.686	13.280	0.	1.624
23	8	7.50	-6.00	8	0.421	0.281	-0.116	0.	-0.105	0.	0.421
24	18	11.00	-3.60	162	0.249	-0.257	-4.574	-7.985	-8.047	0.	0.249
Plasma		5.30	0.40		0.	0.600	5.400	6.400	6.400	0.	0.

Unit : MAT

Table XI-3-4 Coordinate and ampere-turns of PF coils (Case 2)

Coil No.	Block No.	Coil location		Turns No.	Time (sec)						
		R(m)	Z(m)		0.	0.3	5.0	11.0	211.0	226.0	246.0
1	1	1.35	0.35	72	3.683	2.872	-2.564	-2.979	-3.900	0.	3.683
2	2	1.35	0.95	72	3.108	2.489	-2.396	-2.979	-3.756	0.	3.108
3	3	1.35	1.55	72	3.396	2.681	-2.480	-2.979	-3.828	0.	3.396
4	4	1.35	2.15	72	3.217	2.562	-2.428	-2.979	-3.783	0.	3.217
5	5	1.35	2.75	72	3.369	2.663	-2.473	-2.979	-3.821	0.	3.369
6	6	1.35	3.35	72	3.180	2.537	-2.417	-2.979	-3.774	0.	3.180
7	7	1.35	3.95	72	3.964	2.646	-1.159	0.	-0.991	0.	3.964
8	8	1.50	4.70	88	4.341	2.898	-1.270	0.	-1.085	0.	4.341
9	8	2.10	5.50	56	2.857	1.907	-0.836	0.	-0.714	0.	2.857
10	9	3.70	6.50	132	1.771	3.000	6.598	6.341	5.898	0.	1.771
11	8	7.50	6.00	8	0.416	0.278	-0.122	0.	-0.104	0.	0.416
12	10	13.00	4.60	144	0.181	-0.452	-4.631	-7.302	-7.347	0.	0.181
13	11	1.35	-0.35	72	3.677	2.869	-2.563	-2.797	-3.898	0.	3.677
14	12	1.35	-0.95	72	3.117	2.495	-2.399	-2.979	-3.758	0.	3.117
15	13	1.35	-1.55	72	3.377	2.668	-2.475	-2.979	-3.823	0.	3.377
16	14	1.35	-2.15	72	3.248	2.582	-2.437	-2.979	-3.791	0.	3.248
17	15	1.35	-2.75	72	3.312	2.625	-2.456	-2.979	-3.807	0.	3.312
18	16	1.35	-3.35	72	3.280	2.603	-2.446	-2.979	-3.799	0.	3.280
19	7	1.35	-3.95	72	3.779	2.522	-1.105	0.	-0.945	0.	3.779
20	8	1.50	-4.70	92	4.568	3.049	-1.336	0.	-1.142	0.	4.568
21	8	2.10	-5.50	56	2.787	1.860	-0.815	0.	-0.697	0.	2.787
22	17	3.70	-6.50	264	1.624	3.340	11.997	13.179	12.773	0.	1.624
23	8	7.50	-6.00	8	0.421	0.281	-0.123	0.	-0.105	0.	0.421
24	18	13.00	-3.60	174	0.249	-0.299	-5.234	-8.732	-8.794	0.	0.249
Plasma		5.30	0.40		0.	0.600	5.400	6.400	6.400	0.	0.

Unit : MAT

Table XI-3-5 Coordinate and ampere-turns of PF coils (Case 3)

Coil No.	Block No.	Coil location R(m)	Coil location Z(m)	Turns No.	Time (sec) 0.	0.3	5.0	11.0	211.0	226.0	246.0
1	1	1.35	0.35	72	4.055			-3.145	-3.830	0.	4.055
2	2	1.35	0.95	72	3.454			-3.145	-3.729	0.	3.454
3	3	1.35	1.55	72	3.672			-3.145	-3.765	0.	3.672
4	4	1.35	2.15	72	3.662			-3.145	-3.764	0.	3.662
5	5	1.35	2.75	72	3.442			-3.145	-3.727	0.	3.442
6	6	1.35	3.35	72	4.243			-3.145	-3.862	0.	4.243
7	7	1.45	4.20	132	6.767			0.0	-1.143	0.	6.767
8	8	2.50	4.80	38	1.843	TBD	TBD	0.0	-0.311	0.	1.843
9	9	5.00	6.30	174	1.807			8.600	8.295	0.	1.807
10	10	13.00	4.50	192	0.502			-9.583	-9.668	0.	0.502
11	11	1.35	-0.35	72	4.055			-3.145	-3.830	0.	4.055
12	12	1.35	-0.95	72	3.454			-3.145	-3.729	0.	3.454
13	13	1.35	-1.55	72	3.672			-3.145	-3.765	0.	3.672
14	14	1.35	-2.15	72	3.662			-3.145	-3.764	0.	3.662
15	15	1.35	-2.75	72	3.442			-3.145	-3.727	0.	3.442
16	16	1.35	-3.35	72	4.243			-3.145	-3.862	0.	4.243
17	17	1.45	-4.20	132	6.767			0.0	-1.143	0.	6.767
18	18	2.50	-4.80	38	1.843			0.0	-0.311	0.	1.843
19	19	5.00	-6.30	174	1.807			8.600	8.295	0.	1.807
20	20	13.00	-4.50	192	0.502			-9.583	-9.668	0.	0.502

Unit: MAT

Table XI-3-6 Coordinate and ampere-turns of PF coils (Case 4a)

Coil No.	Block No.	Coil location		Turns No.	Time (sec)						
		R(m)	Z(m)		0.	0.3	5.0	11.0	211.0	226.0	246.0
1	1	1.35	0.35	72	3.643	3.032	-2.576	-3.073	-3.991	0.	3.643
2	2	1.35	0.95	72	3.076	2.519	-2.582	-3.073	-3.848	0.	3.076
3	3	1.35	1.55	72	3.363	2.779	-2.579	-3.073	-3.921	0.	3.363
4	4	1.35	2.15	72	3.174	2.608	0.037	0.	-0.800	0.	3.174
5	5	1.35	2.75	72	3.353	2.770	0.039	0.	-0.845	0.	3.353
6	6	1.35	3.35	72	3.088	2.530	0.036	0.	-0.778	0.	3.088
7	7	1.35	3.95	72	3.671	3.319	1.543	3.000	2.075	0.	3.671
8	8	1.35	4.55	72	3.905	3.531	0.045	0.	-0.984	0.	3.905
9	9	1.90	5.30	72	3.558	3.218	0.041	0.	-0.897	0.	3.558
10	10	3.00	6.50	38	1.917	1.322	0.022	0.	-0.483	0.	1.917
11	11	4.50	6.50	38	0.592	0.124	-1.920	1.792	1.643	0.	0.592
12	12	7.50	6.00	8	0.348	0.314	0.004	0.	-0.088	0.	0.348
13	13	11.00	4.50	60	0.237	0.362	2.003	-3.000	-3.060	0.	0.237
14	14	1.35	-0.35	72	3.644	2.321	-2.576	-3.073	-3.992	0.	3.644
15	15	1.35	-0.95	72	3.074	1.806	-2.582	-3.073	-3.848	0.	3.074
16	16	1.35	-1.55	72	3.363	2.067	-2.579	-3.073	-3.921	0.	3.363
17	17	1.35	-2.15	72	3.181	1.903	-2.581	-3.073	-3.875	0.	3.181
18	18	1.35	-2.75	72	3.326	2.033	-2.579	-3.073	-3.911	0.	3.326
19	19	1.35	-3.35	72	3.139	1.865	-2.582	-3.073	-3.864	0.	3.139
20	20	1.35	-3.95	72	3.575	3.233	0.041	0.	-0.901	0.	3.575
21	21	1.35	-4.55	72	3.991	3.609	0.046	0.	-1.006	0.	3.991
22	22	1.90	-5.30	72	3.587	3.244	0.042	0.	-0.904	0.	3.587
23	23	3.00	-6.50	312	1.812	2.873	13.901	15.660	15.203	0.	1.812
24	24	4.50	-6.50	312	0.640	1.814	13.887	15.660	15.499	0.	0.640
25	25	7.50	-6.00	6	0.317	0.287	0.004	0.	-0.080	0.	0.317
26	26	11.00	-4.65	312	0.264	-1.205	-13.777	-15.260	-15.327	0.	0.264
Plasma		5.30	0.40		0.	0.600	5.400	6.400	6.400	0.	0.

Unit : MAT

Table XI-3-7 Study of optimum PF coil distribution

		Case 1 Phase-II A pumped limiter	Case 2 Phase-II A pumped limiter	Case 3 Phase-II A outboard pumped limiter	Case 6 Phase-I divertor
Main characte-ristics	Plasma elongation	1.4	1.5∿1.6	1.5	1.6
	Start-up voltage	35V	35V	35V	50V
	Max. ring-coil radius	11m	13m	13m	12.1m
	No. of TF coils	12	12	12	12
	TF coil bore	6.6×9.3m	6.6×9.3m	6.6×8.9m	7.7×10.7m
Out-of-plane force of TF coil	f_{max}	13.6 MN/m	13.4 MN/m	11.4 MN/m	29.7 MN/m
	M_Z	±239 MN·m	±263 MN·m	±278 MN·m	±368 MN·m
	M_R	213 MN·m	188 MN·m	160 MN·m	237 MN·m
AC loss of TF coil	$<\int \dot{B}_r^2 d\ell>$	8.53×10^{-3} T^2m/S^2	8.27×10^{-3} T^2m/s^2	TBD	34.4×10^{-3} T^2m/s^2 (*1)
				TBD	(32.8×10^{-3})
	$<\int \dot{B}_z^2 d\ell>$	11.3×10^{-3}	11.2×10^{-3}		34.8×10^{-3} (*1) (33.3×10^{-3})
PF coil	AT	83.53 MAT	86.33 MAT	84.19 MAT	97.88 MAT
	B_{max}	7.1T	7.1T	7.8T	9.8T
	$\dot{B}_{max}$	6.4 T/S	6.4 T/S	TBD	8.3 T/S (*1) (5.5 T/S)
	Max. one-turn voltage	105V	144V	TBD	377V (251V)
	Stored energy	4.3 GJ	5.75 GJ	7.18 GJ	15.34 GJ
Power supply (*2)	MG peak power	0.86 GW	1.1 GW	TBD	3.1 GW

Remarks: 1) In case of start-up voltage of 35V.

2) During the plasma start-up phase (0 ∿ 0.3s, the voltages of PF coil are ass-med to be generated by resistances.)

Table XI-3-7 Study of optimum PF coil distribution (Continued)

		Universal-Japan		Universal-INTOR		
		Case 4(a) phase-II A diverter	Case 4(b) phase-II A pumped limiter	Case 5(a) phase-II A divertor	Case 5(b) phase-II A pumped limiter	Case 6 phase-I divertor
Main characte-ristics	Plasma elongation	1.5∿1.6	1.5	1.6	1.5	1.6
	Start-up voltage	35V	35V	35V	35V	50V
	Max. ring-coil	11m	11m	12.35m	12.35m	12.1m
	No. of TF cols	12	12	12	12	12
	TF coil bore	6.6×9.3m	6.6×9.3m	6.6×9.3m	6.6×9.3m	7.7×10.7m
Out-of-plane force of TF coil	f_{max}	27.1 MN/m	12.1 MN/m	32.3 MN/m	13.7 MN/m	29.7 MN/m
	M_Z	±234 MN·m	±229 MN·m	±307 MN·m	±236 MN·m	±368 MN·m
	M_R	164 MN·m	199 MN·m	135 MN·m	184 MN·m	237 MN·m
AC loss of TF coil	$<\int \dot{B}_i^2 d\ell>$	23.7×10^{-3} T^2m/s^2	9.22×10^{-3} T^2m/s^2	TBD	9.35×10^{-3} T^2m/s^2	34.4×10^{-3} T^2m/s^2 (*1) ($32.8\ 10^{-3}$)
	$<\int \dot{B}_z^2 d\ell>$	25.2×10^{-3}	12.0×10^{-3}	TBD	12.4×10^{-3}	34.8×10^{-3} (*1) (33.3×10^{-3})
PF coil	AT	95.74 MAT	87.95 MAT	83.06 MAT	92.05 MAT	97.88 MAT
	$\dot{B}_{max}$	8.2T	7.7T	8.0T	8.0T	9.8T
	B_{max}	6.5 T/S	6.4 T/S	TBD	8.0 T/S	8.3 T/S (*1) (5.5 T/S)
	Max. one-turn voltage	196V	121V	TBD	171V	377V (251V)
	Stored energy	8.09 GJ	5.0 GJ	15.6 GJ	5.77 GJ	15.34 GJ
Power supply (*2)	MG peak power	2.3 GW	0.94 GW	∿3.5 GW	1.06 GW	3.1 GW

Remarks: 1) In case of start-up voltage of 35V.

2) During the plasma start-up phase (0 ∿ 0.3s, the voltages of PF coil are assumed to be generated by resistances.)

Table XI-3-8 Out-of-plane magnetic force

	Case 1 pump limiter R=11m	Case 2 pump limiter R=13m	Case 3 pump limiter R=13m	Case 4a divertor
Moment around horizontal axis (Mx)	213	188	160	164
Moment around vertical axis (Mz)	±239	±263	±278	±234

Units; MN/m-coil

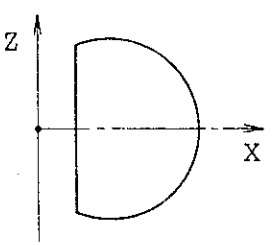

Table XI-3-9 TF coil stress due to electromagnetic force

Unit: MPa

Case		Case 1		Case 2		Case 4a	
Location		Stress due to out-of-plane force		Stress due to out-of-plane force		Stress due to out-of-plane force	
		σ_{1b}	σ_{3b}	σ_{1b}	σ_{3b}	σ_{1b}	σ_{3b}
A	He vessel	±35.57	±1.86	±32.05	±1.67	±30.77	±18.62
	Conductor	±24.40	—	±21.95	—	±21.07	—
B	He vessel	±49.98	±158.76	±48.22	±156.60	±127.30	±315.56
	Conductor	±32.4	—	±33.03	—	±87.12	—
C	He vessel	±60.47	±141.12	±104.37	±131.03	±184.14	±280.18
	Conductor	±41.36	—	±71.44	—	±126.32	—
D	He vessel	±114.95	±142.10	±103.29	±121.52	±169.74	±260.68
	Conductor	±76.69	—	±70.66	—	±116.13	—
E	He vessel	±141.02	±120.05	±132.59	±95.84	±133.57	±109.47
	Conductor	±96.53	—	±90.75	—	±91.43	—
F	He vessel	±34.20	±23.42	±39.79	±9.31	±77.81	±47.73
	Conductor	±23.42	—	±27.24	—	±53.21	—

Note: *1) σ_1, σ_2, σ_3 show the stress direction. σ_m and σ_b show the membrane stress and the bending stress.

*2) The values in parentheses indicate σ_{2m}.

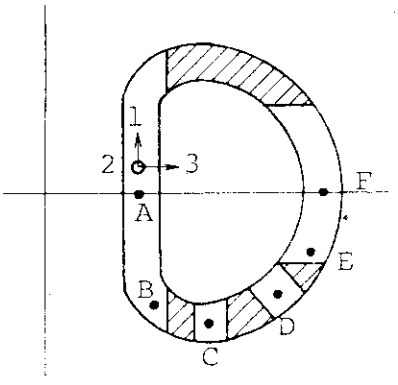

Table XI-3-10 AC losses in PF coils

	Case 1 Pump limiter R=11m	Case 2 Pump limiter R=13m	Case 4a (Divertor)
Superconductors	1.3 kW	1.4 kW	2.0 kW
Coil supports	2.5 kW	2.6 kW	10.4 kW
(Helium leak shields)	(20.3 kW)	(28.9 kW)	(43.0 kW)
Sum	3.8 kW (24.1 kW)*	4.0 kW (32.9 kW)*	12.4 kW (55.4 kW)*

* Taking account of the AC loss in helium leak shields.

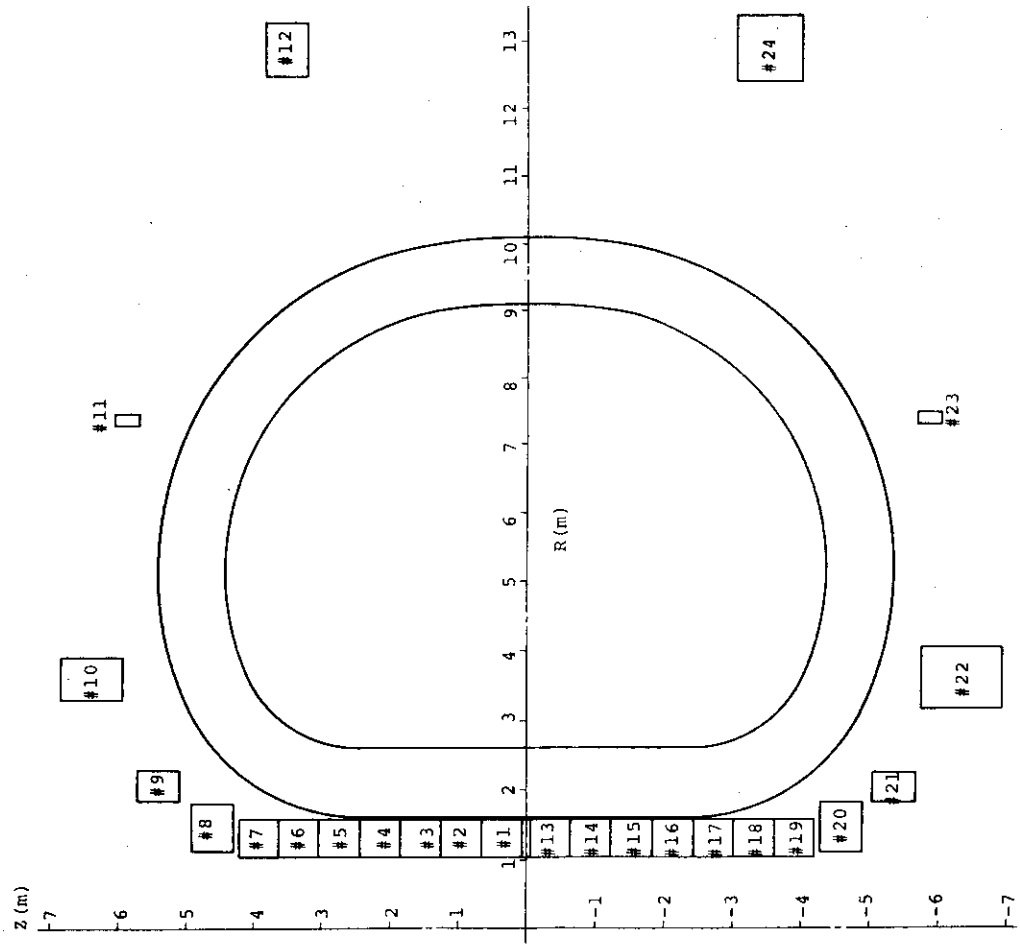

Fig. M-3-2 Poloidal coil location for pump limiter operation (Case 2)

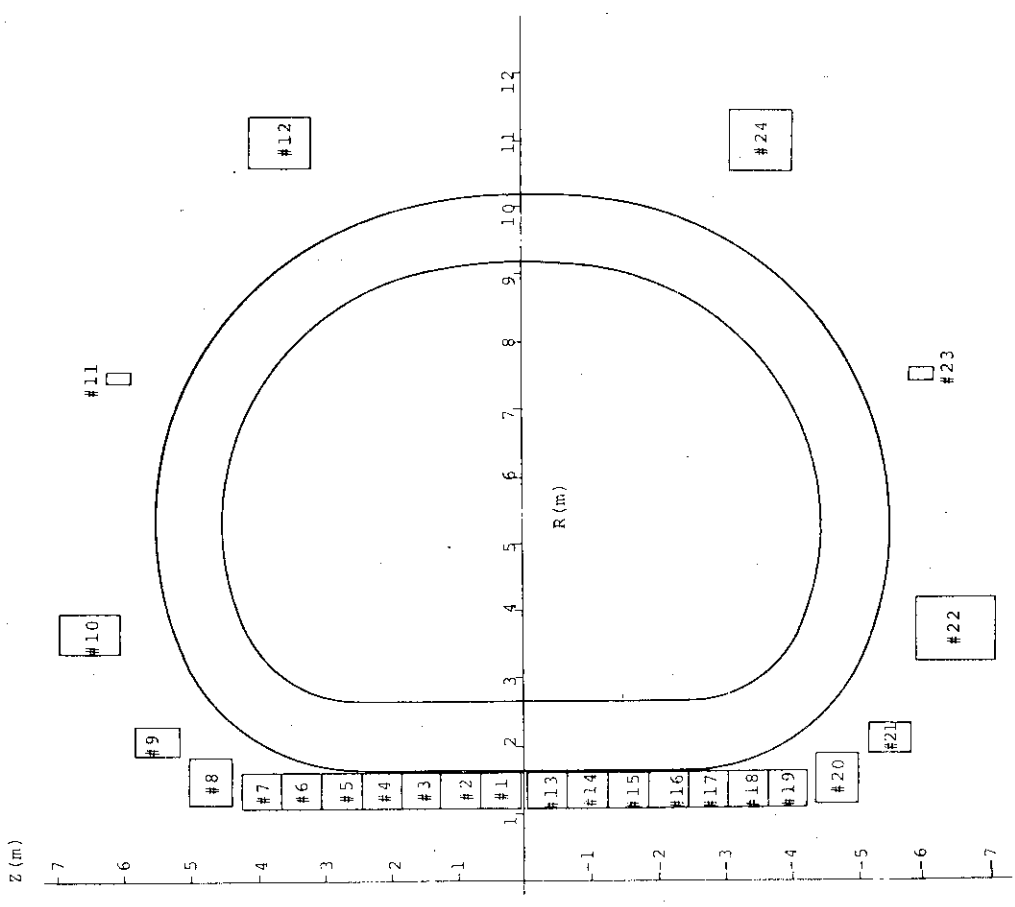

Fig. M-3-1 Poloidal coil location for pump limiter operation (Case 1)

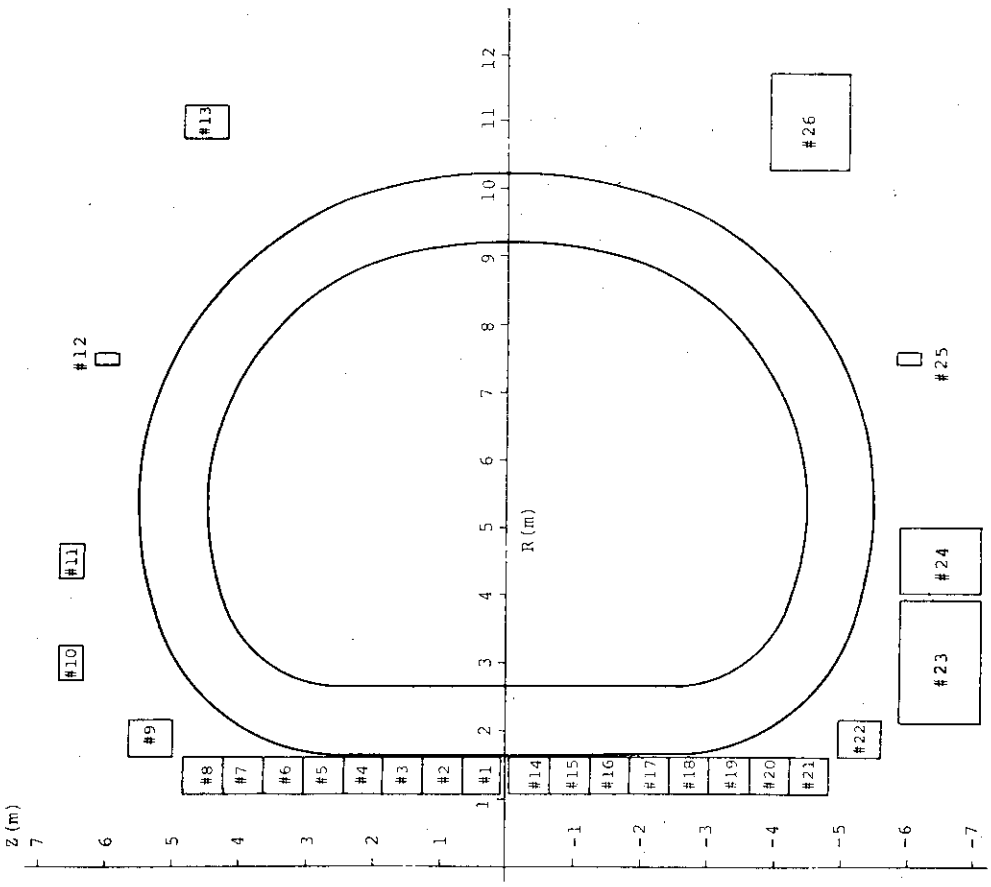

Fig. XI-3-4 Poloidal coil location for divertor operation (Case 4a)

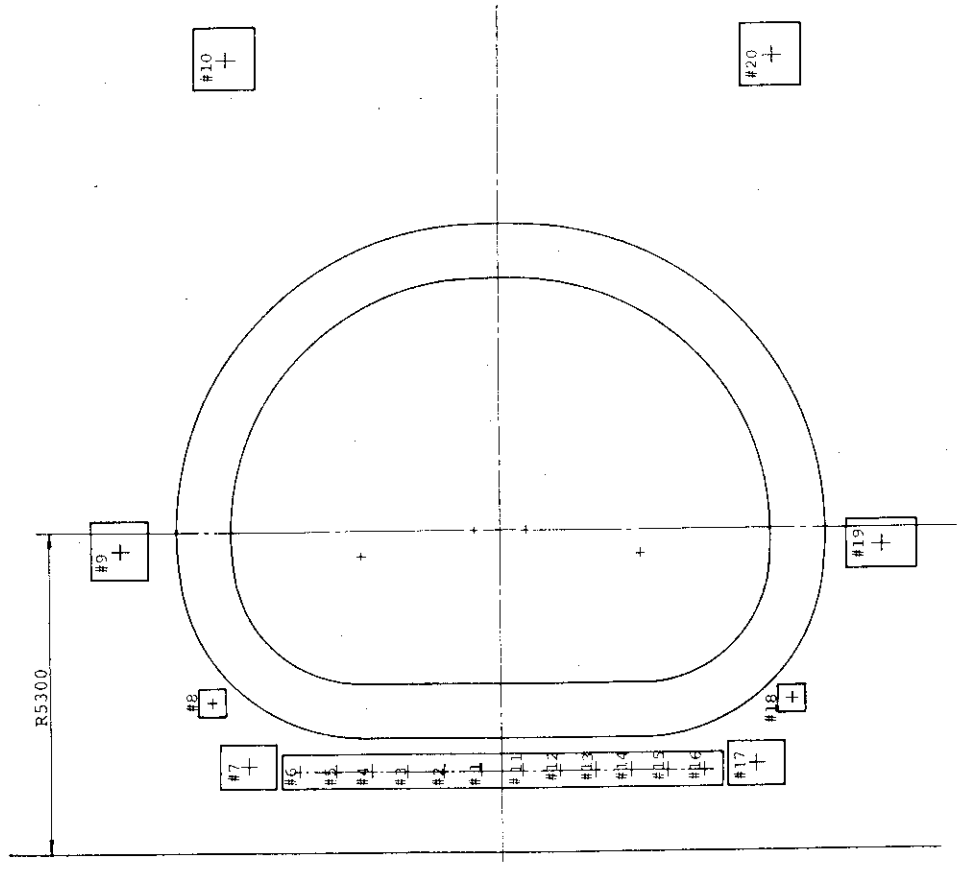

Fig. XI-3-3 Poloidal coil location for pump limiter operation (Case 3)

3.1.3 Poloidal divertor configuration

(Compiled in 3.1.2)

3.1.4 Design optimization (Universal-INTOR Concept)

Concerning the Universal-INTOR type operation, the PF coil arrangement, the ampere-turns, the stored energy and the out-of-plane force acting on TF coil are examined.

The PF coil arrangement is shown in Fig. XI-3-5.
The maximum radius of ring coil is R = 12.35 m.

The ampere-turns of the case of divertor operation and the case of limiter operation are shown in Table XI-3-11(a) and Table XI-3-11(b) respectively.

The total ampere turns are 83.06 MAT in divertor operation and 92.05 MAT in limiter operation.
The stored energy of PF coils are 15.6 MG in divertor operation and 5.8 MG in limiter operation.

The out-of-plane forces acting on TF coil by interaction of PF coil field are shown Fig. XI-3-6(a) for divertor operation and in Fig. XI-3-6(b) for limiter operation.

The overturning moments are M_Z = ±307 MN-m, M_R = 135 MN-m for divertor operation and M_Z = ±236 MN-m, M_R = 184 MN-m for limiter operation.

Table XI-3-11(a) Coordinate and ampere-turns of PF coils for Divertor operation (Case 5(a))

Coil No.	Block No.	Coil location R(M)	Coil location Z(M)	Turns No.	Time 0. S	5.0 S	11.0 S	211.0 S	226.0 S	246.0 S
1	1	1.350	0.350	72	4.006	-2.420	-2.972	-3.231	0.	4.006
2	2	1.350	0.950	72	3.413	-2.364	-3.047	-3.231	0.	3.413
3	3	1.350	1.550	72	3.666	-2.388	-3.015	-3.231	0.	3.666
4	4	1.350	2.150	72	3.682	-2.380	-3.038	-3.231	0.	3.582
5	5	1.350	2.750	72	3.544	-0.339	0.449	0.	0.	3.544
6	6	1.350	3.350	84	3.639	-4.348	0.461	0.	0.	3.639
7	7	1.350	3.950	92	4.486	-0.429	0.568	-4.621	0.	4.486
8	8	1.600	5.100	168	8.537	-0.817	1.081	0.	0.	8.537
9	9	3.500	6.050	108	1.361	3.824	5.466	0.	0.	1.361
10	10	4.950	6.050	100	0.491	-0.047	1.062	0.	0.	0.491
11	11	10.000	5.400	144	0.546	1.327	-2.931	1.000	0.	0.546
12	12	1.350	-0.350	72	4.029	-2.422	-2.969	-3.231	0.	4.029
13	13	1.350	-0.950	72	3.375	-2.360	-3.052	-3.231	0.	3.375
14	14	1.350	-1.550	72	3.736	-2.394	-3.176	-3.231	0.	3.736
15	15	1.350	-2.150	72	3.458	-2.368	-3.041	-3.231	0.	3.458
16	16	1.350	-2.750	72	3.781	-2.399	-3.000	-3.231	0.	3.781
17	17	1.350	-3.350	72	3.157	-0.302	0.400	0.	0.	3.157
18	18	1.350	-3.950	104	5.234	-0.501	0.663	0.	0.	5.234
19	19	1.600	-5.100	150	7.506	-0.718	0.951	0.	0.	7.506
20	20	3.150	-6.200	288	2.118	13.115	14.341	1.000	0.	2.118
21	21	5.650	-6.200	450	0.580	13.263	14.146	22.410	0.	0.580
22	22	12.350	-4.900	500	0.543	-17.689	-19.558	-24.953	0.	0.543
Plasma		5.300	0.400		0.	5.400	6.400	6.400	0.	0.

Table XI-3-11(b) Coordinate and ampere-turns of PF coils for limiter operation (Case 5(b))

Coil No.	Block No.	Coil location R(M)	Coil location Z(M)	Turns No.	Time 0. S	0.3 S	5.0 S	11.0 S	211.0 S	226.0 S	246.0 S
1	1	1.350	0.350	72	4.006	3.034	-2.337	-2.996	-3.910	0.	4.006
2	2	1.350	0.950	72	3.413	2.658	-2.162	-2.966	-3.745	0.	3.413
3	3	1.350	1.550	72	3.666	2.818	-3.165	-2.979	-3.816	0.	3.666
4	4	1.350	2.150	72	3.582	2.765	-2.212	-2.975	-3.793	0.	3.582
5	5	1.350	2.750	72	3.544	2.741	-2.201	-2.973	-3.782	0.	3.544
6	6	1.350	3.350	84	3.639	2.801	-2.229	-2.978	-3.808	0.	3.639
7	7	1.350	3.950	92	4.486	2.852	-1.320	-0.225	-1.249	0.	4.486
8	8	1.600	5.100	168	8.537	5.427	-2.512	-0.429	-2.377	0.	8.537
9	9	3.500	6.050	108	1.361	1.644	3.613	4.929	4.618	0.	1.361
10	10	4.950	6.050	100	0.491	1.091	3.869	4.972	4.860	0.	0.491
11	11	10.000	5.400	144	0.546	0.001	-3.997	-7.168	-7.293	0.	0.546
12	12	1.350	-0.350	72	4.029	3.049	-2.343	-2.997	-3.917	0.	4.029
13	13	1.350	-0.950	72	3.375	2.633	-2.151	-2.964	-3.735	0.	3.375
14	14	1.350	-1.550	72	3.736	2.863	-2.257	-2.983	-3.835	0.	3.736
15	15	1.350	-2.150	72	3.458	2.688	-2.175	-2.969	-3.758	0.	3.458
16	16	1.350	-2.750	72	3.781	2.891	-2.270	-2.985	-3.848	0.	3.781
17	17	1.350	-3.350	72	3.157	2.495	-2.087	-2.954	-3.674	0.	3.157
18	18	1.350	-3.950	104	5.234	3.327	-1.540	-0.263	-1.457	0.	5.234
19	19	1.600	-5.100	150	7.506	4.772	-2.208	-0.377	-2.090	0.	7.506
20	20	3.150	-6.200	288	2.118	2.262	4.040	5.335	4.851	0.	2.118
21	21	5.650	-6.200	450	0.580	1.285	4.492	5.412	5.280	0.	0.580
22	22	12.350	-4.900	500	0.543	-0.554	-7.785	-12.228	-12.352	0.	0.543
Plasma		5.300	0.400		0.	0.600	5.400	6.400	6.400	0.	0.

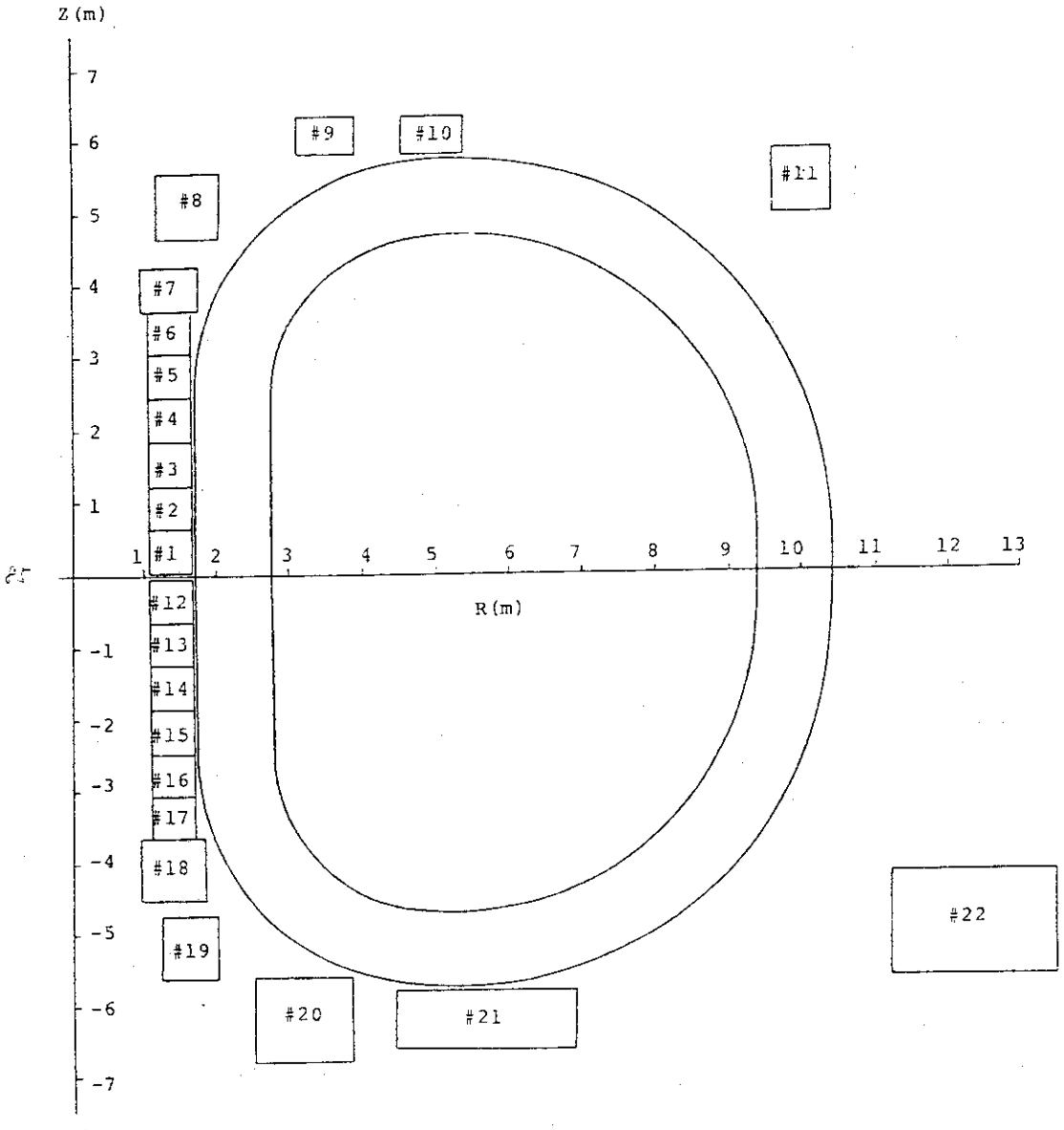

Fig. XI-3-5 Poloidal coil location (Case 5)

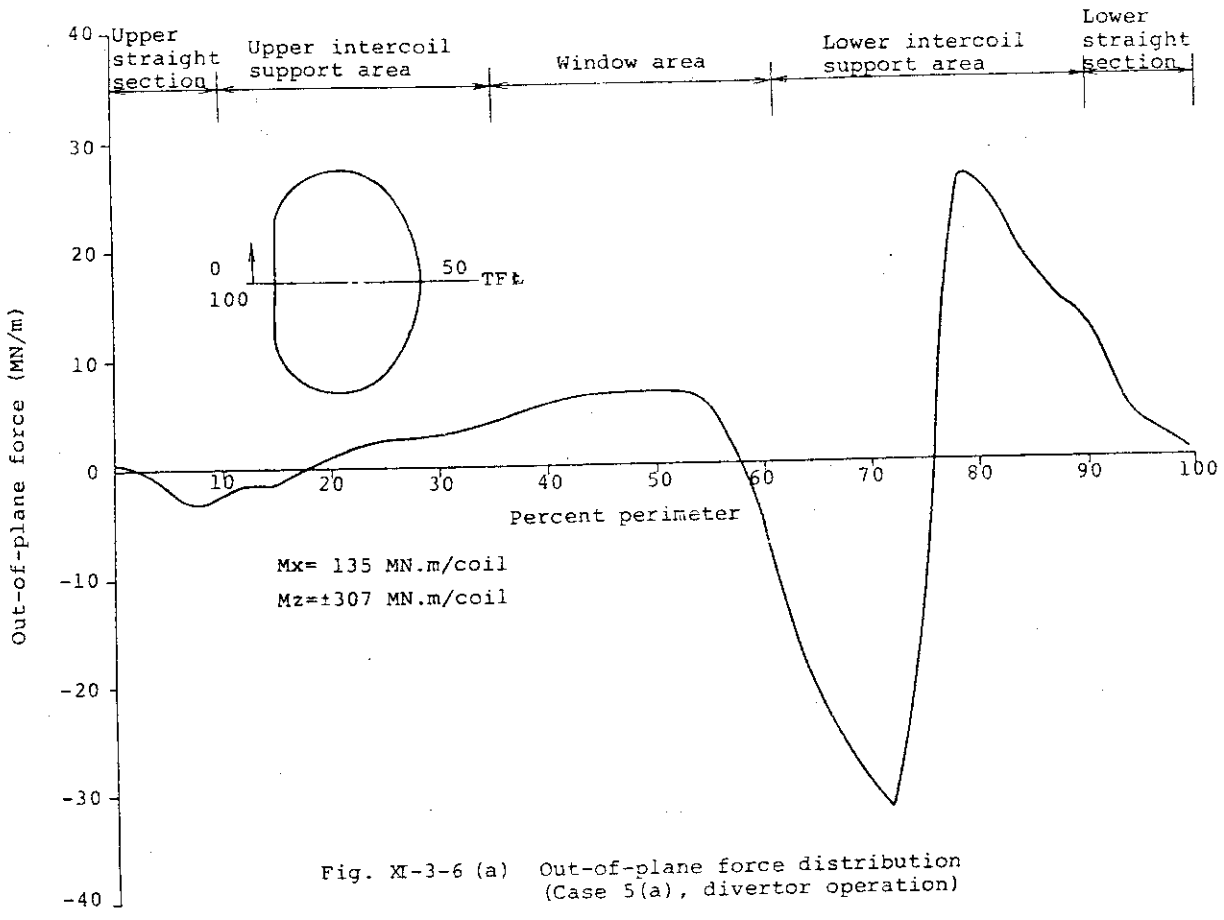

Fig. XI-3-6 (a) Out-of-plane force distribution (Case 5(a), divertor operation)

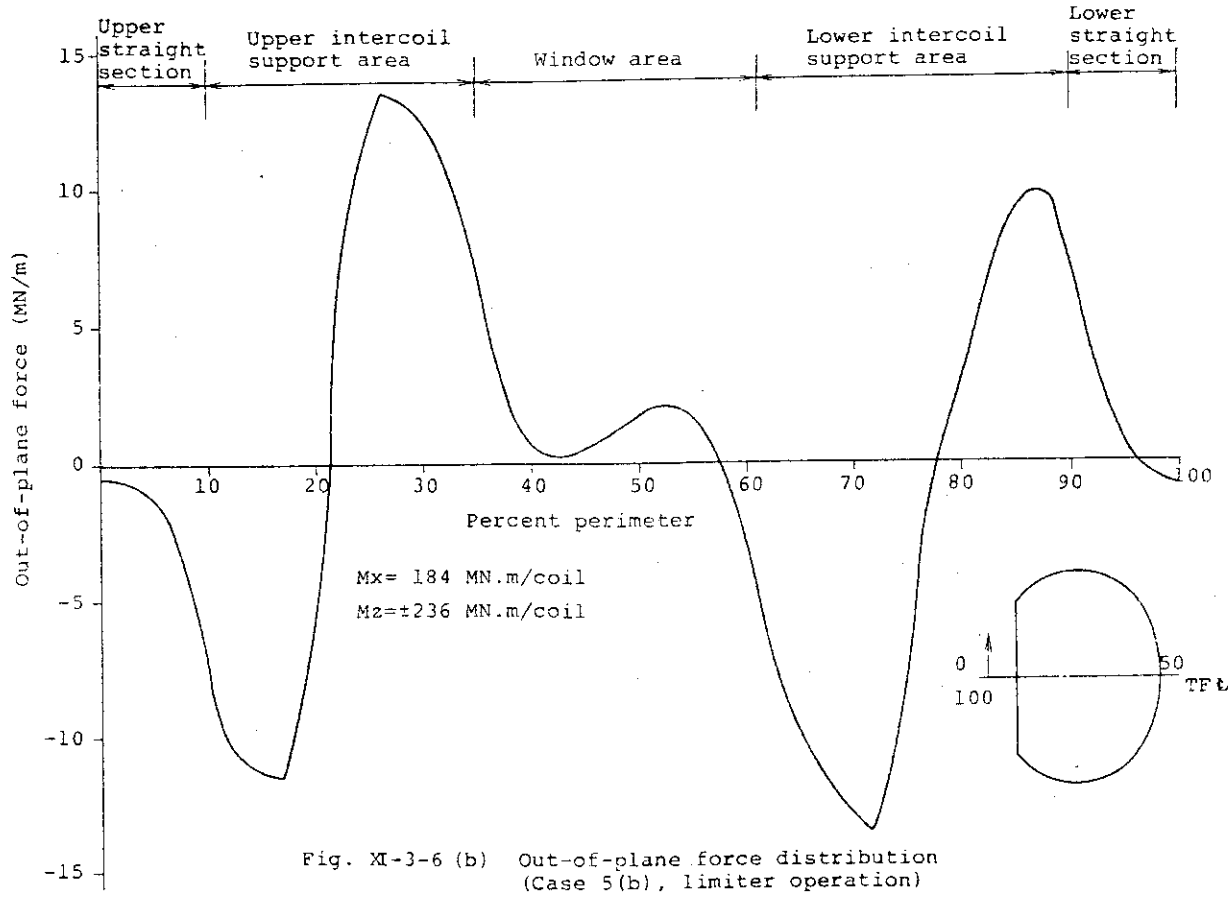

Fig. XI-3-6 (b) Out-of-plane force distribution (Case 5(b), limiter operation)

3.2 The design description

The major design features of the selected PF magnet are specified in Table XI-3-12 ∿ Table XI-3-14 and summarized as shown below.

(a) All PF coils are located outside of TF coil.

(b) A pool boiling system is employed mainly because of efficient cooling and matured technology.

(c) Copper stabilized NbTi superconductor is used.

Three composite superconducting material composed of NbTi, copper and CuNi is used for the achievement of low AC losses. (See Fig. XI-3-7)

(d) Rated maximum conductor currents is 53.8kA and the critical current is 85kA.

(e) A liquid helium vessel is intended to be made of fiber reinforced plastic (FRP) instead of conducting material such as stainless steel in order that the excessive eddy current losses can be avoided.

(f) The maximum field of 7.1T appears on coil #7. The maximum rate of magnetic field change on PF coil is 6.4T/S at coil #7.

(g) Electromagnetic force acting on conductor is mainly supported by both stainless steel mandrel and the stainless steel tape inserted between turns.
The mean current density of the coil including the SS support is 12.1A/mm^2 ∿ 16.5A/mm^2.

(h) The conductor is a flat cable type conductor consisting of 31 subcables wrapped around a central stainless steel mandrel core.
The conductor has the size of 130mm by 18mm.

(i) The conductor is designed so as to satisfy cryogenic stability against the fast field sweep and AC losses such as hysteresis loss, coupling loss and eddy current loss.

(j) The coil is subject to the AC loss due to the changing field. The loss occurs in the superconductors, the coil support and the helium leak shield if used for PF coils.
(if the helium leak shield is used, it is expected that the AC loss might be great due to one turn loop, even though the thickness is as thin as possible.)
If the helium leak shield is not used, the average AC loss of all PF coils amounts to 3.8kW.

(k) The stress produced in SS tape inserted between SS mandrel and turn, is 290MPa maximum which is lower than the allowable value.

Table XI-3-12 Specification of poloidal field coil system

Number of coils	24
Concept of power supply	hybrid
Magnetomotive force/coil	0.421 ∿ 13.69 (MAT)
Cooling method	pool boilding
Superconducting cable	NbTi + CuNi + Cu
Operating current	53.8 (kA)
Critical current	85 (kA)
Average current density	12.1 ∿ 16.5 (A/mm^2)
Maximum field	7.1 T
Coil case material	FRP
Support concept	outer coils supported by TF coils and inner coils by the center post

Table XI-3-13 Parameters of superconductor

1.	Final Level	
(1)	Operating current	53.8 kA
(2)	Critical current	85 kA
(3)	Cable size	130mm × 18mm
(4)	Number of subcables	31
(5)	Mandrel core size	115mm × 4mm
(6)	Cable twist pitch	1300 mm
(7)	Effective perimeter	520 mm
(8)	Conductor current density	23 A/mm^2
(9)	Winding current density	14 A/mm^2
(10)	Maximum field	7.1 T
2.	Subcable	
(1)	Subcable diameter	8 mm
(2)	Number of strands	6
(3)	Core strand material	Stainless steel
(4)	Twist pitch	50 mm
3.	Strand	
(1)	Strand diameter	2.67 mm
(2)	Number of NbTi filaments	6156
(3)	Twist pitch	40 mm
(4)	Surface treatment	Formval
(5)	Number of bundles	18
(6)	NbTi : Cu : CuNi	1 : 9.58 : 1.04
4.	Bundle	
(1)	Bundle diameter	0.338 mm
(2)	Number of filaments	342
(3)	Surface CuNi thickness	11.7 μm
(4)	NbTi : Cu : CuNi	1 : 1.33 : 1.04
5.	Filament	
(1)	NbTi filament diameter	10 μm
(2)	OFHC thickness	2.1 μm
(3)	Surface CuNi thickness	1 μm
(4)	NbTi : Cu : CuNi	1 : 1.02 : 0.59

Table XI-3-14 Conductor characteristics

(1)	Strand loss time constant	2.88 ms
(2)	Subcable loss time constant	0 ms
(3)	Total loss time constant	1.28 ms
(4)	Cu resistivity	5×10^{-10} Ωm
(5)	Heat generation	1.96 w/cm
(6)	Effective perimeter	52 cm
(7)	Required heat transfer	0.37 w/cm^2

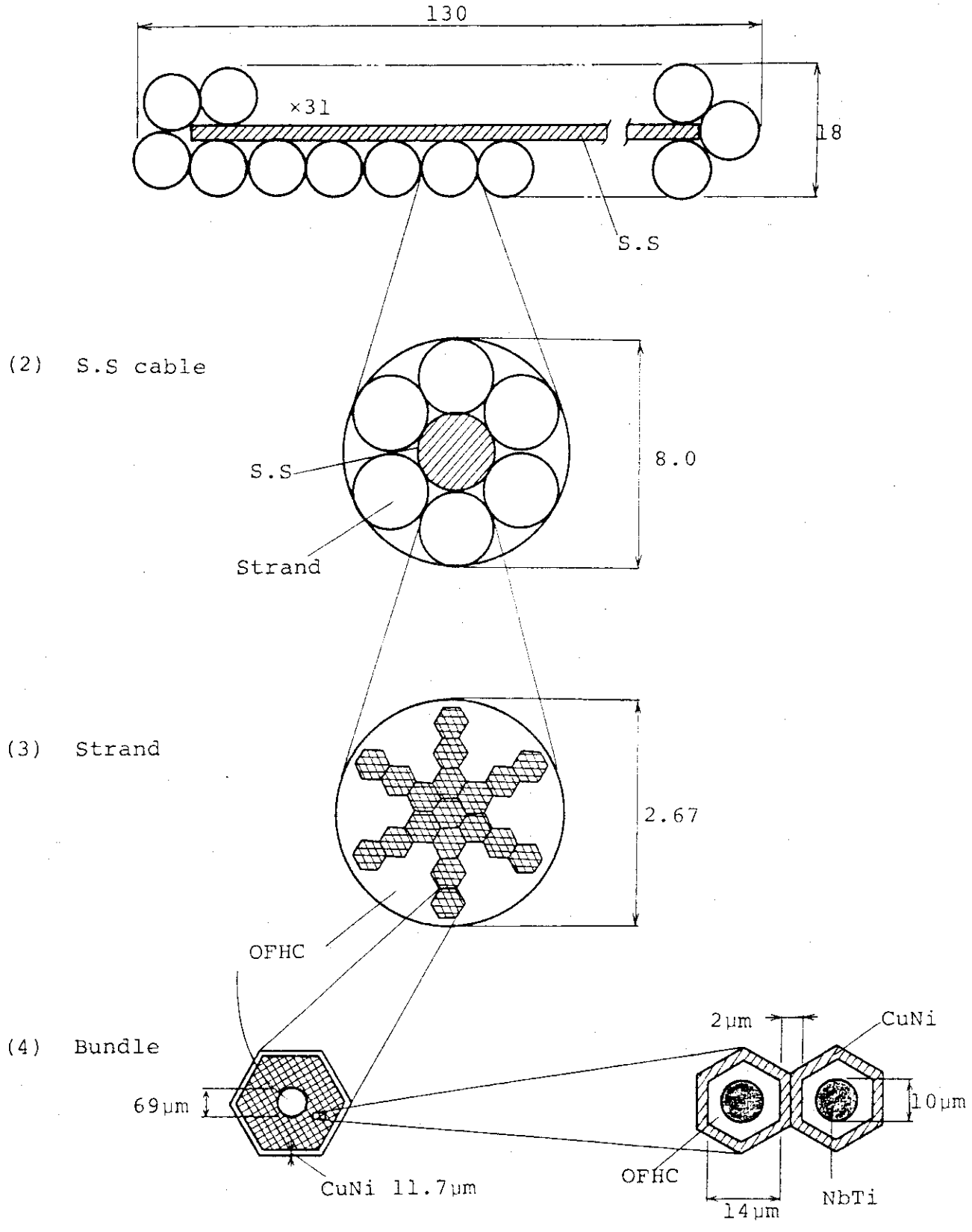

Unit: mm except noted above

Fig. XI-3-7 PF coil conductor

3.3 Supporting analysis

The mechanical stresses due to the electromagnetic forces on PF coils are considered. It is assumed that the hoop force is supported only by the stainless steel reinforcement.

Figure XI-3-8 shows the two-dimensional axisymmetric stress analysis model and loading condition for PF coils. The stainless steel reinforcement is modeled with the two-dimensional plane element. And the superconductor cable and interturn insulation are modeled with the truss element, because the cable and insulation are assumed not to support the hoop force but to carry only the radial load.

Figure XI-3-9 ∿ Fig. XI-3-12 show the stress distribution of PF coils for case 1. Fig. XI-3-13 ∿ Fig. XI-3-16 show the stress distribution for case 2. And Fig. XI-3-17 ∿ Fig. XI-3-20 show the stress distribution for case 4a. The maximum stresses for case 1, case 2 and case 4a are 290 MPa, 280 MPa and 325 MPa, respectively.

Ultimate strength, yield strength and design stress intensity of stainless steel reinforcement (SS316L) are 1580 MPa, 670 MPa and 440 MPa. The maximum stress intensities of reinforcement for three cases are below the allowable value.

The design fatigue stress of SS316L for the design cyclic number of 10^4 is 310 MPa.

The equivalent cyclic stress amplitude is given by

$$S_{eq} = \frac{S_{alt}}{1 - \frac{S_{mean}}{S_u}}$$

where,

S_{alt} : Cyclic stress amplitude

S_{mean} : Modified mean stress

S_u : Ultimate strength

The equivalent maximum cyclic stress amplitudes for case 1, case 2 and case 4a are 160 MPa, 154 MPa and 182 MPa, respectively. These cyclic stress amplitudes are below the design fatigue stress of 310 MPa.

The out-of-plane force is assumed to be supported by stainless steel support structure attached to helium vessel of FRP, because the bending stiffness of conductor and stainless steel tape inserted between turns is felt to be small.

The bending stress (σb) of PF support structure due to the out-of-plane force can be obtained from the following equation.

$$\sigma b = \frac{M}{Z}$$

where

$$M = \frac{W\ell^2}{8}$$

$$W = \frac{F_z}{2\pi r}$$

Fz = Out-of-plane force

r = Radius of PF coil

ℓ = Supporting span

z = Section modules of support structure

The bending stresses of 50 mm thick support structure are about 50 MPa in the largest ring coil. This stress is below the allowable stress.

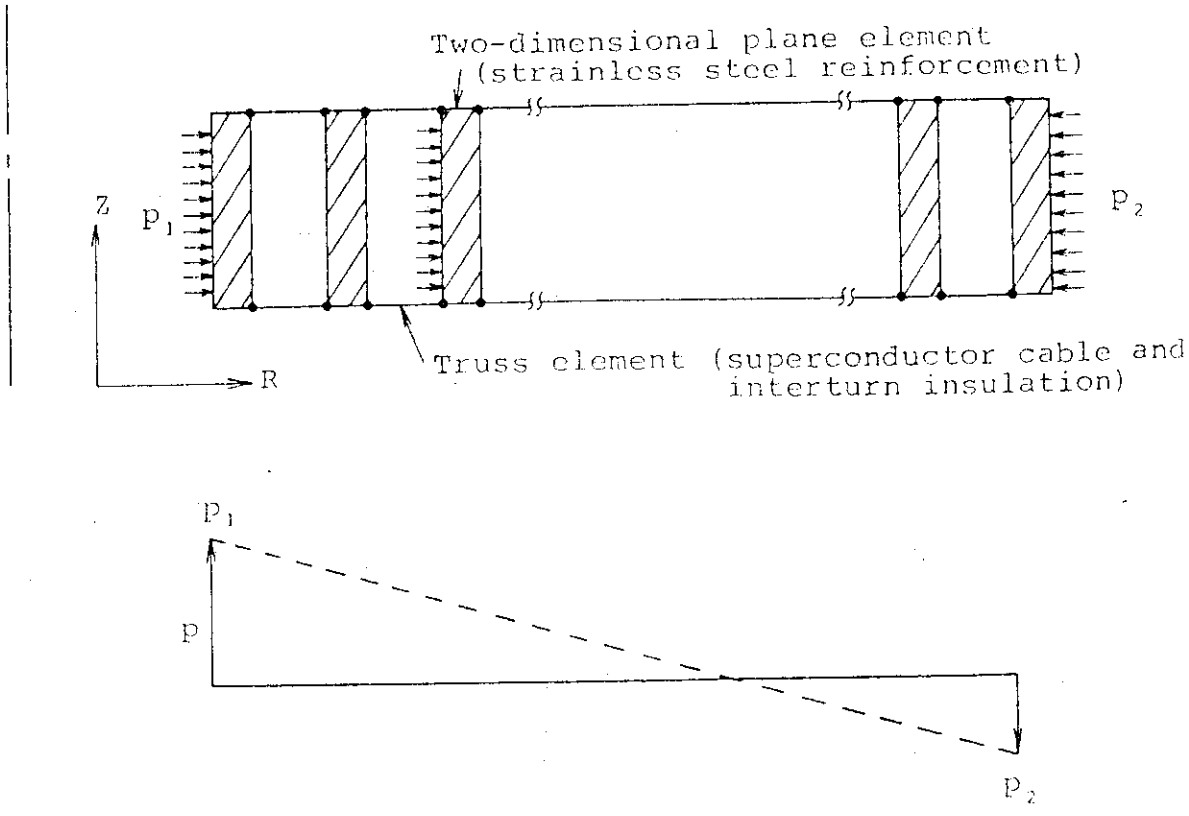

Fig. XI-3-8 Two-dimensional axisymmetric stress analysis model and loading condition for PF coils

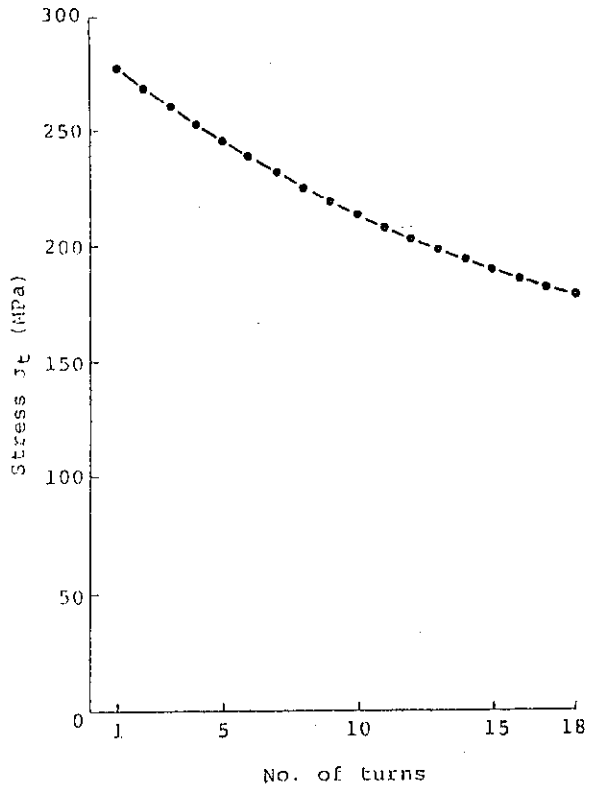

Fig. XI-3-9 Distribution of stress in radial direction of No.1 coil (Case No.1)

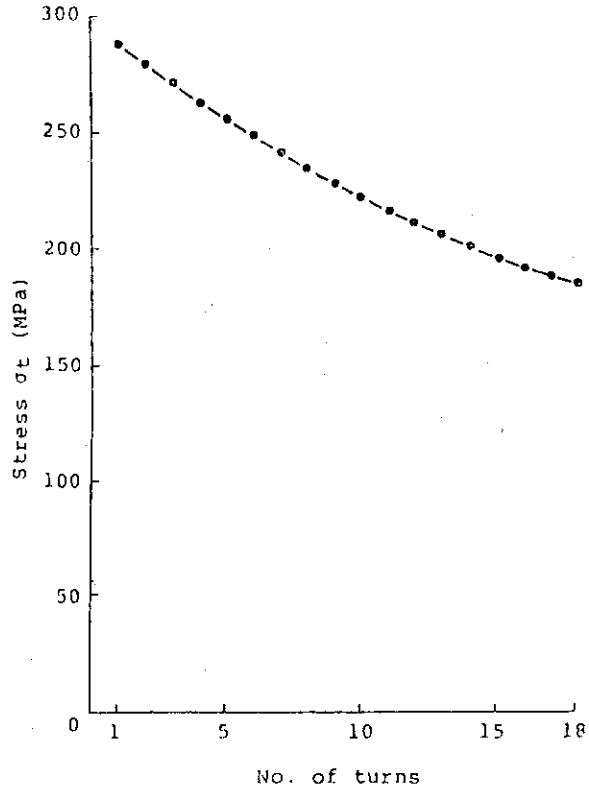

Fig. XI-3-10 Distribution of stress in radial direction of No.7 coil (Case No.1)

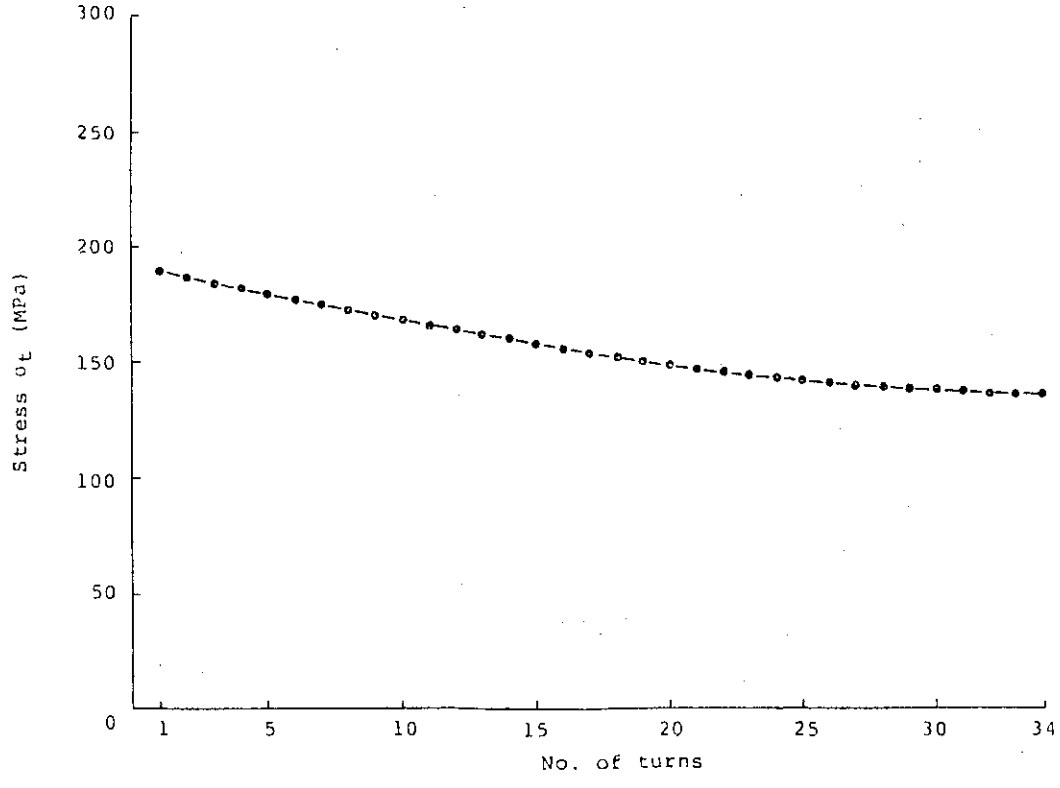

Fig. XI-3-11 Distribution of stress in radial direction of No.22 coil (Case No.1)

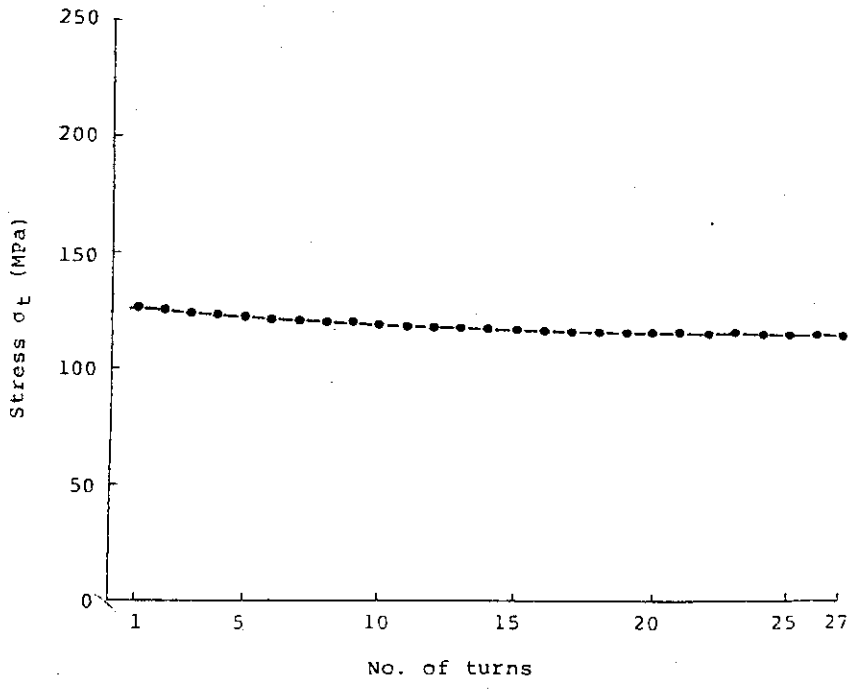

Fig. XI-3-12 Distribution of stress in radial direction of No.24 coil (Case No.1)

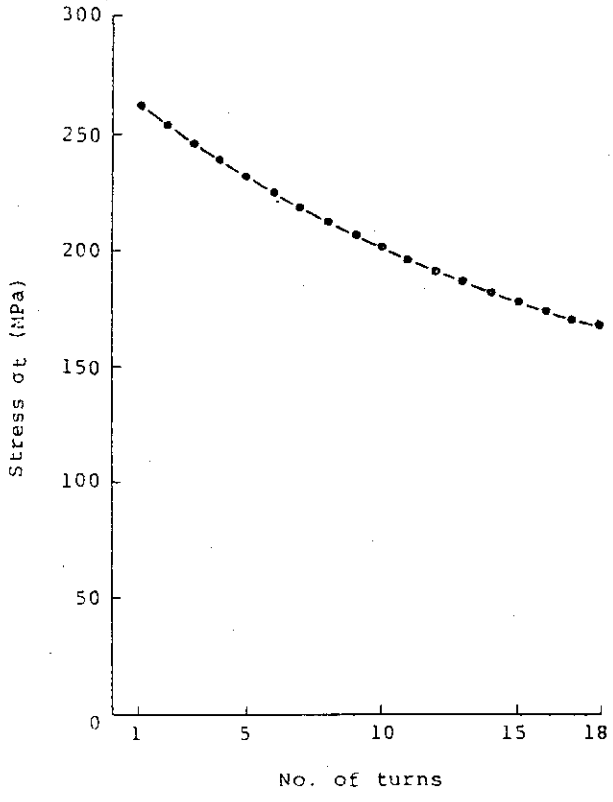

Fig. XI-3-13 Distribution of stress in radial direction of No.1 coil (Case 2)

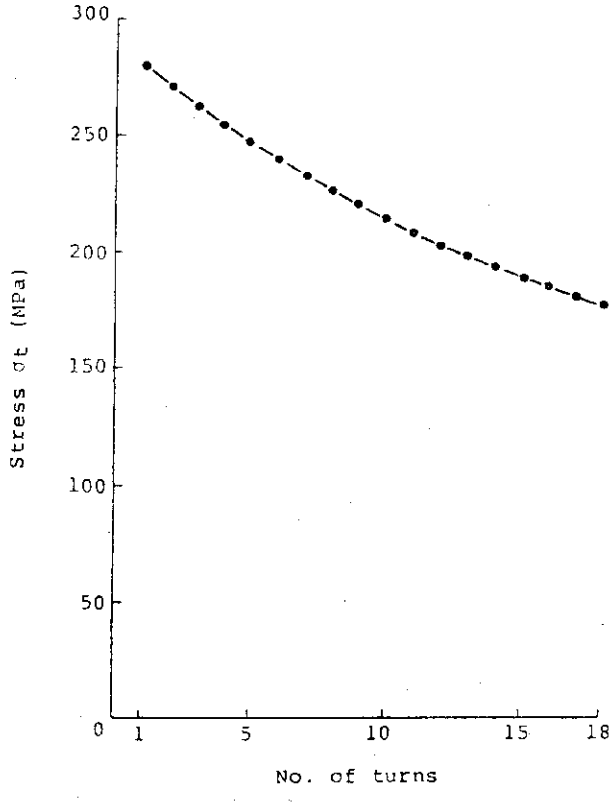

Fig. XI-3-14 Distribution of stress in radial direction of No.7 coil (Case 2)

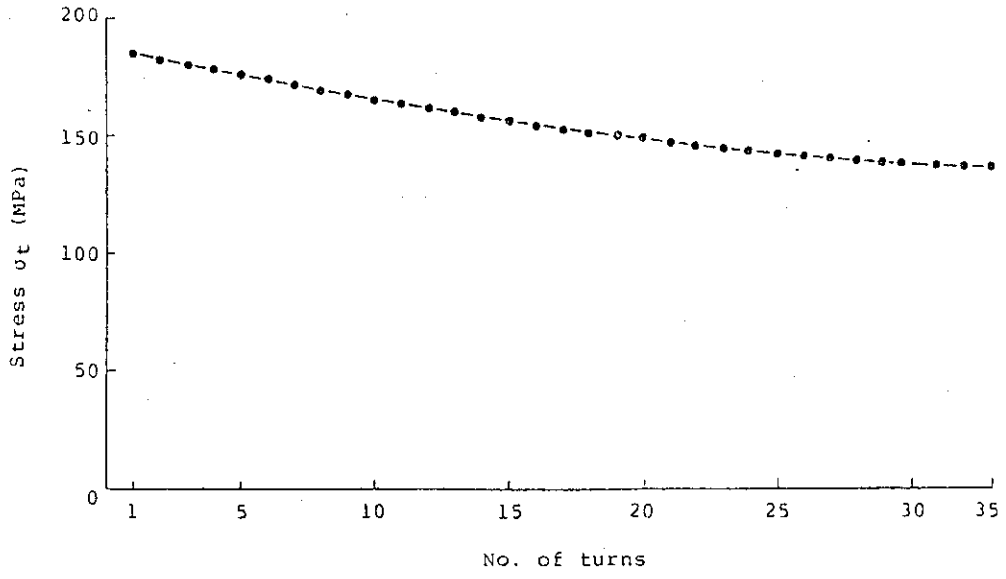

Fig. XI-3-15 Distribution of stress in radial direction of No.22 coil (Case 2)

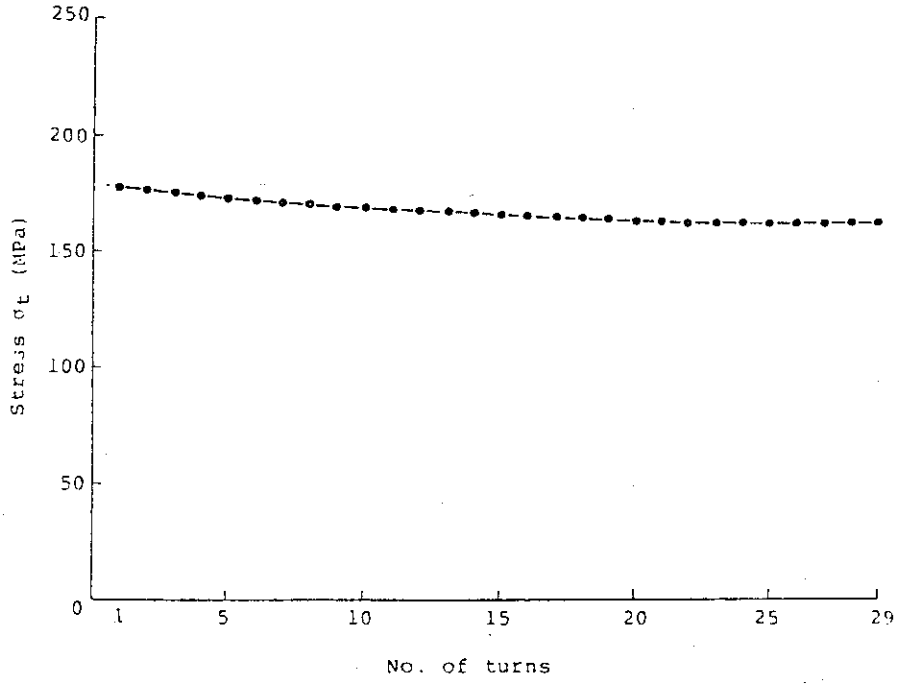

Fig. XI-3-16 Distribution of stress in radial direction of No.24 coil (Case 2)

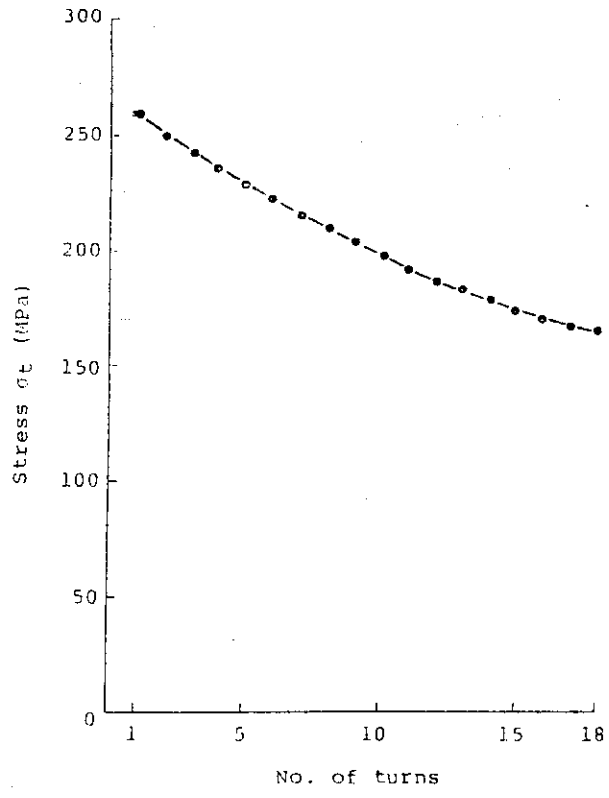

Fig. XI-3-17 Distribution of stress in radial direction of No.1 coil (Case 3)

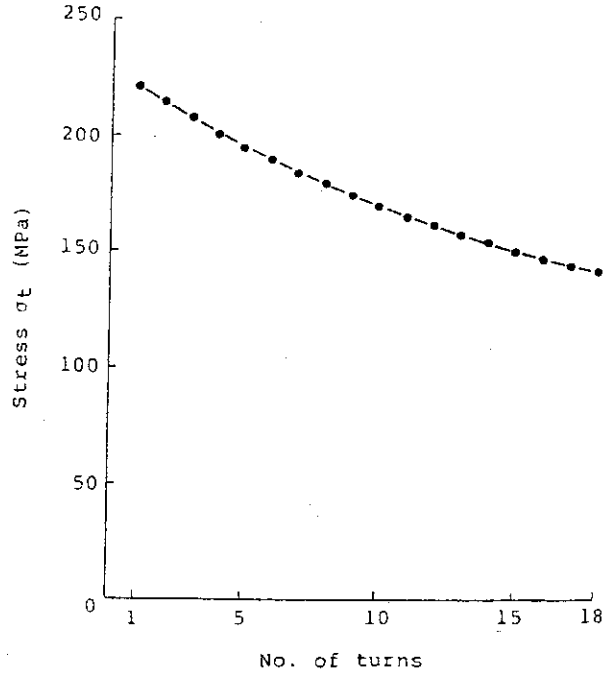

Fig. XI-3-18 Distribution of stress radial direction of No.8 coil (Case 3)

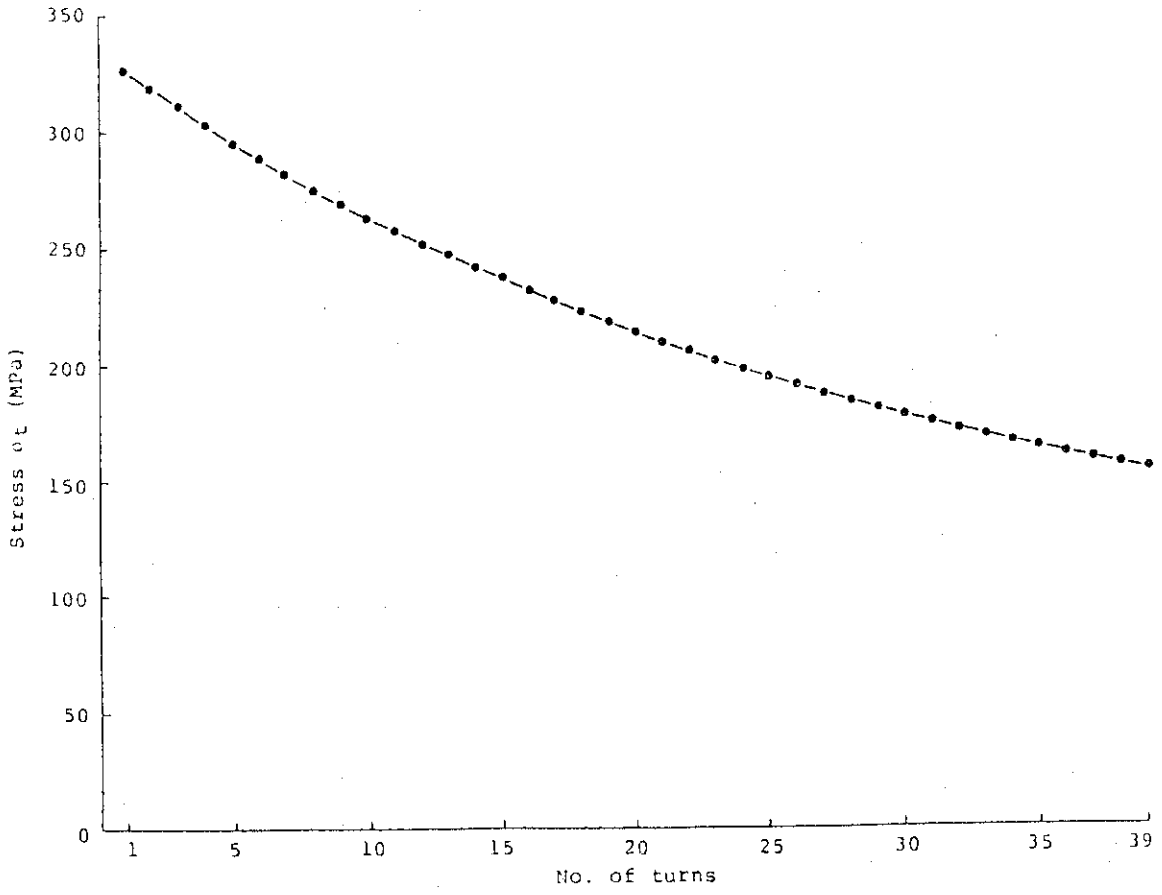

Fig. XI-3-19 Distribution of stress in radial direction of No.23 coil (Case 3)

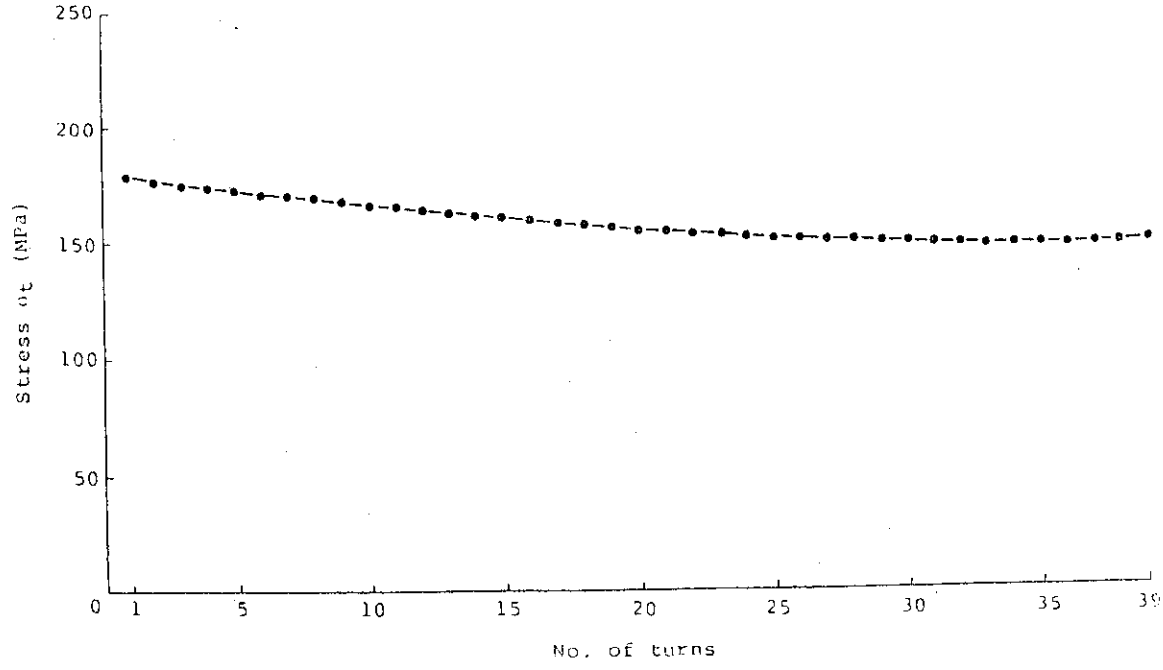

Fig. XI-3-20 Distribution of stress in radial direction of No.26 coil (Case 3)

4. Vacuum boundary

4.1 Design options

The choice of the vacuum boundary configuration should be made according to the consideration taken for the vacuum boundary technical issues such as,

1) Safety
2) Reliability
3) Maintenability
4) Producibility and cost
5) Torus one turn resistance
6) Penetration and accessibility
7) Influence of bake out
8) Influence of electromagnetic force

The comparison study with respect to the above issues are carried out for five following vacuum boundary configurations.

The following options were identified and discussed:

(1) Separate vacuum boundaries with air in-between (Double plasma vacuum boundary). This option is schematically indicated in Fig. Ⅺ-4-1. In this design concept dielectric breaks are backed by double bellows, and field welded joints are sealed by double welded seals to minimize the potential for a leak into the plasma chamber and preclude tritium permeation into the reactor building. The Phase 1 design employs this concept.

(2.) Simplified separate vacuum boundaries with air in-between - (simple plasma vacuum boundary). This option is schematically indicated in Fig. XI-4-2
It is similar to option 1, except that the dielectric breaks are backed by single bellows and field welds can be backed by welded seals.

(3.) Single combined vacuum boundary

This option is schematically indicated in Fig. XI-4-3.
A single vacuum boundary separates the plasma chamber from the TF coil assembly in this option.

(4.) Double vacuum boundary integrated in semi-permanent torus segments, with segmented interspaces.

This option is schematically indicated in Fig. XI-4-4.
This concept is similar to option 3, except that double wall boundary with an intermediate vacuum replaces to single wall in option 3.

(5.) Separate vacuum boundaries with intermediate vacuum in-between (with two separate vacuum closures).

This option is schematically indicated in Fig. XI-4-5.
This concept is also similar to option 3, except that the intermediate vacuum is extended across the face of the torus by the installation of an outboard closure (door) in the open space between adjacent TF coils.

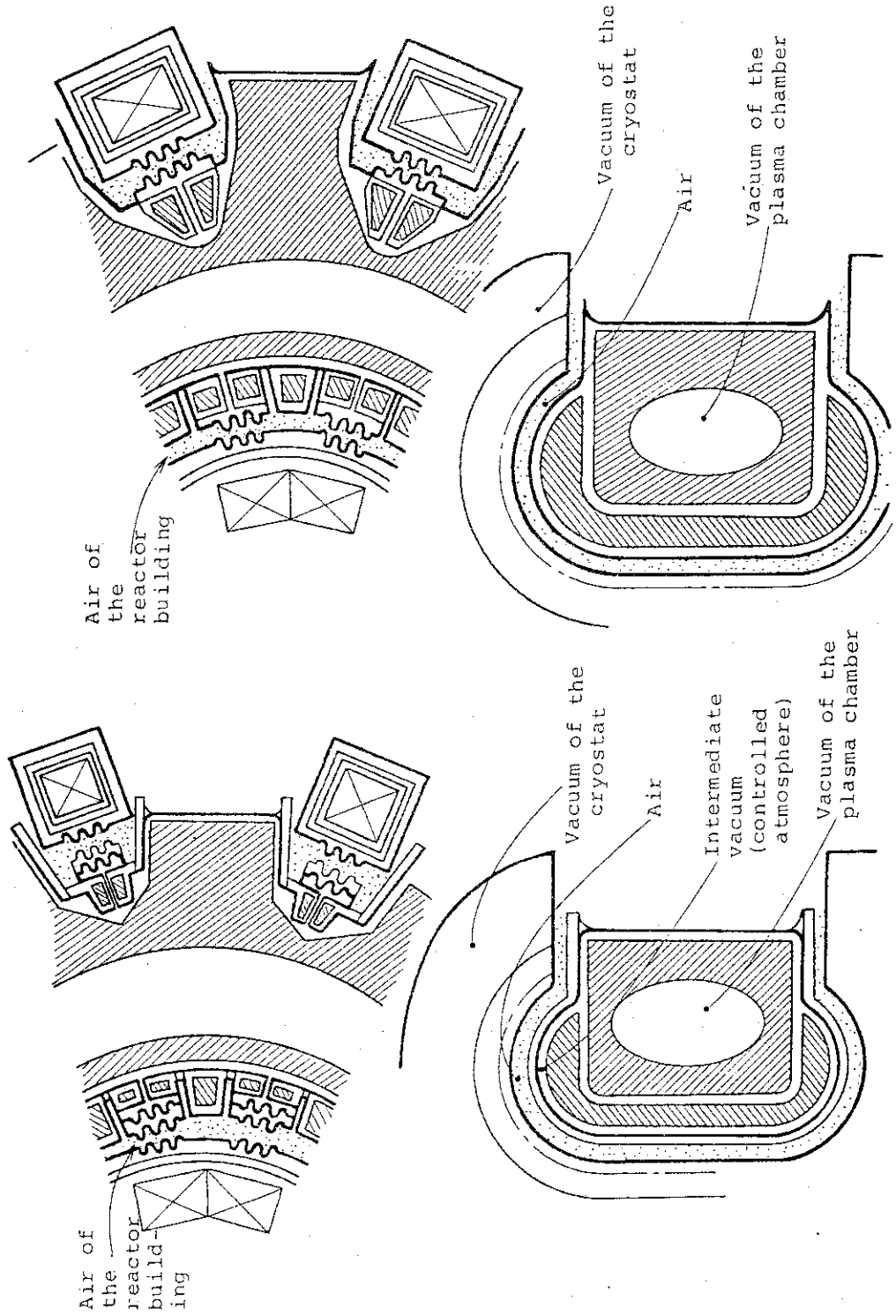

Fig. XI-4-1 ① Separate vacuum boundaries with air between

Fig. XI-4-2 ② Simplified separate vacuum boundaries with air in between

Reference

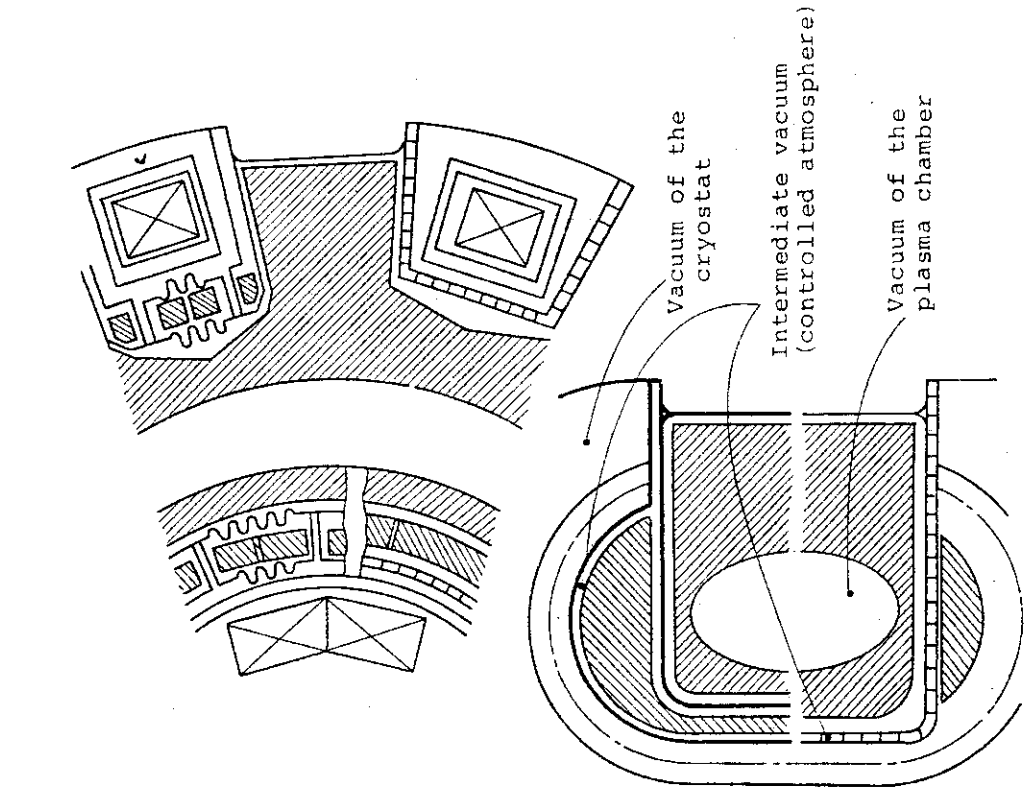

Fig. M-4-4 ④
Double vacuum boundary integrated on semi-parmanent torus segments, with segmented interspaces

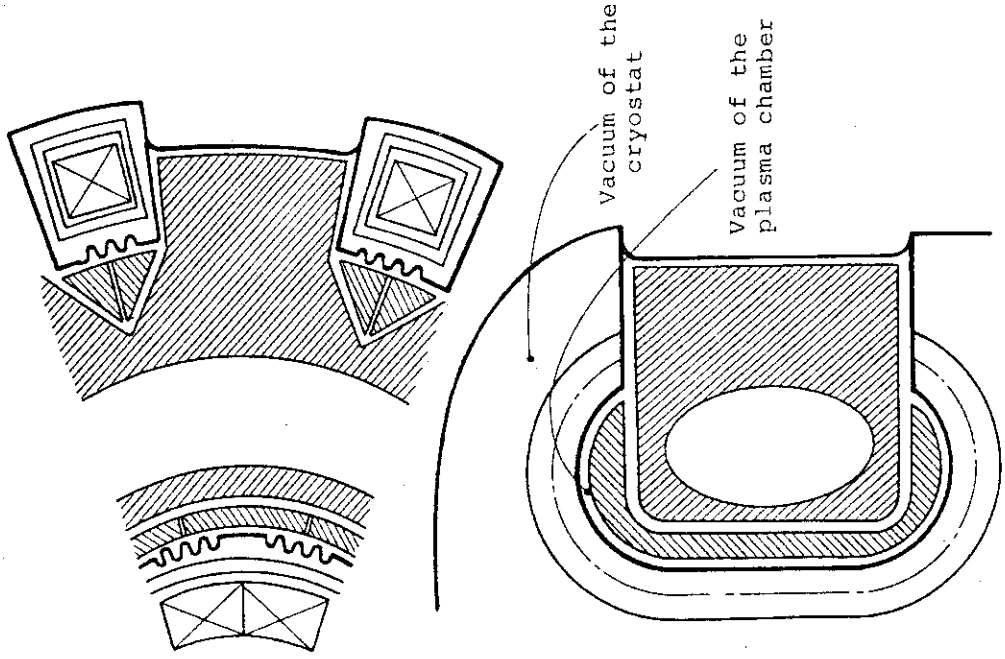

Fig. M-4-3 ③
Single combined vacuum boundary

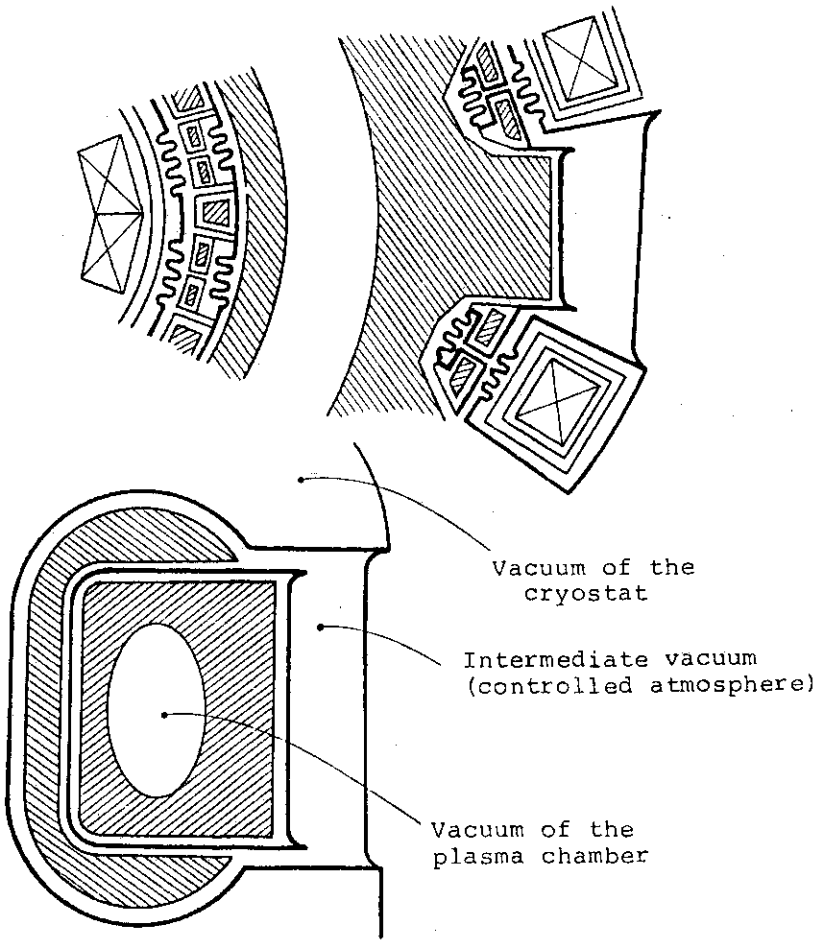

Fig. XI-4-5 ⑤
Separate vacuum boundaries with intermediate vacuum in between with two separate vacuum closures

4.2 Evaluation and Selection

(1) Safety, reliability

(a) Influence on superconducting coils

o Configuration of bellows

The cryostat of option ① consists of single bellow. The plasma vacuum boundary of option ② consists of single bellow.
Adoption of double bellows in these two concept requires more space necessary for one bellow 70mm.
The options ④ and ⑤ consist of double bellows.

o Influence of the rupture of bellows

With respect to the options ① and ② , the temperature elevation of the superconducting coil due to air penetration evaporates the liquid helium in coil case and increase the pressure in coil case which leads to distruction of the rupture disk.
The rapid elevation of temperature of the superconducting coils induces a relatively high thermal stress which exceeds possibly the allowable value of mechanical strength.
On the other hand, concerning the option ③ and ④ , as the bellows is facing to the vacuum boundary, the rupture of bellows do not accompany the elevation of temperature.

However, the bellows should be installed at the access port in order to absorb the thermal displacement produced by bake out. As the bellow is facing to the atmosphere, the rupture of this bellow induces a penetration of air and consequently the elevation of the S.C. coil temperature.

(b) Tritium leakage (by rupture of bellows)

Concerning the concepts ① and ② , the rupture of the bellows in plasma vacuum boundary bring about the tritium diffusion in reactor room. The tritium will be evacuated by emergency tritium processing system.

Concerning the concept ③ and ④ , when the tritium leakage takes place from the bellow in plasma vacuum boundary, the greater part of the tritium is absorbed by He coil case. Therefore, the tritium elimination system should be equipped in vacuum system of the belljar. This tritium elimination system will be operated mainly in time of elevation of coil temperature.

This kind of accident is, however, not frequent. Besides, no person is in the reactor room during reactor operation.

It seems that an exaggerated account should not be given to the accident of tritium leakage.

(c) Tritium leak (permeation through bellows)

Tritium permeation rate depends mainly on the temperature of bellows through which the tritium permeates.

The temperature of the bellows is determined from the nuclear heating of the bellow and its cooling method. The comparative study on five concepts are summarized in Table XI-4-2.

(d) Shielding ability

Shield thickness for inner side of TF coil depends on the space required for the bellows. It concerns the space necessary for installation of bellows in major radial direction of the device.

Available space of shield for each concept is shown in Table XI-4-1.

(2) Maintenability

(a) Accessibility to cryostat

In option ① and ② , the access to the cryostat is possible after disassembling the shielding structures. This maintenance operation is classified as large scale repair.

On the other hand, in option ③ and ④ , the access to the cryostat is possible after retraction of the blanket. This maintenance operation is classified as medium scale.

However, if the bellows is installed behind the shield, the shield structure should be disassembled in order to access the bellow. This maintenance operation should be classified as large scale.

(b) Leak detection

In option ① , the leak test of the double bellows in plasma vacuum boundary can be carried out independently for each toroidal part, however, the leak test of the bellows of cryostat should be performed as a whole torus.
In option ② , the leak test of both the bellows in the plasma vacuum chamber and that of cyostat should be performed as a whole torus.
In option ④ , ⑤ , the leak test of the bellows in both the plasma vacuum chamber and the cyostat is possible if the space between the plasma chamber and cryostat is evacuated and connected to the leak detector. However, in option ⑤ , the detection of leak spot is difficult.

(c) Requirement of temperature elevation of S.C coil at the maintenance operation

For maintenance operation such as replacement of shielding structure, the elevation of the temperature of S.C coil is required for five options because of accessibility and space necessary for retraction.

For maintenance operation such as replacement of the blanket and limiter, the elevation of superconducting coil temperature is not required for five options.

In options ③ and ⑤ , there would be a possibility that the unexpected accident such as rupture of bellows or lip seals due to bad manipulation of maintenance equipment causes an elevation of superconducting coil temperature which leads to the coil damage.

(4) Manufacturing and cost

(a) Cost down by reduction of the reactor size

The options ③ and ④ can save more space than the options ① and ② by about 10cm in major radius direction. As the plasma major radius 5.3m is fixed, this free space can not contribute to the reduction of the reactor size.

(b) Installation time and easiness of installation

As the options ③ and ④ have only one boundary common to plasma and superconducting coil, the time required for installation is shorter and the installation is easier.

(5) One turn resistance

In order to obtain 0.2mΩ torus resistance, the bellows in option ③ requires the lowest resistance (length of the bellows is short), on the other hand, the bellows in option ① requires the highest resistance.

(6) Penetration and access

As the option ⑤ has double vacuum boundaries, the accessibility is very poor and the penetration of pipes through these boundaries is very complex.

(7) Influence of bake out

The bake out is necessary to evacuate the trace of water at the surface of the plasma vacuum boundary. Analysis of thermal displacement and thermal stress for plasma vacuum boundary and cryostat are carried out. The temperature of the torus at the time of bake out is assumed to be 150°C.
The peak value of 410MPa appeared at the edge exceeds slightly the allowable stress of SS304 of ASME criterion.
On the other hand, the option ① and ② does not suffer the thermal stress due to thermal displacement.

≪ Conclusion ≫

Comparisons among five optional vacuum boundaries are listed in Table XI-4-3.

The option ② , simplified separate vacuum boundary, is selected in our design from the following reasons mentioned below.

(1) Maintenability

The option ⑤ has double vacuum boundary which complicates the replacement procedure of blanket and pumped limiter. In particular, the piping through double vacuum boundaries is highly complex. Therefore, the option ⑤ is rejected from our design.

(2) Problem of bake out

Concerning the thermal displacement at the bake out in options ① and ② , there is no problem because the plasma vacuum boundary and the cryostat are independent. In options ③ and ④ , the belljar and the plasma vacuum boundary are connected at the access port where the thermal stress exceeding the allowable criteria appears. However, the bellows installed in belljar will be available in order to reduce this stress. In this case, the bellow is forming a boundary to atmosphere.

(3) Reliability

It is desirable that the components which constitute the reactor should function independently from the other components. It is fundamental from the view point of the safety and reliability that an unexpected accidents should not propagate to other components. From these standpoints, the options ③ and ④ will be rejected because of the possible propagation of unexpected accident.
On the other hand, in option ① and ② , there is no propagation of accident. The components are independent from the structural and functional points.

(4) Shielding ability

In option ① and ② , the option ② is disposable more space for shield structure.
Therefore, the option ② is selected to be reasonable

(2) Tritium permeation

The examinations on the temperature of bellows and the tritium permeation on five type of vacuum topologies are carried out.

The results are shown in Table XI-4-1 and Table XI-4-2.

Table XI-4-1

	① Separate vacuum boundary	② Simplified separate vacuum boundary	③ Single combined vacuum boundary	④ Double vacuum boundary	⑤ Separate vac. boundary with intermediate vac.
Schematic cross section between the inboard shield and TF coil	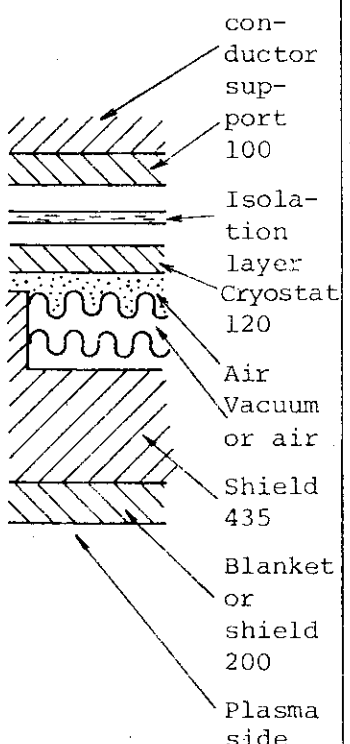	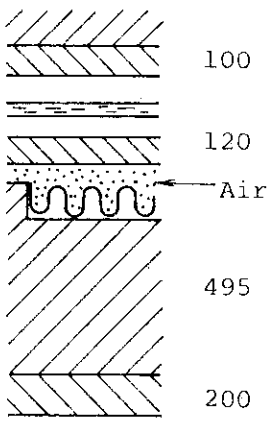	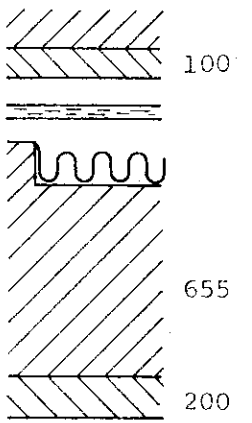	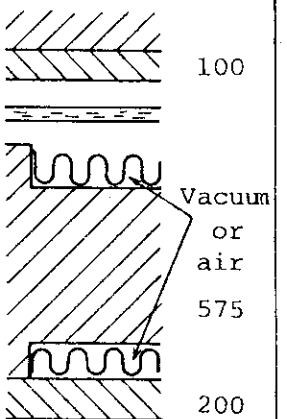	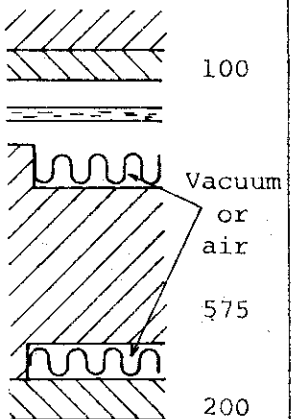
Thickness of shield	(635)	(695)	(855)	(200, 775)	(200, 775)
Thickness of bellows and	0.15, 12 convexities	0.15, 8 convexities	0.15, 5 convexities	0.15, 8 convexities	0.15, 8 convexities
Cooling	Radiation or air cooling	Air cooling	Radiation	Radiation or air cooling	Radiation or air cooling
Nuclear heating of bellow	4×10^{-3}W/cc	2×10^{-3}W/cc	2×10^{-4}W/cc	1.2W/cc 6×10^{-4}W/cc	1.2W/cc 6×10^{-4}W/cc

Table XI-4-2

	Plasma side			Isolation layer side
① Radiation	Plasma 105°C 6.8×10^{-2} Ci/day	⟹	Vacuum 114°C Recovery in vacuum system	Air
Air cooling	Plasma 70°C 1.2×10^{-2} Ci/day	⟹	Air 70°C Recovery in cooling system	Air
② Radiation + Air cooling	Plasma 73°C 7.9×10^{-3} Ci/day	⟹	——	Air
③ Radiation	Plasma 28°C 1.2×10^{-4} Ci/day	⟹	——	Vacuum
④ Radiation	Plasma 830°C 3.5×10^{4} Ci/day	⟹	Vacuum 33°C Recovery in cooling system	Vacuum
Air cooling	Plasma ∿ 150°C 3.3×10^{-1} Ci/day	⟹	Air 70°C Recovery in cooling system	Vacuum
⑤ is same as ④				

Table XI-4-3 Comparison of torus and vacuum boundary

			Weight factor	Case 1	Case 2	Case 3	Case 4	Case 5
1. Safety	1.1	Tritium leak	3	3	2	3	4	5
	1.2	Tritium permeation	4	4	2	3	4	5
2. Reliability	2.1	SC magnet system (in operation)	7	4	4	3	3	4
	2.2	Plasma chamber	5	4	3	3	4	3
	2.3	Shielding ability	8	2	4	5	3	3
	2.4	Influence of bake out	8	5	5	3	3	5
3. Maintenance	3.1	Accessibility to cryostat	3	3	3	4	4	3
	3.2	Leak detection (at shut down)	5	4	3	3	4	3
	3.3	Elevation of SC temperature	7	4	4	2	4	4
4. Manufacturing, Cost	4.1	Machine check-out time and cost down	7	3	4	5	4	4
5. Penetration & Access			9	5	5	5	5	1
				252	254	242	250	231

4.3 Design description

(a) The vacuum boundary of the plasma chamber is located on the inner wall of the shielding structure. This vacuum boundary is connected with the blanket access door through which the blanket is retracted. The concept of this vacuum boundary is shown in Fig. XI-4-6.

As the segment of the blanket or the limiter between the two toroidal coils is devided to several sectors, the T shaped seal will be necessary to seal these sectors. However, it is desirable to aboid the T shaped seal where the mechanical force is acting on. The T shaped seal can be aboided if we use the access port accompagnied with the access door which covers the outer face of shield segment between the two toroidal field coils, as shown in Fig. XI-4-6.
The vacuum seal is carried out around the access door without T shaped sealing.
On this access door called as blanket access door, the smaller opening door called as limiter access door is equipped. The sealing is also carried out around this limiter access door.

(b) The single cryostat is used for the toroidal field coils as well as for the poloidal field coils. This cryostat is equipped independently from the plasma vacuum chamber.
Cryostat for TF coil is shown in Fig. XI-4-7.

(c) Torus resistance

The simplified separate vacuum boundary is employed in this design. As the torus structure should have 0.2mΩ of one turn resistance, the bellows are equipped in the plasma vacuum vessel at the position just behind of each toroidal field coil, as shown in Fig. XI-4-8. These bellows are installed at the outer side of These bellows are installed at the outer side of the shield. With regard to the cryostat of the superconducting magnets, the bellows are also installed just behind each toroidal coil.

As the belljar type single cryostat is used for the toroidal field coils and the poloidal field coils, one turn resistance (0.2mΩ) of the part of belljar structure is sustained with help of the thin wall structure.

(a) One turn resistance

The basic configuration of the bellows is shown in the next figure.

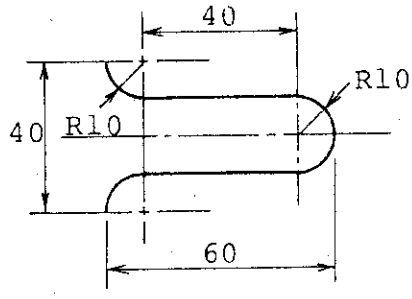

thickness: 1.5 mm
pich : 20 mm
height : 60 mm
Number of convexifies: 8

Basic configuration of bellow

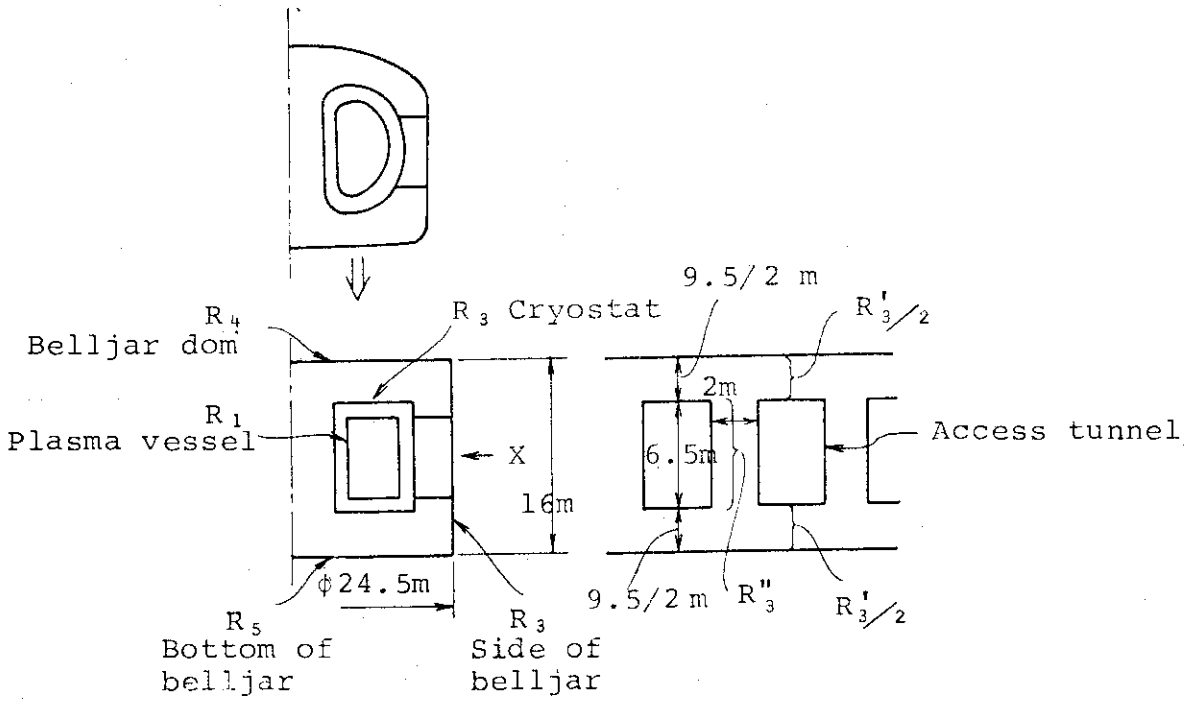

One turn resistance R is given as

$$\frac{1}{R} = \Sigma \frac{1}{Ri}$$

Ri is given as shown in the figure.

where

The resistance of plate is $Ri = \rho \frac{\ell}{a}$

ℓ: length

a: cross sectional area

t: thickness

The resistance of disk is $Ri = \rho \frac{2\pi}{t}$

The specific resistance of Inconel 625 is

$\rho = 129 \times 10^{-6}\ \Omega.cm$ (at room temperature)

The resistance of the outer side wall of belljar made with thin plate is $R_3' = 5.2 \times 10^{-3}\ (\Omega)$

$R_3'' = 2.4 \times 10^{-3}\ (\Omega)$

The resistance of the belljar dome and belljar bottom is R_4, $R_5 = 4.1 \times 10^{-3}\ (\Omega)$

The resistance of the bellows in plasma vacuum vessel is $R_1 = 5.4 \times 10^{-4}\ (\Omega)$

The resistance of the bellows in cryostat is

$R = 5.9 \times 10^{-4}\ (\Omega)$

The integrated resistance is $R = 2.1 \times 10^{-4}\ (\Omega)$

The positions and configurations of the bellows are shown in Fig. XI-4-7 and XI-4-8.

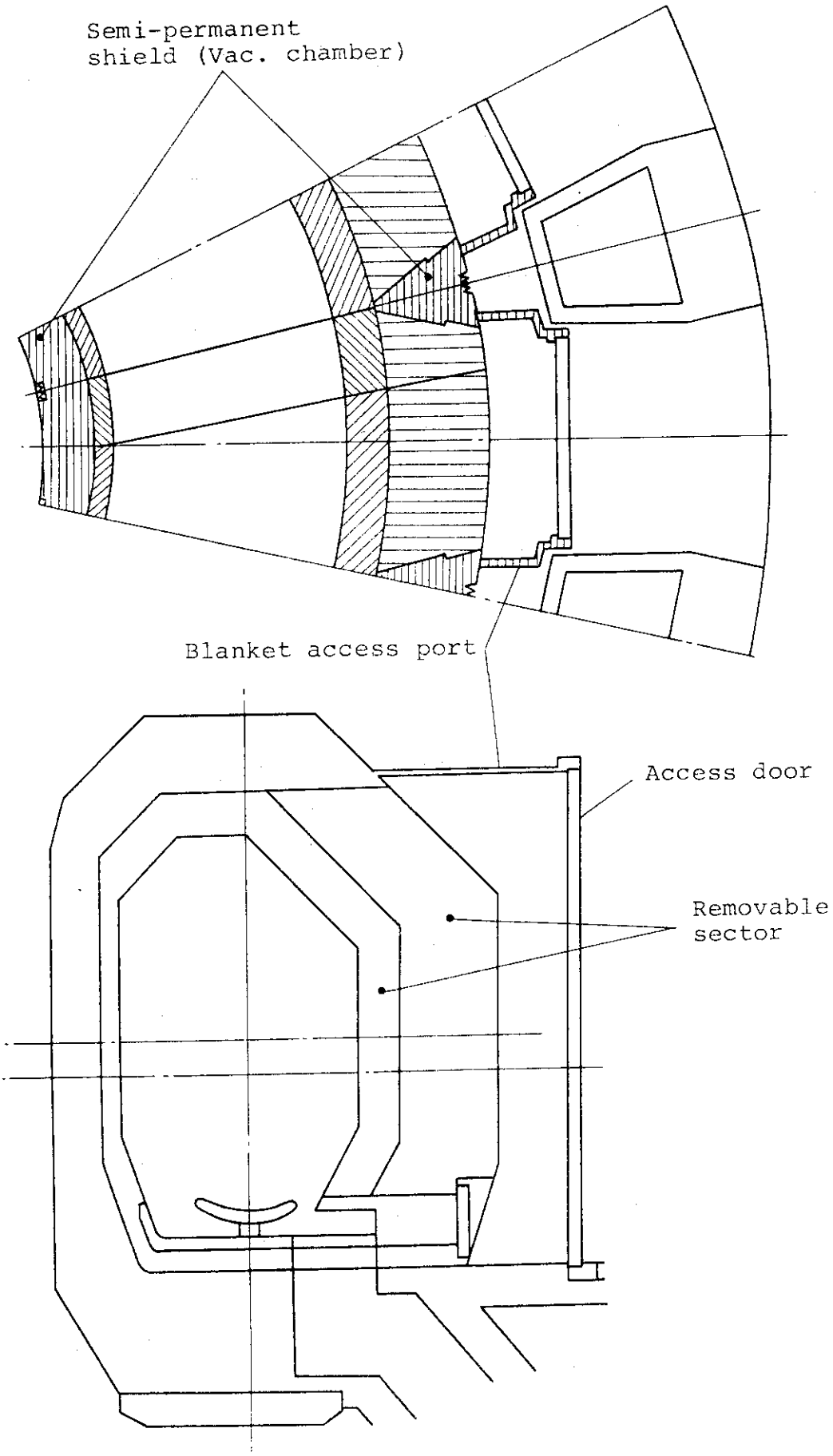

Fig. XI-4-6 Vacuum boundary of plasma chamber

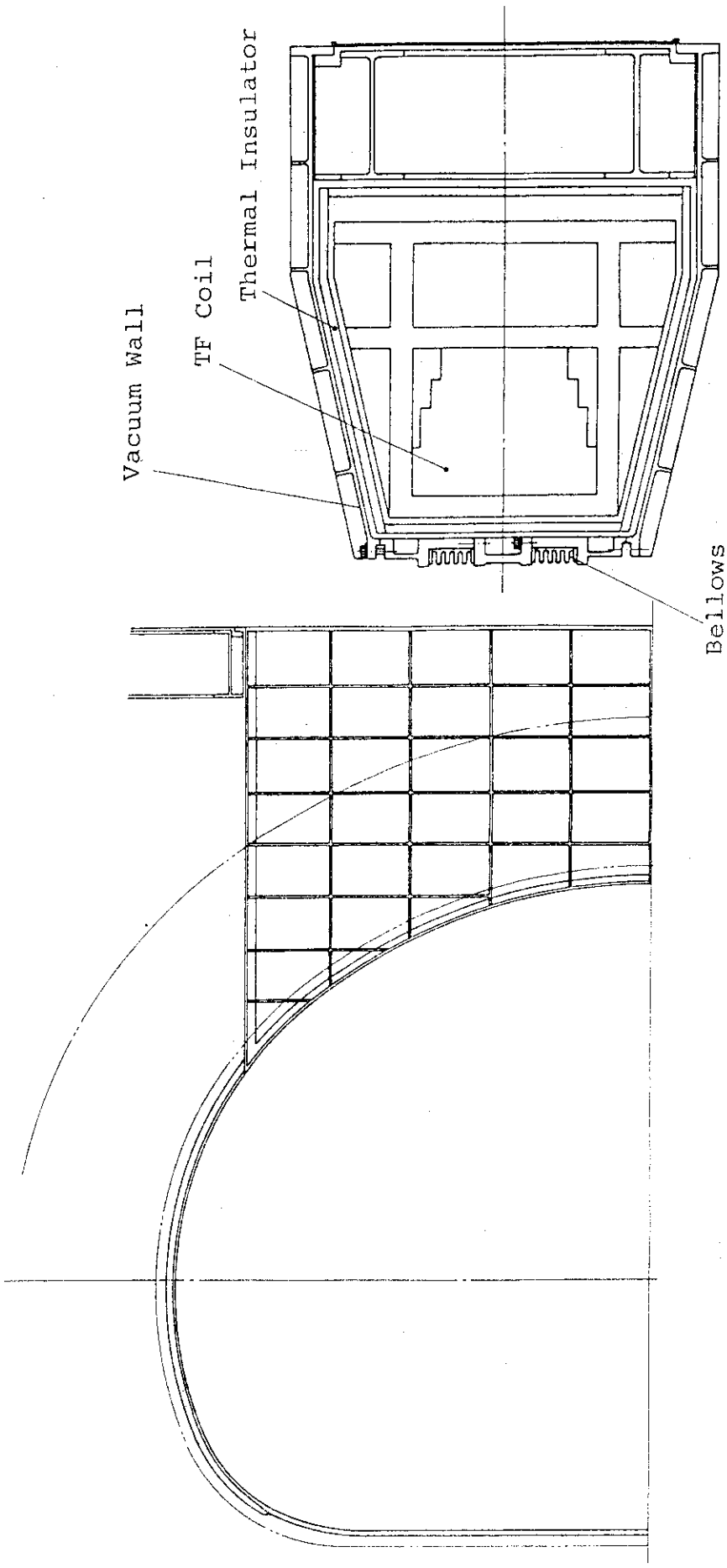

Fig. XI-4-7 Cryostat for TF coil

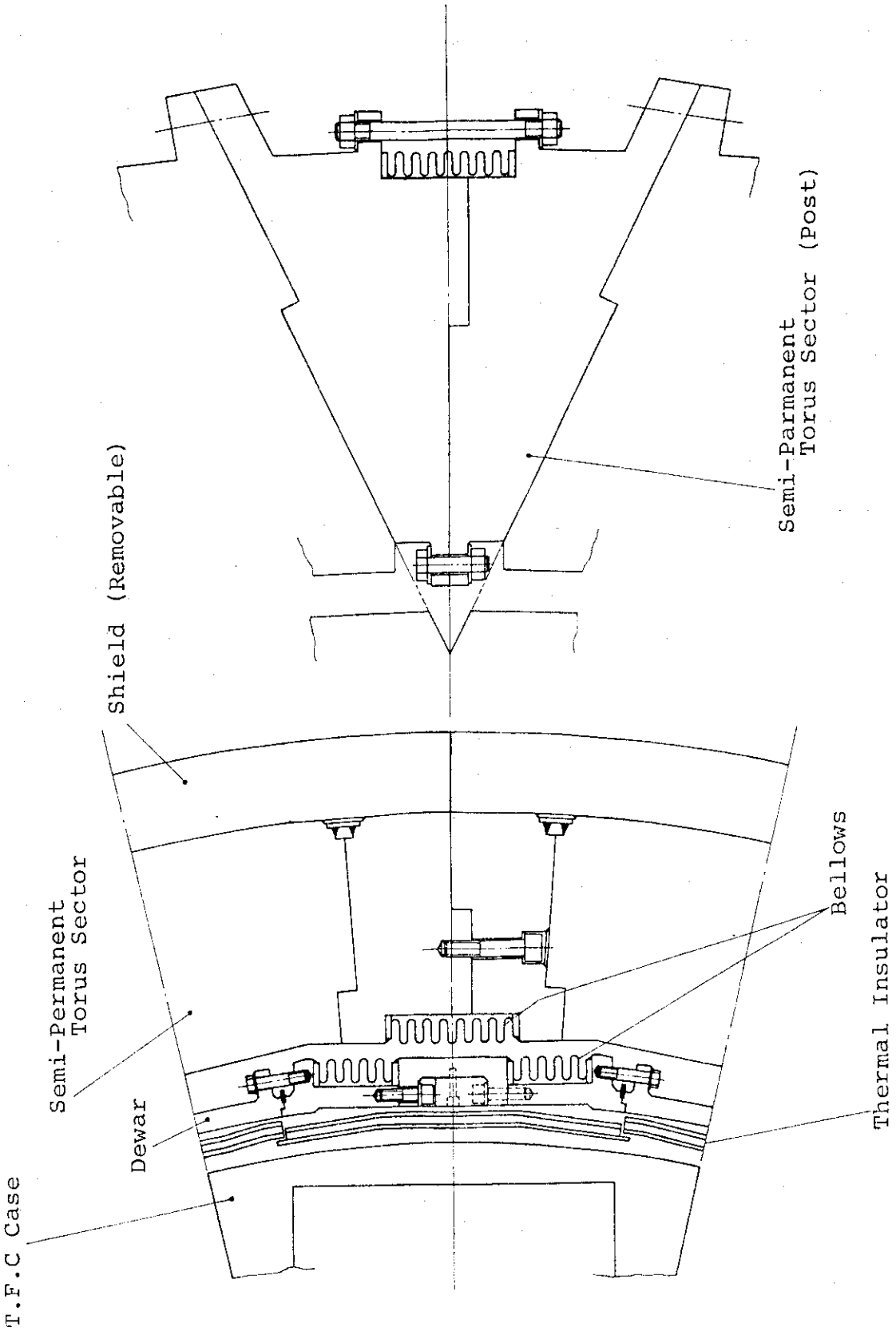

Fig. M-4-8 Torus resistance (bellows)

4.4 Supporting analysis

Thermal stress of the vacuum vessel for the combined boundary is investigated with respect to torus bake-out.

Fig. XI-4-9 shows the three-dimensional stress analysis model of the vacuum vessel for the combined boundary. The torus vacuum vessel, the vacuum duct between torus vessel and bell jar, and the bell jar are modeled with the shell elements of 750 mm, 50 mm and 70 mm thickness, respectively. Temperature rise of torus for bake-out is assumed to be 150°C.

Fig. XI-4-10 and Fig. XI-4-11 show the results of stress analysis by means of a finite element method. The peak value of 410 MPa sit on the margine of ASME criterion, therefore an alternative mechanical configuration between the vacuum boundary and the bell jar must be resolved.

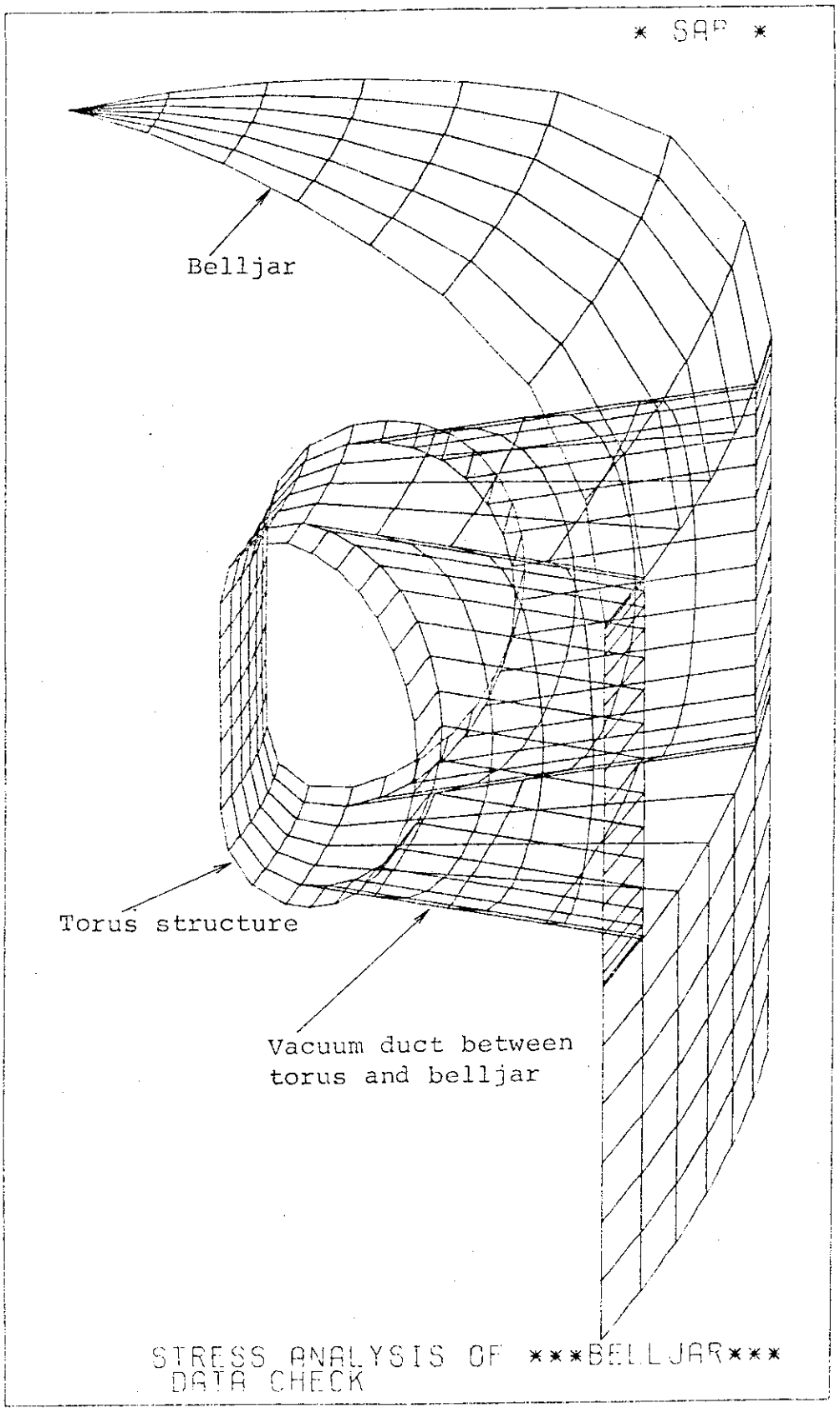

Fig. XI-4-9 Three-dimensional stress analysis model of the vacuum vessel for the combined boundary

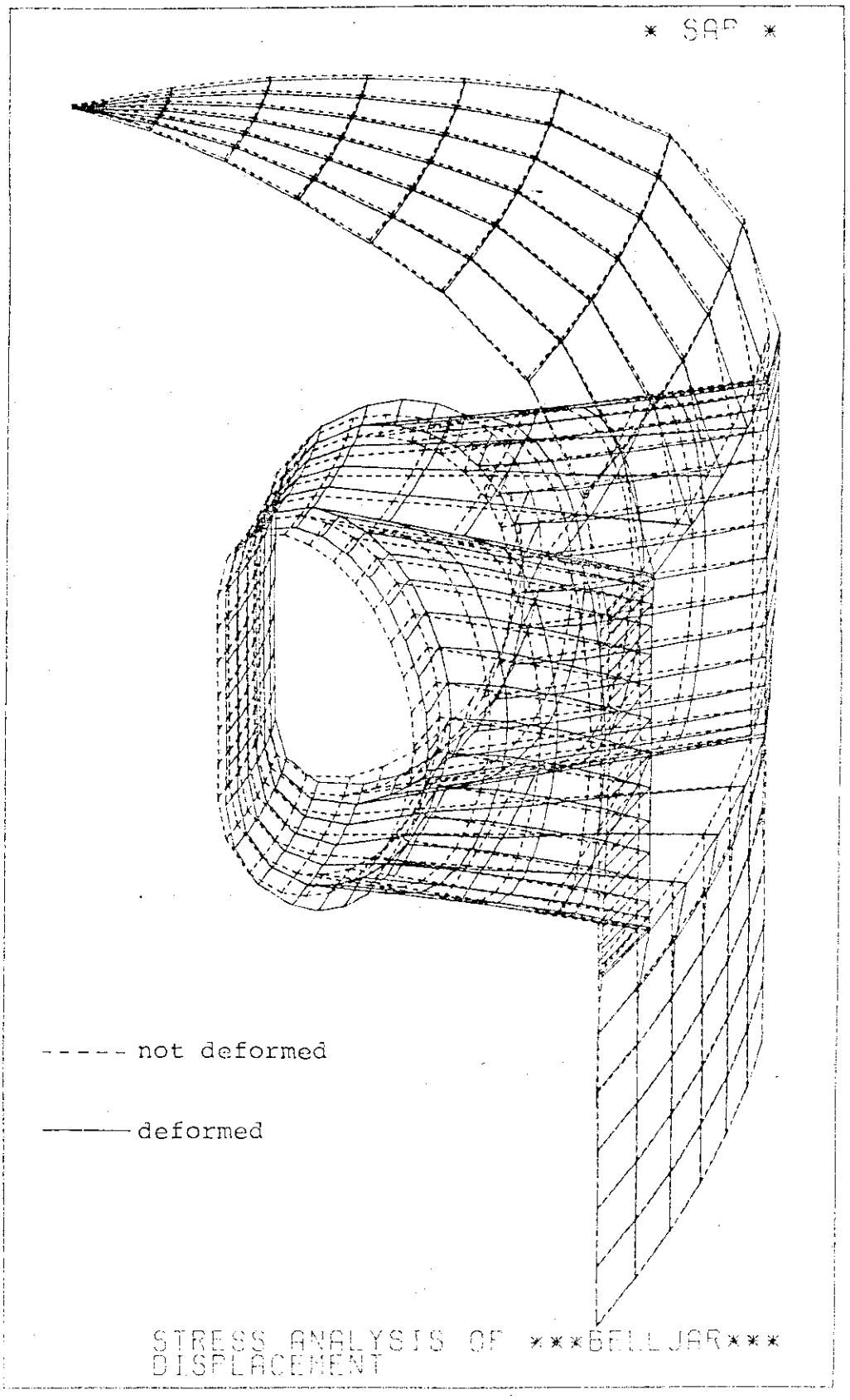

Fig. XI-4-10 Deformation of the combined vacuum vessel due to the torus temperature rise of 150°C for bake-out

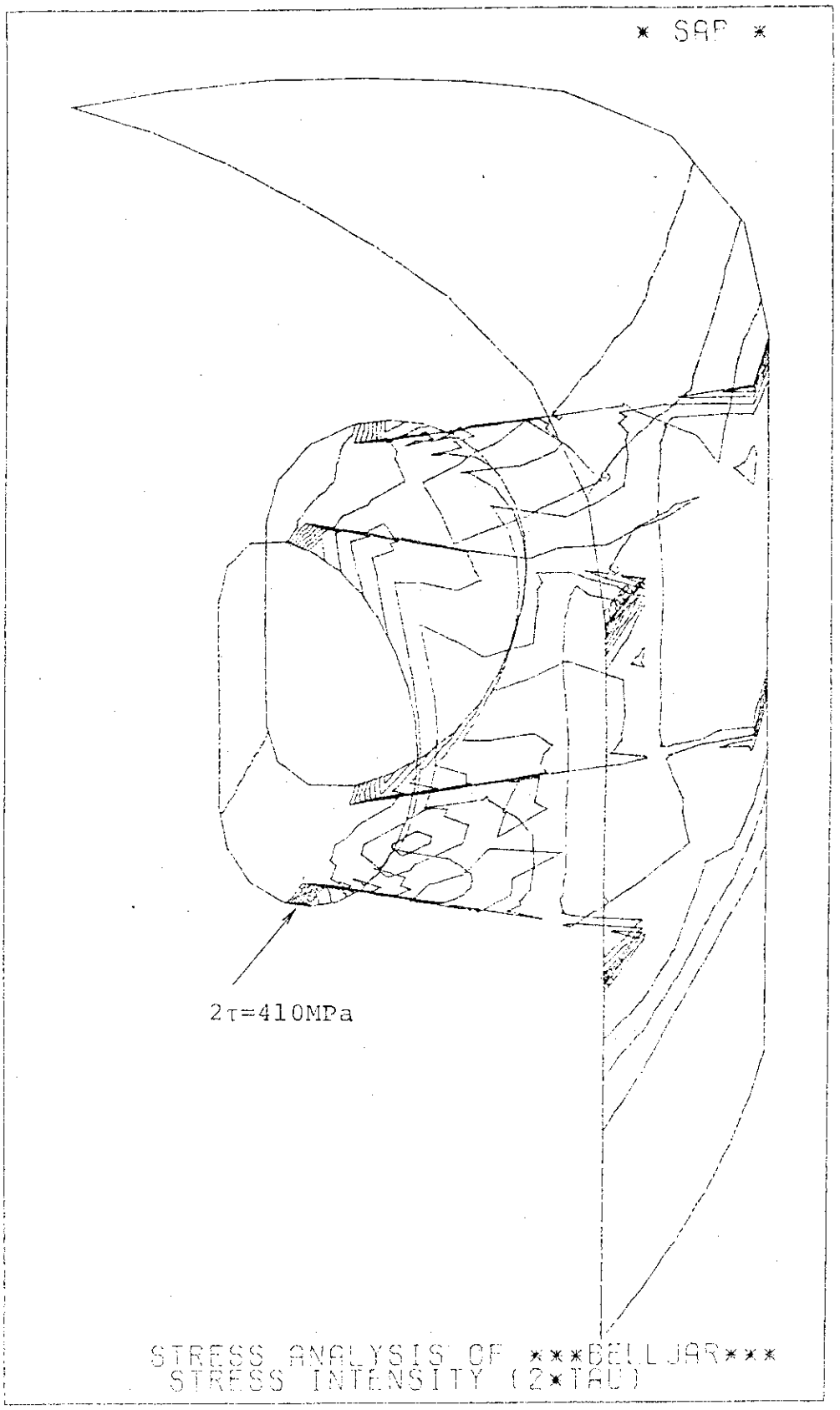

Fig. XI-4-11 Stress distribution of the combined vacuum vessel due to torus bake-out

5. Torus System

5.1 Segmentation options

The relation between the torus segmentation and the maintenability, one of the major concerns in the reactor design, influences greatly the reliability of the reactor system.

Here, the segmentation of blanket and the replacement method of the blanket sector are discussed.

Five representative options mentioned below are considered from the view point of relations between the number of torus segmentation and the replacement procedures.

(a) one sector/TF coil-single motion (straight); Fig. XI-5-1.

(b) two sectors/TF coil-single straight motion (obliquely) ; Fig. XI-5-2.

(c) two sectors/TF coil-two motions (straight and oblique) ; Fig. XI-5-3.

(d) three sectors/TF coil-single motion (straight or oblique) ; Fig. XI-5-4.

(e) three sectors/TF coil-two motion (rotation in toroidal direction + straight) ; Fig. XI-5-5.

5.2 Evaluation and selection

The merits and demerits of each option are discussed below.

(a) One sector/TF coil-single motion (straight)

This concept is the reference design in INTOR Phase-I. The advantage of this concept is simplicity of retraction motion.

Less accidents and high reliability are expected in this concept in comparison with other concepts of two motions.

The disadvantage of this concept is that this concept requires larger coil bore size. In order to maintain the ccil bore 6.6m with this concept, a small fraction of the outer blanket/shield structure just behind the TF coil should be left in the TF coil bore at the time of blanket replacement. Such design brings about reduction of tritium breeding ratio, and requires insitu maintenance of first wall on blanket/shield fraction left in toroidal bore. This operation should be performed with full remote and might be relatively difficult.

(b) Two sectors/TF coil-straight motion (obliquely)

This concept is Japanese option in INTOR Phase-IIa. The advantage is that the retraction motion is single straight motion which is relatively simple and highly reliable. Though two sections/TF coil should be retracted in two different direction respectively, this concept permits a reduction of TF coil bore size.

(c) Two sectors/TF coil-straight motion + oblique motion

The advantage is that the torus consists of the blanket sector having a equally divided angle,

and that there is sufficient space on semi-permanent shield just behind the TF coil in order to install the bellows. However the attention for tritium permeation through this bellow should be payed. The disadvantage is that the second sector requires the two motion in different direction and complicates the maintenance of the blanket.

(d) Three sectors/TF coil-straight motion + oblique motion

The advantage is that the TF coil bore size can be more reduced.

(e) Three sectors/TF coil-straight motion + circumferential motion in toroidal direction

The advantage is that the most reduced TF coil bore size can be realized and that the torus can be consist of equally divided sectors.
The disadvantage is that the two side sectors, with the exception of central sector, need the circumferential motion in toroidal direction which requires sophysticate equipment for replacement operation. Therefore, the reliability concerning the maintenance operation does not seem to be high.

≪ Conclusion ≫

The results of comparative study on five concepts are shown in Table XI-5-1.
Each concept has each merit and each demerit.

However, as the disassembly and assembly operations of blanket/first wall is assumed to be inevitable, the reliability of maintenance is the most important. Therefore, single straight motion is recommended for blanket replacement procedure.

In order to satisfy the reduced TF coil (bore size 6.6m) condition, the concept b and d is favorable.

Table XI-5-1 Comparison of segmentation method of blanket

	Weight factor	a. One sector/ TF coil Single motion (Straight)	b. Two sectors/ TF coil Single motion (Oblique)	c. Two sectors/ TF coil Two- otion (Oblique & Straight)	d. Three sectors/ TF coil Single motion (Straight or Oblique)	e. Three sectors/ TF coil Two-Motion (Rotation in toroidal direction & Straight)
1. Reliability of retraction motion	8	5	4	3	4	2
2. Time required for maintenance	5	5	4	3	3	2
3. Sector region available to be retracted (Reduction ability of TF coil bore)	8	1	3	3	4	5
4. Attachability of limiter/divertor	5	4	3	4	4	4
5. Symmetry of torus sector	5	5	4	4	2	2
6. Tritium breeding ratio	6	2	4	4	4	4
		130	135	128	133	120

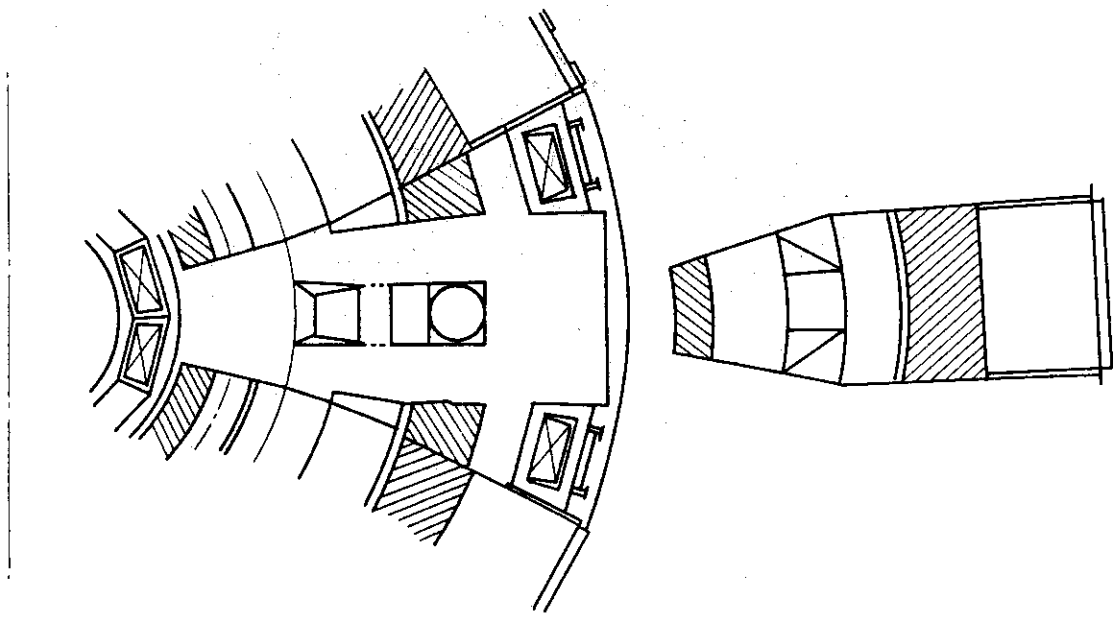

Fig. XI-5-1 Single sector concept

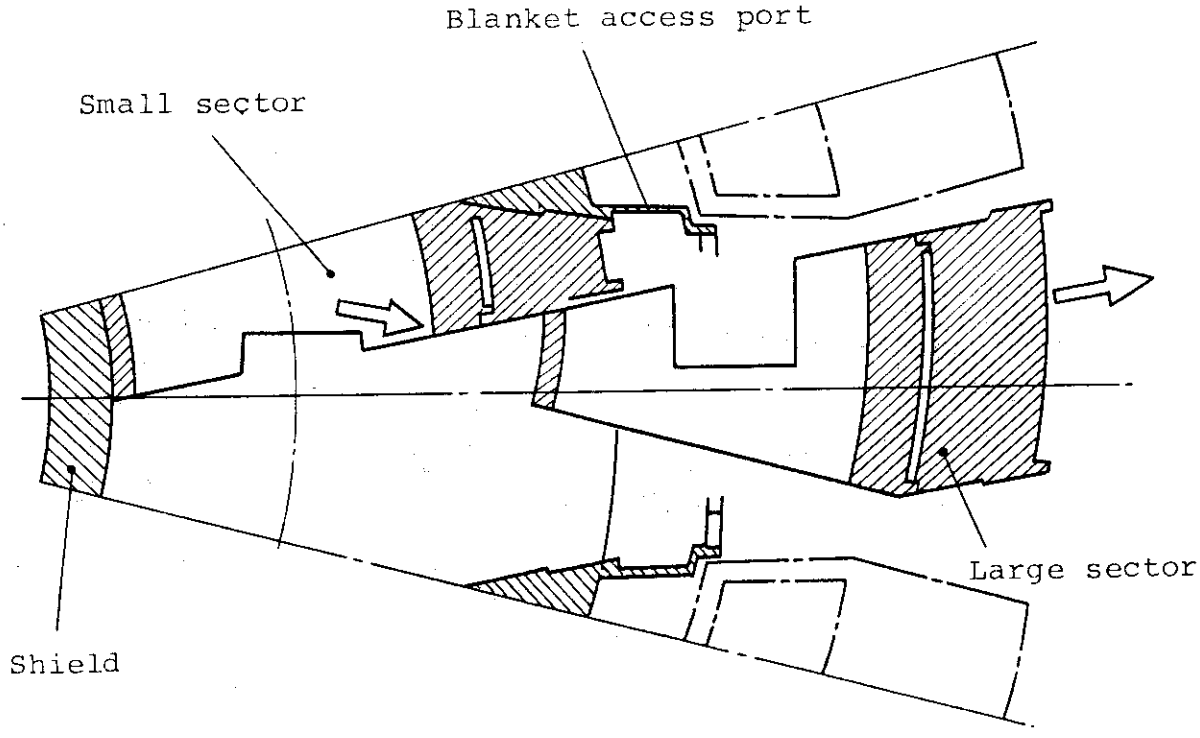

Fig. XI-5-2 Two-sector concept with single notion of both sectors

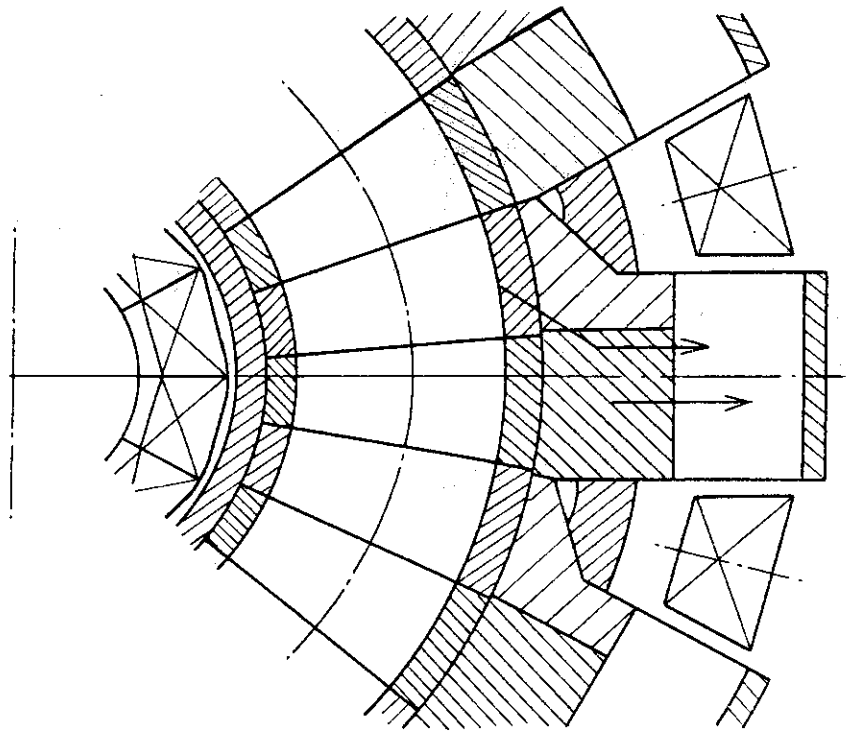

Fig. XI-5-3 Two-sector concept with compound motion of 1 sector

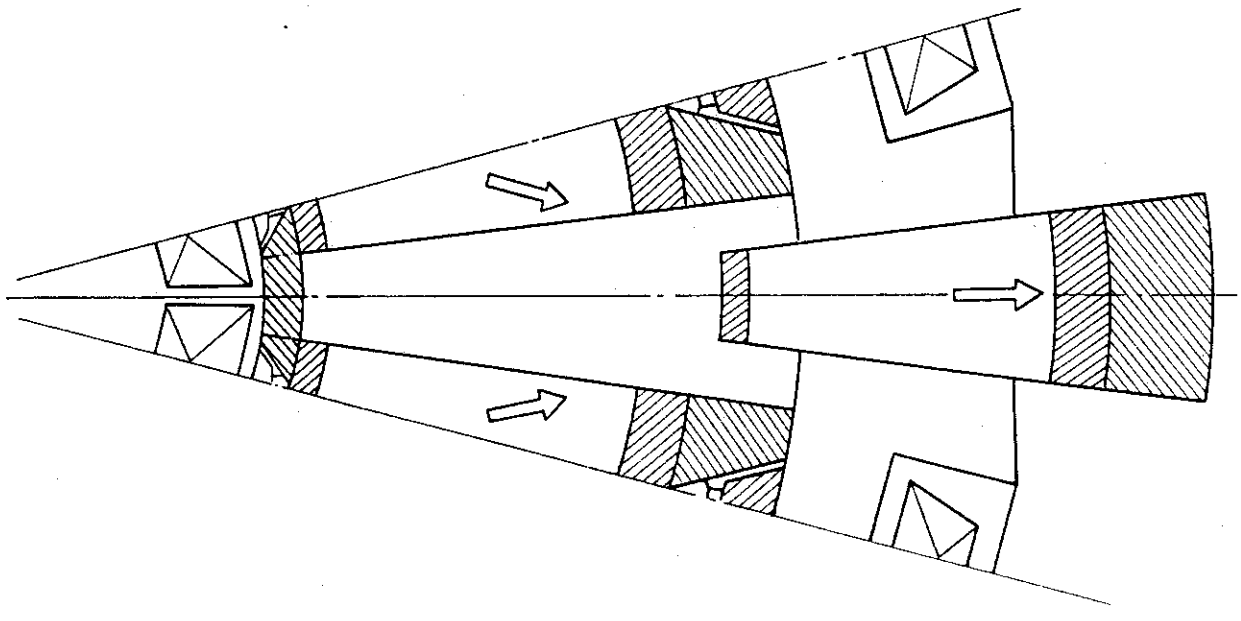

Fig. XI-5-4 Three-sector concept with single motion

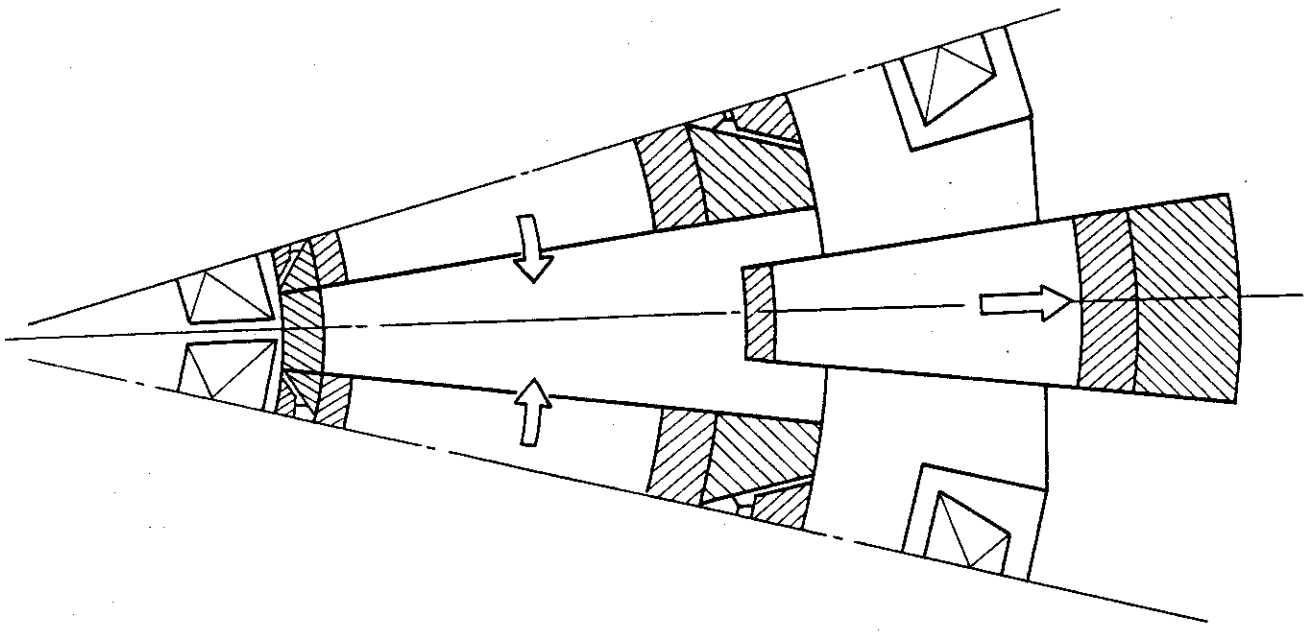

Fig. XI-5-5 Three-sector concept

5.3 Design description

(1) Removable torus sector

In order to reduce the dimension of the reactor, the TF coil size is reduced. This reduction does not allow to replace the blanket on the limiter by simple retraction of the segment of the same member of TF coils.

It is necessary to devise further each 1/12 segment of the blanket or the limiter to several sectors. The methode of segmentation influences strongly the remote maintenance procedure.

Here, in order to simplify the replacement operation and the remote maintenance machine, only the methode of the simple straight motion is adopted.

In Fig. XI-5-6 the segmentation of the blanket structure is shown. The blanket segment between two TF coils is separated to the two sectors, which are large sector and small one.

After pulling out the large sector in the olbique direction, the small sector will be pulled out with straight motion in a slightly inclined direc tion.

Fig. XI-5-7 shows the segmentation of the limiter structure. The segment between two TF coils consists of large sector and small one and each sector has separate opening window located at the outside of the shield where the support structure of limiter

plate is fixed.

In order to replace the limiter segment, the large sector is pulled out after removing the samall sector.

The connections between the blanket and the shield as well as between the limiter and the shield, are performed with mechanical connection only.

The vacuum sealing is carried out at the outside of the access doors.

(2) Segmentation of shield structure

The shield structure is semi-permanent. However, at the maintenance of toroidal field coil, the shield structured should be removed.

In toroidal direction, the shield structure is divided into 36 sectors at the time of manufacturing, but 24 sectors at the time of maintenance operation.

Segmentation of shield structure is shown in Fig. XI-5-8.

The side sectors located behind the toroidal coil equip the bellows for torus resistance and the contact surface between two side sectors is insulated with ceramic coating.

As the each two side sectors are fixed with bolts, the replacement of the two side sectors can be performed as one structure.

The access port connected to the shielding structure can be divided according to the same manner as shield structure.

The connection between the side sectors and the central sector is performed by welding.

(3) Support structures

(a) TF coil support

The force to the torus center in the toroidal field magnets is supported by the pressure acting between the surfaces of wedge parts of the magnet cases which are located on the inner side in the major radius direction.

The toroidal torsion force in the toroidal field magnets is supported by the support beams between toroidal field magnets.

At the upper and lower areas of the TF coil, the support beams are installed. The support beams installed at the lower area of TF coil have the openings to permit the penetration of the support leg for shield and the exhaust duct for pumped limiter.

The gravity of the TF coils is supported from both the torus center and the outside of the torus.

At the torus center, TF coils are supported with the support leg which also supports the solenoid coils.

At the outside of the torus, each TF coil has an independent support leg. These support legs have a shield layer of 77K located between the floor of 300°K and the structures of 4.2K.

(b) PF coil support

The hoop force resulting in PF coils is sustained by the PF coil's own structures.
The gravity and the out of plane force acting on the PF coils (#1 ∿ #9) are supported with the support cylinder situated at the center of the torus.
As regard to the PF coils #10 ∿ #13,
they are supported by the arms on the toroidal field coil.
These PF coils have the same cryogenic temperature as the toroidal field coils, and slide freely in radial direction.

(c) Shield support structure

The shield is installed and fixed with bolts on the base place which is supported by the support legs (12 legs) penetrating the inter TF coil support beam.
This support structure of the shield is surrounded by the cryostat.

(d) Cryostat gravity support

The gravity of the cryostat is supported by the vacuum boundary structure surrounding the support structure of the shield already mentioned in (c).

(4) Maintenance of first -wall and blanket

Replacing the first wall and the blanket is a medium scale repair. Here, disassembly and assembly procedures of the blanket are described.

(i) Maintenance procedure

a) Disassembly procedure for first wall and blanket.

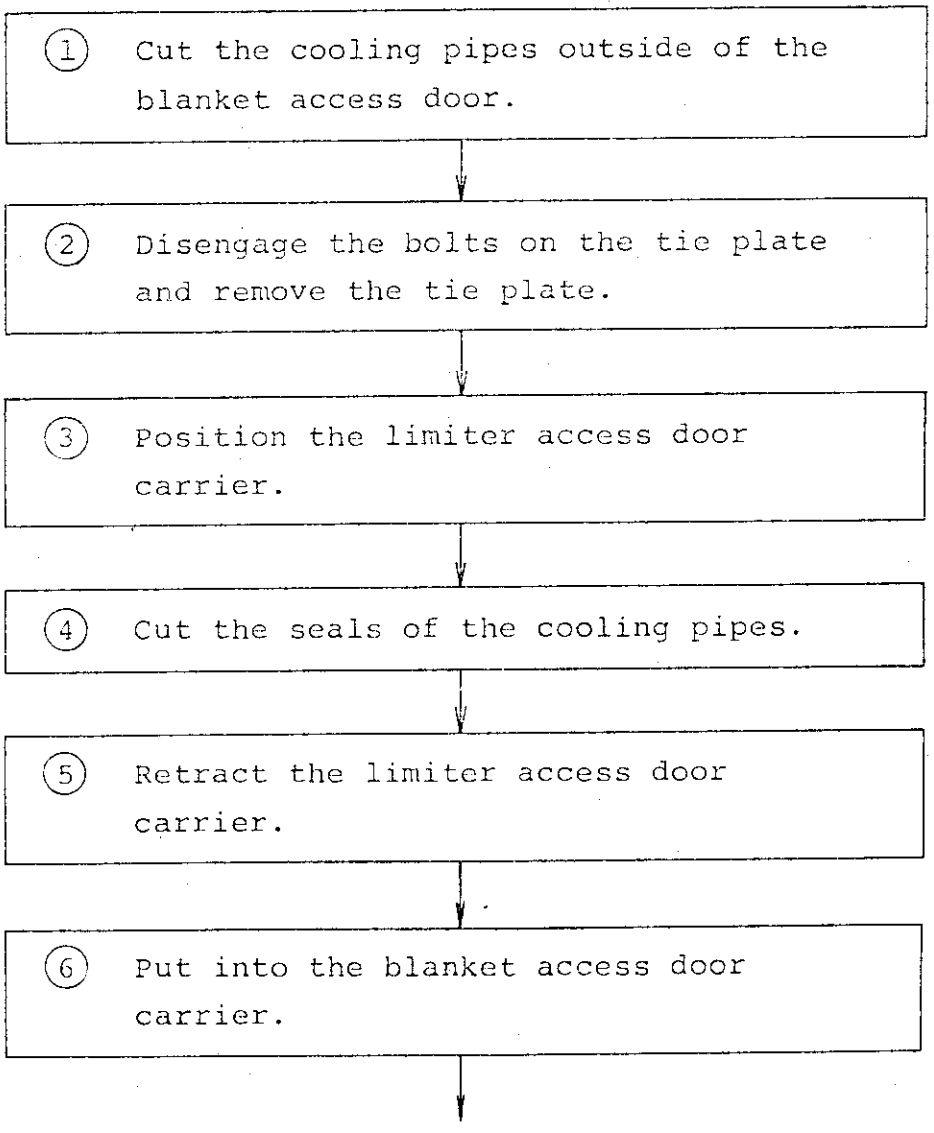

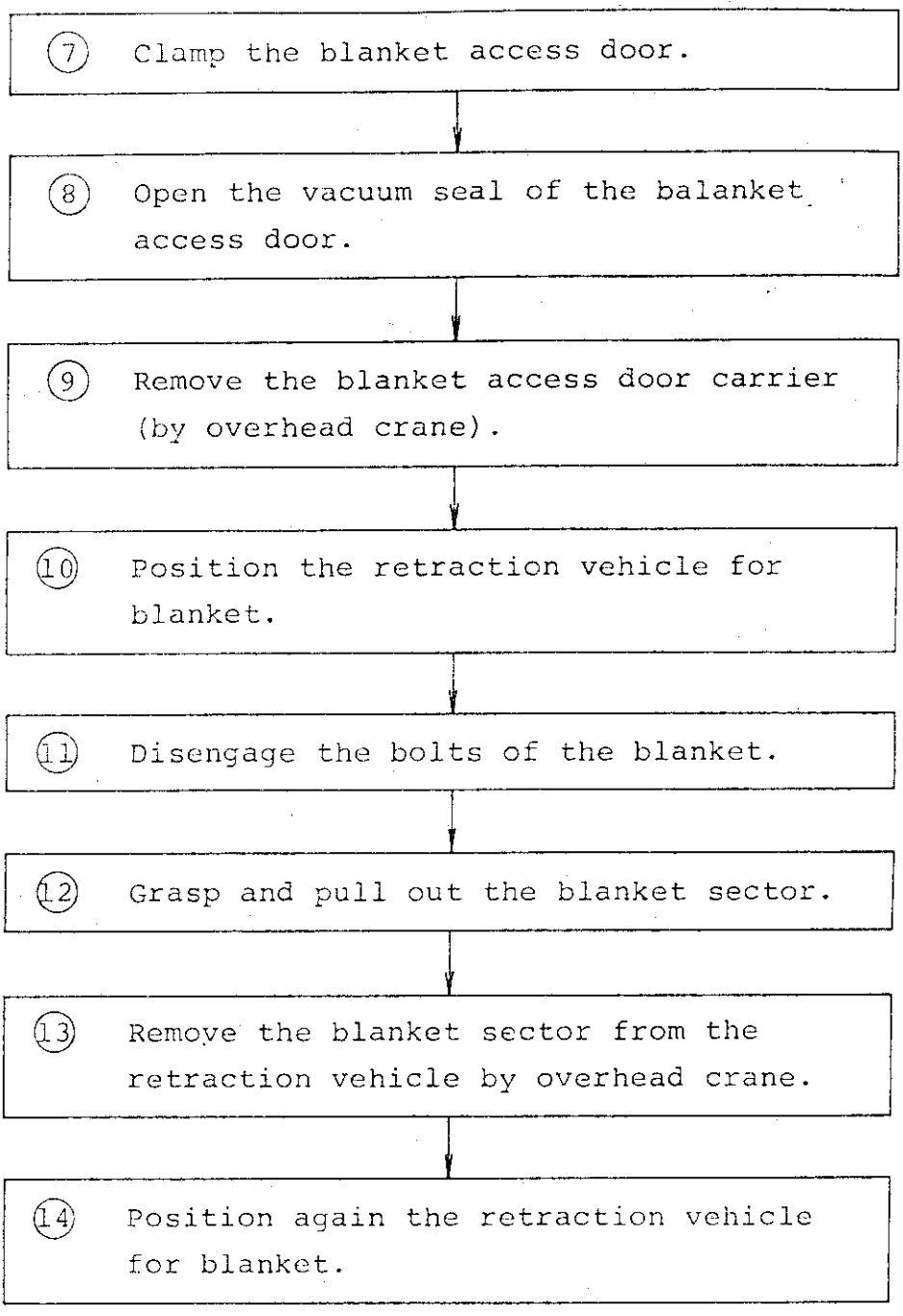

(Repeat ⑩ ∿ ⑬ for two side sectors of blanket)

b) Assembly procedure for first wall and blanket.

Assembly operation of blanket is done basically with the reverse sequence to that of disassembly, provided that the NDT operation is added after welding of the sela in place of ⑧ and ④.

(5) Maintenance equipment

During the blanket replacement operation, overhead crane will be employed frequently in order to remove the blanket sector from the retraction vehicle and to change the direction of the retraction vehicle for blanket.

In order to remove the blanket access door, considerable amount of time will be required to cut the seal of the door which amounts to 14 m in total length.

The following equipments are necessary for the purpose of the maintenance of first wall and blanket.

1 Overhead crane
2 Limiter access door carrier
3 Blanket access door carrier
4 Retraction vehicle for blanket

The equipments listed above have following functions.

1 Overhead crane

During the maintenance operation of the blanket, this crane functions to transfer the blanket sector and also the retraction vehicle for blanket.
100 ton hoist capacity is required for this crane because the maximum weight of the central blanket sector amounts to 100 ton.

2 Limiter access door carrier

This carrier is employed not only for limiter replacement but also for blanket replacement. The manipulator equipped in this carrier serves to weld and cut the seal of pipes situated at the upper part of the blanket access door.

3 Blanket access door carrier

This carrier is composed with, machine for welding and cutting of the sealing part of the blanket access door, machine for handling and positioning of the blanket access door, and traveling system.
The equipments are same as those of the limiter access door carrier except the manipulator.

4 Retraction vehicle for blanket

The retraction vehicle for blanket approaches to the blanket sector along the guide rail equipped on the floor between the toroidal field coils.

This retraction vehicle functions to disengage the bolts fixed between the blanket sectors and to pull out the blanket sector in radial direction with a straight motion.

This vehicle consists of the manipulator which functions to engage and disengage the bolts in moving along the vertical pole, the grasping system which grasps the blanket sector with two points, and the traveling system moving along the guide.

The concept of this vehicle is shown in Fig. XI-5-10 and Fig. XI-5-11.

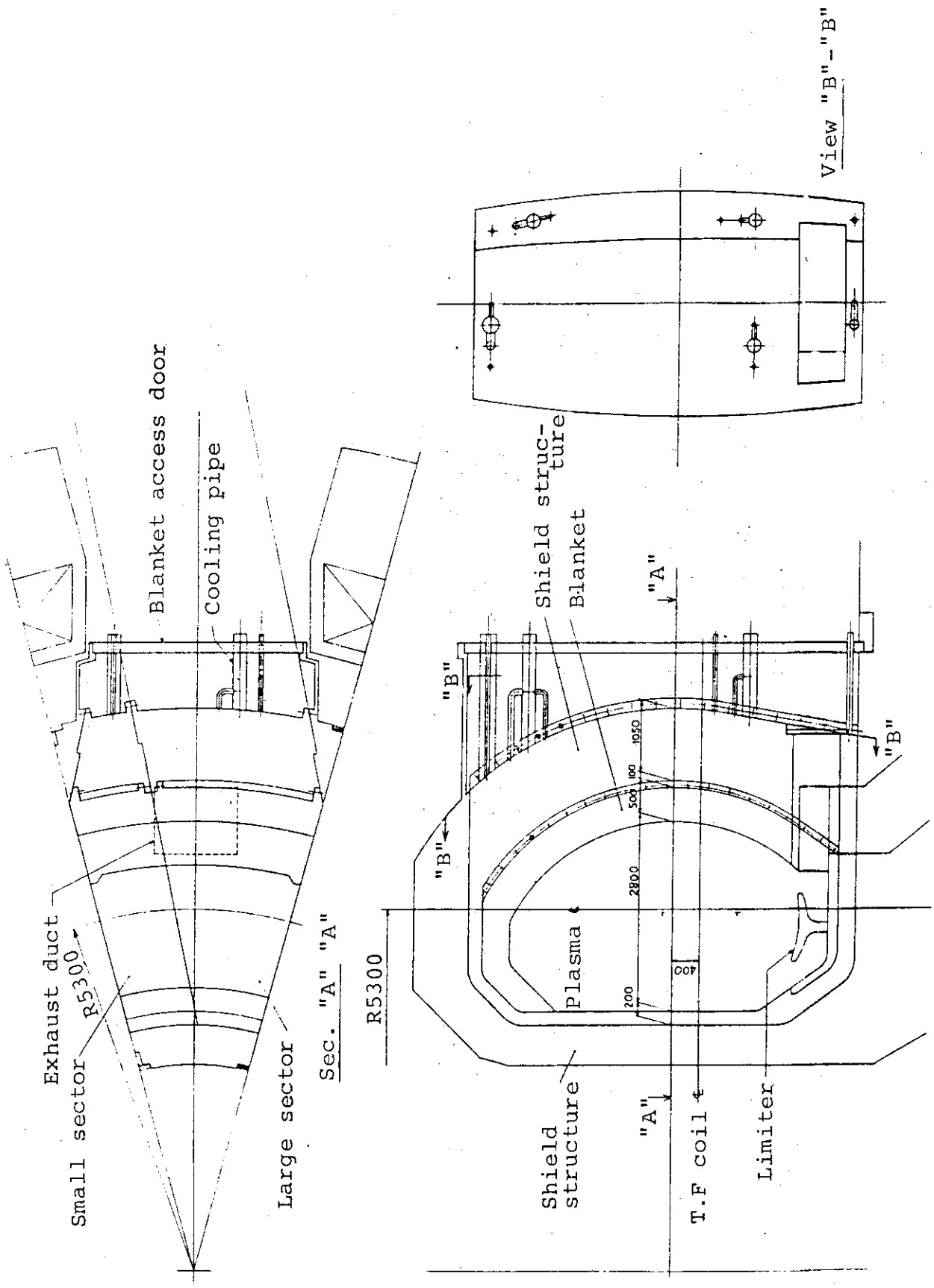

Fig. M-5-6 Blanket configuration

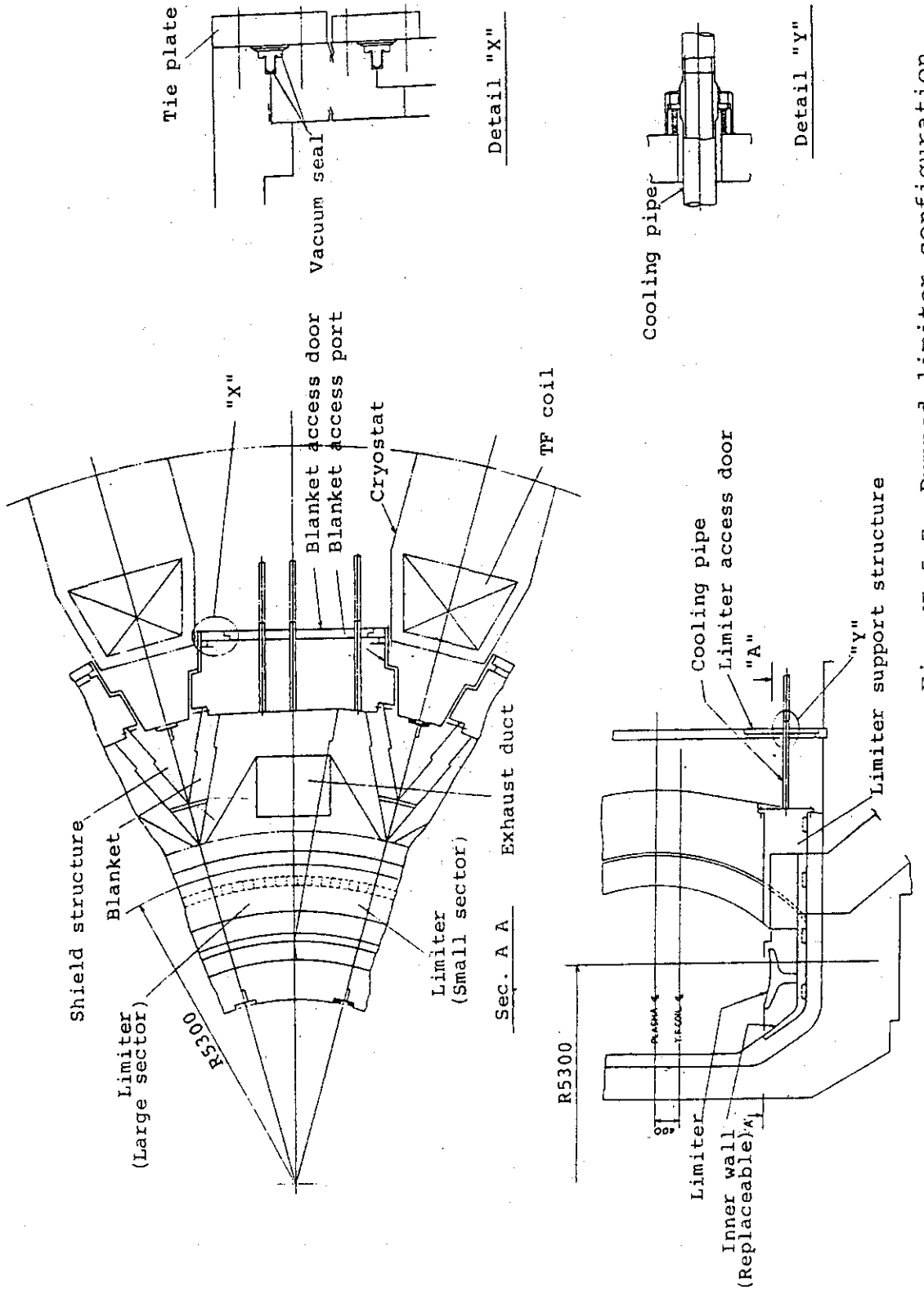

Fig. XI-5-7 Pumped limiter configuration

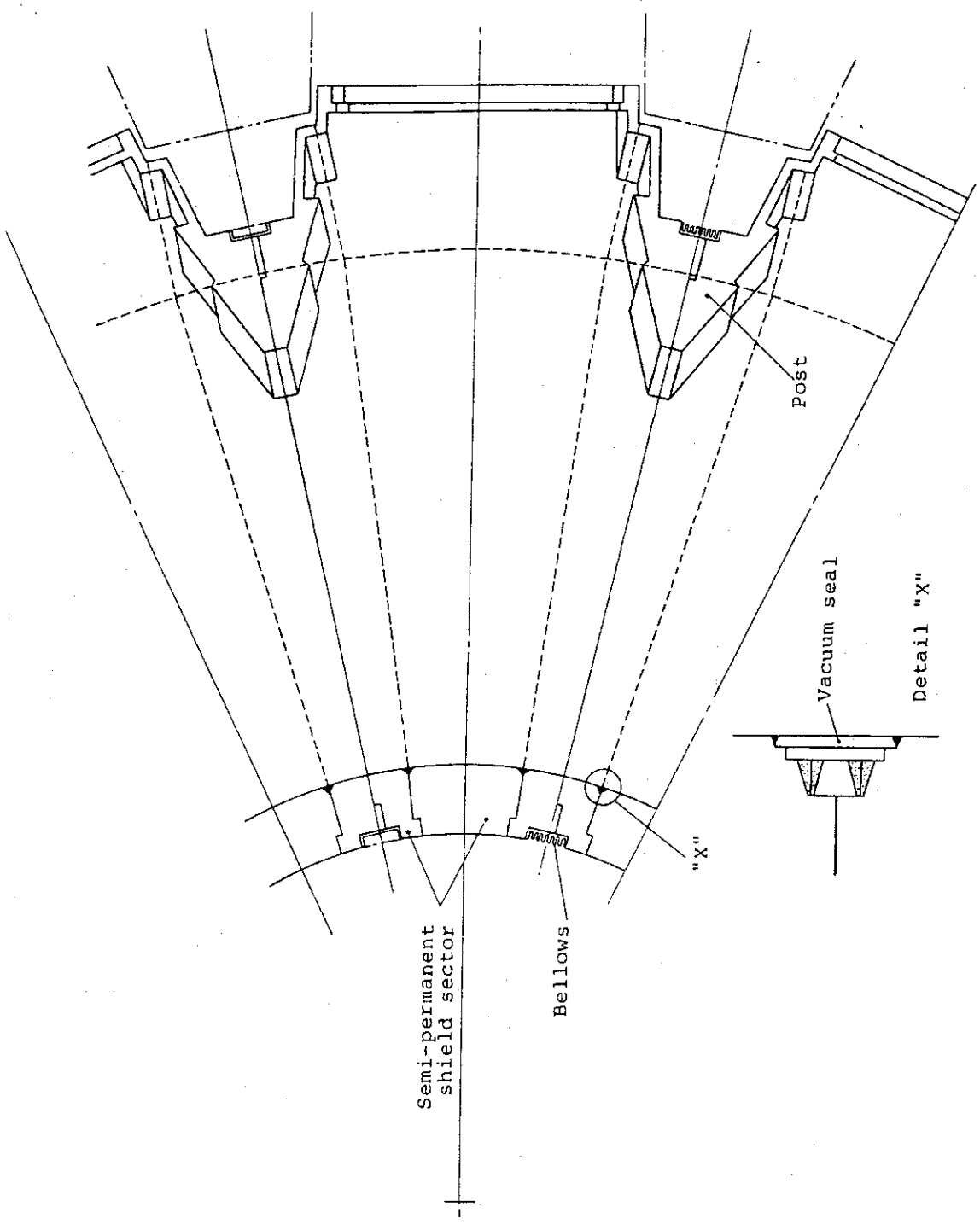

Fig. XI-5-8 Segmentation of semi-parmanent shield

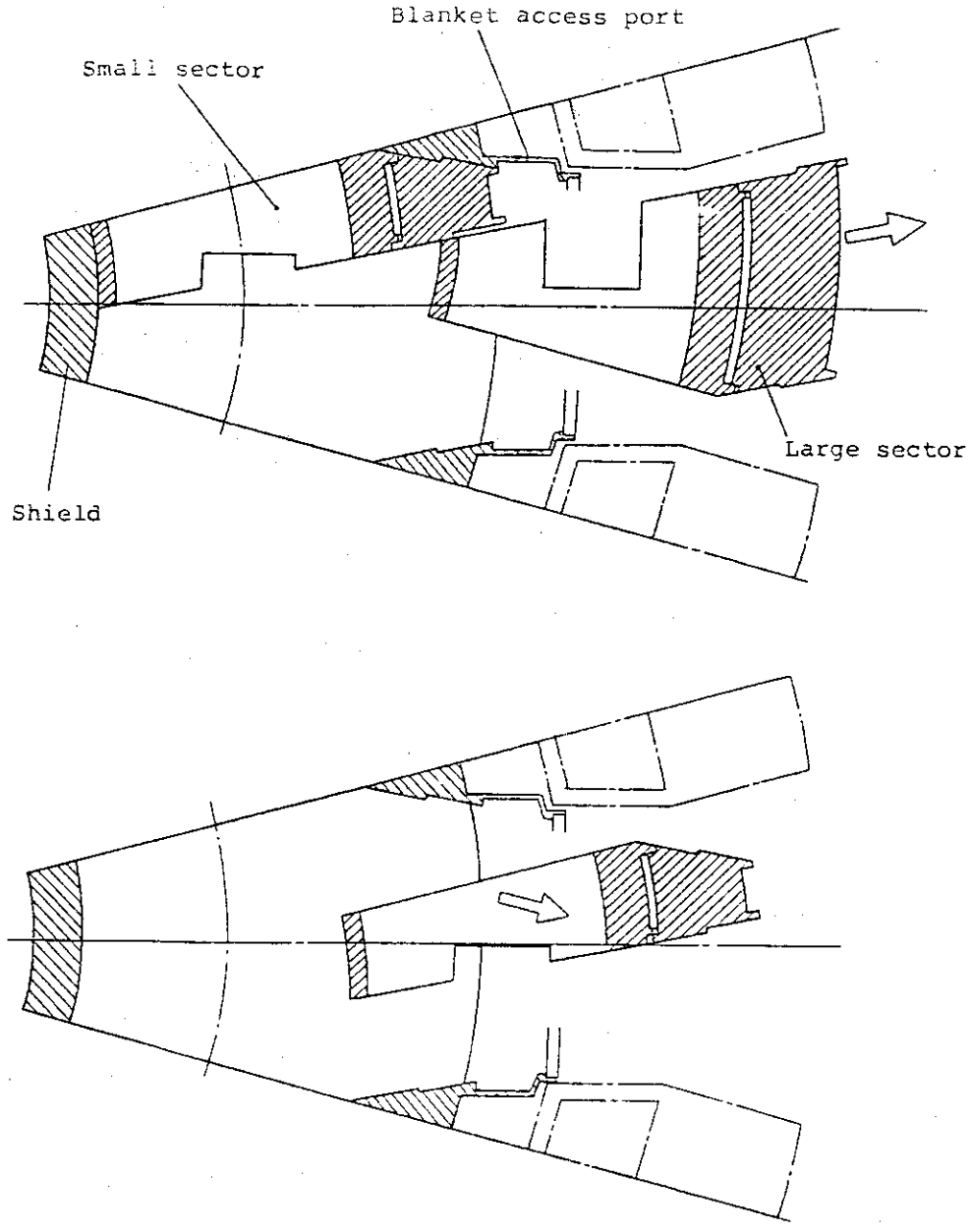

Fig. XI-5-9 Blanket sector replacement process

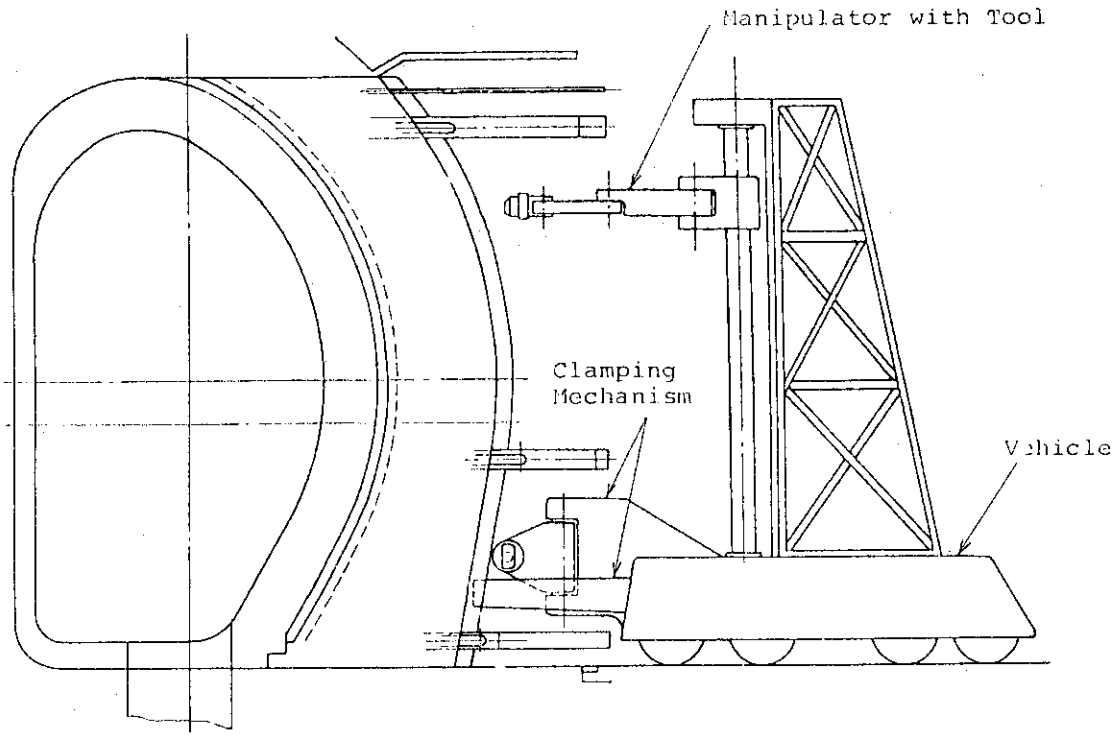

Fig. XI-5-10 Retraction vehicle for the blanket

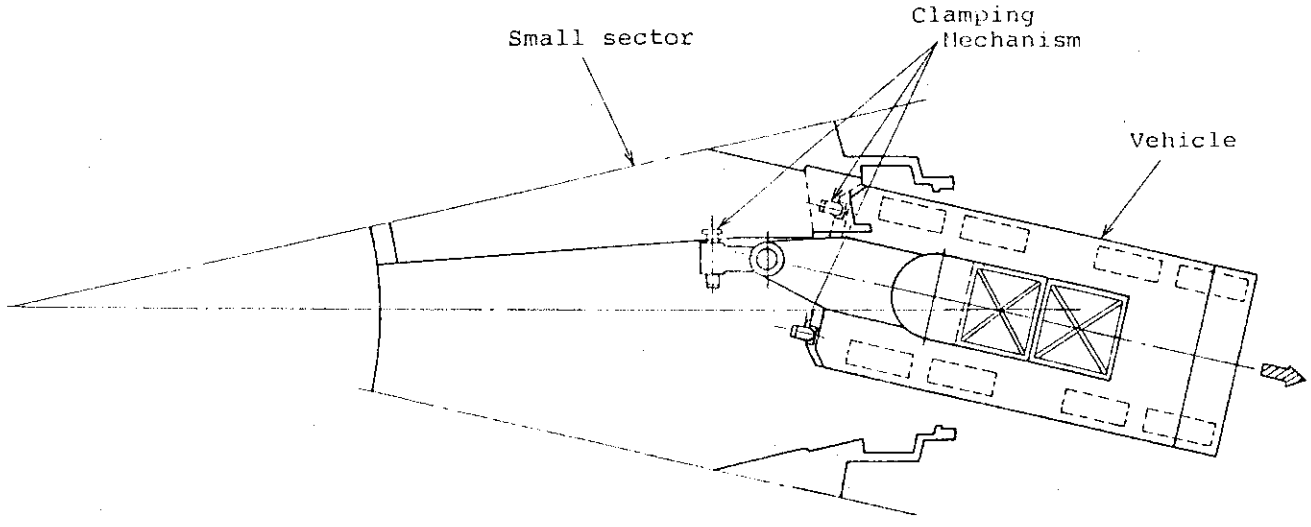

Fig. XI-5-11 Retraction vehicle for the blanket

5.4 Supporting analysis

This section concerns the strength of the support leg for toroidal shield.

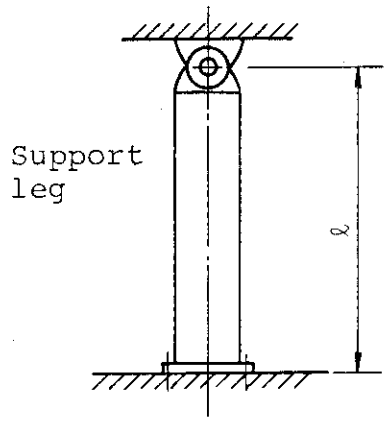

Fig. XI-5-12

The schematic configuration of the support leg of the shield is shown in Fig. XI-5-12.

The supprting of the toroidal shield is carried out by means of the support leg standing from the floor and fixed with the shield structure by pin-joint.

This leg can support the gravity of the shield, blanket, limiter and base plate.

If these structures are supported by 12 leg, the load par one leg (Wg) is 494 ton/leg.

(1) Aseismatic strength

(a) Loard in vertical direction

If we suppose that the dead load (Wg) is multiplied by 1.3 for the load in vertical direction Wv,

$$Wv = 1.3\ Wg = 642 \times 10^3\ (kg)$$

The buckling load Wk of the leg is given as,

$$Wk = \frac{n \cdot \pi^2 \cdot E \cdot I}{\ell^2}\ (kg)$$

here; n : coefficient determined from configuration = 0.25

E : young's modulus = 1.95×10^4 (mm^4)

I : moment of energy (mm^4)

ℓ : length of leg = 5300 (mm)

As the outer radius of the leg is 850 mm, the thickness of the cylinder t = 100 (mm),

The bulcking load is $Wk = 29.2 \times 10^6$ (kg)

Therefore, $Wk = 29.2 \times 16^6$ kg > $Wv = 6.4 \times 10^5$ (kg)

The strength of the leg is sufficient for buckling.

The compressive stress of the leg in this case is $\sigma_c = 2.7$ (kg/mm^2).

(b) Loard in horizontal direction

If we suppose that the gravity loard is multiplied by 0.3 as the horizontal load,

$$Wh = 0.3\ Wg = 148 \times 10^3 \text{ (kg)}$$

bening stress σ_b is expressed as

$$\sigma_b = \frac{M}{Z} = 19.8 \text{ (kg/mm}^2\text{)}$$

here, M : bending moment = $Wh \cdot \ell$

Z : section modulus = 3.97×10^7 (mm^3)

(2) Thermo-mechanical strength at the time of baking

As the connection is carried out with pin-joing system, the deformation is defined as

$$\Delta R = \alpha \cdot R \cdot \Delta T = 11.9 \ (mm)$$

here, α : coefficient of thermal expansion of the S.S 304 = 17.3×10^{-6} (/°C)

R : the radius of the installation of leg = 5300 (mm)

ΔT: temperature elevation the time of baking = (150 - 20) = 130°C

The stress is given is as follow

$$\sigma_{bT} = \frac{3 \cdot E \cdot I \cdot \Delta R}{\ell^2} \times \frac{1}{Z} = 10.7 \ (kg/mm^2)$$

Therefore, the stress appeared in the leg is expressed as

$$\sigma = (\sigma_c + \sigma_b + \sigma_{bT}) = 33.2 \ kg/mm^2$$

This value is higher than the design criteria of the ordinary stainless steel.

Therefore, the use of material of high strength such as high Mn steel or an adjunction of some support structure should be recommended.

The above analysis is carried out only for static load. However, the dynamic seismic analysis will be necessary.

6. Impurity control

6.1 Pumped limiter configuration

6.1.1 Reference concept (PF coil max. radius R = 11 m)

The structure of the reactor system with pumped limiter is shown in Fig. XI-6-1 and Fig. XI-6-2. The radial built is shown in Fig. XI-6-3. This reactor system has the following features.

(1) The bore of the toroidal field coil is 6.6 m width × 9.3 m in height. Number of toroidal field coil amounts to 12. The cross section of the TF coil helium case is 0.9 m × 1.25 m.

(2) All superconducting poloidal field coils are located outside of the toroidal field coils. The distance between the plasma center and the TF coil center is 400 mm.

(3) The pumped limiter is used in order to control the impurities. The limiter plates are installed at the bottom of the reactor core. The curved, double-edged limiter is considered. The configuration of the pumped limiter is shown in Fig. XI-6-4.

(4) Replacement of the blanket/first wall and the pumped limiter is performed by single straight motion. The torus structures of both limiter and blanket are divided into 24 sectors (2 sectors/TF coil).

Each two sectors between two TF coils is retracted in radial direction with different angle

(5) The vacuum boundary of the plasma chamber is located on th inner side of the shielding structure. This vacuum boundary is connected with the blanket access door through which the blanket and th limiter sector are retracted.

(6) The coil cryostat is simplified-separate-vacuum boundary type.

(7) The exhaust duct is lead from the bottom of the toroidal plasma chamber to the cryopump after passing through the space between two toroidal field coils. Number of the exhaust duct is 12. Their conductance is 4.3×10^5 ℓ/s (He).

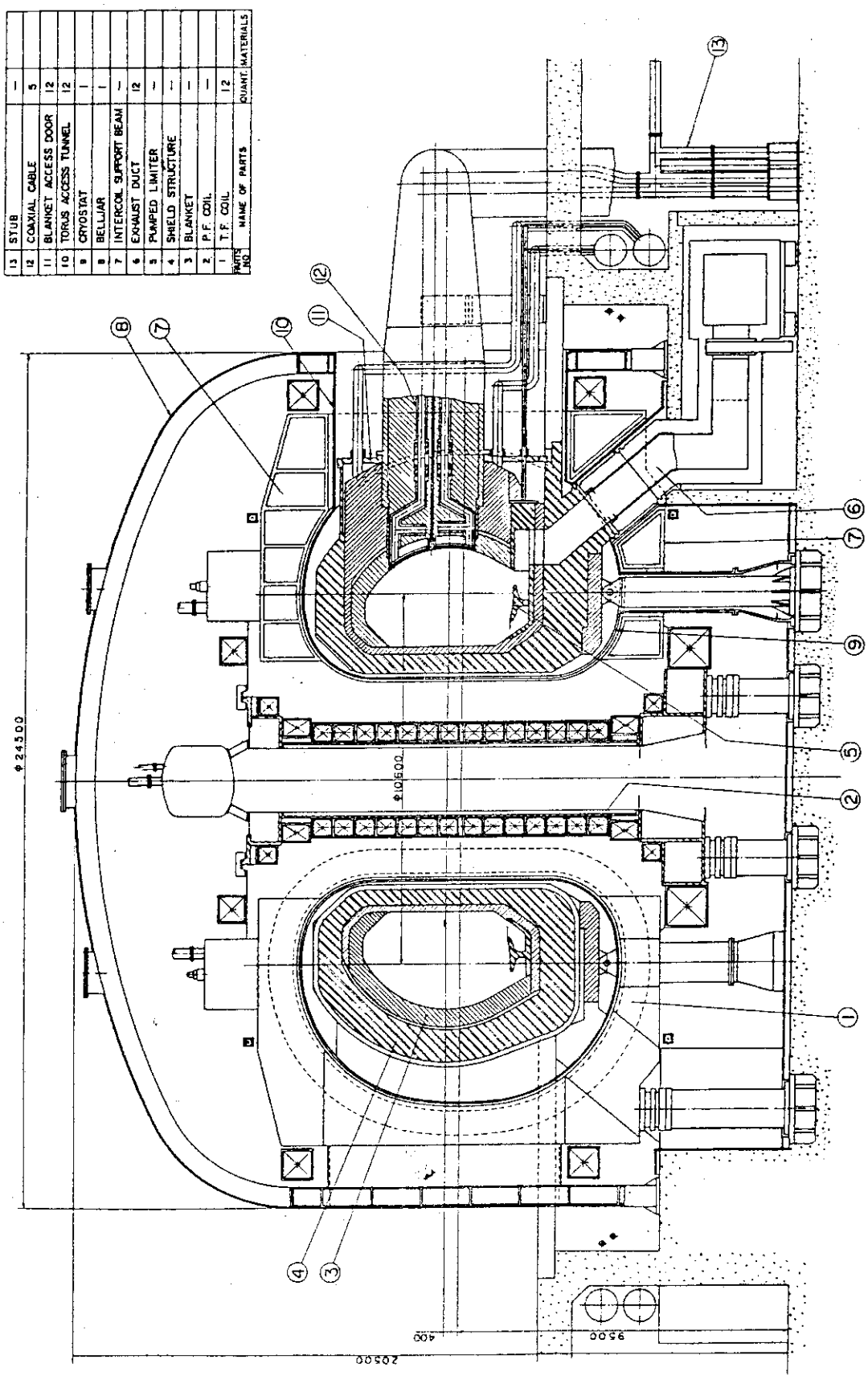

Fig. XI-6-1 INTOR-J-IIA Vertical view of INTOR

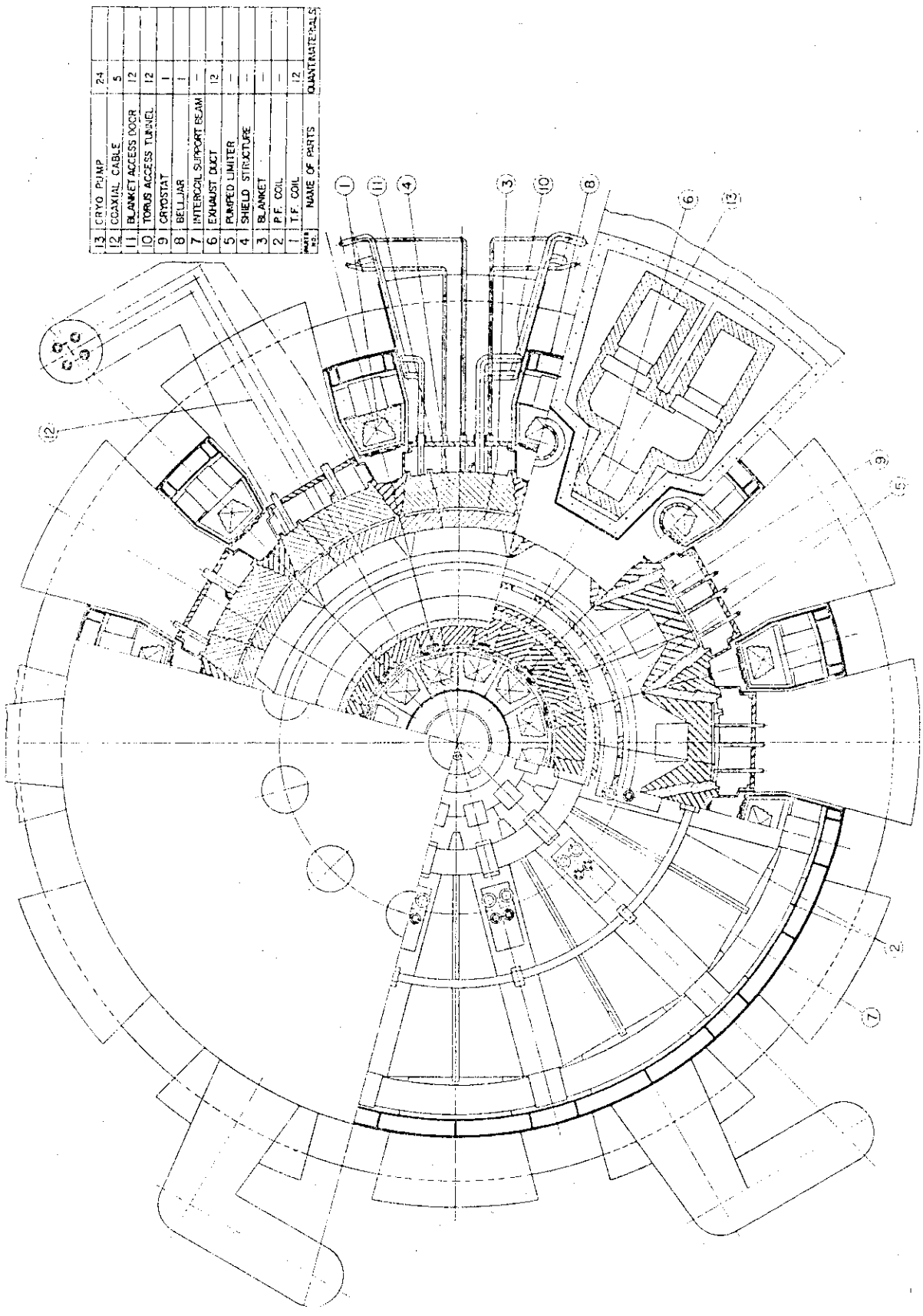

Fig. XI-6-2 INTOR-J-IIA Plan view of INTOR

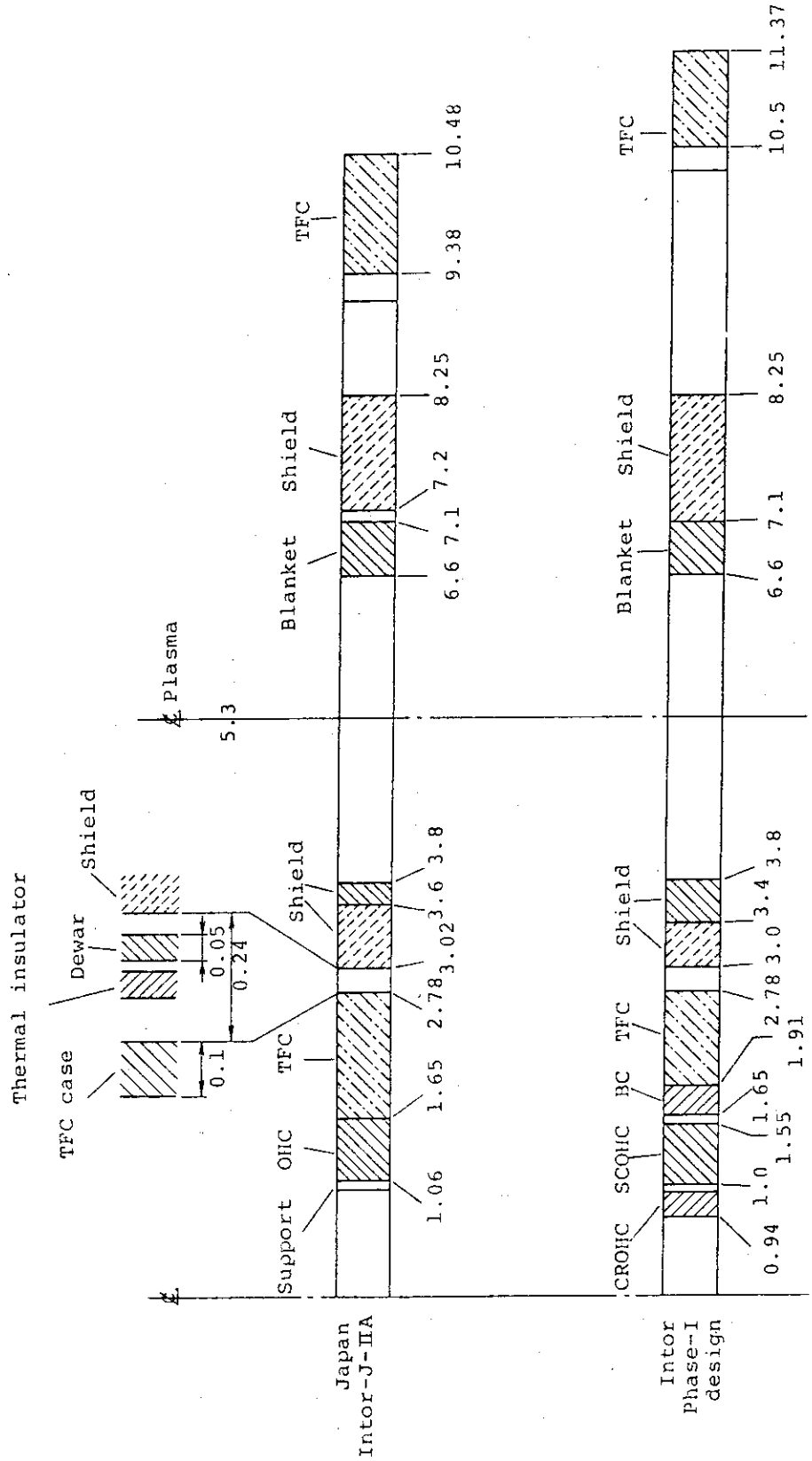

Fig. XI-6-3 Radial build

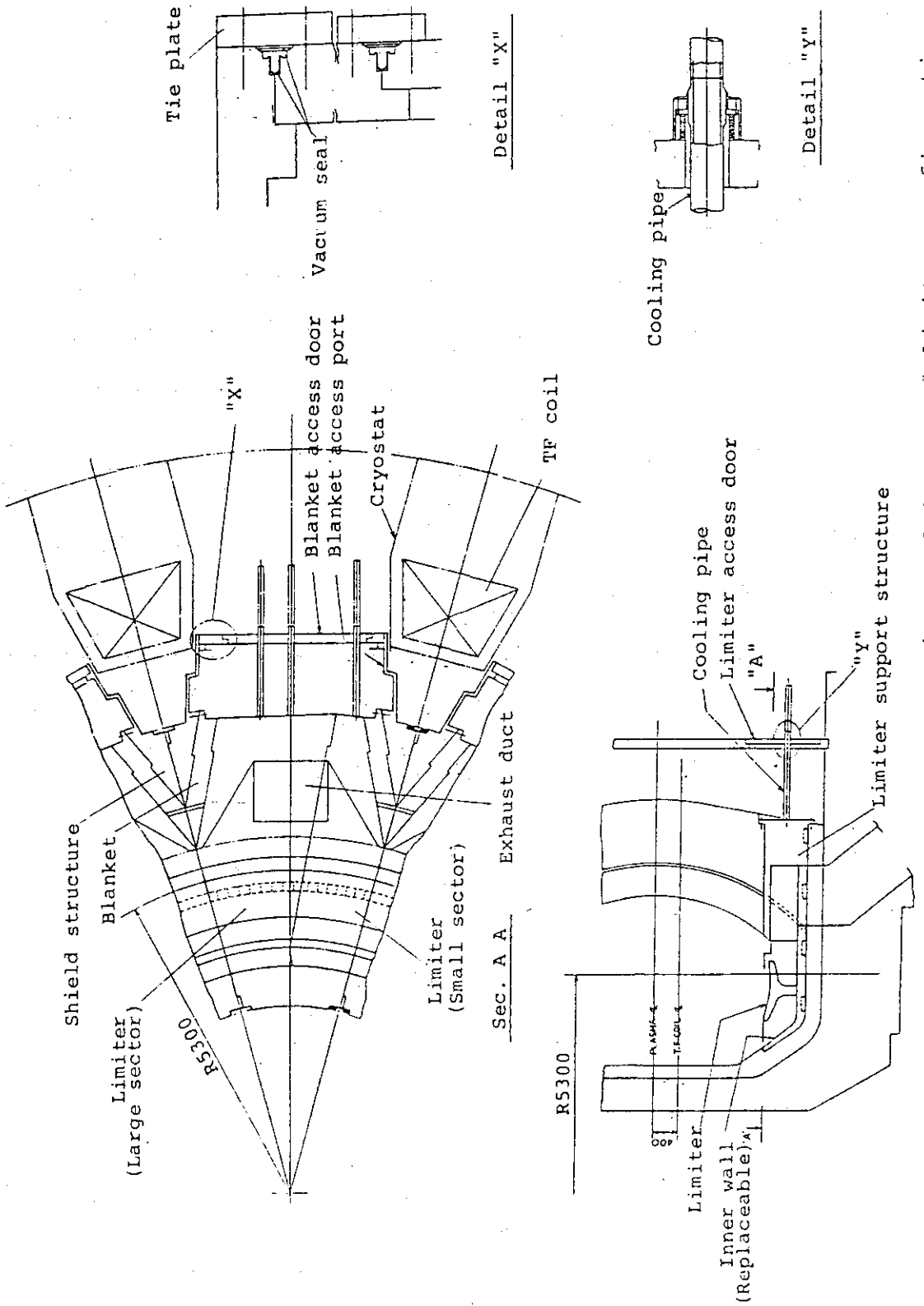

Fig. XI-6-4 Pumped limiter configuration

6.1.2 Alternative concept (Outboard single pumped limiter)

The reactor structure concept, whose plasma center is located on TF coil center, and which is equipped with the outboard single pumped limiter is shown in Fig. XI-6-5. The limiter plate is curved and double-edged configuration.

TF coil bore size 6.6m × 8.9m is determined from the space necessary for maintenance of the limiter and the blanket sectors. In this concept, the single straight motion is supposed.

The torus is segmented as 24 sectors/12 TF coils, and the replacement procedure of the limiter and blanket in this case are shown in Fig. XI-6-6.

The replacement of the outboard pumped limiter is accomplished as the same manner as the case of the bottom pumped limiter which is shown in section 6.4.

PARTS NO.	NAME OF PARTS	QUANT	MATERIALS
13	STUB	—	
12	COAXIAL CABLE	5	
11	BLANKET ACCESS DOOR	12	
10	TORUS ACCESS TUNNEL	12	
9	CRYOSTAT	1	
8	BELLJAR	1	
7	INTERCOIL SUPPORT BEAM	—	
6	EXHAUST DUCT	12	
5	PUMPED LIMITER	—	
4	SHIELD STRUCTURE	—	
3	BLANKET	—	
2	P.F. COIL	—	
1	T.F. COIL	12	

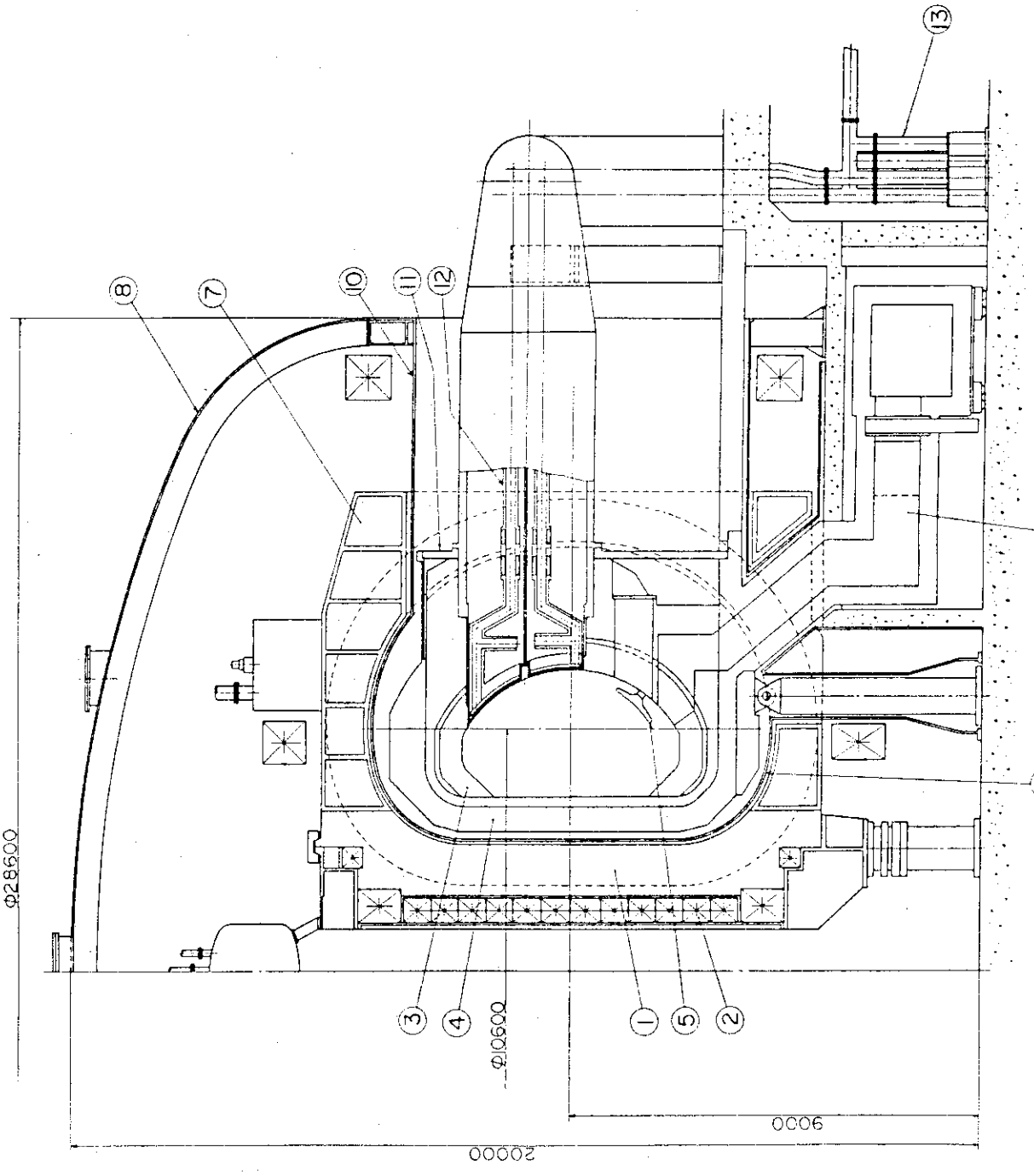

Fig. XI-6-5 Reactor concept with outboard single pumped limiter

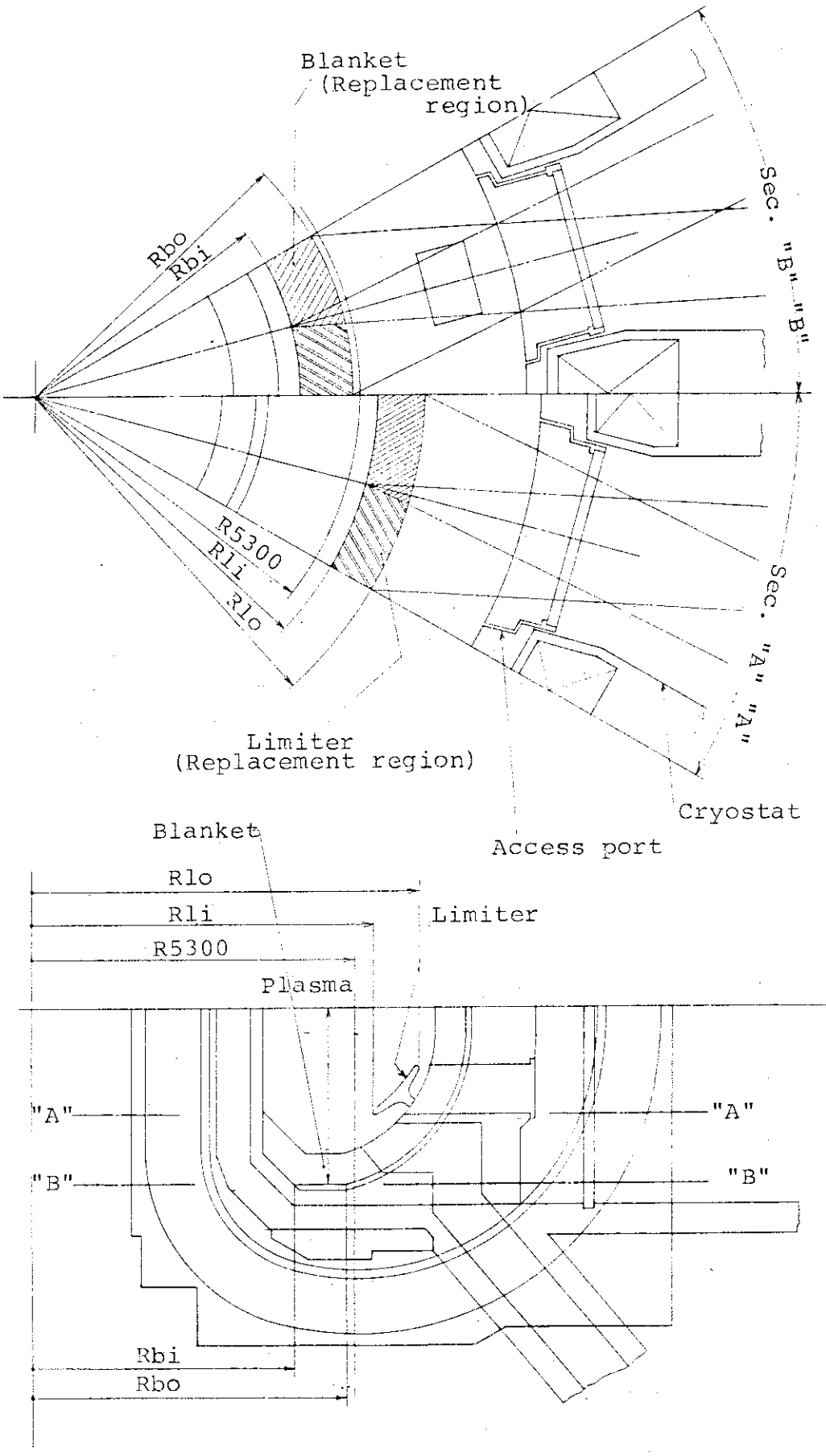

Fig. XI-6-6 Replacement region of blanket and limiter

6.2 Poloidal divertor configuration

The reactor structure with poloidal divertor is examined. The TF coil bore size is fixed as 6.6m × 9.3m. In corresponding to this TF coil bore, location and ampere turn of the PF coil are arranged. The torus and divertor segmentation are determined according to the maintenance method adopted for single motion replacement procedure of the divertor.

- o The configuration of divertor is adopted without modification from that examined in Phase-I.
- o The reactor structure is shown in Fig. XI-6-7. The segmentation of the divertor is shown in Fig. XI-6-8.
- o The replacement of the divertor is performed by retraction of each sector between TF coils with single straight motion. The precise procedure and sequence of the replacement as well as the required remote maintenance equipments are in principle same as those of the limiter.

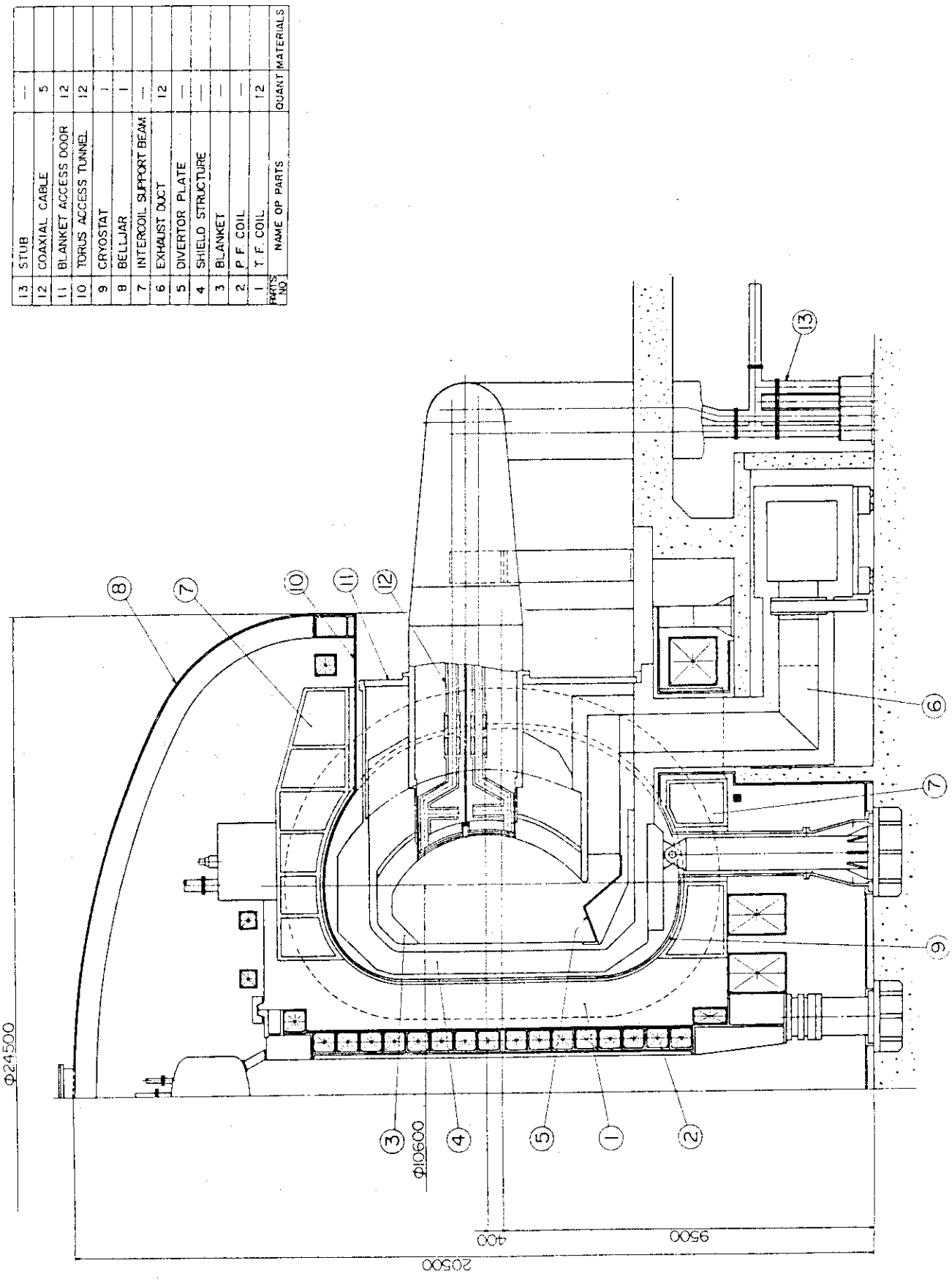

Fig. XI-6-7 Vertical view of INTOR

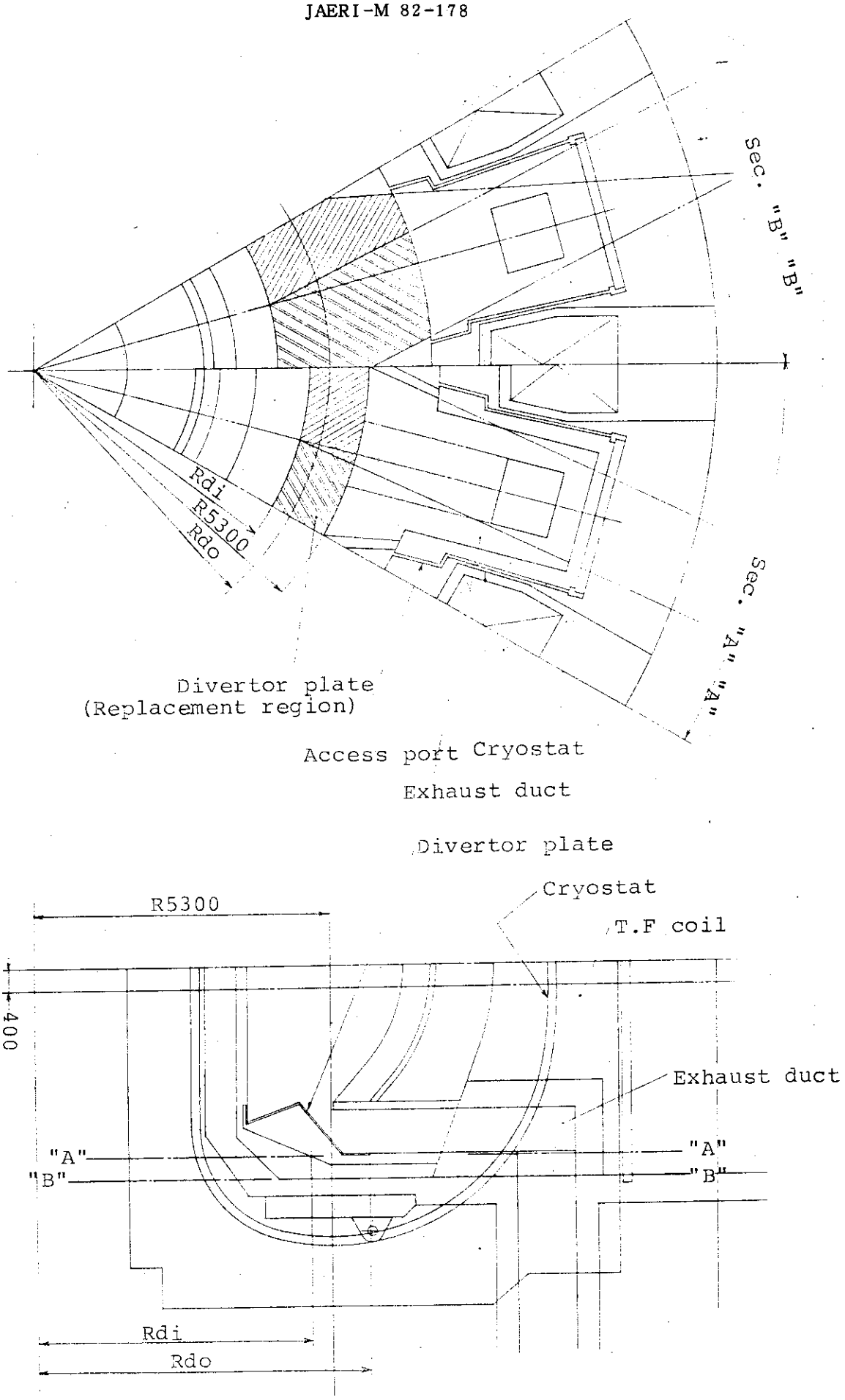

Fig. XI-6-8 Segmentation and replacement region of divertor

6.3 Universal concept

Concerning the Universal-INTOR type PF coil distribution, the reactor structure for both limiter and divertor are considered under the following specifications.

i) Vacuum boundary is combined type

ii) Torus closure is completed without access port

iii) Torus is segmented as 1 ∿ 2 sectors/TF coil

iv) TF coil bore is 6.6m × 9.3m

The reactor concept with divertor is shown in Fig. XI-6-9. The reactor concept with limiter is shown in Fig. XI-6-10. The divertor/limite and the blanket are segmented into 24 sectors in torus (2, small and large sectors/TF coil). The small sector is retracted after the retraction of the large one.

In order to avoid the T shape seal, the structure as shown in Fig. XI-6-11 is adopted.

The segmentation concept of the divertor/limiter and blanket is shown in Fig. XI-6-12.

All TF coils and PF coils are located in the same vacuum boundary (bell jar).

The maximum radius PF coil has a independent cryostat structure. However, this structure is connected with the bell jar and holds the common vacuum boundary.

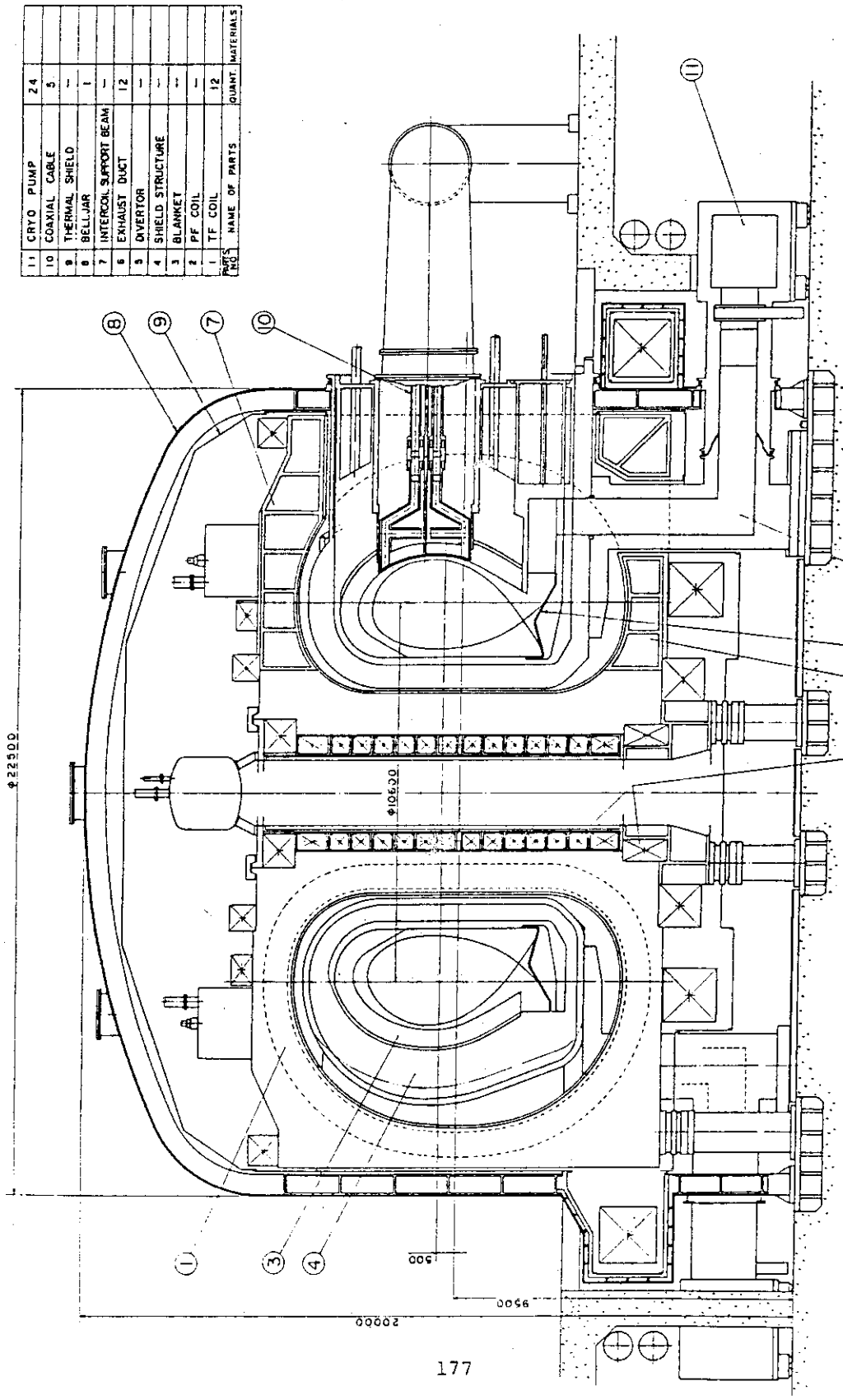

Fig. XI-6-9 Vertical view of INTOR (universal type)

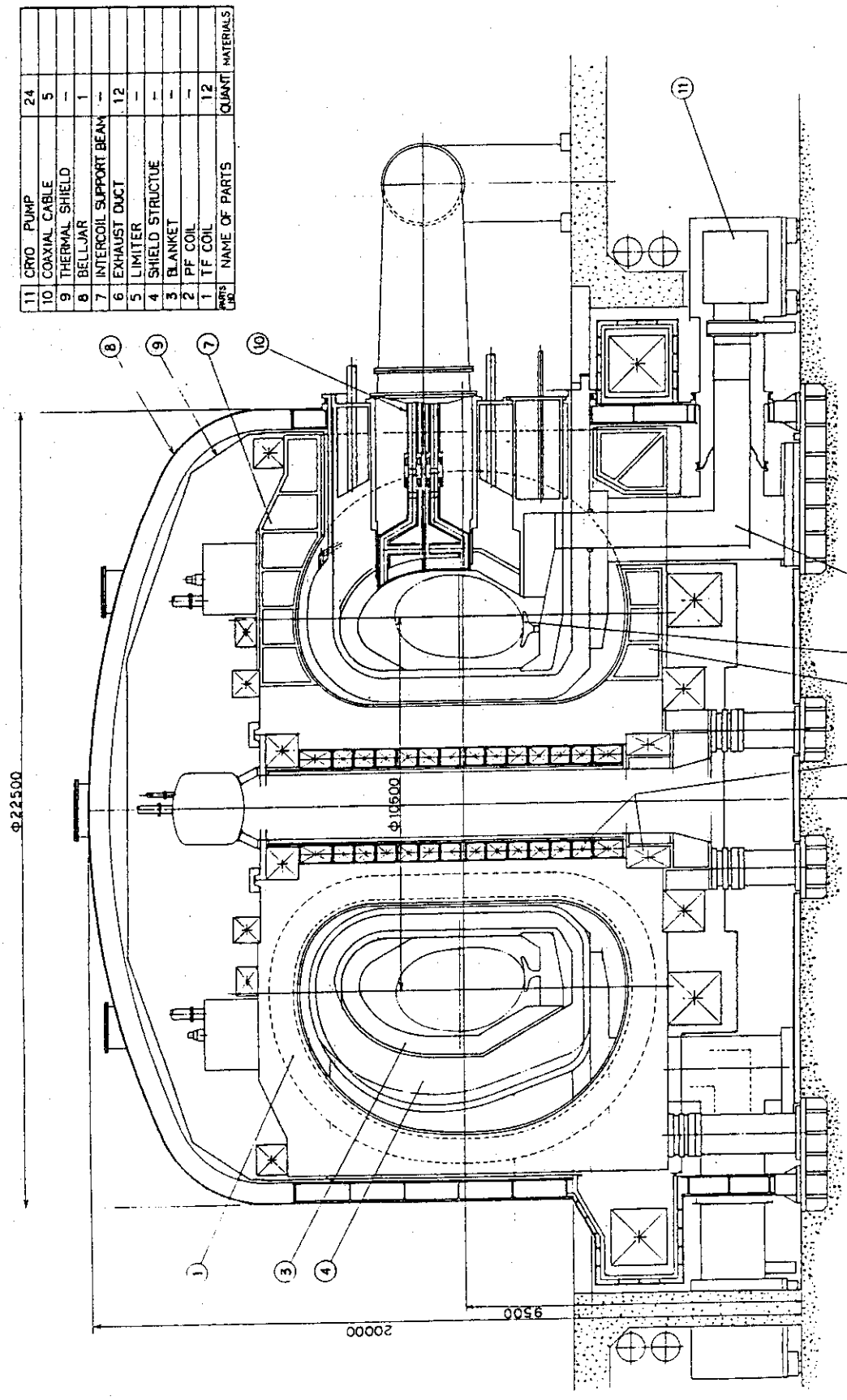

Fig. XI-6-10 Vertical view of INTOR (universal type)

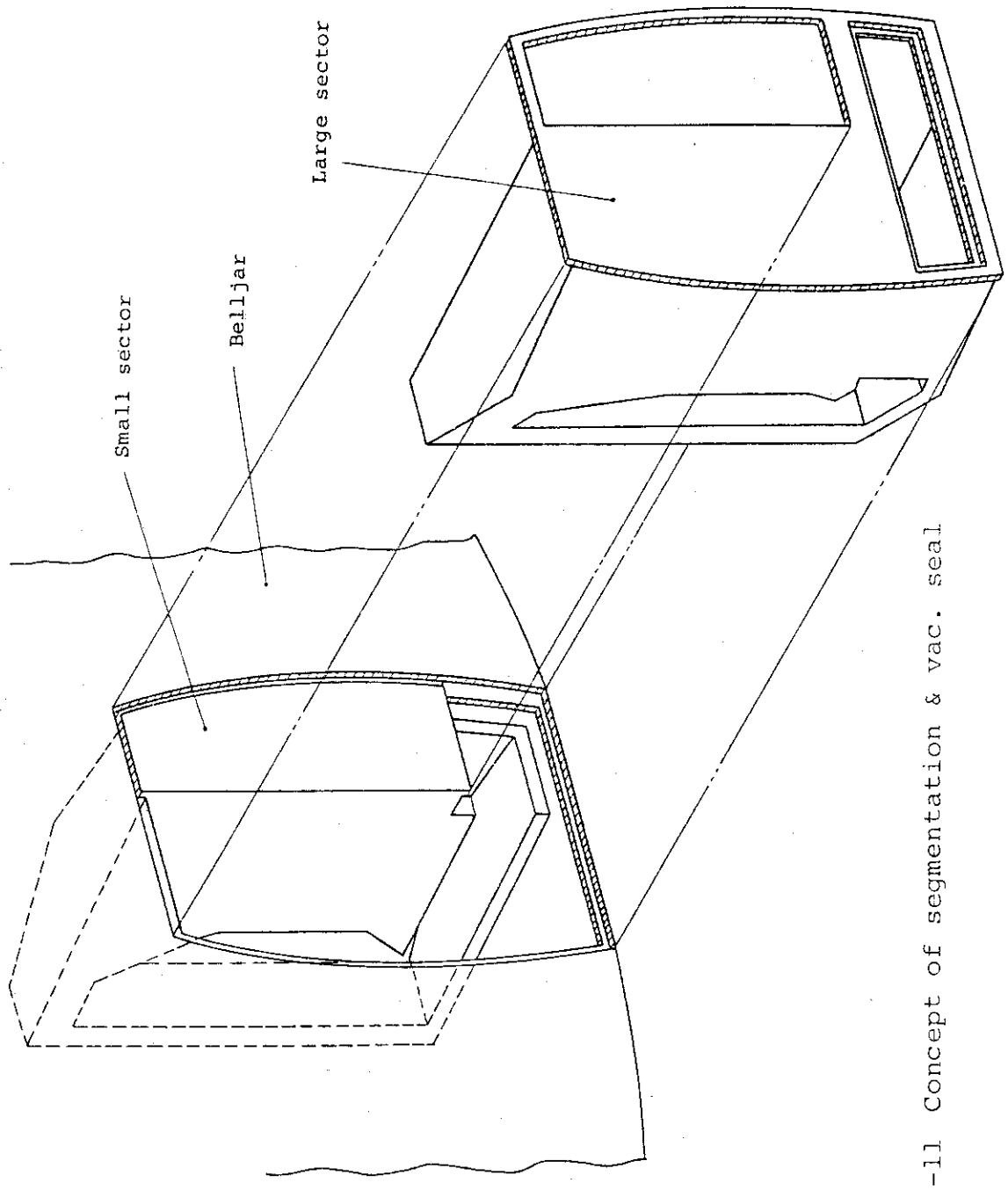

Fig. XI-6-11 Concept of segmentation & vac. seal

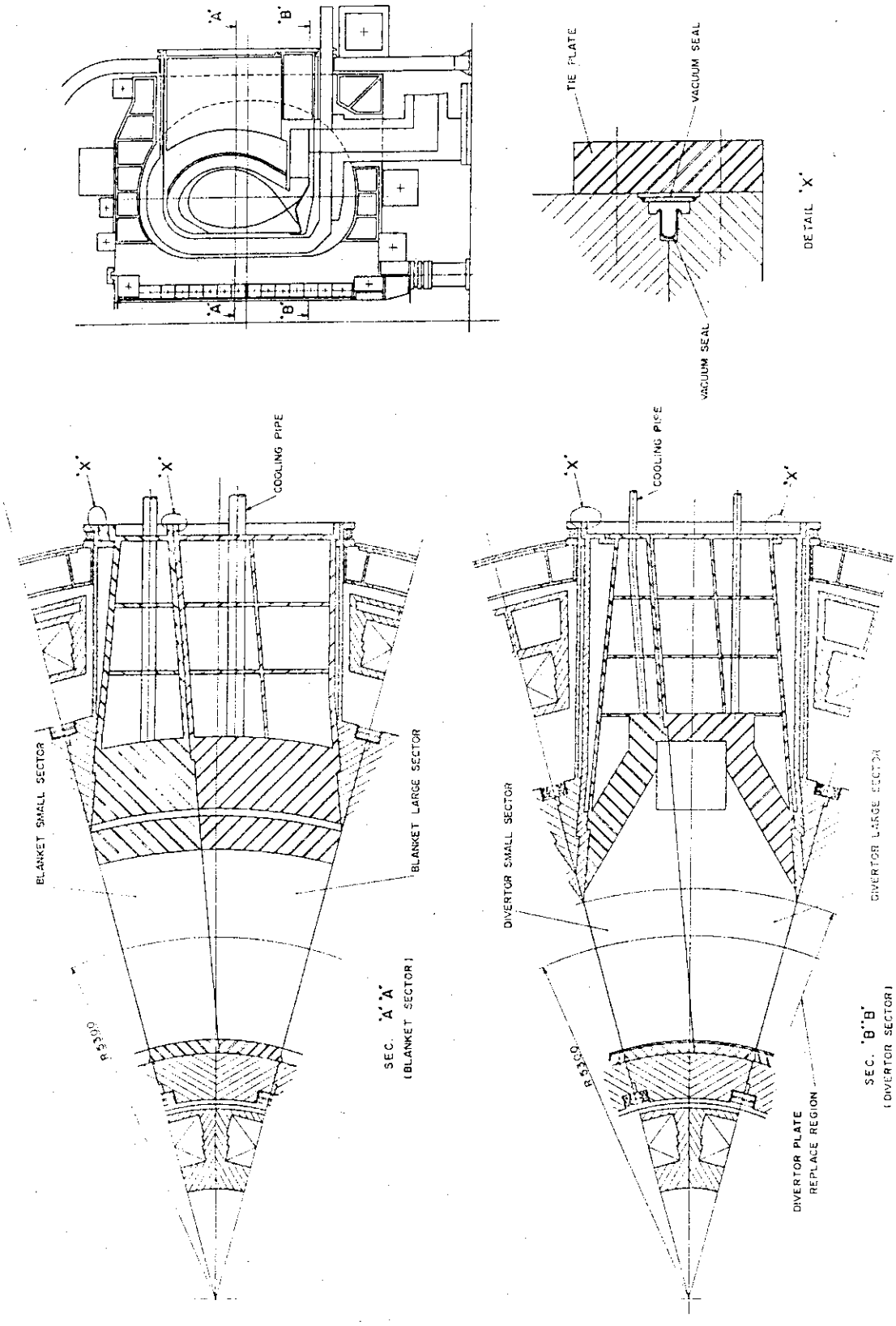

Fig. XI-6-12 Sector of blanket & divertor

6.4 Maintenance and Segmentation

(1) Segmentation and replacement procedure of pumped limiter

The segmentation of the limiter is intimately associated with the segmented blanket sector into which the pumped limiter is inserted and fixed. The space required for limiter replacement is also one of the factor.

The region to be replaced in the limiter is shown in Fig. XI-6-13. The inner radius and outer radius of the limiter blade in 4525mm and 5525mm respectively. Only the outer radius is concerned in maintenance operation space.

Being the TF coil bore size 6.6mm × 9.3m, TF coil the thickness 1.25m and the distance from the TF coil helium vessel to the cryostat wall 0.2m, there is a sufficient space which permits the pump limiter of one sector/TF coil to be replaced as shown in Fig. XI-6-14. However, this concept is possible only when the concept of one blanket sector/TF coil is adopted.

In the case of the concept of two or further blanket sectors/TF coil, the vacuum seal will be T type or + Type which reduce the reliability of the vacuum seal. This concept is not realizable from the view point of the mechanical structure. Therefore, in our design, the pumped limiter is segmented as 2

sectors/TF coil as shown in Fig. XI-6-15. The limiter segment between two TF coils consists of large sector and small sector which are retracted horizontally in radial direction as shown in Fig. XI-6-16.

The pumped limiter is supported from the limiter support structure in which the vacuum duct is integrated as shown in Fig. XI-6-15.

The electromagnetic force acting on the limiter blade at plasma disruption is supported with two keys provided at the two side wall of the limiter support structure.

These keys function effectively as positioning tool at the time of assembly of the pumped limiter sector.

The cooling pipes coming from each limiter sector pass through the access door on which the vacuum sealing is carried out.

(2) Maintenance of pump limiter

Disassembly procedure for pump limiter

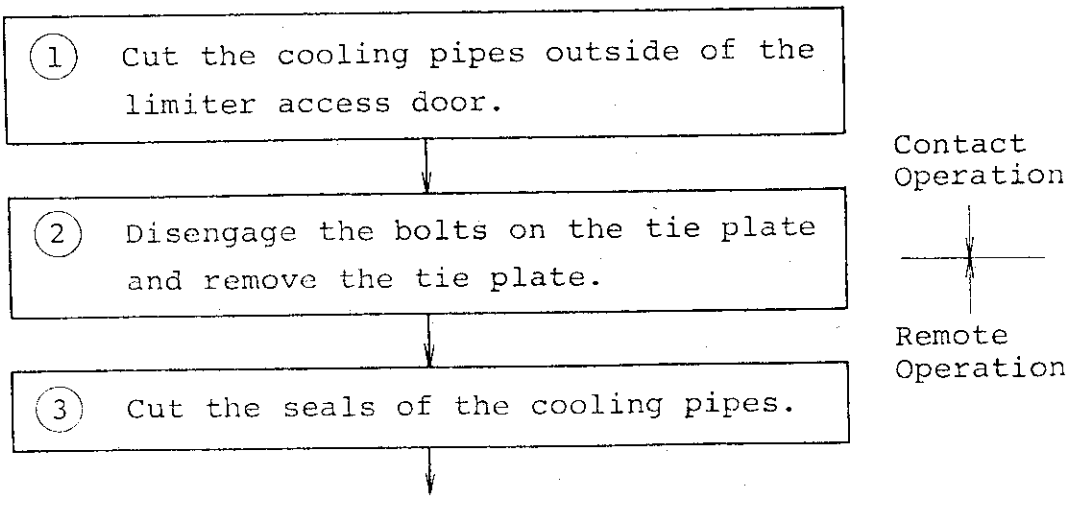

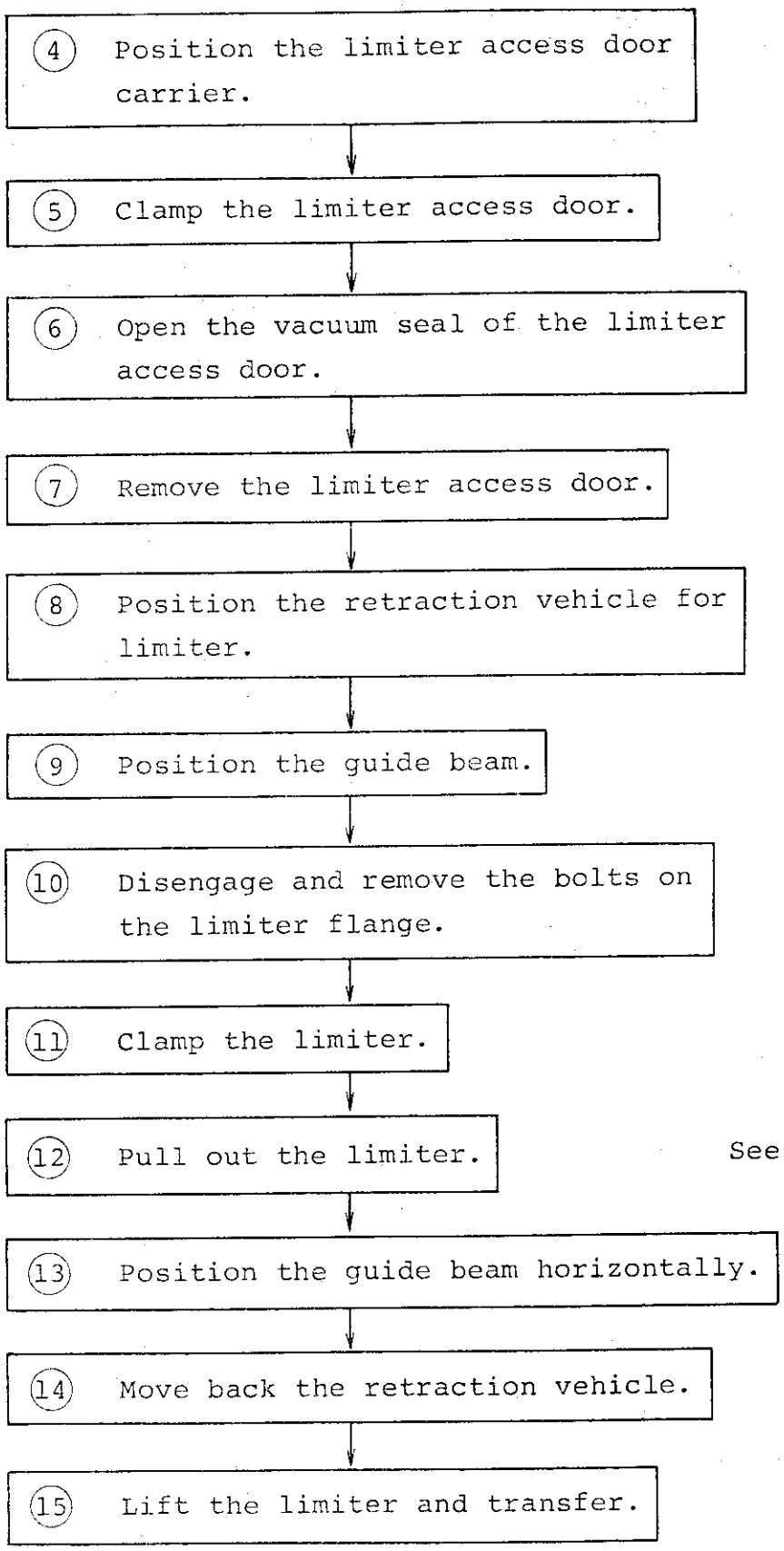

See Fig. XI-6-16

(3) Maintenance equipment

As the replacement frequency of the limiter is thought to be relatively high, the remote maintenance machine for limiter replacement should be designed to be special machine with high efficiency and reliability.

The following equipments are served for the purpose of the maintenance of the pumped limiter.

1 Overhead crane
2 Cutting machine of seal for cooling pipe
3 Welding machine of seal for cooling pipe
4 Limiter access door carrier
5 Retraction vehicle for limiter

The equipments listed above have following functions,

1 Overhead crane

This crane is primarily provided to service the reactor. During the maintenance operation of the limiter, this crane functions to transfer remote manipulator, damaged limiter and new limiters.

Several ten ton capacity should be provided for this crane in order to maintain the pumped limiter.

2 Cutting machine of seal for cooling pipe

This machine is provided to cut and remove the sealing part of the cooling pipe which passes through the limiter access door.

As shown in Fig. XI-6-17, the inserted colet which clamps the pipe from the interior, and which is primarily equipped at the top of the manipulator, permits the positioning and fixing of the cutting machine of seal.

The cutting velocity is considerably reduced in order to reduce the reaction. The cutter is of cylindrical shape, with which the seal ring and the welded part of seal will be cut and removed.

Weight of machine	30 kg
Cutting speed	100 rpm
Feed speed	0.1 mm/rev.

3 Welding machine of seal for cooling pipe

This machine is provided for welding the sealing part of the pipe. The positioning is performed in the same manner as that of the cutting machine for seal.

The welding procedure is schematized in the figure shown in Fig. XI-6-18.

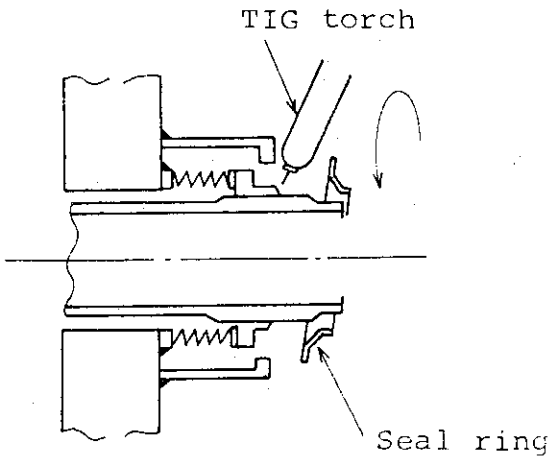

Fig. XI-6-18

The end part of bellows is welded at first, and after inserting and fixing the seal ring, the welding of inner and outer circumferences of the ring is performed.

Method of welding ; TIG
Welding speed ; 20 mm/sec.

4 Limiter access door carrier

This carrier has several machines in order to perform several kind of functions.
This carrier equips the jib which permits to hold the manipulator and which has sufficient capacity to handle it freely.
This carrier also equips a machine for handling and positioning of the limiter access door.
The carrier equips also a machine for welding and cutting of the sealing part of the limiter access door.

These three machines are equipped in the same remote driving vehicle as shown in Fig. XI-6-19.

a) Manipulator

This manipulator handles the cutting and welding machine for cooling pipes and functions to transfer and position the sealing structures.

The manipulator has seven freedoms with 40 kg capacity hoist and is operated by force-reflecting servo-manipulator slave units. The manipulator has an arm of 1.2 m maximum length.

Concerning the jib which is provided for supporting of the manipulator, one articulation is introduced at its central part in order to permit the operation in the vicinity of the floor.

The jib has a front arm of 1.4 m length and a back arm of 2.5 m length, which, on the occasion of the blanket replacement operation, enable to weld and cut the seal of pipes situated at the upper part of the blanket access door.

b) Machine for handling and positioning of the limiter access door.

This machine functions not only to support the limiter access door of 2 tons weight after disengaging the bolts of the limiter access door and opening the pipe sealing, but also to position and fix the orbit of the cutting or welding machine.

In order that the positioning and locking of the machine are just performed, the nails of the machine are inserted to the holes bored at the central part of the limiter access door.
The precise positioning and the strong grasping are required in order to cut the sealing part.

c) Machine for welding and cutting of the sealing part of the limiter access door.

This machine consists of one welding vehicle and two cutting vehicles. They can travel on the orbit installed on the machine for handling and positioning of the limiter access door.

One of the cutting vehicles functions to cut and remove the V shaped sealing structure with ϕ20 end mill, the other cutting

vehicle functions to cut and remove the plate shaped sealing structure with ϕ60 cutter.

Each cutting vehicle has a capability to control the quantity of cutting, the cutter speed and feed speed.

The welding vehicle equips two TIG torches which permit to weld the two end of seal at the same time by only one traveling on the orbit.

The height and the distance between two torches are controlable and adjustable according to the sealing structures: U shaped or plate shaped.

Traveling speed of vehicle	;	0 ∿ 200 mm/min. (continuously variable)
Cutting speed	;	∿ 40 mm/min.
Welding speed	;	∿ 100 mm/min.
Performance of motor for cutting	;	2.2 kW
Cutting speed	;	180 rpm
Performance of motor for traveling	;	1.5 kW

d) Traveling system

Total weight of the limiter access door carrier amounts to about 20 ton. So, the traveling speed kept at low: about 2 m/min.

The transfer of the limiter access door carrier between the sectors is performed by the overhead crane.

5 Retraction vehicle for limiter

This retraction vehicle for limiter is provided to service both large limiter sector and small limiter sector, and functions to fasten and disengage the bolts on the limiter frange. When the limiter should be retracted, with the

6 Other equipments

Maintenance operation of the pumped limiter requires the following additional equipments.

a) Chip treatment equipment
b) Machine tool for bolts fixing
c) Remote viewing equipment
d) Non-destruction-test equipments

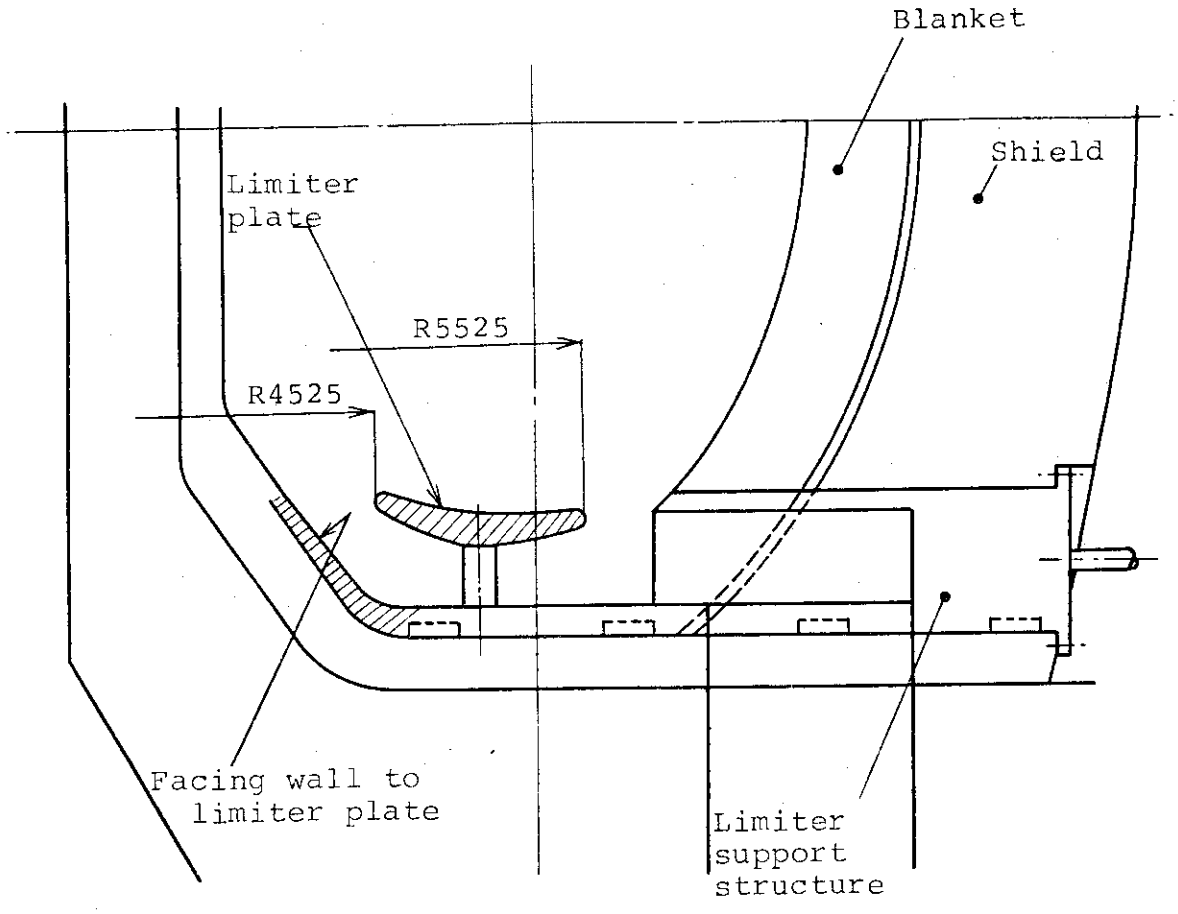

Fig. XI-6-13 Replacement region of pumped limiter

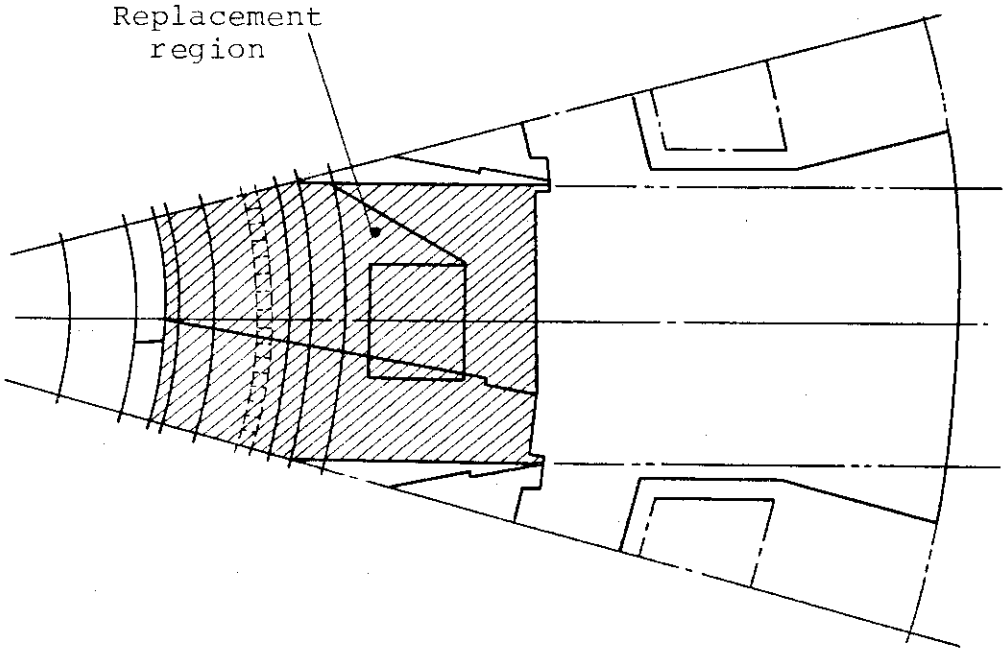

Fig. XI-6-14 Replacement region of pumped limiter

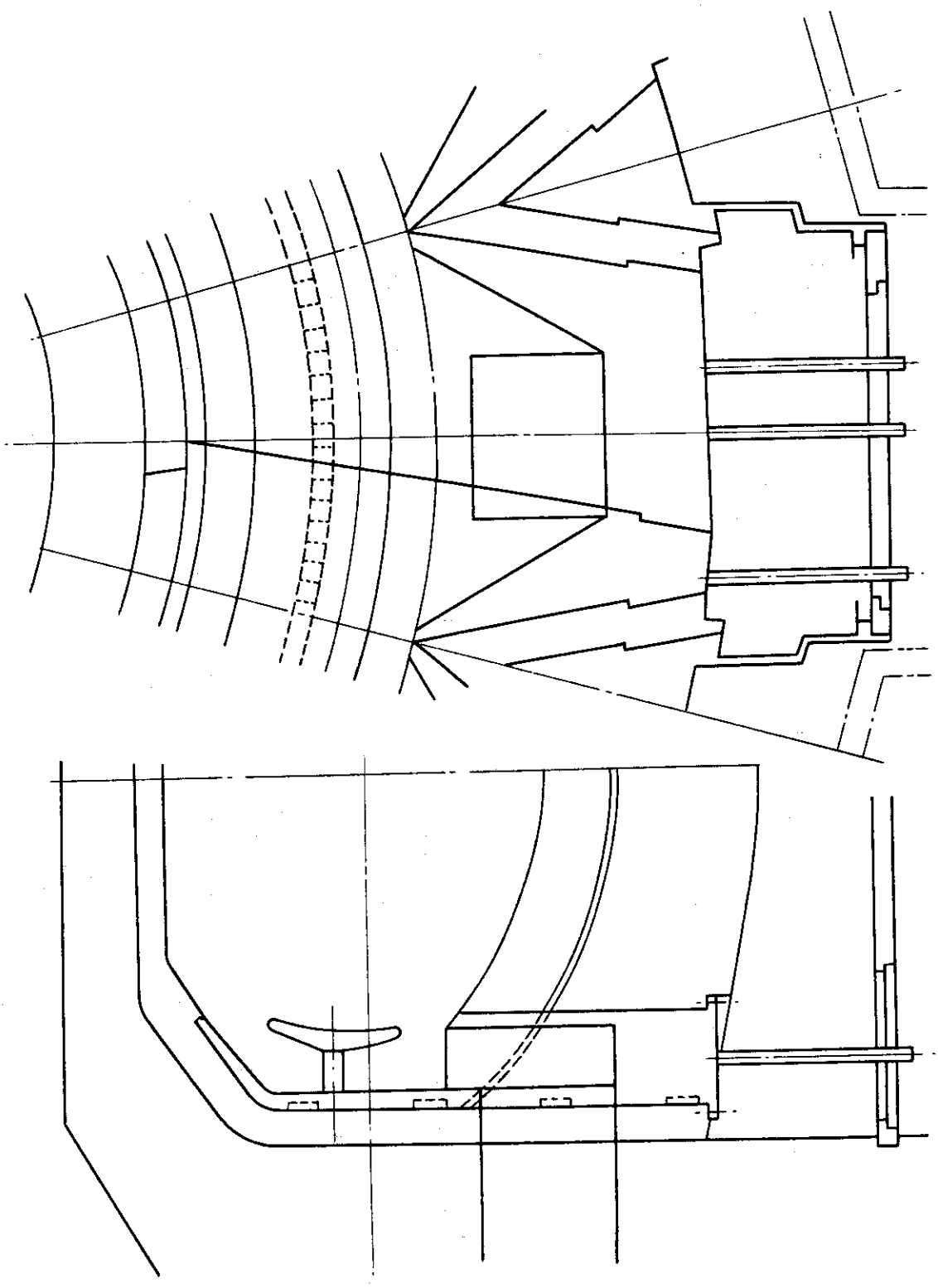

Fig. XI-6-15 Limiter

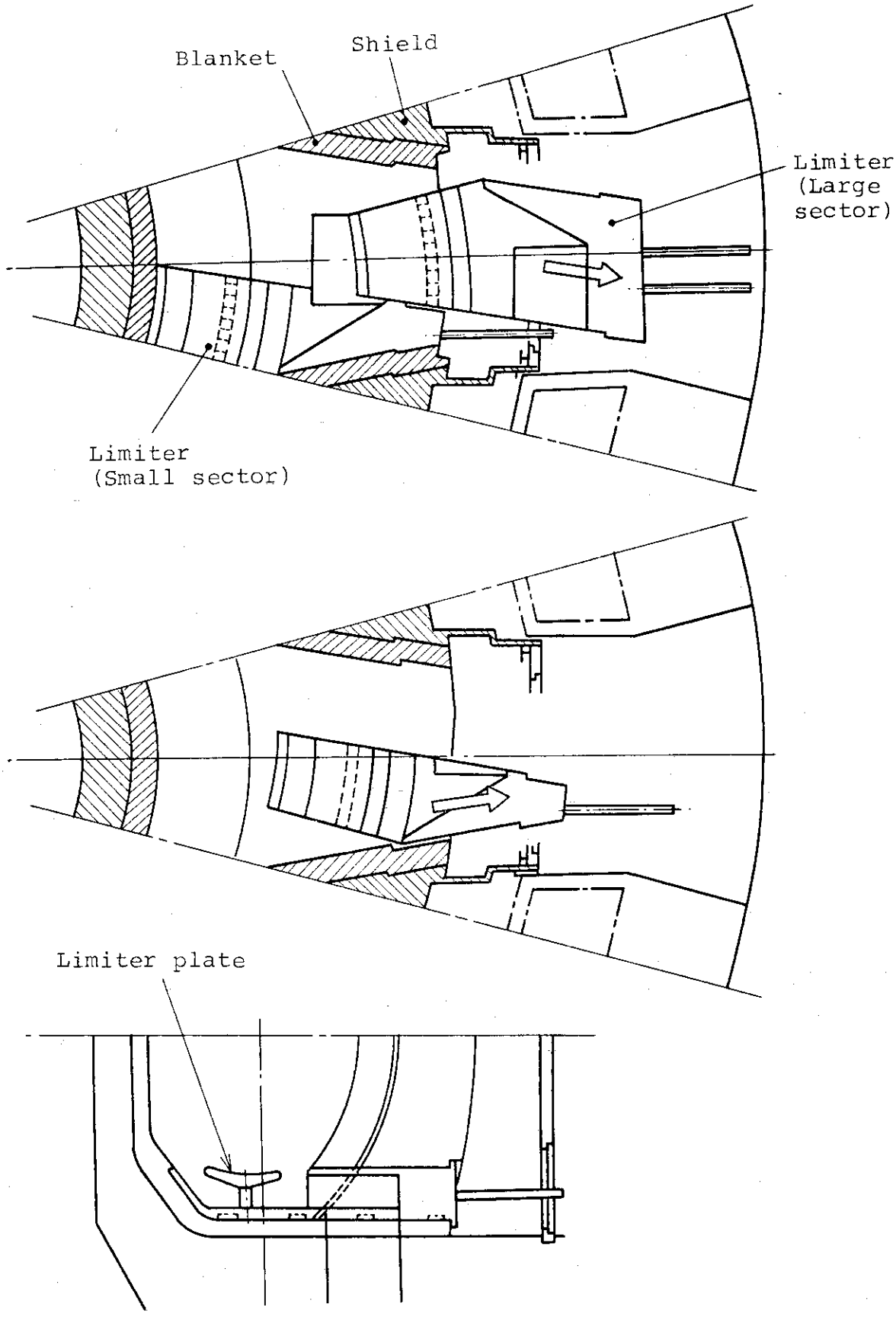

Fig. XI-6-16 Limiter replacement concept

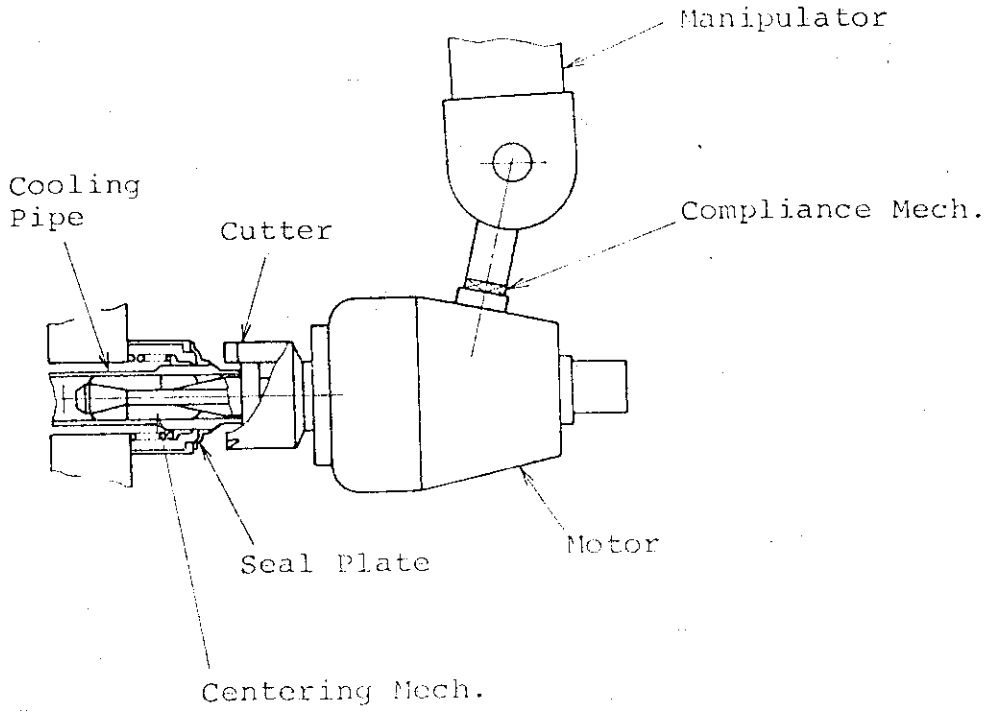

Fig. XI-6-17 Cutting tool

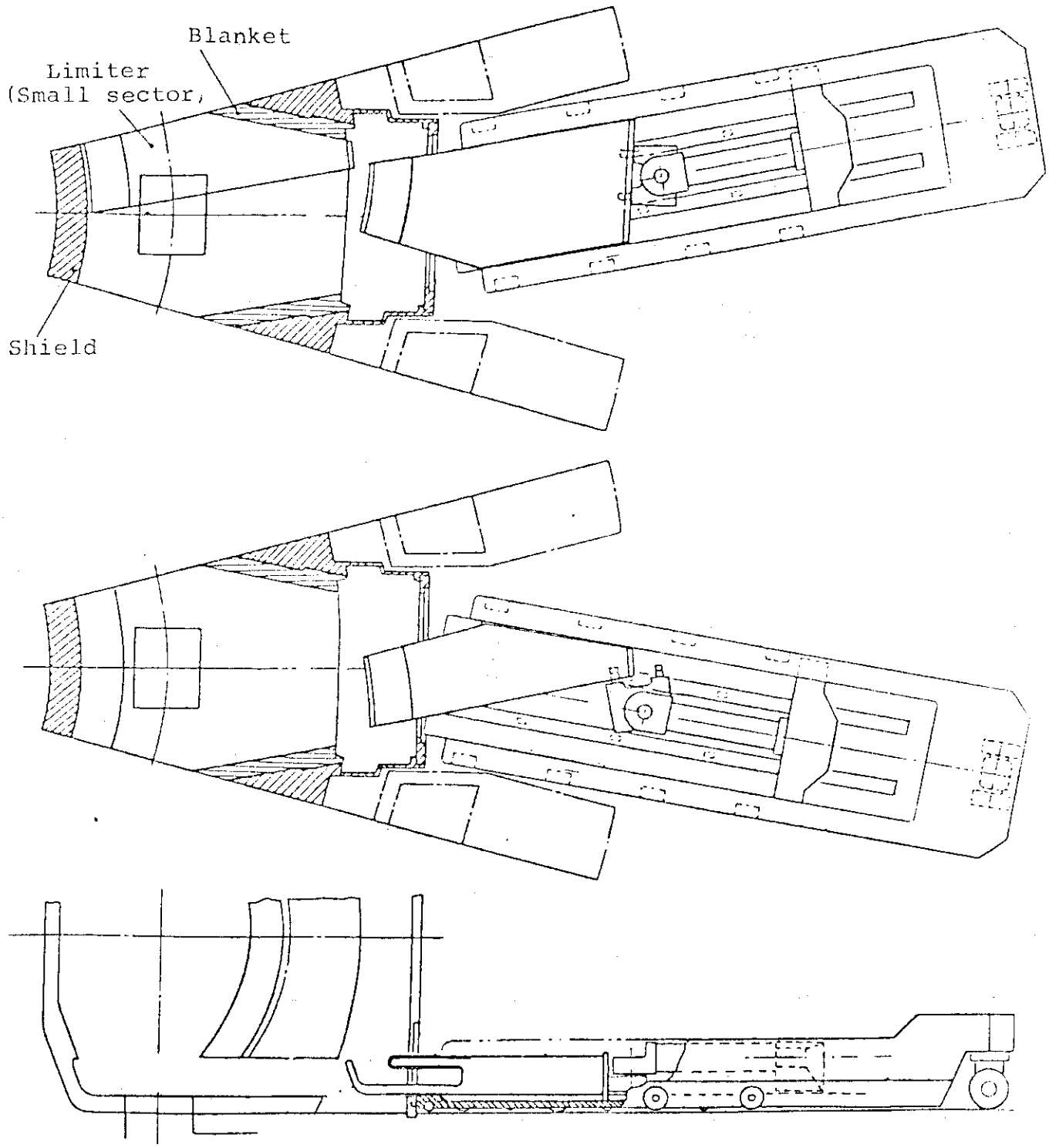

Fig. XI-6-19 Limiter replacement procedures

7. Heating system

As the auxiliary heating system, the concepts of NBI and RF are considered.

The design of the antenna as well as the wave guide structures are accomplished in taking account the compatibility of the overall reactor system and of repair and maintenance system.

7.1 NBI configuration

The same structure and size of the NBI designed in Phase I is adopted.

As shown in Fig. XI-7-1, one beam line of the NBI has 8 ion sources equipped as 2 × 4. The NBI size is 8m (width) × 9.4m (length) × 8m (height).

The connection of the NBI to the reactor is shown in Fig. XI-7-2 .

7.2 RF configurations

(1) ICRH

The installation of antenna, Farady shield and coaxial cable of ICRH to the reactor are considered. The schematic view of the ICRF antenna installed in the reactor is shown in Fig. XI-7-3. The blind like part is the Faraday shield whose position is nearly the first wall surface. As the one port has four antenna, the Faraday shield is divided into four region. The front view of the four ICRF antenna is shown in Fig. XI-7-4.

The central conductor, the return conductor, the end conductor and the coaxial cable are shown in the cross sectional view removed the Faraday shield. The return conductor and the end conductor are fixed in the wall. The lateral cross sectional view of the ICRF antenna is show in Fig. XI-7-5. The center conductor is very near the Faraday shield, and the gap spacing of them is 1.5 cm. The all antenna elements and the coaxial cable have cooling channels.

The vertical entire cross sectional view of the ICRF antenna in the reactor is shown in Fig. XI-7-6. In order to aboid the neutron dammage to the insulators supporting the coaxial cable, the each four coaxial cable has corner covered with shielding structures.

The repair and maintenance of antenna or Faraday shield are carried out by retraction with the shield structure behind the antenna structures.

The main specifications are follows.

(1) RF parameter

Frequency	85 MHz
Input power/port	15 MW
Port Number	4
Total input power	50 (+10) MW
Pulse width	10 sec.
Repetition rate	10 sec/246 sec.

(The number in the parentheses denotes redundancy.)

(2) Antenna parameter

Distance from central conductor to plasma surface	9.2 cm
Distance from central conductor to return conductor	30 cm
Central conductor length	1 m
Central conducdtor width	40 cm
Antenna impedance	
Resistance	9.3 Ω/m
Reactance	95.6 Ω/m

(2) LHRH

The installations of the launcher and the wave guide of LHRH to the reactor are investigated. The port size is horizontally about 2m and vertically about 3m. As the less r.f port number is desirable from the point of view of large branket space, we design the two type structures as shown in Fig. XI-7-7.

The one is composed of only A-type launchers as shown in Fig. XI-7-7 (a). Two ports of this type are required in this design.

The other is composed of 4 A-type launchers and 4 B-type launchers as shown in Fig. XI-7-7 (b).

The 85 MW r.f power can be injected by above three ports, which is less than the ICRF heating system by one port.

The total view of the A-type launchers in the reactor is shown in Fig. XI-7-8. The front surface of the launcher is set as same as the first wall position from the plasma surface.

The total cross sectional view of the R.F port is shown in Fig. XI-7-9. The bundle of waveguides are located in the shield.

The main specifications are follows.

Total input power	85 MW
Plasma heating power	75 MW in duty of 10 sec/ 246 sec.
Current drive power	10 MW in duty of 211 sec/ 246 sec.
Maximum available r.f port number	4
Maximum transport r.f power density	4.5 kW/cm^2
Interval of waveguide for plasma heating	36 mm
Interval of waveguide for current drive	18 mm
Long side width of waveguide	125 mm
R.F frequency	2 GHz
Launcher	Grill type

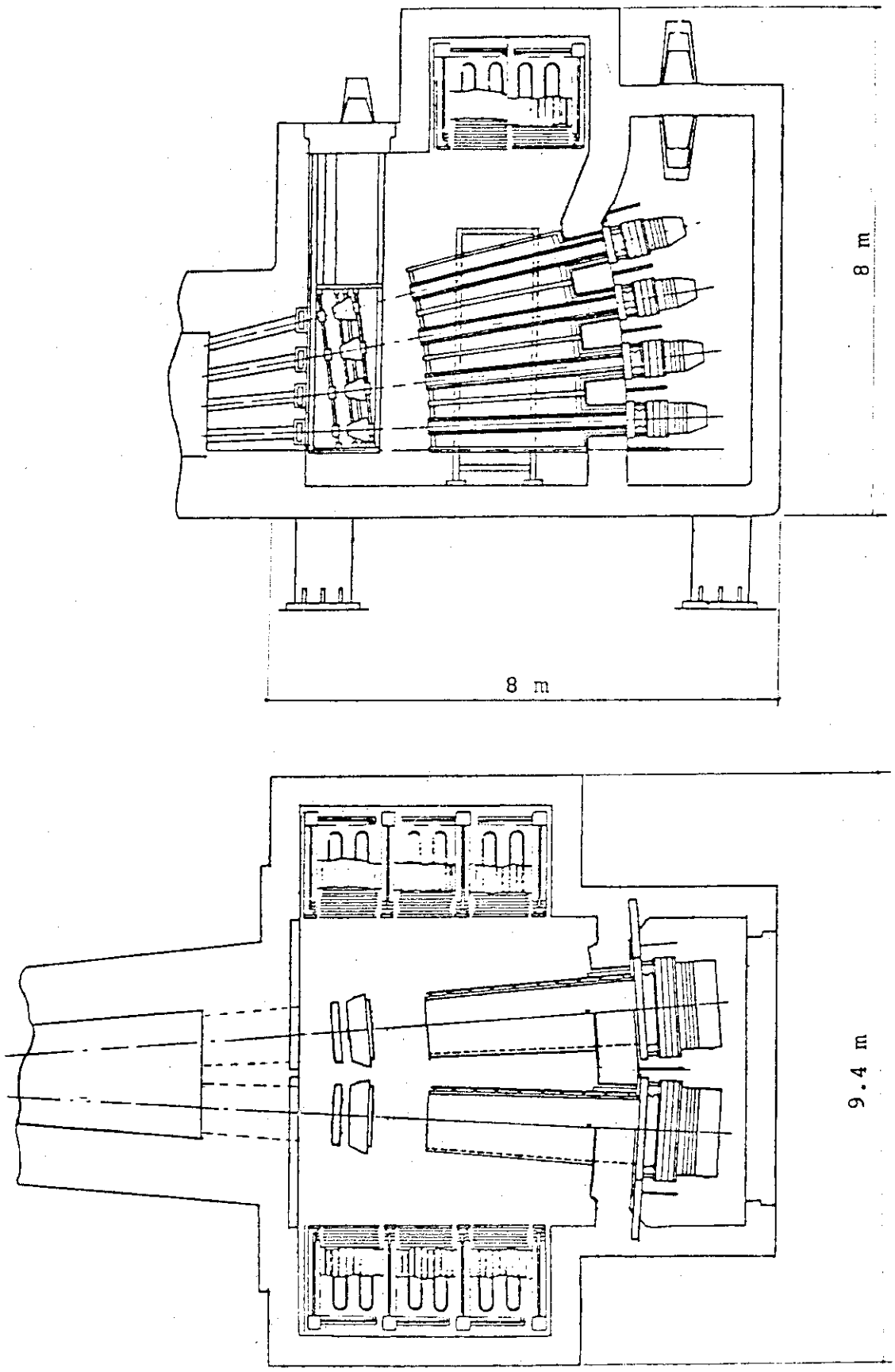

Fig. XI-7-1 Preliminary concept of the neutral beam

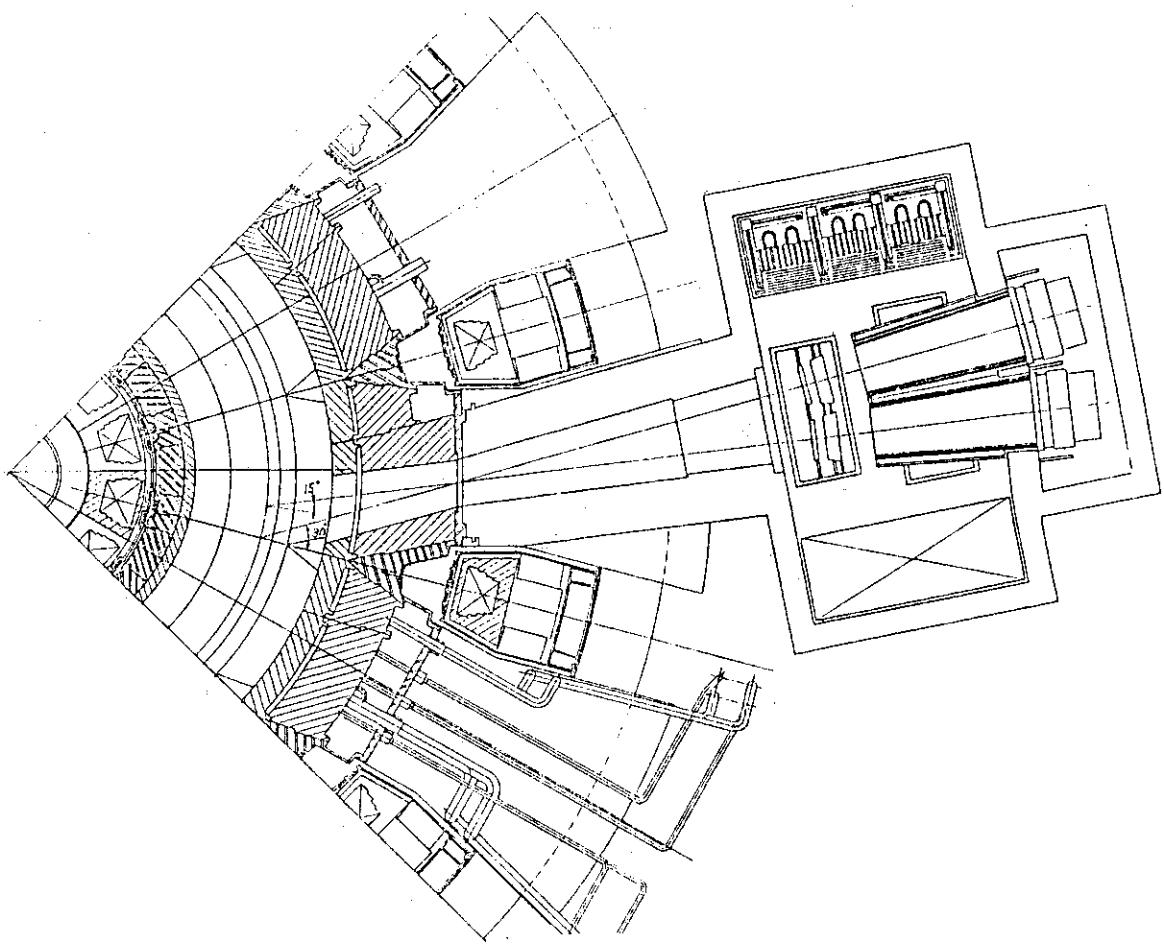

Fig. XI-7-2 Layout of NBI

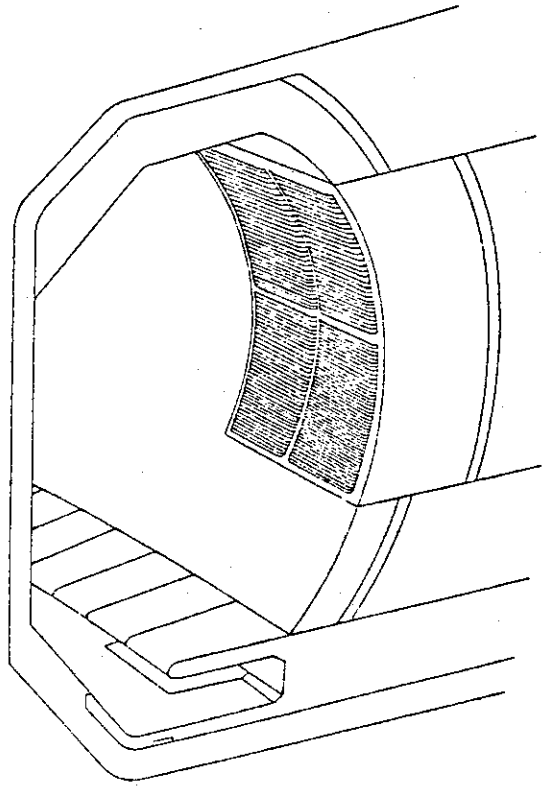

Fig. XI-7-3 Schematic view of ICRF antenna in reactor

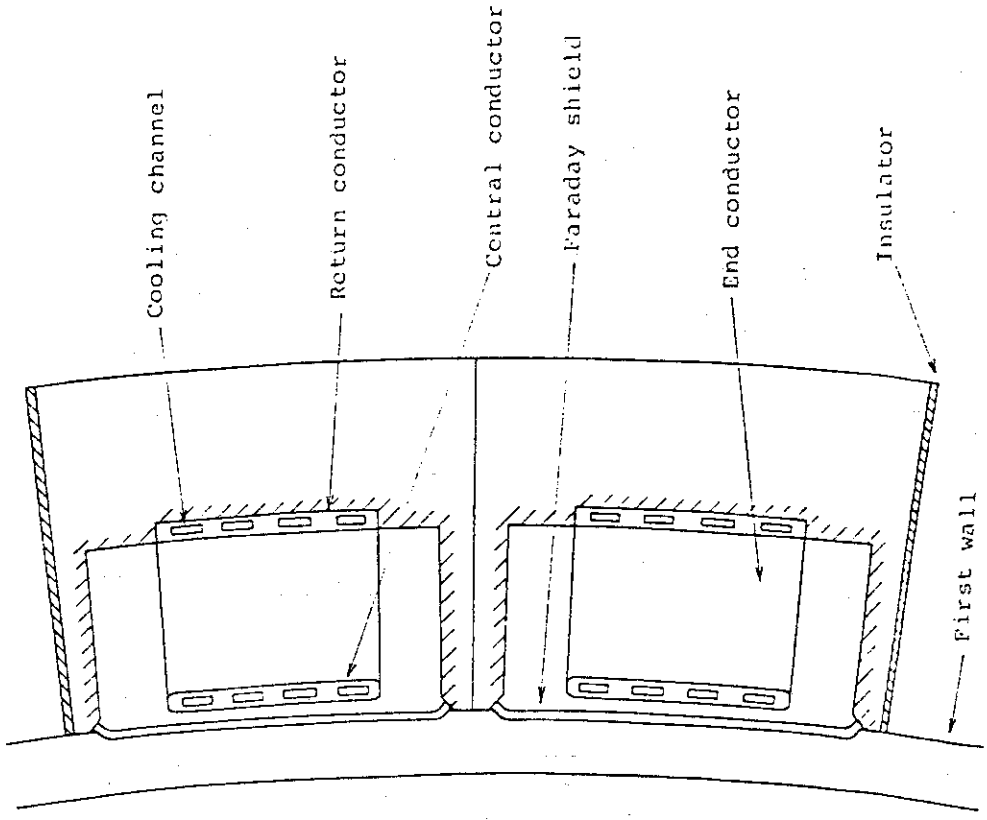

Fig. XI-7-5 Lateral cross sectional view of ICRF antenna

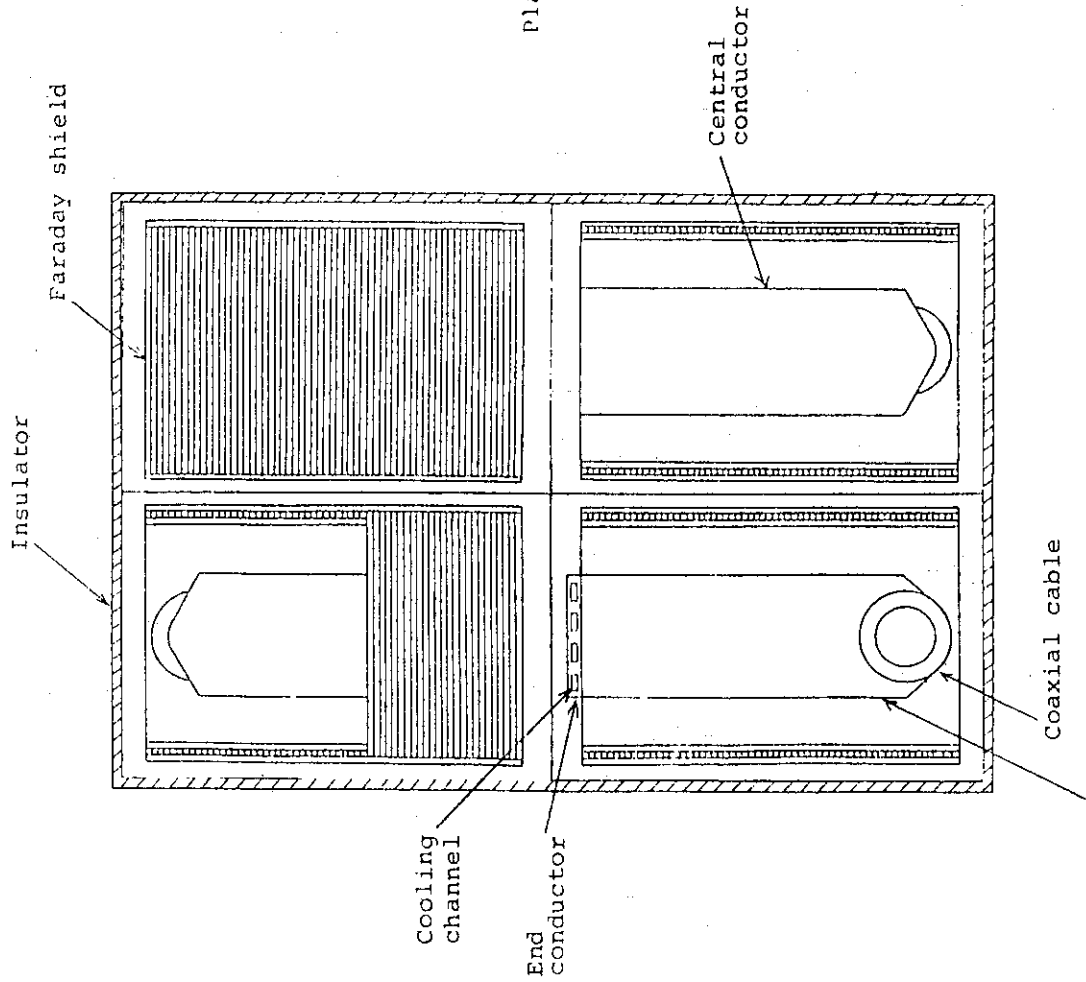

Fig. XI-7-4 Front view of four ICRF antenna

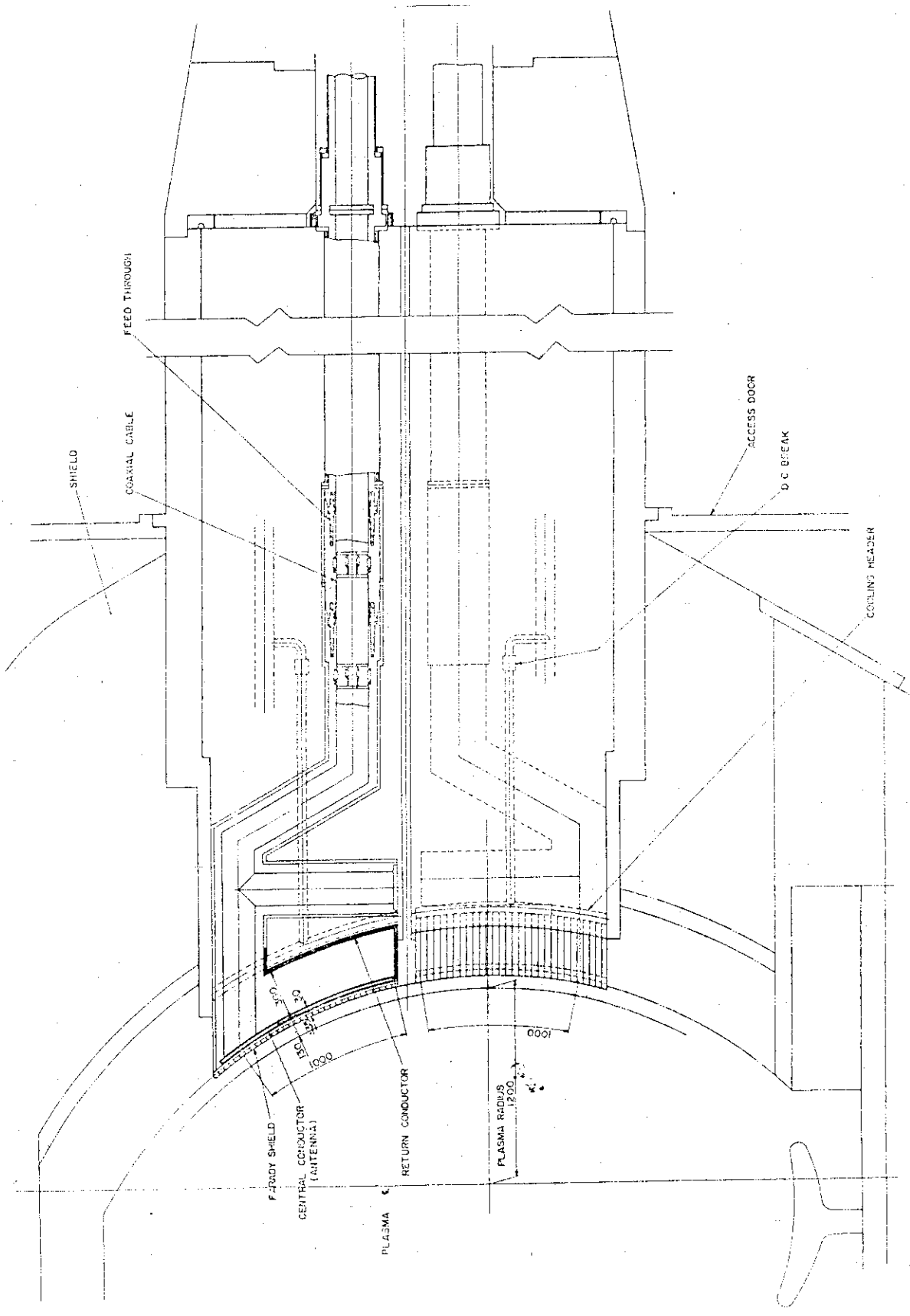

Fig. XI-7-6 ICRF antenna

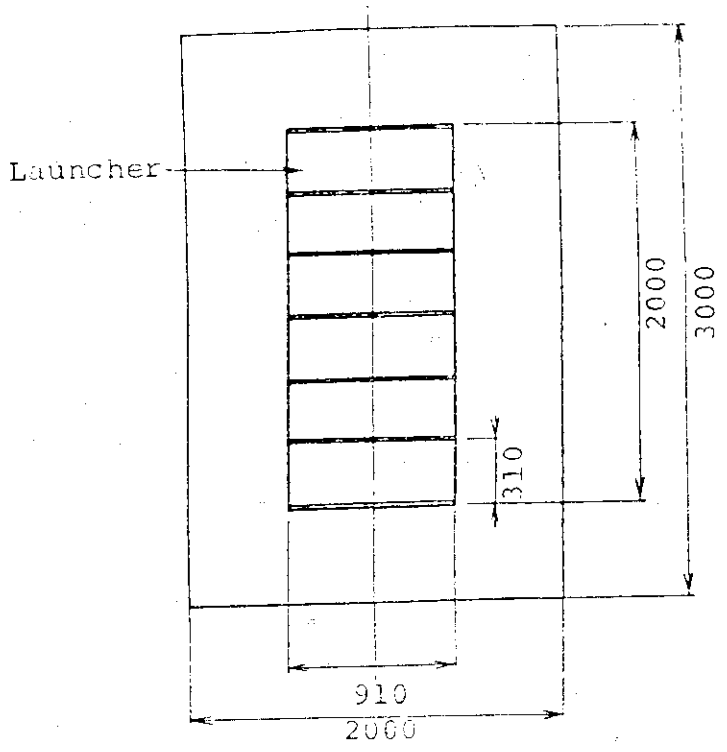

(a)

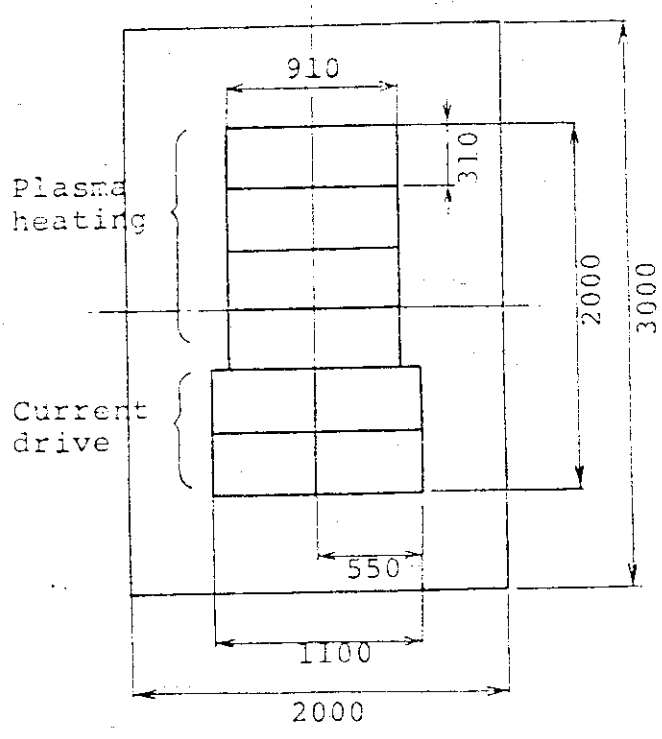

(b)

Fig. XI-7-7 Launcher overview; (a) for plasma heating, (b) for plasma heating + current drive

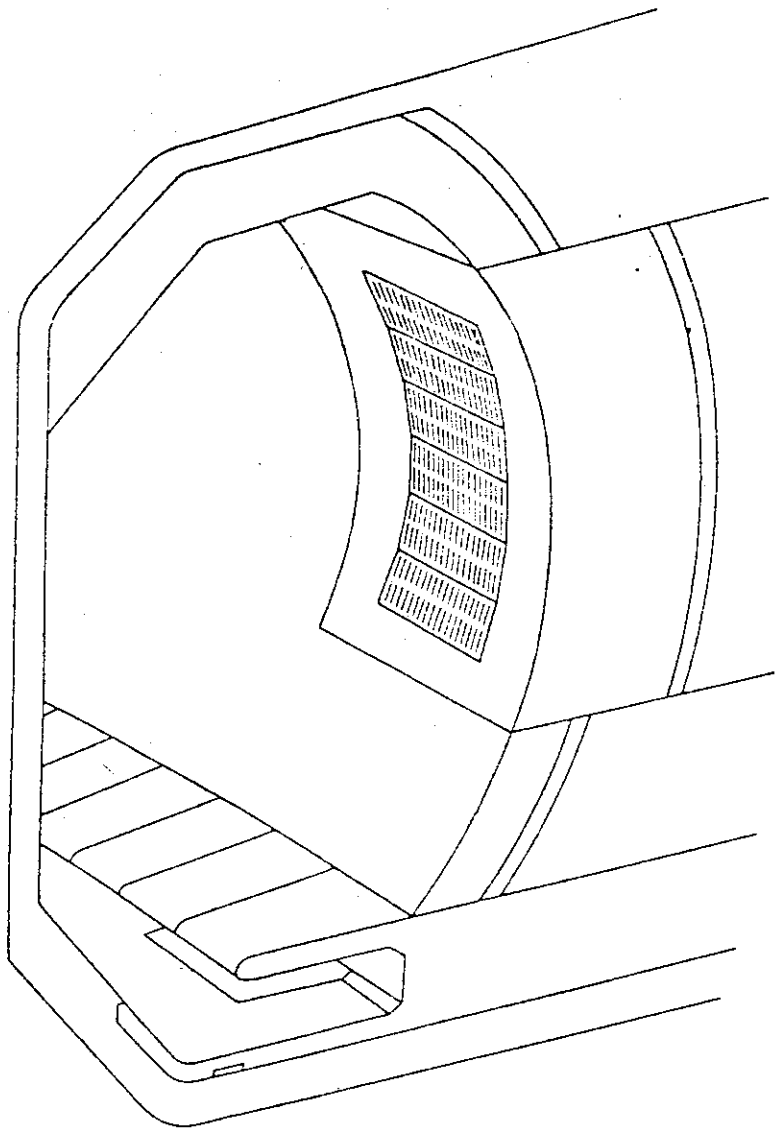

Fig. XI-7-8 Schematic view of LHRF launcher in reactor

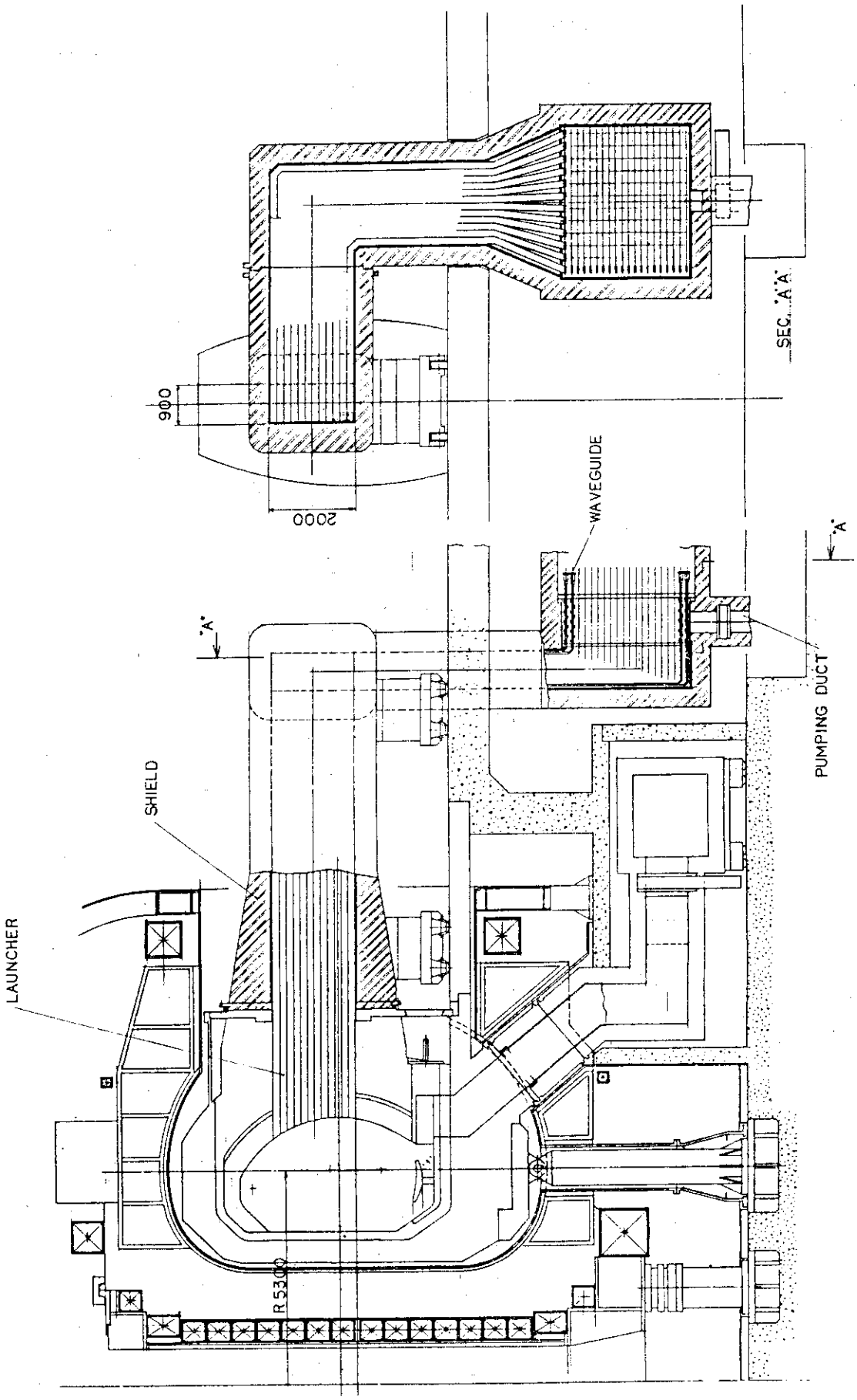

Fig. XI-7-9 Cross sectional view of R.F port

8. Conclusion and Recommendations

In Phase IIa, our efforts are focused on the reduction of reactor size and on the cost reduction.

Concerning the cost reduction, the overall system including the power supply system should be taken into consideration.

As impurities control system, both divertor and limiter operations are investigated for PF coil distribution of 5 cases.

As the results of the examination on the decisive items such as reactor size, out-of-plane force, PF coil arrangement, PF coil stored energy and power supply capacity, the case 1 (limiter operation, PF coil max radius R = 11 m) is found to be most advantageous.

Therefore, the case 1 is adopted as the reference reactor concept in our report. Concerning the limiter operation concept, not only the accumulation of the material data bases for irradiation effects, but also the more in depth design investigation is needed in order to improve the design of the limiter.

Concerning the vacuum boundary configuration, the separate type boundary is adopted.

As regard to the influence of tritium penetration, detailed studies will be necessary.

The reduction of TF coil size obliges to segment the torus in 2 sectors/ TF coil.

Acknowledgment

The authers are grateful to Drs. K. Sako, Y. Seki and T. Tone for fruiteful discussions and useful recommendations. We thank Drs. M. Yoshikawa, K. Tomabechi, Y. Iso and S. Mori for their continuous encouragements.